



# Università degli Studi della Basilicata

Dottorato di Ricerca in  
“Ingegneria per l’innovazione e lo sviluppo sostenibile”

TITOLO DELLA TESI  
“Development and characterization of innovative adsorbent materials for the remediation of  
contaminated water”

Settore Scientifico-  
Disciplinare  
“ICAR/03”

Coordinatore del Dottorato

Prof. Carmine Serio

Dottorando

Dott. Marco Cuccarese

Relatore

Prof. Donatella Caniani

Ciclo XXXIII

## Summary

Abstract .....	6
1. General introduction and adsorption process overview.....	7
1.1 General introduction .....	7
1.2 Water preservation .....	9
1.3 Wastewater treatment plants.....	11
1.3 Groundwater remediation technologies.....	13
1.4.1 Physical control of groundwater .....	13
1.4.2 Ex-situ treatment techniques.....	14
1.4.3 In-situ treatment techniques .....	16
1.5 Adsorption process.....	17
1.5.1 Influence of experimental parameters on adsorption process.....	19
1.5.2 Kinetics of the adsorption .....	20
1.5.2.1 Pseudo-first order model .....	21
1.5.2.2 Pseudo-second order model .....	21
1.5.2.3 Liquid film diffusion model.....	21
1.5.2.4 Intraparticle diffusion model.....	22
1.5.2.5 Elovich model .....	22
1.5.3 Isothermal adsorption model.....	22
1.5.3.1 Langmuir isothermal adsorption .....	24
1.5.3.2 Freundlich isothermal adsorption .....	25
1.5.3.3 Dubinin-Radushkevich isothermal adsorption .....	26
1.5.3.4 Temkin isothermal adsorption .....	26
1.5.3.5 Adsorption on fixed-bed column.....	27
1.5.3.6.1 Adams-Bohart model .....	28
1.5.3.6.2 Thomas model.....	29
1.5.4 Conventional adsorbent material .....	30
1.5.5 Innovative adsorbent material: graphene-based material and expanded graphite .....	32
1.4.6 Morphological modification of expanded graphite and graphene structure .....	33
1.5.6.1 Transformation from powder to granular adsorbent material: physical entrapment.....	33
1.5.6.2 Transformation from insoluble to hydro soluble expanded graphite: sonication .....	35
1.6 Material characterization analysis .....	36
1.6.1 Scanning electron microscopy analysis (SEM) .....	36
1.6.2 Transmission electron microscopy.....	38
1.6.3 Fourier-transformed Infrared spectroscopy (FT-IR) analysis .....	39
1.6.4 X-ray diffraction (XRD) analysis .....	40

1.6.5 Raman spectroscopy .....	41
1.6.6 Brunauer-Emmett-Teller (BET) analysis .....	43
1.7 Analytical methods.....	44
1.7.1 UV-vis spectrophotometric analysis.....	44
1.7.2 Gas-chromatography analysis .....	45
1.8 Hydrocarbons pollutants .....	47
1.8.1 BTEX.....	48
1.8.2 Benzene .....	48
1.8.3 Toluene.....	49
1.8.4 Ethylbenzene .....	50
1.8.5 Xylenes .....	50
1.8.6 Trichloroethylene .....	52
1.8.7 Methylene blue .....	52
1.9 Plasticizers .....	53
1.10 Pharmaceuticals and personal care products (PPCPs) .....	55
1.10.1 Diclofenac .....	55
1.10.2 Carbamazepine.....	56
1.10.3 17- $\alpha$ ethinylestradiol .....	56
1.11 Pesticides and herbicides .....	57
1.11.1 Atrazine .....	57
Reference .....	58
2.1 Removal of methylene blue dye from aqueous solutions using thermo-plasma expanded graphite: adsorption mechanism and material reuse .....	65
Abstract .....	65
1.Introduction.....	66
2.Materials and methods .....	67
3. Results and discussion.....	73
4. Conclusions.....	82
5. References.....	82
2.2 Removal of diclofenac from aqueous solutions using a thermo-plasma expanded graphite: material characterization, adsorption mechanism and material reuse.....	85
Abstract .....	85
1. Introduction.....	86
2. Materials and methods .....	88
3. Results and discussion.....	91
4. Conclusions.....	101

5.Reference .....	102
2.3 “Hydro-soluble” thermo-plasma expanded graphite: preparation, low pressure injectable permeable reactive barrier and adsorption of BTEX study .....	105
Abstract .....	105
1.Introduction.....	106
2.Materials and Methods .....	108
3.Results and discussion.....	113
4.Conclusion .....	133
Reference .....	133
2.4 Trichloroethylene adsorption from aqueous solution by thermo-plasma expanded graphite: investigation of mechanism process .....	138
Abstract .....	138
1. Introduction.....	139
2. Materials and methods .....	140
3 Results and discussion.....	144
4. Conclusions.....	153
5. References.....	154
2.5 Removal of organic micropollutants from water by adsorption on fixed-bed of thermo-plasma expanded graphite encapsulated into calcium alginate .....	157
Abstract .....	157
1. Introduction.....	157
2.Materials and methods .....	159
3. Results and discussion.....	165
4. Conclusion .....	185
5. Reference .....	186
2.6 Removal of phtalathes plasticizers from water by adsorption on fixed-bed of thermo-plasma expanded graphite encapsulated into calcium alginate .....	192
Abstract .....	192
1. Introduction.....	192
2. Materials and methods .....	195
3. Results and discussion.....	196
4. Conclusion .....	204
5.Reference .....	204
2.7 Adsorbent material prepared by soft alkaline activation of spent ground coffee: characterization and adsorption mechanism of methylene blue from aqueous solution.....	206
Abstract .....	206
1. Introduction.....	207

2. Materials and methods .....	208
3.Results and discussions .....	211
4.Conclusions.....	220
5.Reference .....	221
3. General conclusions and outlook .....	226
3.1 General conclusions .....	226
3.2 Outlook.....	228

## **Abstract**

The present thesis deeply investigated the use of a commercial innovative material, the thermoplasma-expanded graphite (TPEG), as adsorbent material for water remediation. This innovative material has never been used for this kind of applications and this thesis would demonstrate its effective use for water and groundwater remediation. TPEG is a promising material for that purpose due to its characteristics, evidenced by the producer, such as: high surface area and very significative expansion of interlayer distance of the plan of graphite. The commercial form of the TPEG is a very light powder that floats on the water, therefore, it was used in its natural form in batch tests. Adsorption of different pollutants, such as methylene blue, thricloethylene and diclofenac, was deeply investigated by evaluating the kinetics and isothermal aspect of the adsorption. Furthermore, other parameters that can affect the adsorption, such as pH, initial concentration of pollutants, ionic strength or presence of interference, were investigated. The possibility of regenerating and reusing the TPEG as adsorbent was also evaluated.

Modification of the morphology of TPEG was conducted in order to use it as adsorbent material for different setup of process, like fixed-bed column. To this aim, the commercial form was transformed into a granular form of thermo-plasma expanded graphite (GTPEG), by entrapping TPEG into calcium alginate, by using a process that was developed and optimized during this thesis work. The GTPEG was then used to treat water by adsorption on fixed bed column. The process was deeply investigated and several pollutants were tested as target compounds, such as short chain phthalates (plasticizers), carbamazepine, bisphenol, 1,7- $\alpha$  ethynilestradiol and atrazine. The effect of adsorbent dosage, flow rate, initial concentration of pollutants, time contact and composition of GTPEG was evaluated. Other tests were conducted to verify the leaching of GTPEG. Adams-Bohart and Thomas models can effectively be applied to modelize the process and to evaluate its scale up.

A sonication process was optimised to transform the not soluble TPEG into a hydrosoluble form, useful to treat groundwater by injecting the adsorbent material to obtain a hydraulic barrier able to contain and remove the pollution. By using this hydrosoluble form, TPEG can be used as material for the installation of injectable permeable reactive barrier. The capacity of

the hydrosoluble TPEG to adsorb BTEX was firstly tested and characterized by using the batch setup to have all the information on the adsorption process. After the deeply characterization of the adsorption process, the use as injectable permeable reactive barrier to remove BTEX from groundwater was investigated.

Innovative commercial materials can be used as adsorbent, but waste materials also represent a source of adsorbent materials. For this reason, a little part of the thesis was reserved to this kind of work. The last chapter reports a study conducted on the reuse of agricultural-food waste as adsorbent material: the spent ground coffee. The ability of spent ground coffee as adsorbent material was demonstrated by deeply investigating its capability to remove methylene blue.

## **1. General introduction and adsorption process overview**

### **1.1 General introduction**

Water remediation is an historical challenge as this natural resource represents the most important element for human life; its damage can irremediably affect the life on the Earth. Several processes have been implemented and optimized for water and wastewater treatment [1, 2, 3, 4, 5, 6, 7, 8, 9, 10] and reuse. By considering the increasing of the pollution and the emerging of new kind of pollutants (known as “emerging pollutants”), several researches are still conducted to improve the performance of the traditional processes and discover new treatments. In the next sections further information on water and treatment waste water will be given, but in this section an overview was reported to better understand the aim and the scope of the thesis.

One of the processes traditionally used for water remediation is the adsorption, that is regulated by transferring the pollutants from the water to the surface of a solid material, called adsorbent material. This process is characterized by some advantages, like its operational simplicity, and the absence of metabolites or new chemical species introduced into the water [8, 9, 10]. The typical and most used adsorbent material is the activated carbon [11, 12]. It is largely used, but its efficiency is not always reliable in removing emerging pollutants or traditional ones, when they are present at concentrations lower than ppm. For these reasons, innovative adsorbent materials are the topic of several scientific research groups and nowadays graphitic and graphenic material are largely investigated [13, 14, 15, 16], due to their very large surface area, a characteristic that ensures good adsorption properties. This thesis investigated the use of a commercial form of thermo-plasma expanded graphite (TPEG), to evaluate the use it as adsorbent material to replace activated carbon or to couple to it. For that reason, the adsorption

ability of the commercial form of TPEG was investigated by batch testing. Diclofenac, methylene blue and trichloroethylene were tested as target pollutants and the adsorption process was deeply investigated. Kinetics and isothermal aspects of the adsorption process were investigated and compared with theoretical models (Langmuir, Freundlich, Dubinin, Temkin, pseudo-first order, pseudo-second order, intraparticle diffusion, liquid film diffusion and Elovich). Furthermore, the effect of other parameters, such as time of contact, pH, ionic strength, concentration of pollutants, on the adsorption capacity of the material, was investigated. The deep knowledge of the process at lab-scale is a mandatory step for real applications because it is necessary to evaluate the performance of the adsorbent material for dimensioning reactors, adsorbent dosages, time of contact and other parameters. Regeneration and reuse as adsorbent material of the TPEG was investigated by testing the thermal regeneration and solvent washing [17, 18, 19, 20].

The commercial form of TPEG is a very light powder with low density, it floats on the water and it represents a limit for different setup applications, such as the use as fixed bed column of adsorbent material [21, 22, 23, 24, 25, 26] (useful for filtration setup) and injectable permeable reactive barrier [27, 28, 29, 30] (useful for the treatment of groundwater and containment of plume). In order to investigate the use of the material for different setup, a modification of the morphology of the material was carried out. Two different form were prepared: granular form of TPEG (GTPEG) and hydrosoluble form of TPEG. The granular form could be used as adsorbent material for fixed bed column. This is the typical setup used into the wastewater treatment plants and it is often used for groundwater remediation when the Pump&Treat system is applied. The preparation of the granular form of the TPEG was performed by using the entrapment approach typically used into nanobioscience for the preparation of enzymatic biosensor [31]. Indeed, TPEG was physically entrapped into calcium alginate sphere. In order to perform that, TPEG was mixed to sodium alginate and mixed until an homogeneous solution was obtained and then dropped into calcium chloride. The presence of the calcium ion facilitates the reticulation of the chain of alginates and TPEG remains entrapped into. Then, the material was dried at 105° in the oven and granular sphere of TPEG was obtained and used to prepare fixed bed column where the water treatment was performed. The adsorption by filtration was tested and deeply investigated by using phthalate (with short chain) normally used as plastizers, bisphenol A, atrazine (herbicide), carbamazepine (anti-epileptic drug) and 1,7- $\alpha$ -ethynilestradiol (hormone) as target pollutants. The process was deeply investigated to obtain enough information that could be used for the scale up of the process. The effect of flow rate, contact time, adsorbent dosage, initial concentration of pollutants and GTPEG composition



were investigated. The fitting of experimental data with theoretical models (Adams-Boahrt and Thomas models) was evaluated and the obtained results were used for dimensioning the possible scale up of the process. A test to evaluate the probably leaking of TPEG from the obtained granular material was also conducted and no leak was observed.

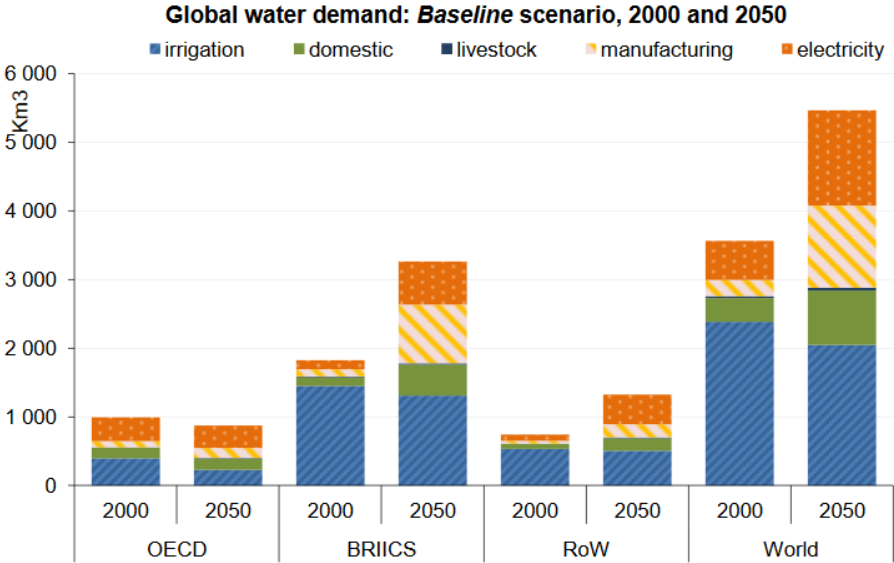
Then, the hydrosoluble form of TPEG was prepared by optimizing the sonication process [32]. The adsorption efficiency of the hydrosoluble form was firstly investigated on batch test for the removal of toluene, xylenes and ethylbenzene (BTEX) and then a simulation of use as injectable permeable reactive barrier for groundwater remediation (BTEX as pollutants as target pollutants again) was performed. The adsorption process was deeply investigated to have complete knowledge on the adsorption process of BTEX on hydrosoluble form of TPEG.

To conclude the thesis, the topic of water preservation was coupled with another aim of the sustainable developing: circular economy. In order to reduce the solid waste production and the water preservation at the same moment, an agricultural-food waste was used to prepare an adsorbent material [33, 34, 35, 36], which was used to remove methylene blue from water. The chosen waste was the spent ground coffee. The adsorption process was investigated by evaluating the kinetics and isothermal aspect. Furthermore, the effect of numerous parameters, such as adsorbent dosage, pH, pollutants concentration, ionic strength was deeply investigated.

The present thesis demonstrates the potentiality of TPEG as innovative adsorbent material for water treatment and remediation. The material performance was comparable with the most performing new material tested and reported in literature. Furthermore, the commercial form of the material presents the advantage that can be easily modified when it is necessary for different setup application from batch reactor, such as injectable permeable reactive barrier or fixed bed columns. The promising results encourage us to perform further modification of the material and the investigation of its adsorption ability of more pollutants. Every chapters focused on the experimental aspect of the thesis contains a deep introduction on the aspect of the novelty, the challenge of the work, the state of the art and other important aspect related to the single work performed to give to the reader all the information that he/she needs. The actual presented chapter is just an overview to gives to the reader the idea of the works performed for this thesis, its logical execution and the context where it is.

## **1.2 Water preservation**

Water is a precious resource used in households, industry, and agriculture. Freshwater on the Earth is very rare and only 0.2% of the total water is directly accessible for human consumption [38] and about 36% of that is actually used [39]. Its distribution in the world is unequal and some countries, where accounting for 30% of the total world population, face freshwater scarcity. The future increase of world population expected in the next years will even increase the problem associated to the freshwater scarcity [40]. As reported in figure 1, the global water demand will increase, and scientific community has to face the problem to avoid global fighting and migration caused by water scarcity, as already happened in some countries where reserve of surface water represent the only source of procurement and they were exhausted due to bad management of the resource and the climate change. An example of what could involves a future decrease of water reserves is represented by the case of lake Chad. Its surface is reduced by about 90% respect the 1870 [41] and it is one of the causes of social tension and migration in that area. Several studies demonstrate that the probability of conflicts is increased of 11% in the African continent respect the 1980 due to the climate change that involves also increase of water scarcity [42]. Furthermore, the increase of water demand and the decrease of water resource will contribute to increase the difference between developed country and not developed country, affected for example the production of cereal. Some models indicate that the production of cereal will be decreased of about 30% in not developed country and increased of about 15% in developed country [43]. It will contribute to the increase of migration phenomena, social inequalities and the negation of the right to choose to live in own country.



Note :BRIICS = Brazil, Russia, India, Indonesia, China and South Africa; RoW = rest of the world  
Source: *Environmental Outlook Baseline*; output from IMAGE suite of models.

**Fig.1 Global water demand: comparison between 2000 and 2050. OECD report on water.**

In this context, the source of freshwater (groundwater and surface water) needs protection and intensive treatment and reuse of wastewater should be aimed for [44]. Wastewater cannot be directly discharged into surface water because normally it contains several hazardous substances that can affect its quality. Nevertheless, globally 80% of the produced wastewater is discharged in surface water without treatment [45]. For this reason an increase of wastewater treatment plants (WWTP) is required to preserve the quality of the water, although this alone will not be enough as a typical WWTP is not able to remove emerging urban pollutants such as herbicides, plasticizers, pesticides and pharmaceutical products that are still detected in WWTP effluent [46, 47, 48, 49, 50]. For this reason, innovative process should be improved to treat urban wastewater, to avoid discharging contaminants that can alter the natural ecosystem into surface water. The pollution of water by urban purpose it is not the only source of water degradation. There are other sources of pollution, such as industrial application and environmental disaster caused by leaking of pipeline or other accidents. In that case, the kinds of pollutants that contaminate water are different from the previous one reported before and the concentration are different (typically for environmental disaster are higher than urban wastewater). Innovative process could be also improved to have more performers treatment able to treat water contaminated after uncontrolled disaster. Normally, pollutants involved in these kinds of events are hydrocarbons or dyes used into tanning industries.

### **1.3 Wastewater treatment plants**

Because of the preservation of water resource, by reusing wastewater after treatment and preservation of freshwater, is necessary to ensure the future human life and developing, wastewater treatment plants (WWTPs) were deeply studied and optimized and nowadays are largely presents into developed country. Different degrees of treatment will be necessary depending on the final use of this reclaimed water. The main function of a WWTP is to minimize the environmental impact of discharging untreated water into natural water systems. The conventional WWTPs consist of two levels of treatment: preliminary and primary (physical and chemical), and secondary (biological) treatment. These treatments may reduce suspended solids, biodegradable organics, pathogenic bacteria and nutrients. This treated wastewater is usually discharge into the sea or rivers but not used for reuse purposes. Also a WWTP may get a resource from wastewater carrying out a tertiary treatment on the treated wastewater which can be reused. The preliminary treatment involves the removal of coarse solids and other large materials often found in raw wastewater. Removal of these materials is necessary to enhance the operation and maintenance of subsequent treatment units. Preliminary treatment operations

typically include coarse screening, grit removal and, in some cases, comminution of large objects. The primary treatment involves the removal of settleable organic and inorganic solids by sedimentation, and the removal of materials that will float (scum) by skimming. Approximately 25 to 50% of the incoming biochemical oxygen demand (BOD<sub>5</sub>), 50 to 70% of the total suspended solids (SS), and 65% of the oil and grease are removed during primary treatment. Some organic nitrogen, organic phosphorus, and heavy metals associated with solids are also removed during primary sedimentation but colloidal and dissolved constituents are not affected. Primary sedimentation tanks or clarifiers may be round or rectangular basins, typically 3 to 5 m deep, with hydraulic retention time between 2 and 3 hours. Settled solids (primary sludge) are normally removed from the bottom of tanks by sludge rakes that scrape the sludge to a central well from which it is pumped to sludge processing units. Primary sludge is then treated by anaerobic or aerobic digestion and dewatering. The objective of secondary treatment is the further treatment of the effluent from primary treatment to remove the residual organics and suspended solids. In most cases, secondary treatment follows primary treatment and involves the removal of biodegradable dissolved and colloidal organic matter using aerobic biological treatment processes. Aerobic biological treatment is performed in the presence of oxygen by aerobic microorganisms that metabolize the organic matter in the wastewater producing CO<sub>2</sub>, NH<sub>3</sub> and H<sub>2</sub>O. The microorganisms are then separated from the treated wastewater by sedimentation to produce clarified secondary effluent. The sedimentation tanks used in secondary treatment, often referred to as secondary clarifiers, operate in the same basic manner as the primary clarifiers described previously. The biological solids removed during secondary sedimentation, called secondary or biological sludge, are normally combined with primary sludge for sludge processing. Secondary treatment, in combination with primary sedimentation, typically remove 85 % of the BOD<sub>5</sub> and SS originally present in the raw wastewater and some of the heavy metals. Tertiary and/or advanced wastewater treatment is employed when specific wastewater constituents which cannot be removed by secondary treatment must be removed. Because advanced treatment usually follows secondary treatment, it is sometimes referred to as tertiary treatment. However, advanced treatment processes are sometimes combined with primary or secondary treatment or used in place of secondary treatment. Normally, tertiary treatments consist of adsorption, reverse osmosis filtration, dephosphatizing, denitrification and sterilization. One or more of them can be conducted. Because adsorption process is the topic of this thesis, it will be largely discussed in next sections. The developing of adsorption process and adsorbent materials can be useful to remove emerging pollutants detected in wastewater that are not removed by the typical WWTPs.

Normally, emerging pollutants require very expensive and complex solution for the removal. To have cheap, high removal efficient and easily adsorption process will allow to have it as mainstream tertiary treatment of WWTPs. [51]

### **1.3 Groundwater remediation technologies**

Groundwater remediation operation is very expensive, time consuming, not always effective and normally pertinent information is usually not available for the aquifer and the geological system. All these considerations, promote the governmental strategies focused on reduction of the risk of exposition to pollutants of the sensitive receptor. However, events of pollution of groundwater could happen and remediation is necessary. Many different methods of physical, chemical and biological technologies have been proposed for the protection/clean up of groundwater reservoir. The remediation methods can include hydrodynamic or physical containment of polluted plume and then extraction of the groundwater by pumping it and treat it. After the remediation treatment water is pumped again into the aquifer system. This system is called pump and treat and it is an ex-situ treatment technology. In-situ treatment technologies are also developed and normally reagents, microorganism etc. useful for the pollutants removal are directly pumped into the groundwater.

#### **1.4.1 Physical control of groundwater**

Different techniques are available for the physical control of the flow of groundwater and therefore of the flow of polluted groundwater (plume): grouting, slurry walls and sheet piling. Grouting is a technique used in the construction industry. It is based on the injection of a stabilizing liquid slurry under pressure into the soil that can also be used to create an impermeable wall. The grout is injected into the soil until all the pores are completely filled. Then, the grout solidifies and sets, resulting in a mass of solid material that will reduce the soil permeability to zero when properly constructed. The success of the grouting operation depends on several variables like the soil composition and geology, the soil temperature and pollutants contained (acid and alkaline conditions degrade the grout wall). An important consideration during the grouting process is the pressure of injection of the grout. A high pressure of injection may weaken the strata and increase the permeability. Other disadvantages of grouting is that it is limited to granular types of soils, having pore space large enough to accept grout fluids under pressure. Another method of impermeable wall formation is the use of slurry walls. It represents a technology to prevent groundwater pollution or restrict the movement of contaminated groundwater. It is very simple and involves digging a deep trench and concurrent

in situ blending of a bentonite clay with the native soils. The advantages of the method are the simplicity and the widely use in the construction industry, bentonite minerals will not break down with the age and as long as the wall remains wet it will swell and maintain an excellent impermeable seal, slurry walls are not attacked by the typical contaminants and low maintenance are necessary. The disadvantages are that the excavation is necessary and bentonite degradation has occurred where there has been exposure to higher ionic strength leachate. Sheet piling technique involves driving lengths of steel that are connected via a tongue and groove mechanism into the ground to form an impermeable barrier to flow. Sheet piling materials include steel and timber. It is a simple technique, no excavation is necessary and no contaminated soils need disposal. For small project, construction can be economical and there is no maintenance after the construction. Furthermore, the steel can be coated for corrosion protection to extend its service life. The presence of acidic groups may attack the steel.

#### **1.4.2 Ex-situ treatment techniques**

In addition to the physical containment of the groundwater, it can be also treated by ex-situ processes to remove pollutants at the surface and then reinject it. The ex-situ treatment available are air stripping, adsorption, biological treatment and chemical treatment. Air stripping is a process by which volatile or semi-volatile compounds are removed from the water and transferred to gas phase. The transfer step is favoured by an air flow through the water. The driving force of the process is the difference between the initial concentration of the pollutant in the air phase ( $C_i=0$ ) and the concentration associated to the equilibrium between the gas and the liquid phase regulated by the Henry's law, expressed by the following equation:

$$C_G = H \times C_L$$

Where  $C_G$  is the concentration in the gas phase,  $H$  is the Henry's law coefficient and  $C_L$  is the concentration in the liquid phase. High values of  $H$  ensure high removal of the pollutants by transferring it to the gas phase. Normally, compound with a  $H$  values higher than  $10^{-4} \text{ atm m}^3 \text{ mol}^{-1}$  are considered strippable. Chlorinated hydrocarbon compound used as solvent and normally detected as pollutants of groundwater have a lower value of  $H$  and are not removed by this technique. Different types of equipment are available for the operation that ensure the transfer of the pollutants from the water to the air. The most widely used is the packed column system. The packing material is useful to ensure the maximum surface area of contact for the countercurrent flow of water coming down and air being forced up. Contaminated water is

cascade from the top of the column and splashed against the packing material while air is forced in from the bottom and out from the top by carrying the volatile and semivolatile pollutants. The key design variables in air stripping project are the diameter of the columns, the liquid loading rate that depends by the amount of the groundwater to treat, the air-water ratio, the packing height and its characteristic. Knowing the flow rate, the diameter of the column can be derived from the loading rate. Fixed the liquid loading rate and the diameter of the column, the height of the packing is a trade off with the air-water ratio. By increasing the air-water ratio a decrease of the height is involved. The design of the column can be obtained by considering the following equation:

$$Z = \frac{L}{K_L D_w} \frac{R}{R-1} \ln \left( \frac{C_i / C_0 (R-1) + 1}{R} \right)$$

Where Z is the packing height (m), L the liquid loading rate ( $\text{kg mol h}^{-1} \text{ m}^{-2}$ ),  $K_L$  is the liquid mass transfer rate times,  $D_w$  the molar density of the water ( $\text{mol m}^{-3}$ ),  $C_i$  is the influent concentration of water,  $C_0$  is the effluent concentration of water and R is the stripping factor defined as reported in the following equation:

$$R = \left( \frac{H \times G}{P \times L} \right)$$

Where H is the Henry's law constant, G is the air velocity ( $\text{kg mol h}^{-1} \text{ m}^{-2}$ ) and P is the total system pressure (atm). The equation allows to define the trade-off between height of the packing and air-water ratio by plotting Z versus R for different values of  $C_i / C_0$ . The methods can be easily applied to the volatile organics compounds. The capital cost of air stripping are relatively small but because of the length of the time to treat the plume, annual cost can be substantial. Biological treatment represent another option to treat groundwater ex-situ. Heterotrophic microorganism are the most common group that provide the metabolic process for removing organic compounds from contaminated groundwater. They use the contaminants as source of carbon and energy. Portion of contaminants are oxidized to provide energy and the other portion are used as building blocks for cellular synthesis. Energy are obtained by fermentation, aerobic respiration and anaerobic respiration. The biological treatment are normally divided into two categories, the suspended growth system (activate sludge processes) and fixed-film system. The activated sludge system consist of a large basin in wich the contaminated water is introduced along with air or oxygen by diffusers or mechanical aeration devices and nutrients like nitrogen and phosphorous. The microorganism are present as

suspended material and grow by using the pollutants present in the water. At the end of the process, microorganism required to be separated from the water phase, therefore a gravity settling is present. The described process is the typical process used into the WWTPs. The fixed-film system differs from the activate sludge in that microorganism are fixed to media that provide an environment for them. Rotating biological contactors are the most common forms of fixed system. It consists of a series of rotating disk connected by a shaft and set in a basin or trough. Microorganism are fixed on the disk and they are in contact with the water. This system ensure lower cost because oxygen are naturally provided thanks to the continuous rotation of the disk that ensure moment outside the water for the microorganism. Biological treatment are normally useful to remove organic compounds. Chemical precipitation is another technology useful to remove inorganic pollutants. Three common techniques are available for the precipitation of the inorganic compounds at specific pH and they are carbonate system, hydroxide system and sulphide system. The sulphide system ensure the removal of all the the inorganics but the handling the chemicals after the precipitation is not easy and resolubilization can be observed. Carbonate system is managed by pH adjustment between 8.2 and 8.5 by using soda ash. The hydroxide system is most used for inorganic metal removal. The system responds to pH adjustment by adding lime or sodium hydroxide. The metals precipitate as hydroxide. Another important process for the ex-situ treatment is the adsorption. As topic of that thesis, it will be discussed deeply in the next section. Adsorption represents the most widely used method because of its feasibility, lower cost and no complex maintenance.

### **1.4.3 In-situ treatment techniques**

A major problem with in situ technologies is delivering the right reagents to the right locations at the right concentration and the right time. The problem to overcome is mixing of the feed material into the aquifer which is a very slow process. In situ physical/chemical treatment involves the installation of a bank of injection at the head of the plume. A treatment agent is pumped into the groundwater. In situ physical/chemical treatment include air sparging, hot water/steam flushing/stripping, in-well air stripping, circulating wells and passive/reactive treatments walls (permeable reactive barriers). Air sparging involves injection of air into contaminated groundwater. Injected air traverses through the soil column, creating a stripper that removes volatile and semivolatile compounds. Pollutants reach the unsaturated zone, where a vapor extraction system is present to remove the generated contaminated gas-phase. The addition of oxygen to the system can also enhance the biodegradation. Some limitation exist for that process like the possible not uniform flow of the air through the soil, depth of the



contamination can reduce the efficiency of the process and soil heterogeneity could represent a limitation and some zone can be unaffected by the process. In-well air stripping is a similar process to the ex-situ air-stripping. Air is injected into a double-screened well, lifting the water in the well and forcing it out the upper screen. Circulating wells is a variation of the in-well air stripping. Hot water/ steam flushing/stripping involves the forcing of hot water/steam into an aquifer through injection wells to vaporize volatile and semivolatile organic compounds. After the vaporization they reach the unsaturated zone where they are removed by vacuum extraction and then treated. Permeable reactive barriers involve the installation of a permeable wall across the flow of the contaminated plume. These barriers allow the passage of water while prohibiting the movement of contaminants by entrapping or degrading them into not dangerous substances. These technology is normally used for long-term operation to control migration of contaminants in groundwater. The limitation are represented by the fact that the barrier lose their activity and replacemet are required, depth and width of barrier could limit the application to small plume, biological activity or chemical precipitation can limit the permeability of the barrier and the long-term monitoring is mandatory. Some of that limitation are the topic of researcher community, like the regeneration of the barrier by coupling adsorption and biodegradation process or the limitation of the installation of the barrier for small and no depth plume by developing low-pressure injectable barrier. In-situ biological remediation technologies are also developed. They can involves inoculation of microorganism, nutrients and primary substrate or oxygen to enhance the natural biodegradation. The biologic remediation technology are already available and other develop are now conducting to improve the efficiency of the process. As reported for the previous section, research on adsorption process is actually largely conducted and, for in-situ treatment, focused on the developing of injectable adsorbent permeable barrier and coupling with biodegradation. Traditional adsorbent barrier is also subject of evaluation of coupling with biodegradation. [52]

### **1.5 Adsorption process**

Adsorption is a chemical-physical mass transfer process with which atoms or molecules of compounds present in the liquid or gas phase are fixed on a solid porous surface, concentrating at the separation interface, due to the bonds of both a physical and physical nature. chemistry between the adsorbate and the adsorbent solid. Adsorbate is the substance that is removed from the liquid phase, the adsorbent is the solid (most common case), liquid or gaseous phase on which the adsorbate accumulates. The adsorption phenomenon is widely exploited in scientific and industrial applications, such as chromatographic analysis or even in many depuration or discoloration technologies. Many substances present in the environment have adsorbent

properties, but the materials most used for this purpose are materials based on silica gel, activated alumina, zeolites and activated carbon. The latter is the most common one for the removal of organic molecules given its high specific surface area, good affinity with many compounds, ease of regeneration and relatively low costs [53]. Based on the type of relationship that is established between the adsorbate and the adsorbent, the adsorption can be defined as physical or chemical. We find ourselves in the first case if weak bonds are involved, such as van der Waals bonds; in the second when strong bonds are involved (type  $\pi$ - $\pi$  and chemical bonds). Since the adsorption process occurs in several steps, the slower step is identified as the kinetically limiting step [54]. In general, it is possible to distinguish four phases during the adsorption process, as shown in Figure 2, and they are:

- transportation within the solution;
- transport by diffusion within the liquid film;
- transportation within the pores;
- adsorption.

The first phase concerns the movement made by the substances to be adsorbed inside the solution, until the stagnant liquid film that surrounds the surface of the adsorbent is reached. The second phase consists in the transport of the substances of interest, according to diffusion processes, through the stagnant liquid film, until the pores of the adsorbent are reached. The following phase consists in the transport of the substance to be adsorbed inside the pores of the adsorbent due to the effect of molecular diffusion mechanisms in the liquid contained in the pores and diffusion on the surface of the solid material. The actual adsorption phase occurs when the substances bind to the adsorbent at the active adsorption sites.

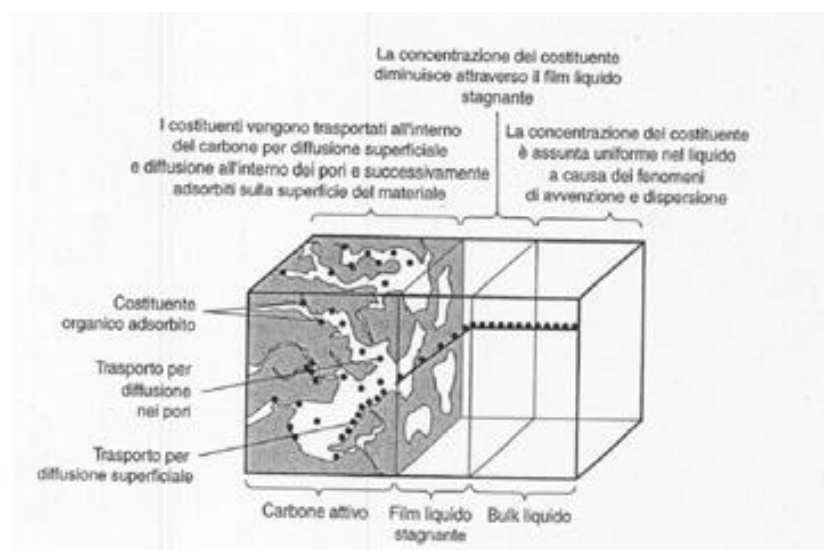


## *Fig.2 Schematic representation of adsorption process*

### **1.5.1 Influence of experimental parameters on adsorption process**

The adsorption capacity is highly variable and depends on the type of adsorbent used, the type of contaminant to be removed and the operating conditions [53]. It is calculated as the mass of pollutant removed per unit of mass of the adsorbent substance and the factors that most influence it are:

- surface area of the adsorbent;
- porosity of the adsorbent;
- solubility;
- nature of the adsorbate (polarity, branching of the structure, presence of aromatic rings etc.);
- pH;
- temperature;
- interaction with other substances present;
- concentration of the solute (adsorbate) and adsorbent material;
- contact time.

Adsorption is a superficial phenomenon and appears to be dependent on the specific surface area of the adsorbent, defined as that portion of the total area involved during the process. In general, the adsorption capacity grows with the specific surface but it is not always closely related to it as it depends on the size of the molecules and the characteristics of the solution [53]. The adsorption capacity is also greater when porosity increase and granulometry of the material decrease. In this case, most of the area available for the process is located in the pores of the adsorbent. If the adsorbent used is not porous or, although porous, the process is limited to the transport of substances through the stagnant liquid film, then the adsorption capacity will be inversely proportional to the diameter of the particles. If, on the other hand, the adsorbent is porous but the adsorption process is based on interparticle transport, then the adsorption efficiency will be the reciprocal of some power of the particle diameter. In addition, the speed and adsorption capacity of a given material vary linearly with the quantity of adsorbent (the adsorption capacity increases only if the number of active sites limits the number of adsorbed molecules) [54]. The adsorption process is also strongly influenced by the properties of the solute. In the case of inorganic compounds, it depends on the presence of solute in neutral or ionic form [55]; in the case of organic compounds, however, the main factor is the solubility of

the compound. Specifically, the Lundelius rule allows you to predict the degree of adsorption of a given solute based on its chemical properties. According to this rule, a compound is all the more adsorbable the lower its solubility in the solvent. This can be explained considering that the greater the solubility, the greater the solute-solvent bond and, therefore, the lower the adsorption capacity due to the lower energy gain derived from the adsorbent-adsorbed interaction. However, Lundelius' rule is not always respected: there are many cases in support of this theory, but also many exceptions. Another parameter that influences the adsorption process is the molecular structure: the compounds with a branched chain are generally less adsorbable than those with a linear chain [56]. The pH affect the process by changing the solubility of the adsorbate (a low solubility promotes adsorption) but also because can provoke protonation or deprotonation of the surface of the adsorbent. The temperature influences both the kinetics of the process and the adsorption capacity. The increase of the temperature involves the increase of the rating of the process due to increase of the energy of the system that ensure a bigger number of molecules with energy equal or major of activation energy of the process. The effect on the adsorption capacity depends on the thermodynamic of the process. Simple assumption can be done and the increase of temperature improves the adsorption process when they are endothermic or an increase of entropy is involved. When several compounds are present at the same time, in general, the adsorption capacity towards each of them tends to decrease, even if it is not said that the total adsorption capacity is lower than that which would occur with a single species in solution [54]. It occurs because the compounds present in the solution compete to interact with the active site of the adsorbent. Finally, the contact time also contributes to the adsorption process. The increase of the contact time involves an increase of adsorption capacity because adsorbate and adsorbent have more time to interact. Normally, after a long time a plateau is reached due to the saturation of the adsorbent material. By increasing the concentration of the adsorbate an increase of the adsorption capacity is observed because the gradient of the concentration between the solution and the surface of the adsorbent is observed. The increase of the concentration of the adsorbent involves an increase of removal efficiency because a major number of active sites are free to interact with the adsorbate.

### **1.5.2 Kinetics of the adsorption**

Kinetic models are useful for understanding the adsorption mechanism and its rate. The evaluation of the kinetics of the process allows to understand what is the slowly step of adsorption process previously described (diffusion in the pores or liquid film, interaction between adsorbate and adsorbent). They are also useful to evaluate the performance of

adsorbents in the removal of contaminants and compare them [57]. They allow to graphically represent and evaluate the variation of adsorption capacity as a function of time. The reported model can be used for adsorption test conducted in batch mode (adsorbent and adsorbate are in contact by mixing it in the same solution).

### 1.5.2.1 Pseudo-first order model

The pseudo-first order model is regulated by the following equation:

$$\ln(q_e - q_t) = \ln q_e - k_1 t$$

where  $q_e$  and  $q_t$  are respectively the quantities of adsorbed solute for gram of adsorbent ( $\text{mg g}^{-1}$ ) at equilibrium and at time  $t$ ,  $k_1$  is the adsorption constant. The values of the constant  $k_1$  are calculated from the trend line equation (linear regression line) obtained by linear regression analysis of the graph obtained reporting the time on the abscissa axis, and the value corresponding to  $\ln(q_e - q_t)$  on the ordinate axis. It is therefore possible to determine the kinetic constant and the theoretical adsorption capacity [58]. This model is generally observed in the case where the slow step of the adsorption process is the physical interaction between adsorbent and adsorbed.

### 1.5.2.2 Pseudo-second order model

The pseudo-second order model is regulated by the following equation:

$$\frac{t}{q_t} = \frac{1}{k_2 q_e^2} + \frac{t}{q_e}$$

Where  $k_2$  is the adsorption constant and  $q_e$  and  $q_t$  are respectively the quantities of adsorbed solute for gram of adsorbent ( $\text{mg g}^{-1}$ ) at equilibrium and at time  $t$ . The values of the constant  $k_2$  are calculated from the trend line equation (linear regression line) obtained by linear regression analysis of the graph obtained reporting the time on the abscissa axis, and the value corresponding to the ratio  $\frac{t}{q_t}$  on the ordinate axis. The theoretical adsorption capacity can be also calculated. This model is generally observed in the case where the slow step of the adsorption process is the chemical interaction between adsorbent and adsorbed.

### 1.5.2.3 Liquid film diffusion model

The model is regulated by the following equation:

$$\ln\left(1 - \frac{q_t}{q_e}\right) = -k_{fd}t,$$

where  $k_{fd}$  is the diffusion constant in the liquid film. To represent this model, on the abscissa axis, the value of the time  $t$  considered and, on the ordinate axis, the value of the  $\ln\left(1 - \frac{q_t}{q_e}\right)$  are reported [59]. The linear regression analysis allows to verify if the model fits the data and the diffusion constant is calculated. This model is generally observed in the event that the slow step of the adsorption process is the diffusion of the adsorbed into the film of stagnant liquid formed near the surface of the adsorbent.

#### 1.5.2.4 Intraparticle diffusion model

The model is regulated by the following equation:

$$q_t = k_{dif}t^{\frac{1}{2}} + C,$$

where  $k_{dif}$  is the intra-particle diffusion constant and  $C$  is the intercept of the straight line that represents the trend line of the graph. Reporting on the abscissa axis, the value of time  $t^{1/2}$  and, on the ordinate axis, the value of the adsorption capacity  $q_t$  the intraparticle diffusion constant can be obtained after the linear regression analysis if the model fits the experimental data [57]. This model is generally observed if the slowest step of the adsorption process is the diffusion of the adsorbed into the pores of the adsorbent.

#### 1.5.2.5 Elovich model

The model is regulated by the following equation:

$$q_t = \frac{1}{\beta} \ln(\alpha\beta) + \frac{1}{\beta} \ln(t)$$

Where  $\alpha$  and  $\beta$  are the initial adsorption rate of the Elovich equation and the desorption constant related to the extent of surface coverage and activation energy constant for chemisorption ( $\text{mg g}^{-1} \text{ min}^{-1}$ ) ( $\text{g mg}^{-1}$ ),  $t$  is the time and  $q_t$  is the adsorption capacity at the time  $t$ . By reporting on the graph, the adsorption capacity versus the time it is possible to evaluate if the model fits the experimental data by doing the linear regression analysis. From the model it is possible to evaluate  $\alpha$  and  $\beta$ . This model is generally observed in the event that the slow step of the adsorption process is the chemical interaction between adsorbent and adsorbed, the surface of which however is not homogeneous.

### 1.5.3 Isothermal adsorption model

The amount of adsorbate that can be absorbed by an adsorbent material is a function of both the characteristics and the concentration of the adsorbate and the temperature. Usually the quantity of adsorbed material is determined as a function of the concentration at constant temperature; what results is called the adsorption isotherm [52]. It represents the variation of the adsorption capacity with respect to the concentration of solute in the fluid to be treated and is developed by placing a variable concentration of contaminant in a fixed volume of liquid containing the adsorbent in a known quantity, for a certain period of time. At the end of the time foreseen for this test, the quantity of adsorbate that remains in solution is measured, at the variation of the initial concentration values of the considered contaminant and it is reported on a graph according to the adsorption capacity. A favorable isotherm is obtained when these have downward concavities, unfavorable isotherms when they have upward concavities and linear isotherms when the mass of solute varies linearly with the mass of adsorbent. Furthermore, there is irreversible adsorption isotherms when such strong bonds are established between adsorbent and adsorbed that it is impossible to reverse the adsorption operation by treating the bed with fresh fluid (regeneration). In this case, the desorption cycle would highlight no adsorbate release after the adsorption cycle. Normally, irreversible isotherms are obtained in the case of strong chemical adsorption. In the figure 3 the different adsorption isotherm previously described are reported.

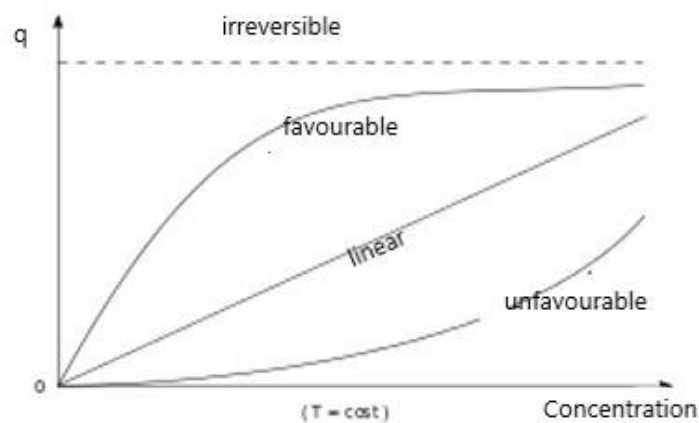


***Fig.3 Representation of favourable, linear, unfavourable and irreversible isothermal adsorption.***

A further classification of the isothermal adsorption exists and five different categories of isothermal adsorption are categorized. They can involve favourable, unfavourable or both the

previous type of isothermal adsorption. The figure 4 reports the further different type of isothermal curves. The categories are listed here:

- Type I: indicate favorable adsorption, have a downward concavity (favourable), are characteristics of microporous materials and typical of single-layer coatings of the adsorbent surface;
- Type II: they have an inflection point that indicates the beginning of the multilayer coating of the adsorbent surface and are typical of macroporous materials;
- Type III: indicate an unfavorable adsorption, typical of systems with weak interactions;
- Type IV: they have an inflection point which indicates the beginning of the monolayer coating of the adsorbent surface and are typical of mesoporous materials;
- Type V: like type III, they are typical of systems with weak interactions.

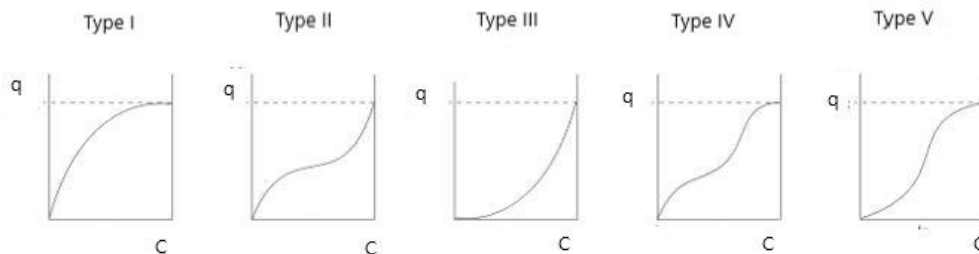


**Fig.4 Schematic representation of type I, II, III, IV and V isothermal adsorption.**

### 1.5.3.1 Langmuir isothermal adsorption

The Langmuir isotherm, typical of single-layer adsorption on a homogeneous surface, was developed to evaluate the absorption of gas on solids and is based on the following assumptions [60]:

- the adsorption energy is constant in all sites and the surface is uniform;
- the adsorbed-adsorbed interaction is considered negligible compared to the adsorbed-adsorbent interaction;
- adsorption cannot proceed beyond the coating of a single layer;
- adsorption is reversible.

In solid-liquid systems, the model is regulated by the following equation:

$$q_e = \frac{q_m k_L C_e}{1 + k_L C_e}$$



$q_e$  is the quantity of solute adsorbed per unit of mass of adsorbent ( $\text{mg g}^{-1}$ ),  $q_m$  is the solid phase concentration corresponding to all available sites that have been occupied or the maximum adsorption ( $\text{mg g}^{-1}$ ),  $C_e$  is concentration in equilibrium ( $\text{mg L}^{-1}$ ),  $k_L$  is associated with the adsorbent / adsorbed affinity (Langmuir constant,  $\text{L mg}^{-1}$ ). The previous equation can be rewritten in the following linear form:

$$\frac{C_e}{q_e} = \frac{1}{q_m K_L} + \frac{C_e}{q_m}$$

By reporting on the graph the ratio  $\frac{C_e}{q_e}$  vs the  $C_e$  and by doing a linear regression analysis it is possible to verify if the system respect this model and eventually evaluate the maximum adsorption capacity ( $q_m$ ), Langmuir constant and it is also possible evaluate if the adsorption is favourable, unfavourable or linear by calculating the parameter  $R$  as following [57]:

$$R_L = \frac{1}{1 + K_L C_0}$$

Where  $C_0$  is the initial concentration. The process resulted to be irreversible when  $R_L$  is equal to 0, linear when  $R_L$  is equal to 1, unfavourable when  $R_L > 1$  and favourable when  $0 < R_L < 1$ .

### 1.5.3.2 Freundlich isothermal adsorption

Freundlich's isotherm, typical of multilayer adsorption on a heterogeneous surface, is used very commonly to describe the adsorption characteristics of the adsorbent used in wastewater treatments [24]. Empirically obtained in 1912, the Freundlich isotherm is defined by the following equation:

$$q = K_f C_e^{1/n}$$

Where  $q$  is the adsorption capacity ( $\text{mg g}^{-1}$ ),  $K_f$  is the Freundlich constant ( $\text{L mg}^{-1}$ )<sup>1/n</sup> and it approximates the maximum adsorption capacity,  $C_e$  is the equilibrium concentration ( $\text{mg L}^{-1}$ ). The parameter  $1/n$  is an indicator of the strength of the adsorption. Furthermore, it is  $<1$  when the adsorption is “normal” and  $>1$  when the adsorption is cooperative. The ratio  $1/n$  indicates also the heterogeneity of the surface of the adsorbent material (an increase of that value is normally related to the increase of homogeneity). The equation can be written in the following linear form:

$$\ln(q) = \ln K_f + \frac{1}{n} \ln(C_e)$$

By reporting on the graph the  $\ln(q)$  vs the  $\ln(C_e)$  and linear regression analysis it is possible to evaluate if the system respect the model and evaluate the Freundlich constant and the ratio  $1/n$ .

### 1.5.3.3 Dubinin-Radushkevich isothermal adsorption

The Dubinin-Radushkevich isotherm is an empirical model initially conceived for the adsorption of subcritical vapors on micropores following a pore filling mechanism. The model is regulated by the following linear equation [57]:

$$\ln q_e = \ln q_m - \beta \varepsilon^2$$

$$\varepsilon = RT \ln \left( 1 + \frac{1}{C_e} \right)$$

$$E = \frac{1}{-\sqrt{2\beta}}$$

where  $q_e$  is the adsorption capacity ( $\text{mg g}^{-1}$ ),  $q_m$  is the theoretical maximum adsorption capacity ( $\text{mg g}^{-1}$ ),  $C_e$  is the concentration of solute at equilibrium,  $\beta$  is the constant associated with the adsorption energy ( $\text{mol}^2 \text{J}^{-2}$ ),  $R$  is the universal gas constant,  $T$  is the temperature expressed as Kelvin and  $E$  is related to the free energy ( $\text{kJ mol}^{-1}$ ). By plotting  $\ln(q_e)$  vs  $\varepsilon^2$  and by doing the linear regression analysis it is possible to verify if the system respects the model and evaluate the theoretical maximum adsorption capacity and the free energy of the process. One of the unique features of the Dubinin-Radushkevich isothermal model lies in the fact that it depends on the temperature: when the adsorption data at different temperatures are reported on a graph as a function of the logarithm of the quantity adsorbed in relation to the square of the energy potential, all data deemed suitable will be on the same curve, called the characteristic curve [54]. This model is typical of adsorption on heterogeneous surfaces where the adsorbed molecules generate steric hindrance for those entering the pores.

### 1.5.3.4 Temkin isothermal adsorption

The model is typical for single-layer adsorption where the adsorbent / adsorbed affinity decreases linearly with the increase of the covered adsorbent surface (heterogeneous surface). The model is regulated by the following equation[61, 62]:

$$q_e = B_1 \ln A + B_1 \ln C_e$$

where  $A$  is the equilibrium binding constant ( $\text{L g}^{-1}$ ),  $B_1$  is related to the heat of adsorption ( $\text{J mol}^{-1}$ ),  $q_e$  is the adsorption capacity at the equilibrium ( $\text{mg g}^{-1}$ ) and  $C_e$  is the equilibrium

concentration ( $\text{mg L}^{-1}$ ). By plotting  $q_e$  vs  $C_e$  and by doing the linear regression analysis it is possible to evaluate if the system respects the model and eventually calculate A and B to estimate the binding constant and the heat of adsorption.

### 1.5.3.5 Adsorption on fixed-bed column

Adsorption process can be conducted by filtration of contaminated water through a fixed-bed column of an adsorbent material. The figure 5 is a schematic representation of the process of adsorption by filtration on fixed bed at lab scale.

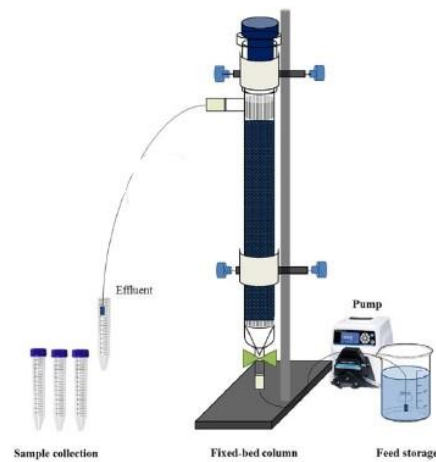


*Fig.5 Schematic representation of adsorption process on fixed-bed column.*

The mechanism of the adsorption is the same of the previous described but the models that regulate the process are different because the different setup of the system that involves different mechanism of diffusion from the liquid solution and the surface of the adsorbent. The models that regulate the process are described on the next section. The parameters that influence the adsorption capacity are the same of the process in batch but in this case also the flow rate, the section of the column and the fixed-bed height affect the adsorption capacity and the removal efficiency. In the figure 6 a detail on the mechanism of the adsorption on fixed-bed column is reported.

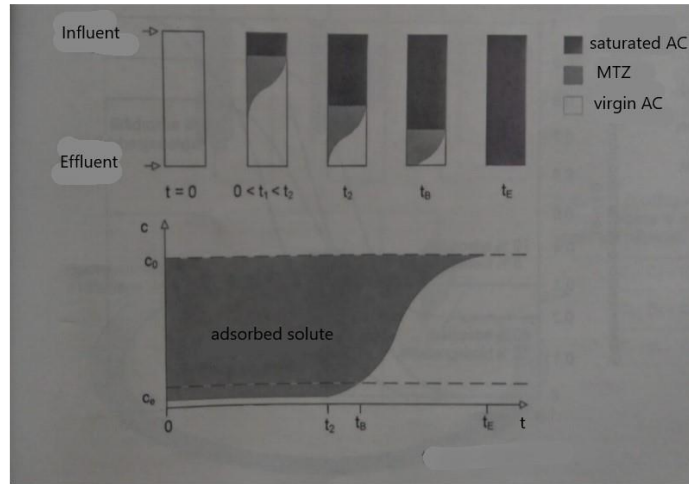


**Fig.6 Detail on the mechanism of adsorption on fixed-bed column.**

The figure 5 is useful to understand a detail on the adsorption process on fixed-bed column and the typical breakthrough curve of the adsorption process. At the time 0, the adsorbent material (reported as AC) is not saturated and adsorption occurs on all the surface of it. After a specified time of filtration, the adsorbent material started to be saturated and normally the saturation proceeds from the part of the filter closed to the influent to the part closed to the effluent. When saturation starts, a mass transferred zone (MTZ) exist that involves the transfer of adsorbate from saturated adsorbent material to the not saturated one. By proceeding with the filtration, MTZ go on until to reach the end of the filter. By considering the breakthrough curves of the filtration ( $C_{eff}/C_{inf}$ ) vs time, it is possible to observe a plateau closed to 0 when the MTZ does not reach the end of the filter. When MTZ reaches the end of the filter, the ratio starts to increase until to reach the value of 1 when all the adsorbent material is saturated and breakthrough point is reached. The described mechanism can explain the typical breakthrough curves obtained for the filtration system. The fixed bed is normally used for industrial application and for the ex-situ groundwater remediation. Before to conduct the industrial remediation, pilot scale tests are necessary to obtain the optimum contact time, bed depth, pretreatment requirement, breakthrough characteristic, reactor dimension and adsorbent dosage[63]. The model reported in the next section are useful to conduct the pilot tests.

### **1.5.3.6.1 Adams-Bohart model**

The Adams-Bohart model assumes that the adsorption rate is proportional to the residual capacity and the concentration of adsorbed micropollutants. Normally, this model can be applied well in the first stage of the adsorption when  $C_{eff}/C_{inf} < 0.15$ . The Adams-Bohart model

used for the description of the initial part of the breakthrough curve is expressed by the following equation:

$$\frac{C_{eff}}{C_{inf}} = e^{(KC_{inf}t - KN_0 \frac{Z}{F})}$$

Where K is the kinetic constant ( L  $\mu\text{g}^{-1} \text{min}^{-1}$ ), t is the time (min),  $N_0$  is the saturation concentration (mass of adsorbate adsorbed for unit of volume of bed,  $\mu\text{g L}^{-1}$ ), Z is the bed depth of the column (cm) and F is the linear velocity (cm  $\text{min}^{-1}$ ). By plotting the natural logarithm of  $C_{eff}/C_{inf}$  versus the time is possible to obtain the value of the kinetic constant and saturation concentration when bed depth and column section area are already known. After the determination of K and  $N_0$ , evaluation of reactor dimension when done. The previous equation can be transformed in the following equation:

$$\ln \frac{C_{eff}}{C_{inf}} = KC_{inf}t - KN_0 \frac{Z}{F}$$

If the breakthrough point is reached, the value of dependent variable of the previous equation is zero, therefore previous equation can be arranged in the following equation:

$$KN_0 \frac{Z}{F} = KC_{inf}t$$

Equation can be rearranged in the following equation:

$$\frac{Z}{tF} = \frac{C_{inf}}{N_0}$$

By programming an excel sheet, it is possible evaluate one of variable Z, t or F by fixing all the other parameters. In this work, F was evaluated by fixing Z and assuming to reach the breakthrough in one day by treating 10000 liter of contaminated water (flow rate 10000 liter for day). After evaluation of F, surface area of the reactor was calculated by the following equation:

$$\text{surface area reactor (s)} = \frac{\text{flow rate}}{F}$$

By assuming to use a circular reactor, diameter of it can be calculated by using the equation to calculate surface of circle.[64, 65]

### 1.5.3.6.2 Thomas model

The Thomas model is one of the most general and used methods in column performance theory. The model assumes Langmuir kinetics of adsorption–desorption and no axial dispersion is

derived with the adsorption that the rate driving force obeys second-order reversible reaction kinetics. By using this model, it is possible to evaluate the adsorption capacity of the system. The linear form of the model is regulated by the following equation.

$$\ln\left(\frac{C_{inf}}{C_{eff}} - 1\right) = k_{Th} \cdot q_e \cdot \frac{x}{v} - k_{Th} \cdot C_{inf} \cdot t \quad (10)$$

Where  $k_{Th}$  is the Thomas constant rate ( $\mu\text{g}^{-1} \text{L min}^{-1}$ ),  $q_e$  is the adsorption capacity of the system ( $\mu\text{g g}^{-1}$ ),  $x$  is the amount of the adsorbent material (g) and  $v$  is the flow rate ( $\text{L min}^{-1}$ ). From the Thomas model, after the calculation of kinetics constant and theoretical adsorption capacity, the necessary amount of adsorbent material was estimated by fixing the initial concentration of wastewater, the breakthrough concentration, the flowrate and the time to reach the breakthrough. After the evaluation of the mass of adsorbent material, it is possible to obtain information on the dimension of the reactor by considering the density of the adsorbent. [64, 65]

#### 1.5.4 Conventional adsorbent material

The main characteristics required for a good adsorbent are:

- a porous structure that provides a high surface area value;
- a rather short time to reach balance, so that contaminants can be removed quickly.

Typical materials used in the adsorption process are listed here.

- silica gel based materials: it is the term commonly used for colloidal silica (a polymer of silicon dioxide), when it is used for its dehydrating and adsorbent properties. The colloidal suspension, obtained by acidifying a sodium silicate solution, provides a white, granular, porous and amorphous solid, with a particle size ranging from a few millimeters to a few microns, also called silica gel. Silica gel has the characteristic of being an excellent dehydrator and is therefore used as a desiccant and for local humidity control. Although its action is called "desiccant", in reality the chemical-physical process with which water vapor is removed from the air consists of an adsorption operation: the water vapor molecules bind to the surface of the silica gel, which it is intended not only as an external surface, but also as a whole surface. The silica gel, in fact, has a considerable porosity, and this translates into a greater total area available for the exchange of matter, or rather a fairly high speed of the dehumidification process,

- activated alumina: it is generally obtained by heating and dehydrating aluminum hydroxide. It belongs to the category of chemical alumina and is mainly used in adsorbents, water purifiers, catalysts and catalyst supports. The activated alumina has a selective adsorption power for gas, water vapor and some liquids. After the adsorption has been saturated, the water can be removed by heating to around 175-315 ° C. Adsorption and reactivation can be done multiple times. In addition to being used as a desiccant, activated alumina can also adsorb hydrogen, carbon dioxide, natural gas and other similar compounds,
- zeolites are silicates and constitute a family of minerals with a very open crystalline structure and interconnected channels. The zeolitic structure can be imagined as a set of SiO<sub>4</sub> and AlO<sub>4</sub> tetrahedra that bind together, according to simple geometric shapes, to form complex units such as chains, rings or cages. Zeolites represent a class of molecular sieves with a high selectivity with respect to silica or activated carbon and can be used for industrial, agricultural or wastewater purposes. In the industry field they are used to dried, purify and separate chemical substance thank their selectivity. Into the agriculture field they are added to the soil and used to release slowly water during drought period. Into wastewater purpose they are used to retain and neutralize selective molecules such as ammonium, heavy metals and various organic substances as well as adsorb odorous gases such as ammonia and hydrogen sulfide.
- activated carbons are materials mainly made up of amorphous carbon, with a highly porous structure and a high specific area. Thanks to this last feature, the activated carbons are able to retain many molecules of other substances inside, being able to accommodate them on its extensive internal surface area. They are known as material with high adsorbing capacities. They are used for several purpose, such as decoloration, industrial wastewater treatment, water purification, recovery of solvents and air treatment. The accumulation of substances on the surface of the activated carbon causes the gradual loss of the adsorption power until it is canceled. In this case, the spent activated carbon must be replaced or regenerated through a regeneration or reactivation process which causes the adsorbent properties to regain the carbon. Several processes are already developed to regenerate activated carbons. Chemical methods, or with chemical reagents that oxidize the adsorbed organic substances, or with solvents that cause their extraction. Steam or inert gas flow (typically nitrogen) at relatively high temperatures (150-220 ° C) for the desorption of adsorbed volatile organic compounds (VOCs) can be used. Biological regeneration processes are also available and thermal

processes (reactivation) are carried out by heating the material in controlled atmosphere rotating ovens (so as not to oxidize the coal) up to temperatures of 800-900 ° C, causing the pyrolysis of the adsorbed substances. The latter is the most effective even if it causes a partial loss of the treated carbon. [53]

### **1.5.5 Innovative adsorbent material: graphene-based material and expanded graphite**

Among the materials studied for the high adsorption capacity, in recent years attention has focused on a graphitic form of carbon, called graphene, composed of single layers of hybridized atoms in the  $sp^2$  form arranged hexagonally to form a nest structure two-dimensional honeycomb. This material is characterized by high rigidity, thermal conductivity, high electronic mobility, impermeability to gases, as well as low specific weight and high specific surface which make it a good adsorbent, especially for aromatic compounds in water treatment. There are different methods by which graphene is produced. One of the main concerns the mechanical exfoliation, based on the experiment conducted by Konstantin Novoselov and Andrei Geim, in which an adhesive is applied on a graphite crystal which captures several layers by means of a small pressure, and then folds up several times until obtain a single layer of graphene. Graphite is formed by several layers of carbon atoms, so it is possible to imagine it as multilayer of graphene. Other techniques concern liquid phase exfoliation, chemical vapor deposition, electrochemical exfoliation and chemical reduction of graphene oxide. Every technique gives characteristics to the material produced in particular in terms of purity, but also of yield, so the appropriate one must be evaluated based on the use for which the product is intended. One of the most used production processes is thermal exfoliation which has the advantage of being faster than the others, since, for high temperatures, it takes place in a few seconds. During the heating process, the functional groups connected to the graphite layers decompose and produce gases that create pressure between the adjacent layers; exfoliation occurs when it exceeds the Van der Waals attraction forces between the layers. Anyway, the graphene is obtained every time from graphite as raw material, that is subjected to different mechanism of expansion and exfoliation. When the expansion or exfoliation process is not able to ensure the formation of single layer of carbon atoms, expanded graphite is obtained (normally the product is called graphite when the number of layers is more than 5). Expanded graphite, like for the graphene, has different properties from the graphite and it normally has a higher surface area, electrical conductivity, mechanical strength and so on. Therefore, even if graphene is not obtained, expanded graphite ensures good potential adsorption capacity due to the increased surface area. Some industrial processes are developing to prepare expanded graphite



or graphene. In this work, a commercial material produced by industrial plasma-thermal expansion of graphite is used and its adsorption properties were characterized. Nowadays, graphitic materials and graphene adsorption properties are widely evaluated and compared with that of activated carbons. In the figure 7 the representation of graphitic and graphene-based material is reported. [66]

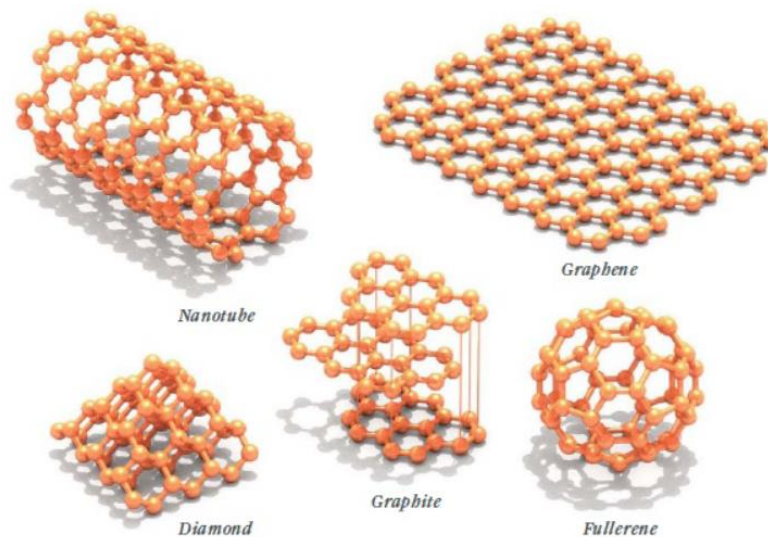


*Fig.7 Allotropic form of carbon.*

#### **1.4.6 Morphological modification of expanded graphite and graphene structure**

Normally, expanded graphite and graphene-based materials present a powder morphology and they are not soluble in the water. Often, their density is lower than the density of the water and they float on it. These characteristics could be a problem for some industrial environmental remediation or can represent a limit for the use of the material for different application from the simple batch adsorption. For example, filtration of the contaminated water on a fixed bed is not possible if the adsorbent material float on the water. Furthermore, the low-pressure injection of adsorbent material into contaminated groundwater to prepare a reactive barrier to confine the pollution is not possible if the adsorbent material is not soluble in water. To solve that problem and ensure the potential application of very low-density insoluble powder of graphitic or graphene-based material, morphological modification can be implemented.

##### **1.5.6.1 Transformation from powder to granular adsorbent material: physical entrapment**

This transformation can be achieved with encapsulation, which consists in preparing capsules composed of a core of encapsulated material covered by capsular formation material, also called encapsulation material [67]. Sodium alginate ( $\text{NaC}_6\text{H}_7\text{O}_6$ ) can be used for this purpose. It is the alginic acid salt obtained from the cell walls of brown algae, widely used in food and in the pharmaceutical industry. It is a non-toxic and biodegradable polymer, consisting of  $\alpha$ -L-guluronic acid (block G) and  $\beta$ -D-mannuronic acid (block M) chains arranged in blocks of homopolymer regions called MM and GG or alternating sequence MG [67]. In contact with water under stirring, it changes its consistency becoming gelatinous. The powder material is added to a sodium alginate solution and homogenized. This phase is followed by the cross-linking of the molecules of alginate through interaction with divalent ions, such as  $\text{Ca}^{2+}$ , obtained from calcium chloride ( $\text{CaCl}_2$ ) dissolved in water. The cross-linking step is conducted by dropping the solution of powder adsorbent material and sodium alginate into a solution of calcium chloride. The dropping addition ensures the formation of granular shape of the polymer. The powder adsorbent material remains entrapped into the polymer of calcium alginate formed after the cross-linking. After that, the material can be dried in the oven and a granular form of the adsorbent material is obtained. The process guarantees a change of the morphology and of the density of the material. The last parameter depends on the amount of sodium alginate used and a material with density higher of the water can be obtained and used as fixed bed filter. The figure 8 and 9 report a schematic representation of physical entrapment process.

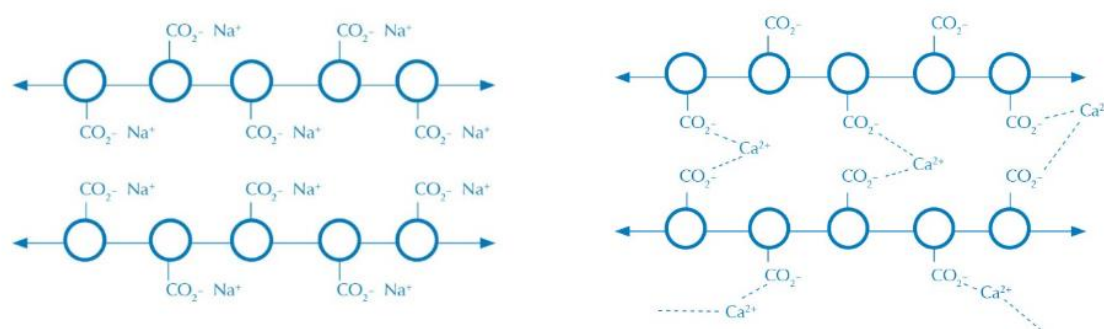


**Fig.8 Cross-linking mechanism of alginate chain. Alginates chains are represented by the arrow with spherical structure (monomer). On the monomers are also reported the carboxylic group involved into the ion exchange necessary for the cross-linking.**

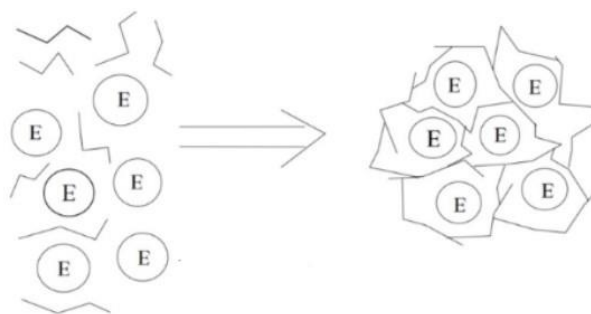


**Fig.9 Schematic representation of physical entrapment. *E* represent the powder adsorbent material and the chain represent the alginate chain.**

### 1.5.6.2 Transformation from insoluble to hydro soluble expanded graphite: sonication

Sonication was already described as one of the methods to produce graphene. Sonication is a term used to describe the use of acoustic waves (ultrasonic waves) for various purposes. Normally, sonification is carried out by using a sonifier that generates mechanical vibrations amplified by exploiting high frequency electric current produced by a generator. The ultrasounds are transmitted in a tank containing water. Sonic cavitation is the energetic effect that is basically exploited. Mechanical exfoliation is involved with the sonication, indeed, bubbles which collapsing on the surface of the graphite, generate compression waves, leading to the exfoliation. A secondary process can also occur as a lateral compression wave can be generated which is able to separate two adjacent layers of graphite with a cutting effect or through a "wedge" effect. The cutting effect could reduce the dimension of the particle of graphite until dimension that allows the formation of colloids or dispersion[32]. The figure 10 reports a schematic representation of process involved in sonication of expanded graphite.

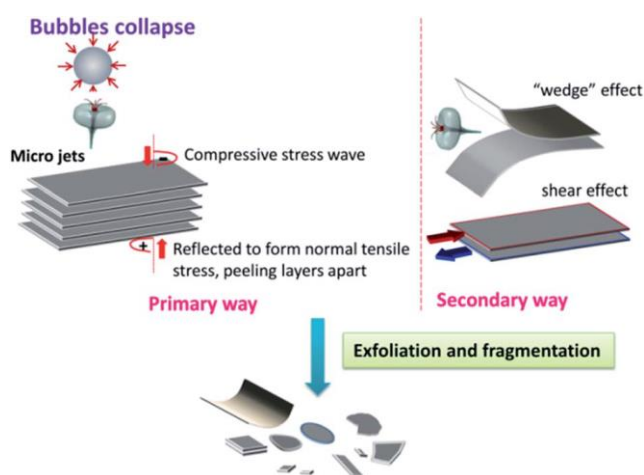


***Fig.10 Schematic representation of exfoliation and fragmentation involved in the sonication process.***

The exfoliation and the fragmentation involve a modification in the morphology of the material. The solid particles assume lower dimension and more exfoliation means lower interaction between layers of graphite. Normally, sonication could also oxidize the surface of the graphite and hydroxyl groups hydro soluble are formed on it. All this modification could increase the hydro solubility of the graphite and an adsorbent material with higher solubility can be obtained. The increase of solubility guarantees the increase of contact with the adsorbate (therefore higher adsorption capacity) and also the possibility to inject graphite into ground water to prepare a reactive barrier by using the low-pressure injection setup.

### **1.6 Material characterization analysis**

The characterization of the adsorbent material is an important step to have preliminary information on the chemical and physical characteristic of it to preliminary evaluate its potential adsorption properties. As reported in the adsorption section, the adsorption capacity depends on the properties of the adsorbent material. Therefore, by that analysis it is possible to check if the material is porous and have a good surface area, two necessary parameters to have a good adsorption. For example, another previously analysis of characterization useful to evaluate adsorption properties is the evaluation of the chemical functional group present on the surface of the adsorbent material. When several polar groups are detected on it, it is possible to conclude that the material will have a good affinity with polar adsorbate. Therefore, that adsorbent material will be chosen to remove that pollutants. The typical characterization analysis conducted on adsorbent material are scanning electron microscopy (SEM), transmission electron microscopy (TEM), X-ray diffraction analysis (XRD), Raman analysis, Infrared spectroscopy (FT-IR) and BET analysis. In the next section an overview on that analysis will be conducted.

#### **1.6.1 Scanning electron microscopy analysis (SEM)**

SEM is a versatile technique used in many industrial labs, as well as for research and development. Due to its high lateral resolution, its great depth of focus and its facility for X-ray microanalysis, SEM is used in materials science to elucidate the microscopic structure. The figure 11 represent schematically the scheme of work of a scanning electron microscope.

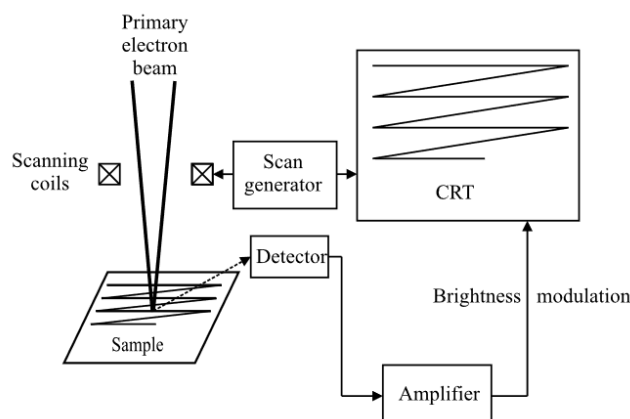


***Fig.11 Schematic representation of scanning electron microscope scheme***

The electronic source (normally tungsten filament) emits the primary electron beam focused by several lens present into the evacuated microscope column. The primary electron beam scans line by line over the surface of the sample and forms signals based on the interactions between the beam and the sample, which are electronically detected and amplified by suitable equipment. The useful effect of the interaction between sample and primary electron beam is the emission by the sample of secondary electron, generated by the energy transferred to the sample by the primary electron beam. The energy transferred and so on the energy of secondary electrons emitted depends on the depth of the sample. For these reason, higher energy of electrons emitted (higher current signal) correspond to thinner sample portion. Therefore, the electronic signal measured is transformed in an imagine by a computer. In this way an imagine with different scale of grey allows to have information on the morphological structure of the material by having a topography information on it. To ensure the interaction between primary electron beam and the sample the column of the microscope operate at vacuum condition to avoid interaction between electron and air. Another requisite for the analysis is the electrical conductivity of the sample, otherwise electron can interact with the first “layers” of the sample. When the material has not electrical conductivity, it can be coated by gold. The figure 12 reports the schematic representation between primary electron beam and sample. As reported previously, the secondary electrons are the result “useful” to obtain the topography information, but other effect are caused by the interaction of the sample and the primary electron beam. X-ray are also emitted and the wavelength of that X-ray depends on the nucleus, therefore an elemental analysis can be conducted for all the surface of the material to evidence the presence of different phase in the sample. Other effect of the interaction is the back scattering of the electron (BSE). The intensity of BSE depends on the atomic weight of the atom present in the sample. For this reason, BSE detection can be used to evidence contrast of phase present in the

sample. Auger emission is an emission present because an X-ray emission is present. It is caused by the transferring of electron into free core shell that caused a release of energy that provoke an emission of external shell electron. The energy of emitted electron depends on the atomic nucleus and it allows to have information on elemental analysis of the sample as reported for the X-ray emission. [68]

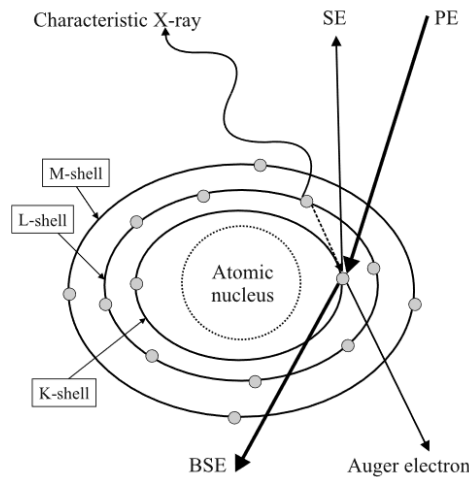


**Fig.12 Schematic representation of interaction between primary electron beam and sample**

### 1.6.2 Transmission electron microscopy

A transmission electron microscope (TEM) operates by accelerating a beam of electrons to sufficient energy so that when incident on a very thin sample (<100 nm), electrons are transmitted through it. Conventional TEMs work on the same principle as light microscopes but utilise a beam of electrons which travel in vacuum and originate from an electron gun source, rather than using a light source. The figure 13 reports the schematic representation of the TEM microscope. The main components consist of: the electron gun (source of electrons), gun alignment controls, condenser lenses (to collimate the beam), objective lens (to focus and initially magnify the image), apertures (to limit the diameter of the electron beam), intermediate lens, projective lens, sample holder, viewing screen and detectors to pick up the main and secondary signals. Atomic resolution images can be obtained because electron are used for the interaction with the mater and topography information are obtained because the intensity of electron that across the sample and reach the fluorescent screen depends on the depth of the sample. The TEM column operate in vacuum condition to avoid interference of the air on the electron way like the SEM. For the TEM analysis are required sample with light transparency. [69]

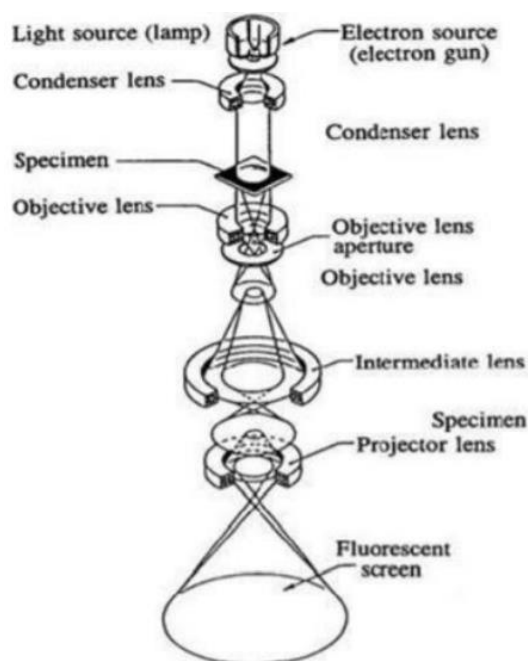


*Fig.13 Schematic representation of transmission electron microscope scheme*

### **1.6.3 Fourier-transformed Infrared spectroscopy (FT-IR) analysis**

IR spectroscopy provides valuable and practical information about the identification of both organic and inorganic materials. The information about a sample, given by each compound's IR spectrum, can be used to characterize unknown materials, as well as to determine molecular structures. An IR spectrum shows detector response and is sketched in absorbance or % transmittance (% T) versus IR frequency (normally reported in wavenumbers [ $\text{cm}^{-1}$ ]). A frequency of radiation that interacts with the sample produces an absorption band that is characteristic of the energy required for a particular molecular group. The collective position and pattern of these absorption bands designate the combination of molecular groups found in any specific compound. The energy of the radiation is transferred to the sample and generate a vibrational transition of the bond between the atoms. Every functional group has typical band of absorbance depending on its structure. Therefore, the frequency of the absorbance is typical for a specific functional group. In this way, by evaluating which band of absorbance the material present, it is possible to establish the functional group that characterize the structure of the sample. To manage the analysis, the solid sample is mixed to KBr powder (it does not absorb IR radiation) and pellets are prepared and inserted in the sampler, which has a window that allows the IR radiation through the sample. Therefore, the sample is crossed by all the IR radiation (IR band is into the range 700 nm – 1 mm) in the same moment and the intensities of

the radiation after the interaction with the sample is measured. Thanks to elaboration of software the Fourier transformation can be applied and the IR spectrum is obtained very fast. The ratio between the intensity of the radiation after the interaction and before the interaction represent the absorbance and it is measured for all the IR spectrum. During the preparation of the sample as KBr pellets it is important to avoid having trace of humidity to have in the spectrum the typical large and intense band of water adsorption. In the figure 14 the schematic representation of FT-IR spectrophotometer is reported. The figure 15 shows the sampler for solid materials. [70]

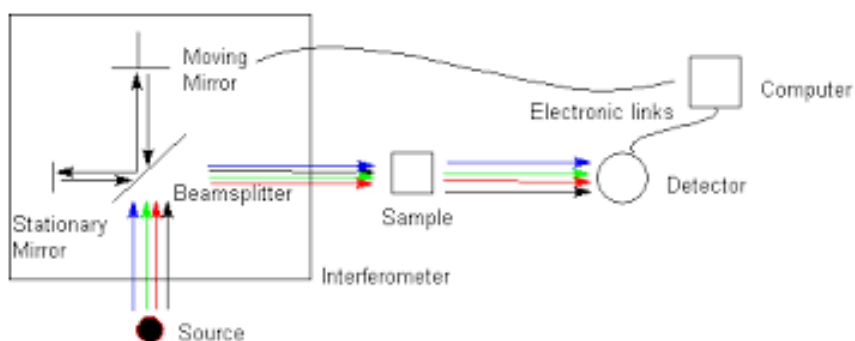


***Fig.14 Schematic representation of FT-IR spectrophotometer.***



***Fig.15 Sampler for solid material. KBr plus sample pellets is fixed into the IR transparent window.***

#### **1.6.4 X-ray diffraction (XRD) analysis**

X-ray powder diffraction (XRD) is a rapid analytical technique used for phase identification of a crystalline material and can provide information on unit cell dimensions. The analysed material is finely ground, homogenized, and average bulk composition is determined. X-ray diffraction is based on constructive interference of monochromatic X-rays and a crystalline



sample. These X-rays are generated by a cathode ray tube, filtered to produce monochromatic radiation, collimated to concentrate, and directed toward the sample. When the Bragg's Law ( $n\lambda=2d\sin\theta$ ) is respected the interaction of the incident rays with the sample produces constructive interference and a diffracted ray. These diffracted X-rays are then detected, processed and counted. Conversion of the diffraction peaks to d-spacings allows identification of the mineral because each mineral has a set of unique d-spacings. The figure 16 and 17 reports the schematic representation of X-ray diffractometer scheme and schematic visualization of Bragg's law and X-ray diffraction. [71]

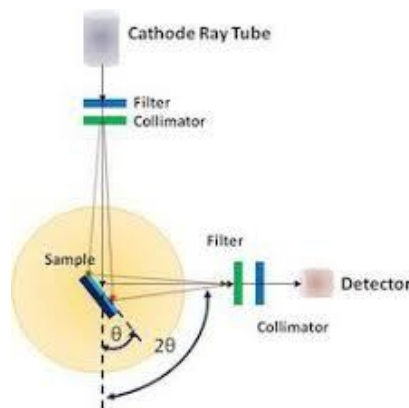


**Fig.16 Schematic representation of X-ray diffractometer.**

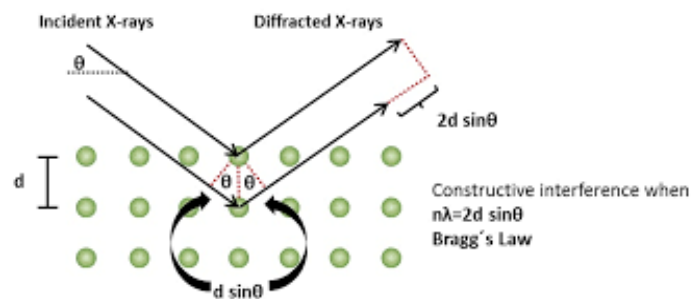


**Fig.17 Schematic visualization of Bragg's law and X-ray diffraction.**

### 1.6.5 Raman spectroscopy

Raman Spectroscopy is a non-destructive chemical analysis technique which provides detailed information about chemical structure, phase and polymorphy, crystallinity and molecular interactions. It is based upon the interaction of light with the chemical bonds within a material. It is a light scattering technique, whereby a molecule scatters incident light from a high intensity laser light source. Most of the scattered light is at the same wavelength as the laser source and does not provide useful information (Rayleigh Scatter). However, a small amount of light (typically 0.0000001%) is scattered at different wavelengths, which depend on the chemical

structure of the analyte (Raman Scatter). A Raman spectrum features a number of peaks, showing the intensity and wavelength position of the Raman scattered light. Each peak corresponds to a specific molecular bond vibration, such as C-C, C=C, N-O, C-H etc., and groups of bonds such as benzene ring breathing mode, polymer chain vibrations etc. As reported for the FT-IR analysis, the interaction between light and the sample involves vibrational energy transition for Raman analysis too. The incident photon brings the system from the vibrational state  $v = 0$  (fundamental level) to a virtual level placed at a higher energy equal to  $E=hv_0$ . From this virtual state the system can relax by returning to the same vibrational level  $v = 0$  and a Rayleigh scattering is obtained or relax on the first excited vibrational level  $v = 1$  giving rise to the Raman scattering. The energy difference between the higher energy level equal to  $E=hv_0$  and the excited vibration level  $v=1$  depends on the type of bond, crystallinity, phase and molecular interaction of the sample, therefore typical Raman spectrum (intensity of Raman scattering light vs wavelength) is obtained for every different compound. The Raman analysis offers the advantage to manage analysis microanalysis by coupling the typical Raman spectrometer with an optical microscope. By the coupling, the laser light incident on the sample can be directed on specific portions of the sample identified by the operator. In this way, it is possible to analyze different portions of the sample and evaluate difference in chemical structure, phase and polymorphy, crystallinity and molecular interactions present on the sample. The figure 18 shows the schematic representation of the light interaction that regulates the Raman spectroscopy. The figure 19 reports the schematic representation of the vibrational transition involved into the Raman spectroscopy. [72]

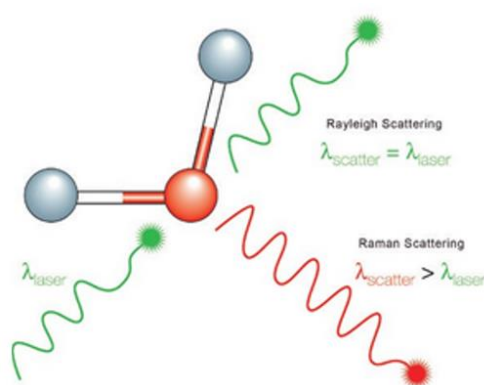


***Fig. 18 Schematic representation of the light interaction involved into the Raman spectroscopy.***

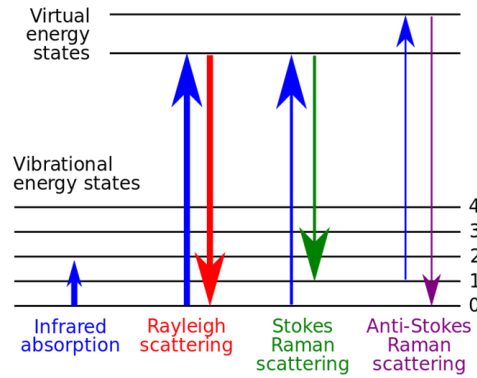


**Fig. 19 Schematic representation of the vibration transition involved into the Raman spectroscopy.**

### 1.6.6 Brunauer-Emmett-Teller (BET) analysis

BET theory explains the physical adsorption of gas molecule on a solid surface and represents the basis for the analysis technique for the measurement of the specific surface area of materials. The BET theory applies to systems of multilayer adsorption and utilizes gases that do not chemically react with material surfaces as adsorbates to quantify specific surface area. Normally the gas used for this purpose is the N<sub>2</sub> at the boiling temperature (77 K). The BET theory is based on an extension of the Langmuir theory to multilayer adsorption by considering the following hypothesis:

- gas molecules only interact with adjacent layers;
- gas molecules physically adsorb on a solid in layers infinitely;
- the Langmuir theory can be applied to each layer;
- the enthalpy of adsorption for the first layer is constant and greater than the second (and higher);
- the enthalpy of adsorption for the second (and higher) layers is the same as the enthalpy of liquefaction.

The equation that regulates the BET theory is the following:

$$\frac{1}{v\left[\frac{p_0}{p} - 1\right]} = \frac{c - 1}{v_m c} \left(\frac{p}{p_0}\right) + \frac{1}{v_m c}$$

Where  $\frac{p}{p_0}$  is the relative pressure of the gas in the adsorption system,  $v$  is the weight of gas adsorbed,  $v_m$  is the weight of adsorbate as monolayer and  $c$  is the BET constant. By the linear

plotting of  $\frac{1}{v[\frac{p_0}{p}-1]}$  vs  $\frac{p}{p_0}$ , the slope  $\frac{c-1}{v_m c}$  and the intercept  $\frac{1}{v_m c}$  can be obtained. From the slope and the intercept, the  $v_m$  can be obtained from the following equation:

$$v_m = \frac{1}{\text{slope} + \text{intercept}}$$

Therefore, total surface area can be obtained by the following equation:

$$S_t = \frac{v_m N A_{cs}}{M}$$

Where  $S_t$  is the total surface,  $N$  is the Avogadro's number,  $A_{cs}$  is the adsorbate cross sectional area (16.2 Å for nitrogen) and  $M$  is the molecular weight of the adsorbate. Specific surface area is then calculated by the following equation:

$$S = \frac{S_t}{w}$$

Where  $S$  is the specific surface area and  $w$  is the weight of the sample. For this reason, by considering the practical aspect, the mass of adsorbed gas is evaluated at different relative pressure of the gas and the data analysis is conducted by considering the previous equation reported. Other parameters can be calculated like the pore volumes. [73]

## 1.7 Analytical methods

During the experimental procedures, different chemical analysis was conducted to evaluate the concentration of different pollutants in the water before and after the adsorption. The chemical analysis conducted were UV-vis spectrophotometry, gas-chromatography analysis (GC) with the barrier ionization discharge detector (GC-BID) and mass spectrometer detector (GC-MS).

### 1.7.1 UV-vis spectrophotometric analysis

Ultraviolet and visible light (UV-vis) spectrophotometry is one of the faster and easier chemical diagnostic tools used for the detection and quantification of some substances into the water. The substances that can be analysed are all the compounds with the "capacity" to absorb the UV-vis light or they can be transformed in compounds able to. When the UV-vis light interacts with the sample, the energy of photon is transferred to promote an electron transition from the fundamental levels to excited levels. The frequency of absorbance is characteristic for every molecules or chromophore groups and the intensities of adsorption depends on the

concentration of the molecules into the solution. The absorbance of UV-vis light is regulated by the Lambert-Beer equation:

$$A = \epsilon bC$$

Where  $A$  is the absorbance (intensity),  $\epsilon$  is the coefficient of absorbance ( $\text{L mol}^{-1} \text{ dm}^{-1}$ ),  $b$  is the optical length (cm) and  $C$  is the concentration ( $\text{mol L}^{-1}$ ). The coefficient  $\epsilon$  is depending by the frequency of the UV-vis light wavelength and it is different for every compounds. Before to move to the quantification analysis, the spectrum of the analysed molecules needs to be conducted to determine the wavelength which the maximum value of  $\epsilon$  is observed. This step is necessary to increase the limit of the detection of the method. After that step, quantitative analysis can be conducted by measuring the intensity of the absorbance. As can be observed by the previous equation, a linear relation between concentration and absorption intensity exists. Therefore, the quantitative analysis is normally conducted by using the calibration line method. The calibration line is evaluated and determined by measuring the absorbance of the analytes for different known concentration. In this way, when absorbance of solution with unknown concentration of analytes is measured, it can be easily related to the concentration by considering the calibration line. The figure 20 reports the schematic representation of UV-vis spectrophotometer scheme. [74]

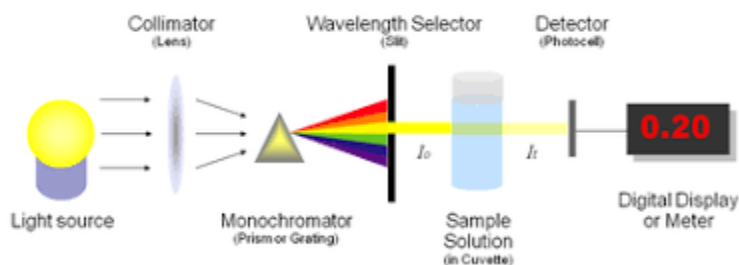


**Fig.20 Schematic representation of UV-vis spectrophotometer scheme.**

### 1.7.2 Gas-chromatography analysis

Chromatography is used to separate the mixture in its individual compounds. Chromatographical methods are classified as liquid (LC) or gas (GC) chromatography depending on the chemical nature of the mobile phase (either a gas or a liquid). The choice between either gas or liquid chromatography depends on the physico-chemical characteristics of the analyte. GC is normally used for the separation of mixtures that contain non-polar, (semi-)volatile compounds. LC is typically preferred for the analyses of polar and non-volatile substances. In the GC procedure, the components of a sample are dissolved in a solvent and

vaporized. The resulting vaporized sample is then mixed with the mobile phase, consisting of a chemically inert gas (typically helium, nitrogen or hydrogen). The mobile phase carries the molecules to the heated GC column, where separation takes place. After elution from the GC column, the separated compounds pass over a detector that generates a signal corresponding to the concentration of the compound. Each component elutes at a different time, also called the retention time of the component, because different interaction between each compound interact in different way with the fixed phase (GC-column). At the end of the analysis a chromatogram is obtained, where peaks are reported for different elution time. The area of the peaks is proportional to the concentration of the analytes. Therefore, before to conduct a quantitative analysis, the calibration line is evaluated by considering the same principles reported in the UV-vis spectroscopy analysis. Also, the elution times are previously evaluated by injecting and analysing standard sample of the analytes examined. The gas-chromatograph is constituted by an injector, composed of a closed and thermally stabilized box with a glass insert and a heating block. Two injection-mode exists: split and splitless mode. The split is used when the sample could saturate the response of the detector and going out of scale distort the result of the analysis due to its high concentration. The split dilutes the sample in the carrier gas, releases a part to the outside by means of a breather and after a certain period of time it enters the column. The splitless mode is used when the sample is diluted and all the sample enters into the column. The column is the other constituent of the chromatograph directly connected to the injector. The column is installed into a thermo-controlled oven to monitor and control the temperature of the column during the separation step. Two different types of columns exist and they are capillary and packed. The capillary columns are very thin fused silica open tubular columns with a diameter generally not greater than 0.53 millimeters and a length of not less than 10 meters coiled on a support metallic. The stationary phase is spread evenly on the internal surface of the column, where it forms a film of constant thickness which generally varies between 0.5 and 2.5  $\mu\text{m}$ . The packed columns are similar to those of traditional column chromatography; are tubes of Teflon, steel or deactivated borosilicate glass with a diameter of the order of one centimeter and with a length that can vary from one meter up to 10 meters, spiral or U-folded and filled with the stationary phase consisting of a support solid and a non-volatile liquid. At the end of the column a detector is installed to convert the presence of the analytes into an electric signal proportional to the concentration of the analytes. BID detector and mass spectroscopy detector were used during the works reported in that dissertation. BID is a highly sensitive device that creates ionization from a Helium-based dielectric barrier discharge plasma. A 17.7eV plasma is generated by applying a high voltage to a quartz dielectric chamber, in the presence of helium

at a relatively low temperature. The BID detector ionizes the analytes that reach the detector and they are directed on a cathode to generate an electric signal proportional to the concentration of the analytes. The mass detector coupled to the GC resulted to be one of the most advanced way to detect analytes. It allows to conduct a disruptive analysis and to obtain indication on the structure of the analytes. The principle of mass spectrometry is based on the ionization of chemical compounds, to produce charged molecules which are separated and measured according to their mass to charge ( $m/z$ ) ratio. After chromatographical separation, the compounds enter into the mass spectrometer through a GC interface. The target molecules undergo an ionization step. Electron-impact ionization (EI) is the most common method of ionization being used in gas chromatography. During this process, the molecules ( $M$ ) are bombarded by an electron beam with an energy of 70 eV, which produced a single charged molecular ion ( $M^+$ ). Most energetic ionization can be conducted to obtain information on molecular structure by considering its fragmentation. Normally, EI does not provoke fragmentation of the molecules and just the molecular ion is obtained and the ion with the molecular weight of the compounds is obtained and registered on the mass spectrum. If fragmentation is obtained, the different molecular fragments are separated as a function of time or space by a quadrupole analyser to distinguish the different  $m/z$  fragments. The chromatogram obtained by GC-MS analysis has the intensity of the electric signal registered for the different elution time, where the intensity reported is proportional to electric signal of a manually defined  $m/z$  ratio. As previously reported, the signal of analytes has a peak shape because distribution of the analytes on the column. Furthermore, when GC-MS chromatogram is obtained, for every elution time detected a mass spectrum is obtained, where are reported all the  $m/z$  ratio signal detected and their intensities. The figure 21 reports the schematic representation of a gas chromatograph. [75]

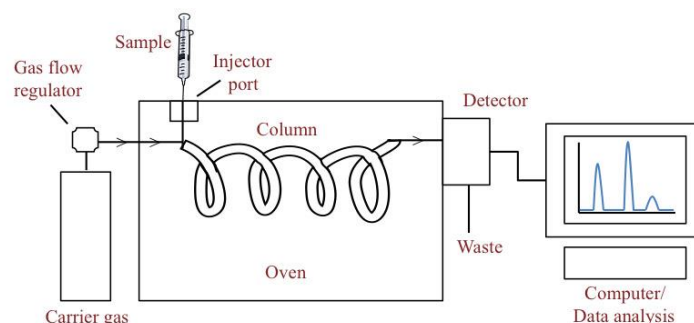


*Fig.21 Schematic representation of the gas chromatograph.*

## 1.8 Hydrocarbons pollutants

### **1.8.1 BTEX**

BTEX stands for benzene, toluene, ethylbenzene and xylene, aromatic hydrocarbons, which are part of the volatile organic compounds (VOCs) found in petroleum products. BTEXs are often reported as contaminants of soil and groundwater that occurs mainly in the vicinity of oil and natural gas refineries, service stations and other areas with underground storage tanks or raised tanks containing petrol or other petroleum products. The nomenclature of these hydrocarbons provides a prefix indicating the hydrogen substituent and the suffix 'benzene' so, for example, the common paraxylene is 1,4-dimethylbenzene since it has two methyl groups, in positions 1 and 4, which they replace two hydrogen atoms. [76]

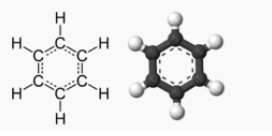
### **1.8.2 Benzene**

Benzene is a chemical compound in the form of a volatile, colorless and highly flammable liquid, with a characteristic odor, similar to that of petrol at room temperature and atmospheric pressure. Benzene is a monocyclic aromatic hydrocarbon having a brute formula  $C_6H_6$  and it is a natural constituent of petroleum. Until the 1920s, benzene was often used as an industrial solvent, especially for degreasing metals; subsequently, once its carcinogenic properties and its toxicity were discovered, it was gradually replaced with other less dangerous solvents. Until the fifties, benzene was almost entirely derived from the production of carbon coke in the steel industry, subsequently, it was also produced from oil, in order to meet the growing requests from plastic factories. Benzene is currently mainly produced by the petrochemical industries. Exposure to benzene can cause serious damage to human health: inhalation of a very high rate of benzene can lead to death; a five to ten minute exposure to a 2% benzene rate in the air (i.e. 20000 ppm) is sufficient to lead a man to death. Lower exposure rates can generate drowsiness, dizziness, tachycardia, headache, tremors, confusional state or loss of consciousness. The lethal dose by ingestion is about  $50 \div 500$  mg / kg (milligram of substance ingested compared to the individual's weight expressed in kilograms) and the ingestion of food or drinks containing high rates of benzene can trigger vomiting, gastric irritation, dizziness, sleepiness, convulsions, tachycardia, and, in severe cases, cause death. The most dangerous way to absorb benzene is by inhalation, since, once it arrives in the pulmonary alveoli, it is absorbed by the dense capillaries. Dermal absorption can only occur if benzene is present in the liquid state. The World Health Organization (WHO) and the International Cancer Research Agency (IARC) classify benzene as a group one carcinogen. WHO has not set an environmental standard for benzene concentrations, stating that there is no safe level of exposure. Many countries use an average



annual standard of  $3.6 \mu\text{g m}^{-3}$ . Its main chemical-physical characteristics are reported in Table 1. [77]

**Tab.1 Physical and chemical properties of benzene.**

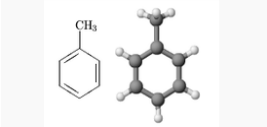
Parameters	
IUPAC name	Benzene
Molecular structure	$\text{C}_6\text{H}_6$
Density	$0.8765 \text{ g cm}^{-3}$
Solubility (in water)	$1.770 \text{ g L}^{-1}$
Structure	

### 1.8.3 Toluene

Toluene is a volatile and colorless liquid, with a strong characteristic odor similar to that of benzene and with the brute formula  $\text{C}_7\text{H}_8$ . It is an aromatic hydrocarbon, cheap, simple to produce and is widely used in industrial processes as a solvent, in place of benzene. It is classified as a harmful and highly flammable substance, however it is less toxic than benzene and has no mutagenic effects. Toluene, whose main characteristics are shown in Table 2, solidifies at  $-95^\circ \text{C}$ , boils at about  $111^\circ \text{C}$  and in the water it is almost insoluble ( $0.52 \text{ g L}^{-1}$ ), while it is miscible in any relationship with the carbon disulphide, ethanol and ethyl ether. It also dissolves well in acetone, chloroform and in most other organic solvents. Exposure, for short or long periods, to low concentrations of environmental toluene in humans causes the main toxic effects on the central nervous system. Typical symptoms include effects such as insomnia, manifestation of concentration difficulties, mental confusion, tiredness, intoxication states like ethanol intake, memory loss and appetite, these effects that vanish when exposure is stopped. Toluene concentrations can also lead to changes in hearing and visual perception of colors. [78]

**Tab.2 Physical and chemical properties of toluene.**

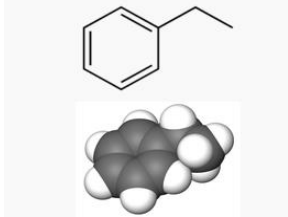
Parameters	
IUPAC name	Methylbenzene

Molecular structure	C <sub>7</sub> H <sub>8</sub>
Density	0.87 g cm <sup>-3</sup>
Solubility (in water)	0.52 g L <sup>-1</sup>
Structure	

### 1.8.4 Ethylbenzene

Ethylbenzene is an aromatic organic compound consisting of a benzene group to which an ethyl group is linked, as visible in Table 3, where its main chemical-physical characteristics and the structure are reported. It is used in the petrochemical industry as a reaction intermediate to obtain styrene, which in turn is used to produce polystyrene and ABS, which are plastic materials, but is also used as a solvent in inks, dyes and gasoline. It appears as a colorless liquid with a characteristic odor, similar to that of benzene. Ethylbenzene boils at 136°C, solidifies at -95°C and its solubility in water is equal to 0.15 g L<sup>-1</sup>. The effect on the human health of the ethylbenzene are the similar of toluene previously described. [79]

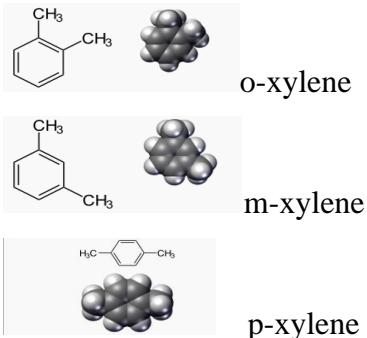
*Tab.3 Physical and chemical properties of ethylbenzene.*

<b>Parameters</b>	
IUPAC name	Ethylbenzene
Molecular structure	C <sub>8</sub> H <sub>10</sub>
Density	0.8665 g cm <sup>-3</sup>
Solubility (in water)	0.15 g L <sup>-1</sup>
Structure	

### 1.8.5 Xylenes

The term xylene refers to the mixture of three isomer compounds derived from benzene, called ortho-xylene, meta-xylene and para-xylene respectively. The prefixes *o*-, *m*- and *p*- indicate the positions where the methyl groups are linked to the benzene ring. In the IUPAC nomenclature, the isomer *o*- is called 1,2-dimethylbenzene, the *m*-1,3-dimethylbenzene and the *p*-1,4-dimethylbenzene. Xylene is a clear, oily, colorless, insoluble in water, flammable and harmful liquid. It is a product that is naturally found in oil, tar but can also form in forest fires and its chemical properties vary slightly from isomer to isomer. The chemical industries produce xylene from petroleum and it is used as a solvent in printing, for the processing of rubbers and leather. It is also used as a cleaning agent for steel, as a component and as a paint thinner. Another frequent use of xylene occurs in analysis laboratories that process histological samples. These samples, after being paraffin embedded, must be paraffin refined; since paraffin is a by-product of oil refining, it is 100% soluble with xylene which is precisely used to eliminate all traces of paraffin from histological sections. Exposure to this substance can cause effects ranging from headache, lack of coordination in the muscles, dizziness, confusion and mood changes to irritation of the skin, eyes and respiratory tract, difficulty in breathing, lung damage, timing of person's reaction slowed, memory loss, stomach pains, liver and kidney damage. In the case of very high levels of concentration, it can cause unconsciousness and sometimes even death. In the table 4 the main physical and chemical properties are reported. [80]

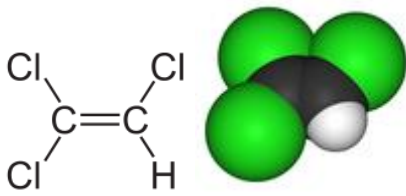
**Tab.4 Physical and chemical properties of xylenes.**

Parameters	
IUPAC name	Dimethylbenzene
Molecular structure	C <sub>8</sub> H <sub>10</sub>
Density	0.88 g cm <sup>-3</sup> (o-xylene) 0.86 g cm <sup>-3</sup> (m-xylene, p-xylene)
Solubility (in water)	Not soluble
Structure	 <p>o-xylene</p> <p>m-xylene</p> <p>p-xylene</p>

### 1.8.6 Trichloroethylene

Trichloroethylene has been widely used as solvent in different kind of industry and often was detected in surface/ground water, contaminated via direct discharge or leaching from disposal operation<sup>1</sup>, furthermore, EPA identified TCE as a priority environmental pollutant<sup>2</sup> and set 5 ppb for the maximum level of contamination of TCE. TCE contamination is a great problem because of its high solubility in water (1100 mg L<sup>-1</sup> at 25°C) and high resistance to biological degradation, therefore contaminated water remains polluted for a long time. The agency for the Toxic Substance and Disease Registry has reported that 852 of 1430 National Priority List sites in 1997 present TCE<sup>3</sup>. When inhaled, trichloroethylene produces central nervous system depression resulting in general anesthesia. Its high blood solubility results in a less desirable slower induction of anesthesia. At low concentrations it is relatively non-irritating to the respiratory tract. Research from Cancer bioassays performed by the National Cancer Institute showed that exposure to trichloroethylene is carcinogenic in animals, producing liver cancer in mice, and kidney cancer in rats. The National Toxicology Program's 11th Report on Carcinogens categorizes trichloroethylene as “reasonably anticipated to be a human carcinogen”, based on limited evidence of carcinogenicity from studies in humans and sufficient evidence of carcinogenicity from studies in experimental animals. In the table 5 the physical and chemical properties of trichloroethylene are highlighted. [81]

**Tab.5 Physical and chemical properties of trichloroethylene.**

Parameters	
IUPAC name	Trichloroethene
Molecular structure	C <sub>2</sub> HCl <sub>3</sub>
Density	1.46 g cm <sup>-3</sup>
Solubility (in water)	1.1 g L <sup>-1</sup>
Structure	

### 1.8.7 Methylene blue

Methylene blue is not very toxic, it generates some disease in human, such as vomiting, diarrhea, increasing of heart rate, shock, cyanosis, jaundice, quadriplegia and tissue necrosis<sup>s</sup>. Furthermore, it can adsorb other pollutants, such as heavy metals or suspended solids. It is normally used as dye for textile industries and it is detected in their wastewater. Because it properties to absorb the light and easily concentration evaluation, it is normally used for preliminary investigation and evaluation of adsorbent properties of new material. In the figure 22 the structure of methylene blue is reported. [82]

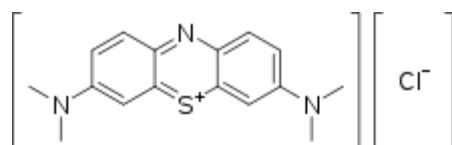


**Fig.22 Structure of methylene blue.**

### 1.9 Plasticizers

Plastic is currently one of the most practical and economical ways to hold food, sanitary products, cosmetics or other products. The development and extensive use of plastics as containers has led the packaging industry to significantly change the chemical composition of plastics in recent years. To this end, chemical additives are added to their composition to increase their malleability, brilliance and workability. Among these additives, the most commonly used are phthalates and bisphenol A (BPA). Phthalates (or phthalate esters, PAE) are compounds synthesized by the double esterification of 1,2 benzenedicarboxylic acid (phthalic acid) with linear or branched alcohols, starting from methanol or ethanol (C1-C2), up to isotridecanol (C13). Depending on the molecular weight they can be used in various industrial applications. Low molecular weight phthalates, such as diethylphthalate (DEP) and dibutylphthalate (DBP), have been used since 1930 in personal hygiene products (in the preparation of perfumes, shampoos, soaps, lotions, cosmetics and fabric softeners, or added as plasticizers of cellulose acetate), in the process industry (e.g. production of lacquers, paints, lubricating oils, adhesives, inks, insecticides, coatings) and in the pharmaceutical industry (in some drugs it is used to regulate the rate of release ). High molecular weight phthalates, such as bis (2-ethylhexyl) phthalate (DEHP), diisononyl phthalate (DINP) and di-n-octyl phthalate (DnOP) are mainly used as plasticizers in vinyl production, which is often used in products such as flooring. and wall coverings, toys, food packaging and medical devices. Plasticizer phthalates, which also include diisodecyl phthalate (DIDP), dimethyl phthalate (DMP), diethyl phthalate (DEP), dibutyl phthalate (DBP) and benzyl butyl phthalate (BBP), are used as

intermolecular lubricants which confer hardness, flexibility, malleability and elasticity. The chemical and physical properties vary with the structure, that is, with the length of the chain and branches. They are generally colorless, odorless and lipophilic and have a high boiling point and low vapor pressure, both parameters that influence their high stability and presence in the environment. Worldwide, up to 8 million tons of phthalates are produced annually, of which over 2 million are DEHP only. PAEs are molecules that are not covalently linked to the matrix and show a tendency to migrate, especially in case of mechanical or thermal stress, so they can be dispersed in the environment during their production, use or after disposal [83, 84]. Their potential for migration and leaching in the environment is a function of various parameters, including the pH, the time of contact, the temperature, the chemical structure and the lipophilia of the surrounding environment. Therefore, PAEs represent ubiquitous contaminants and decompose both with exposure to sunlight and with aerobic microbial activity; by affinity with the natural organic substance, they tend to absorb themselves to the soil, sediment and humus particles where they are also protected from sunlight. From an environmental point of view, PAEs have a duration (and therefore a permanence) of several hours in the atmosphere and months in the soil, while they can persist for years in the sediments; they can bioaccumulate in invertebrates, fish and plants, while in complex animals they are metabolized and excreted efficiently. The accumulation of PAE in human tissues can cause chronic intoxication causing serious damage to the liver and / or reproductive system. Exposure can arise from four main routes, namely ingestion (sources may be contamination of food during the preparation or packaging process, drugs and nutritional preparations, children's toys), inhalation (mainly DEP and DEHP, even if they show low volatility; they can come from medical devices, for example bags or tubes, or from dust present in closed environments, furniture, clothes, building materials, plastic components), intravenous (from PVC medical devices that transport fluids for intravenously as nutrients or blood; the migration of DEHP varies according to some parameters such as lipid content, temperature and duration of exposure) and dermal (mainly DEP with contamination through clothing, footwear, gloves, cosmetics, sunscreen, insecticides, products for hygiene, paints, toys). The toxicity of phthalates is still under study, however it has been shown that many types of them, such as DEHP, DBP, BBzP and various phthalate metabolites, are carcinogenic to the liver of rodents and teratogenic to other animals [83]. The working group of the International Agency for Research on Cancer (AIRC) classifies DEHP as a possible carcinogen for humans (group 2B) since toxic and carcinogenic effects have been found in rats in numerous target tissues such as liver and testicles. It has also been shown how phthalates affect children's neurodevelopment, decreasing

their readiness and creating attention deficit hyperactivity disorder among girls [84]. In the figure 23 is reported the general structure of phthalates. The group R and R' can be the same or different and it determine the name and properties of structure. For example, for R=R' and R=methyl, the compound will be dimethyl phthalate. [84]

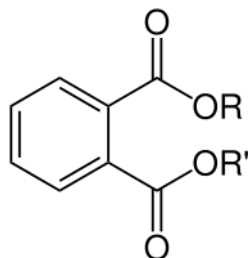


*Fig.23 General structure of phthalates*

### **1.10 Pharmaceuticals and personal care products (PPCPs)**

Pharmaceuticals and Personal Care Products (PPCPs) have increasingly been found in surface water and, even though they are normally present at very low concentrations, several scientific studies have proved their negative impact on aquatic life. Conventional wastewater treatment plants cannot completely remove PPCPs because of their high polarity and solubility in water. These characteristics represent the main challenge for the removal of PPCPs from water solution.

#### **1.10.1 Diclofenac**

Diclofenac sodium (DCF, fig. 24) is an analgesic drug included in the class of PPCPs, generally prescribed to treat inflammatory disorders because of its nonsteroidal anti-inflammatory potential. The DCF neutral form presents free acid groups (-COOH), whereas the anionic form presents deprotonated acid groups (-COO<sup>-</sup>). Chronic exposure to DCF generates hemodynamic changes and thyroid tumors in Humans<sup>2</sup>. Furthermore, negative effects have been observed on natural ecosystems, causing the death of several animal species. Particularly, Oaks et al. investigated on the death of a popular specie of vultures in South Asia, proving that eating carcasses of animals nursed with DCF may cause visceral gout in vultures, mainly due to the crystallization of their internal organs. DCF has largely been detected in both natural water and wastewater worldwide because of its common use in large quantities. [85, 86]

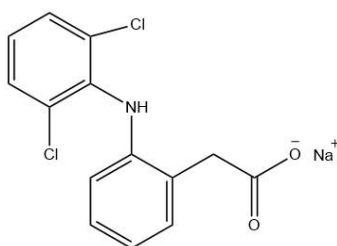


**Fig.24 Structure of diclofenac sodium salt.**

### 1.10.2 Carbamazepine

Carbamazepine (CBZ), sold under the trade name Tegretol among others, is an anticonvulsant medication used primarily in the treatment of epilepsy and neuropathic pain. Carbamazepine is typically used for the treatment of seizure disorders and neuropathic pain. It is used off-label as a second-line treatment for bipolar disorder and in combination with an antipsychotic in some cases of schizophrenia when treatment with a conventional antipsychotic alone has failed. Carbamazepine and its (bio-)transformation products have been detected in wastewater treatment plant effluent and in streams receiving treated wastewater. Field and laboratory studies have been conducted to understand the accumulation of carbamazepine in food plants grown in soil treated with sludge, which vary with respect to the concentrations of carbamazepine present in sludge and in the concentrations of sludge in the soil; taking into account only studies that used concentrations normally found, a 2014 review found that "the accumulation of carbamazepine into plants grown in soil amended with biosolids poses a *de minimis* risk to human health according to the approach." [84]. The structure of carbamazepine is reported in figure 25. Regarding the chemical point of view, it is a molecule with a tricyclic structure 6-7-6 of the class of imminestilbene. Due to its larger use it is often detected into water and it can affect the ecosystem and generates disease for human that use that water.

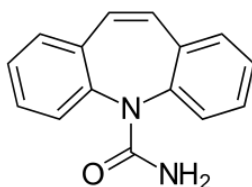


**Fig.25 Structure of carbamazepine.**

### 1.10.3 17- $\alpha$ ethinylestradiol

Ethinylestradiol is an estrogen medication which is used widely in birth control pills in combination with progestins. In the past, EE was widely used for various indications such as



the treatment of menopausal symptoms, gynecological disorders, and certain hormone-sensitive cancers. It is usually taken by mouth but is also used as a patch and vaginal ring. The general side effects of ethinylestradiol include breast tenderness and enlargement, headache, fluid retention, and nausea among others. In men, it can additionally cause breast development, feminization in general, hypogonadism, and sexual dysfunction. Rare but serious side effects include blood clots, liver damage, and cancer of the uterus. The figure 26 reports the structure of the 17- $\alpha$  ethinylestradiol. As reported for the previous compound, it is often detected into the water due to its large use and inability of WWTPs to remove it. It can affect the ecosystem and affect the human that drink or use that water for agricultural purpose. [86]

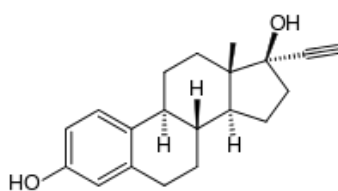


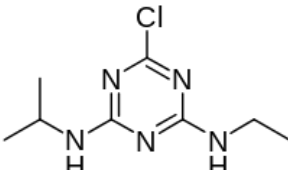
**Fig.26 Structure of 17- $\alpha$  ethinylestradiol.**

## **1.11 Pesticides and herbicides**

### **1.11.1 Atrazine**

Atrazine is a herbicide of the triazine class. It is used to prevent pre-emergence broadleaf weeds in crops such as corn and sugarcane and on turf, such as golf courses and residential lawns. As of 2001, atrazine was the most detected pesticide contaminating drinking water in the United States. Studies suggest it is an endocrine disruptor, an agent that can alter the natural hormonal system. Its use was banned in the European Union in 2004, when the EU found groundwater levels exceeding the limits set by regulators. Atrazine remains in soil for a matter of months (although in some soils can persist to at least 4 years) and can migrate from soil to groundwater; once in groundwater, it degrades slowly. It has been detected in groundwater at high levels in some regions of the U.S. where it is used on some crops and turf. Atrazine degrades in soil primarily by the action of microbes. The half-life of atrazine in soil ranges from 13 to 261 days. Atrazine's effects in humans and animals primarily involve the endocrine system. Studies suggest that atrazine is an endocrine disruptor that can cause hormone imbalance. The table 6 summarized the main physical and chemical properties. [87]

**Tab. 6 Physical and chemical properties of atrazine.**

<b>Parameters</b>	
IUPAC name	6-chloro- <i>N</i> <sup>2</sup> -ethyl- <i>N</i> <sup>4</sup> -(propan-2-yl)-1,3,5-triazine-2,4-diamine
Molecular structure	C <sub>8</sub> H <sub>14</sub> Cl <sub>3</sub> N <sub>5</sub>
Density	1.19 g cm <sup>-3</sup>
Solubility (in water)	70 mg L <sup>-1</sup>
Structure	

## Reference

- [1] Crimi, M.L., Taylor, J., 2007, Experimental Evaluation of Catalyzed Hydrogen Peroxide and Sodium Persulfate for Destruction of BTEX Contaminants, Soil and Sediment Contamination: An International Journal, 16, 29-45
- [2] Liang, C., Huang, C.-F., Chen, Y.-J, 2008 Potential for activated persulfate degradation of BTEX contamination, Water Research, 42, 4091-4100.
- [3] Kang, N., Hua, I., 2005, Enhanced chemical oxidation of aromatic hydrocarbons in soil systems, Chemosphere, 61, 909-922
- [4] Christofolletti Mazzeo, D.E., Levy, C.E., de Franceschi de Angelis, D., Marin-Morales, M.A., 2010, BTEX biodegradation by bacteria from effluents of petroleum refinery, Science of the Total Environment, 408, 4334-4340
- [5] Lovanh, N., Hunt, C.S., Alvarez, P.J.J., 2002, BTEX biodegradation by bacteria from effluents of petroleum refinery, Water Research, 36, 3739-3746
- [6] Khoadei, K., Nassery, H.R., Asadi, M.M., Mohammadzadeh, H., Mahmoodlu, M.G., 2017, BTEX biodegradation in contaminated groundwater using a novel strain (*Pseudomonas* sp. BTEX-30), International Biodeteration and Biodegradation, 116, 234-242
- [7] Caetano, M.O., Schneider, I.A.H., Gomes, L.P., Kieling, A.G., Miranda, L.A.S., 2017, A compact remediation system for the treatment of groundwater contaminated with BTEX and TPH, Environmental Technology, 38, 1408-1420

- [8] Nourmoradi, H., Nikaeen, N., Khiadani, M., 2012, Removal of benzene, toluene, ethylbenzene and xylene (BTEX) from aqueous solutions by montmorillonite modified with nonionic surfactant: Equilibrium, kinetic and thermodynamic study, *Chemical Engineering Journal*, 191, 341– 348
- [9] Azizi, A., Torabian, A., Moniri, E., Hassani, A.H., Panahi, A.H., 2016 Adsorption performance of modified graphene oxide nanoparticles for the removal of toluene, ethylbenzene, and xylenes from aqueous solution, *Desalination and Water Treatment*, 57, 28806-28821
- [10] Bhadra, B.N., Cho, K.H., Khan, N.A., Hong, D.Y., Jhung, S.H., 2015 Liquid -phase adsorption of aromatics over a metal-organicframework and activated carbon: effects of hydrophobicity /hydrophilicity of adsorbent and solvent polarity, *J. Phys. Chem. Lett.*, 119, 26620-26627.
- [11] Yu, Z., Peldszus, S., Huck, P.M., 2008. Adsorption characteristic of selected pharmaceuticals and an endocrine disrupting compound-naproxen, carbamazepine and nonylphenol-on activated carbon, *Water Res.*, 42, 2873-2882.
- [12] Wei, H., Deng, S., Huang, Q., Nie, Y., Wang, B., Huang, J., Yu, G., 2013. Regenerable granular carbon nanotubes/alumina hybrid adsorbent for diclofenac sodium and carbamazepine removal from aqueous solution, *Water Res.*, 47, 4139-4147.
- [13] Hu, X., Cheng, Z., 2015. Removal of diclofenac from aqueous solution with multi-walled carbon nanotubes modified by nitric acid, *Chin. J. Chem. Eng.*, 23, 1551-1556.
- [14] Jaurius, I.M., Matos, C.F., Saucier, C., Lima, E.C., Zarbin, A.J.G., Fagan, S.B., Machado, F.M., Zanella, I., 2016. Adsorption of sodium diclofenac on graphene: a combined experimental and theoretical study, *Phys. Chem. Chem. Phys.*, 18, 1526-1536.
- [15] Nam, S.W., Jung, C., Li, H., Yu, M., Flora, J.R.V., Boateng, L.K., Her, N., Zoh, K.D., Yoon, Y., 2015. Adsorption characteristic of diclofenac and sulphamethoxazole to graphene oxide in aqueous solution, *Chemosphere*, 136, 20-26.
- [16] T. Madrakiana, A. Afkhami, M. Ahmadi, H. Bagheri, Removal of some cationic dyes from aqueous solution using magnetic-modified multi-walled carbon nanotubes, *Journal of Hazardous Materials*, 2011, 196, 109-114.

- [17] L. Chen, A. Ramadan, L. Lu, W. Shao, F. Luo, J. Chen, Biosorption of Methylene Blue from Aqueous Solution Using Lawny Grass Modified with Citric Acid, *Journal of Chemical and Engineering Data*, 2011, 56, 3392-3399.
- [18] P. Sharma, M.R. Das, Removal of a Cationic Dye from Aqueous Solution Using Graphene Oxide Nanosheets: Investigation of Adsorption Parameters, *Journal of Chemical and Engineering data*, 2013, 58, 151-158.
- [19] P. Wang, M. Cao, C. Wang, Y. Ao, J. Hou, J. Qian, Kinetics and thermodynamics of adsorption of methylene blue by a magnetic graphene-carbon nanotube composite, *Applied Surface Science*, 2014, 290, 116-124.
- [20] Mohammed N., Grishkewich N., Waeijen H.A., Berry, R.M., Tam, K.C. (2016) Continuous flow adsorption of methylene blue by cellulose nanocrystal-alginate hydrogels beads in fixed bed columns. *Carbohydrate Polymers*, 136, 1194-1202
- [21] Jang, J., Lee, D.S. (2016) Enhanced adsorption of cesium on PVA-alginate encapsulated Prussian blue-graphene oxide hydrogel-beads in a fixed-bed column system. *Bioresource Technology*, 218, 294-300
- [22] Han, R., Ding, D., Xu, Y., Zou, W., Wang, Y., Li, Y., Zou, L. (2008) Use of rice husk for the adsorption of congo red from aqueous solution in column mode. *Bioresource Technology*, 99, 2938- 2946
- [23] Han, R., Wang, Y., Zhao, X., Wang, Y., Xie, F., Cheng, J., Tang, M. (2009) Adsorption of methylene blue by phoenix tree leaf powder in a fixed-bed column: experiments and prediction of breakthrough curves. *Desalination*, 245, 284-297
- [24] Lezehari, M., Baudu, M., Bouras, O., Basly, J.-P. (2012) Fixed-bed column studies of pentachlorophenol removal by use of alginate-encapsulated pillary clay microbeads. *Journal of Colloid and Interface Science*, 379, 101-106.
- [25] Kumar, A., Jena, H. M. (2016) Removal of methylene blue and phenol onto prepared activated carbon from Fox nutshell by chemical activation in batch and fixed-bed column. *Journal of Cleaner Production*, 137(20), 1246-1259.
- [26] Y. Wang, S. Pleasant, P. Jain, J. Powell, T. Townsend, Calcium carbonate -based permeable reactive barriers for iron and manganese groundwater remediation at landfills, *Waste Management*, 2016, 53, 128-135

- [27] Y. Liu, H. Mou, L. Chen, Z.A. Mirza, L. Liu, Cr(VI)-contaminated groundwater remediation with simulated permeable reactive barrier (PRB) filled with natural pyrite as reactive material: Environmental factors and effectiveness, *Journal of Hazardous Materials*, 2015, 298, 83-90
- [28] X. Zhao, W. Liu, Z. Cai, B. Han, T. Qian, D. Zhao, An overview of preparation and applications of stabilized zero-valent iron nanoparticles for soil and groundwater remediation, *Water Research* 2016, 100, 245-266
- [29] V.R. Vermeul, J.E. Szecsody, B.G. Fritz, M.D. Williams, R.C. Moore, J.S. Fruchter, An Injectable Apatite Permeable Reactive Barrier for In Situ <sup>90</sup>Sr Immobilization, *Groundwater Monitoring and Remediation*, 2014, 34, 28-41
- [30] El-Maiss, J., Cuccarese, M., Maerten, C., Lupattelli, P., Chiummineto, L., Funicello, M., Schaaf, P., Jierry, L., Boulmedais, F. (2018) Mussel-Inspired Electro-Cross-Linking of Enzymes for the Development of Biosensors. *Applied Materials and Interfaces*, 10, 22, 18574-18584.
- [31] M. Yi, Z. Shen, A review on mechanical exfoliation for the scalable production of graphene, *Journal of Materials Chemistry A*, 2015, 3, 11700-11715
- [32] T. Wang, S. Tan, C. Liang, Preparation and characterization of activated carbon from wood via microwave-induced ZnCl<sub>2</sub> activation, *Carbon*, 2009, 47, 1867-1885
- [33] R. Pietrzak, Sawdust pellets from coniferous species as adsorbent for NO<sub>2</sub> removal, *Bioresource Technology*, 2010, 101, 907-913
- [34] J.M.R. Rodriguez Arana, R.R. Mazzocco, Adsorption studies of methylene blue and phenol onto black stone cherries prepared by chemical activation, *Journal of Hazardous Materials*, 2010, 180, 656-661
- [35] Dilek, Production and characterization of activated carbon from sour cherry stones by zinc chloride, *Fuel*, 2014, 115, 804-811
- [36] Oki, T., Kanae, S., Global hydrological cycles and world water resources. *Freshwater Resources*, 2006, 313(5790), 1068-1072.
- [37] Kummu, M., Guillaume, J. H., A., De Moel, H., Eisner, S., Flörke, M., Porkka, M., Siebert, S. Veldkamp, T. I. E., Ward, P. J., The world's road to water scarcity: shortage and stress in the 20th century and pathways towards sustainability. *Nature*, 2016, 6, 38495.

- [38] Gude, V. G., Desalination and water reuse to address global water scarcity. *Reviews in Environmental Science and Bio/Technology*, 2017, 16, 591-609.
- [39] <https://www.oecd.org/env/indicators-modelling-outlooks/49844953.pdf>
- [40] J. Lemoalle, G. Magrin, Development of lake Chad-current situation and possible outcomes, IRD, 2014.
- [41] T. Carleton, S. Hsiang, Social and economic impact of climate, *Science*, 2016, 353, 6304.
- [42] F.N. Tubiello, L'impatto dei cambiamenti climatici su agricoltura e foreste, in *I cambiamenti climatici come problema globale*, Franco Angeli Editore, 2006.
- [43] Sophocleous, M., Global and regional water availability and demand: prospects for the future. *Natural Resources Research*, 2004, 13(2), 61-75.
- [44] WWAP, The United Nations World Water Development Report 2016: Water and Jobs, UNESCO, Paris (France), 2016.
- [45] Gosling, S. N., Arnell, N. W., A global assessment of the impact of climate change on water scarcity, *Climatic Change*, 2016, 134, 371-385.
- [46] Mekonnen, M. M., Hoekstra, A. Y., Four billion people facing severe water scarcity. *Science Advances*, 2016, 2(2), e1500323.
- [47] WWAP (United Nations World Water Assessment Programm)/UN-water, The United Nations World Water Development Report 2018: Nature-Based Solutions for Water, UNESCO (United Nations Educational Scientific and Cultural Organization), Paris (France), 2018.
- [48] OECD (Organization for Economic Co-operation and Development), *OECD Environmental Outlook to 2050: The Consequences of Inaction*, OECD Publishing, Paris (France), 2012.
- [49] M.B. Pescod, Wastewater treatment and use in agriculture - FAO irrigation and drainage paper 47, 1992.
- [50] Lehr, J., Hyman M., Gass, T. E., Seevers, W.J., *Handbook of complex environmental remediation problems*, 2001.
- [51] Bonomo L. (2008), "Trattamenti delle acque reflue", *McGraw-Hill Education*.

- [52] Metcalf & Eddy (2006), “Ingegneria delle acque reflue. Trattamento e riuso.”, *Milano: The McGraw-Hill Companies*, 4th ed.
- [53] Weber W.J.Jr (1972), “Physicochemical processes for water quality control”, *John Wiley & Sons*.
- [54] Cooney D.O. (1999), “Adsorption design for wastewater treatment”.
- [55] Kul A.R., Koyuncu H. (2010), “Adsorption of Pb(II) ions from aqueous solution by native and activated bentonite: Kinetic, equilibrium and thermodynamic study“, *Journal of Hazardous Materials*, Volume 179, pp. 332–339.
- [56] Rampazzo E. (2018), “Funzionalizzazione con plasma di grafite e grafene per lo sviluppo di nanocompositi epossidici”, *tesi.cab.unipd.it*.
- [57] Qiu H., Lv L., Pan B., Zhang Q., Zhang W., Zhang Q. (2009), “Critical review in adsorption kinetic models”, *Journal of Zhejiang University-SCIENCE A*, Volume 10, pp. 716-724.
- [58] Thomas C. Voice and W.J. Weber Jr (1983), “Sorption of hydrophobic compounds by sediments, soils and suspended solids”, *Water Research*, Volume 17, pp. 1433-1441.
- [59] Dada A.O, Olalekan A.P, Olatunya A.M., DADA O (2012), “Langmuir, Freundlich, Temkin and Dubinin–Radushkevich Isotherms Studies of Equilibrium Sorption of Zn<sup>2+</sup> Unto Phosphoric Acid Modified Rice Husk”, *IOSR Journal of Applied Chemistry (IOSR-JAC)*, Volume 3, pp. 38-45.
- [60] Eckhard Worch, Adsorption technology in water treatment: fundamentals, processes, and modeling, De Gruyter, pp. 169-176.
- [61] Han, R., Ding, D., Xu, Y., Zou, W., Wang, Y., Li, Y., Zou, L. (2008) *Use of rice husk for the adsorption of congo red from aqueous solution in column mode*. *Bioresource Technology*, 99, 2938-2946
- [62] Han, R., Wang, Y., Zhao, X., Wang, Y., Xie, F., Cheng, J., Tang, M. (2009) *Adsorption of methylene blue by phoenix tree leaf powder in a fixed-bed column: experiments and prediction of breakthrough curves*. *Desalination*, 245, 284-297
- [63] Hu, X., Cheng, Z., Removal of diclofenac from aqueous solution with multi-walled carbon nanotubes modified by nitric acid, *Chin. J. Chem. Eng.*, 2015, 23, 1551-1556.

- [64] Wei, H., Deng, S., Huang, Q., Nie, Y., Wang, B., Huang, J., Yu, G., Regenerable granular carbon nanotubes/alumina hybrid adsorbent for diclofenac sodium and carbamazepine removal from aqueous solution, *Water Res.*, 2013, 47, 4139-4147.
- [65] Ahmed, M.J., Hameed, B.H., 2018, Removal of emerging pharmaceutical contaminants by adsorption in a fixed-bed column: A review, *Ecotoxicology and Environmental Safety*, 149, 257-266
- [66] Yang, G., Li, L., Lee, W.B., Ng, M.C., 2018, Structure of graphene and its disorder: A review, *Science and Technology of Advanced Materials*, 19:1, 613-648.
- [67] Blandino, A., Macias, M., Cantero, M., Formation of calcium alginate gel capsules: Influence of sodium alginate and CaCl<sub>2</sub> concentration on gelation kinetics, *Journal of Bioscience and Bioengineering*, 1999, 88, 686-689.
- [68] (2008) Scanning Electron Microscopy (SEM). In: *Electron Microscopy of Polymers*. Springer Laboratory. Springer, Berlin, Heidelberg.
- [69] Pennycook S.J. et al. (2006) Scanning Transmission Electron Microscopy for Nanostructure Characterization. In: Zhou W., Wang Z.L. (eds) *Scanning Microscopy for Nanotechnology*. Springer, New York, NY.
- [70] Coates, J., Interpretation of Infrared Spectra, A Practical Approach, *Encyclopedia of Analytical Chemistry*, 1-23.
- [71] Dutrow, B.L., Clarck, C.M., X-ray Powder Diffraction (XRD)
- [72] <https://www.horiba.com/it/scientific/products/raman-spectroscopy/raman-academy/raman-faqs/what-is-raman-spectroscopy/>
- [73] [https://en.wikipedia.org/wiki/BET\\_theory](https://en.wikipedia.org/wiki/BET_theory)
- [74] Passos, M. L. C., Saraiva, M. L. M. F. S., Detection in UV-visible spectrophotometry: Detectors, detection systems, and detection strategies, *Measurement*, 2019, 135, 896-904
- [75] Coskun, O., Separation techniques: Chromatography, *North Clinic of Instabul*, 2016, 3(2), 156-160.
- [76] <https://it.wikipedia.org/wiki/BTEX>
- [77] <https://it.wikipedia.org/wiki/Benzene>
- [78] <https://it.wikipedia.org/wiki/Toluene>



[79] <https://it.wikipedia.org/wiki/Etilbenzene>

[80] <https://it.wikipedia.org/wiki/Xilene>

[81] <https://it.wikipedia.org/wiki/Tricloroetilene>

[82] [https://it.wikipedia.org/wiki/Blu\\_di\\_metilene](https://it.wikipedia.org/wiki/Blu_di_metilene)

[83] Abdel-Daiem, M.M., Rivera-Utrilla, J., Ocampo-Perez, R., Mendez-Diaz, J.D., Sanchez-Polo, M., Environmental impact of phthalic acid esters and their removal from water and sediments by different technologies, a review, *Journal of Environmental Management*, 2012, 109, 164-178

[84] Boyda, G.R., Reemtsma, H., Grimmb, D.A., Mitrac, S., 2003. Pharmaceuticals and personal care products (PPCPs) in surface and treated waters of Louisiana; USA and Ontario, Canada, *Sci. Total Environ.*, 311, 135-149.

[85] Oaks, J.L., Gilbert, M., Virani, M.Z., Watson, R.T., Meteyer, C.U., Rideout, B.A., Shivaprasad, H.L., Ahmed, S., Chaudhry, M.J.I., Arshad, M., Mahmood, S., Ali, S.A., Khan, A.A., 2004. Diclofenac residues as the cause of vulture population decline in Pakistan, *Nature*, 427, 630-633.

[86] <https://it.wikipedia.org/wiki/Etinilestradiolo>

[87] <https://it.wikipedia.org/wiki/Atrazina>

## **2.1 Removal of methylene blue dye from aqueous solutions using thermo-plasma expanded graphite: adsorption mechanism and material reuse**

### **Abstract**

The adsorption of methylene blue dye (MB) on thermo-plasma expanded graphite (TPEG) from water solution was investigated. The adsorbent material was characterized by SEM, TEM, BET, Raman and X-ray diffraction analysis. The influence of pH on the adsorption capacity was evaluated by varying its value in the range 1-11 and the adsorption mechanism was determined by kinetic and isothermal studies. Pseudo-first order, pseudo-second order, intraparticle diffusion, liquid film diffusion and Elovich models were used to fit our kinetics experimental data, whereas the isothermal experimental data were fitted by using Langmuir, Freundlich, Temkin and Dubinin-Radushkevich isotherms models. Pseudo-second order and Langmuir models agreed with the theoretical value of adsorption capacity (i.e. 196 and 208 mg g<sup>-1</sup>,

respectively), thus resulting the best fit for our experimental data. The thermodynamics of the process was evaluated by plotting the adsorption capacity/concentration ratio at the equilibrium as a function of different values of the multiplicative inverse of temperature. The process results to be spontaneous for temperature above 271 K and the increase of entropy is the driving force of the process. Moreover, the adsorbent regeneration was also investigated, by using the thermo-regeneration. The thermo-treatment was carried out by regenerating the exhausted material in an oven at 105°C for 2 hours, firstly, and then at 200°C for 4 hours. The thermo-treatment ensures a recover of at least 50 % of initial performance after 4 cycles of use and regeneration.

## **1.Introduction**

Surface water contamination is a growing concern and different kinds of contaminants and remediation techniques have been widely investigated in literature. The presence of dyes in the wastewater of cotton, wood and silk industry. The methylene blue (MB), a cationic dye, is largely used in these kinds of industries<sup>r</sup> and wastewater that contains it require a treatment to eliminate or reduce the MB concentration. In fact, even if MB is not very toxic, it generates some disease in Human, such as vomiting, diarrhea, increasing of heart rate, shock, cyanosis, jaundice, quadriplegia and tissue necrosis<sup>s</sup>. Furthermore, it can adsorb other pollutants, such as heavy metals or suspended solids. The adsorption process results to be one of the most investigated method by scientific community to remove MB, due its inexpensive maintenance, simplicity of design, simplicity of the process, insensitivity to toxic pollutants and smaller amount of harmful substances [1]. A large variety of substance was used and investigated as adsorbent materials, such as iron terephthalate [2], sawdust [3], palm kern fiber [4], pineapple leaf powder [5], activated carbon [6], carbon nanotubes [7], graphene [8] and graphene oxide [9]. Activated carbon is the typical and more used adsorbent material, but carbon nanotube, graphene and other carbonaceous nanomaterials are emerging as adsorbent materials and several studies investigate their industrial application. Their structural characteristic ensure strong interaction with organic molecules by mean of  $\pi$ - $\pi$  interactions, H-bonding, electrostatic forces, van der Waals forces and hydrophobic interactions [9,10]. They are capable to reach the equilibrium very fast thanks to their nanostructure, furthermore they have high adsorption capacity thanks to their high surface area. In this study, thermo-plasma expanded graphite (TPEG) was proposed as adsorbent material and its performance in term of adsorption capacity was evaluated. Furthermore, the kinetics, the adsorption isotherm, the thermodynamics of the

process and the possibility of regenerate and reuse the material for adsorption purpose were investigated.

TPEG used in this study is produced by means of an innovative process, that ensure a higher expansion than classical methods, consisting in the chemical intercalation of natural graphite followed by high temperature thermal plasma expansion. This process confers excellent physico-chemical properties to TPEG, i.e. apparent density [11] in the range 2.3 to 9 g L<sup>-1</sup>, that make it an excellent adsorbent material. TPEG is an innovative carbon-based material used to remove different kinds of hydrocarbons, like exhausted lubricating oil [12], BTEX [13] and PPCPs, such as diclofenac [14], with a removal efficiency of more than 80%, both treating soil and water.

## **2. Materials and methods**

### ***2.1 Materials***

TPEG was obtained from Innograf. TPEG is produced from natural graphite by using the chemical intercalation followed by the thermal plasma expansion. This process ensures the separation of graphite in different individual sheets, with a volume expansion of up to 300 units, compared to an average of 200 units obtainable by other standard methods. TPEG has good structural properties, such as mechanical strength of about 1 TPa, a thermal conductivity of about 500 W mK<sup>-1</sup>, a diameter between 60 and 300 μm<sup>a</sup> and high apparent density that could be associated with high surface area, property that can confer high adsorption capacity.

The initial pH of the solutions was adjusted by adding NaOH and HCl purchased from Carlo Erba reagents (Carlo Erba, Rodano, Milano, Italy) and MB was supplied from Carlo Erba reagents (Carlo Erba, Rodano, Milano, Italy, purity: 99.9%). The stock solution of MB was prepared in distilled water at a concentration of 1000 mg/L. All reagents were of extra pure grade and used without further purification.

### ***2.2 Material characterization***

SEM (scanning electron microscope) images were obtained by using a high-resolution field emission scanning electronic microscopy (HR-FESEM), Auriga Zeiss model, at CNIS laboratory of the University of La Sapienza (Rome, Italy).

TEM images was obtained by using transmission scanning electronic microscopy (TEM), FEI-TECNAI G2 20 TWIN model, with a value of 120 kV of acceleration voltage.

XRD (X-ray powder diffraction) spectra have been acquired by a X-Perth-Pro Philips X-ray diffractometer, operating at 40 kV and 32 mA, using CuK $\alpha$  radiation (wavelength of 1.5406 Å) in a q-2q configuration. The spectra have been acquired at 2 $\theta$  10°–80°, step size 0.040°, time per step 4 s. The Scherrer equation was used to calculate the average dimension of crystallite (stacking of graphene's sheet), while the average number of sheets of each stacking was obtained by dividing the dimension of crystallite for the reticular distance obtained by using the Bragg equation. Scherrer and Bragg equation are reported.  $\tau$  is the main size of the ordered crystalline domains,  $K$  is the shape factor,  $\lambda$  is the X-ray wavelength,  $\beta$  is the line broadening at half maximum intensity,  $\theta$  is the Bragg angle,  $n$  is a positive integer and  $d$  is the interplanar distance.

$$\tau = \frac{K\lambda}{\beta \cos\theta} \quad (\text{Scherrer equation})$$

$$n\lambda = 2d\sin\theta \quad (\text{Bragg equation})$$

Micro-Raman analysis was carried out by using a Jobin-Yvon Horiba LabRam microRaman-spectrometer, equipped with a He-Ne laser ( $\lambda = 632.8$  nm), an edge filter and an Olympus microscope with 10 $\times$ /50 $\times$ /100 $\times$  objectives. A spectral resolution of about 5 cm $^{-1}$  was obtained by a holographic grating with 600 grooves/mm. Spectra were acquired with an accumulation time of 60 s and a laser power of 20mW.

Specific surface area was measured with MONOSORB quantachrome instrument by applying the BET single point technique and by using N $_2$ /He 30% as gas to adsorb/desorb and BET multipoint technique by using ASAP 2020 instrument of Micromeritics.

The pH of zero charge was also evaluated by adding different amount of GTPEG in a solution with different initial pH and evaluating the final pH after 24 hours of contact. The  $\Delta$ pH observed for the different initial pH was reported in a graph and the pH $_{ZPC}$  was identified as the point with a value of  $\Delta$ pH of 0.

FT-IR spectrum was obtained in the range 400-4000 cm $^{-1}$  (4 cm $^{-1}$  of resolution) by using a JASCO FT-IR 460 Plus spectrophotometer. The sample was measured in the form of KBr pellet.

### ***2.3 Experimental setup***

To investigate how pH influences the adsorption process, experimental batch adsorption tests were performed by adding 10 mg of TPEG to 50 mL of MB solution (50 mg L $^{-1}$ ) in a conical flask at room temperature. The initial pH was brought at different values (i.e., 1, 2.5, 4, 7, 9 and 11) by adding NaOH and HCl and checked by an Orion 420A pH meter (ThermoFisher

Scientific, Waltham, Massachusetts, USA). The conical flask was placed on a magnetic stirrer (IKA RH digital) and was mixed at room temperature for 20 minutes at 650 rates per minute (rpm). At the end of adsorption treatment, the supernatant was aspirated to remove TPEG and the residual MB was measured, by UV-vis spectrometry analysis at 661 nm (Dr. Lange Cadas 200 spectrophotometer) with the calibration line method. Therefore, the adsorption capacity was evaluated at different pH values, as follows:

$$q = \frac{\text{mass of MB adsorbed (mg)}}{\text{mass of adsorbent (g)}} \quad (1)$$

$$q = (c_i - c_f) \frac{V}{m} \quad (1 \text{ bis})$$

where V is the initial solution volume (L), m is the adsorbent weight (g),  $c_i$  and  $c_f$  ( $\text{mg L}^{-1}$ ) are the MB concentrations at the beginning and after each adsorption experiment.

The influence of initial concentration of MB was evaluated by measuring the adsorption capacity at different initial concentration of MB (100, 70, 50, 30, 20 and 10  $\text{mg L}^{-1}$ ). Therefore, 50 mL of MB at different initial concentration and pH 9 was mixed with 10 mg of TPEG and stirred at 650 rpm for 20 minutes. Then, the residual concentration of MB was evaluated by spectrophotometric analysis and adsorption capacity was calculated.

Each test was repeated three times to have a main value.

#### **2.4 Adsorption kinetics study**

The kinetics models investigate the velocity of the process, providing the relationship between contact time and adsorption capacity. Therefore, to evaluate the kinetic of the process, experimental tests were executed by mixing 50 mL sample of contaminated water with a MB concentration of 50  $\text{mg L}^{-1}$  with 10 mg of TPEG, at 9 as the initial pH and 650 rpm as the stirring speed. Using different contact times, i.e. 5, 10, 15, 20, 30, 40 and 60 minutes, the adsorption capacity was determined. All tests were repeated three times to obtain the main value. The obtained data were plotted to evaluate the correlation between contact time and adsorption capacity and were fitted to different kinetic models, i.e. pseudo-first order, pseudo-second order, intraparticle diffusion, Elovich and liquid film diffusion models, and the  $R^2$  coefficient of linear regression and  $\chi^2$  were calculated for each fitting, in this way the mechanism of interaction was determined. Table 7 shows the linear form of model equations.

**Tab. 7 Overview of the kinetics models.  $q_e$ : equilibrium adsorption capacity ( $\text{mg g}^{-1}$ ),  $q_t$ : adsorption capacity at time  $t$  ( $\text{mg g}^{-1}$ ),  $k_1$ : rate constant of pseudo-first order ( $\text{min}^{-1}$ ),  $k_2$ : rate**

*constant of pseudo-second order (g mg<sup>-1</sup> min<sup>-1</sup>),  $\alpha$  and  $\beta$ : initial adsorption rate of the Elovich Equation and the desorption constant related to the extent of surface coverage and activation energy constant for chemisorption (mg g<sup>-1</sup> min<sup>-1</sup>) (g mg<sup>-1</sup>),  $k_{fd}$ : liquid film rate diffusion constant (min<sup>-1</sup>),  $k_{dif}$ : rate constant of intraparticle diffusion (mg g<sup>-1</sup> min<sup>-1/2</sup>)*

Model	Equation	References
Pseudo-first order	$\log(q_e - q_t) = \log(q_e) - k_1 t$	15
Pseudo-second order	$\frac{t}{q_t} = \frac{1}{k_2 q_e^2} + \frac{t}{q_e}$	15
Elovich	$q_t = \frac{1}{\beta} \ln(\alpha\beta) + \frac{1}{\beta} \ln(t)$	16
Liquid film diffusion	$\ln\left(1 - \frac{q_t}{q_e}\right) = -k_{fd} t$	17
Intraparticle diffusion	$q_t = k_{dif} t^{1/2} + C$	17

The pseudo-first order model involves a proportional correlation between the reaction velocity and the concentration of adsorbed molecule, the pseudo-second order model involves a quadratic correlation between velocity and the concentration of adsorbed molecule. The Elovich model is the best fit for materials with heterogeneous surface and slow adsorption. In the case of diffusion of adsorbate into the pores of adsorbent material is the slow step of the process, the intraparticle diffusion model is followed, while the liquid film diffusion is the model followed in case of the slow step is the diffusion in liquid/solid phase.

## 2.5 Adsorption isotherms

To identify the mechanism of interaction between the residual concentration of pollutant in water samples and the adsorption capacity of the adsorbent is necessary to analyze the adsorption isotherms. Therefore, adsorption capacity was evaluated for different MB concentrations (i.e. 10, 20, 30, 50, 70 and 100 mg L<sup>-1</sup>). 50 mL of MB solution were mixed with 10 mg of TPEG, stirred for 20 minutes at 650 rpm at pH 9 (optimal pH) and the residual MB was determined. The obtained experimental data were fitted using Langmuir [18], Freundlich [19,20], Temkin [21] and Dubinin-Radushkevich [22] isotherm models. To evaluate the best fit of the isotherms to the experimental data, the coefficient of linear regression (R<sup>2</sup>) and  $\chi^2$  were calculated. All the tests were repeated in triplicate.

The Langmuir model is valid for monolayer adsorption on a surface containing a finite number of identical sites and the adsorption is uniform. The linear form of Langmuir equation is:

$$\frac{C_e}{q_e} = \frac{1}{K_L q_m} + C_e / q_m \quad (2)$$

Where  $C_e$  is the concentration of adsorbate at equilibrium ( $\text{mg L}^{-1}$ ),  $q_e$  is the adsorption capacity at equilibrium ( $\text{mg g}^{-1}$ ) and  $K_L$  ( $\text{L mg}^{-1}$ ) is associated to free energy of the process and  $q_m$  ( $\text{mg g}^{-1}$ ) is the maximum adsorption capacity ( $\text{mg g}^{-1}$ ).

The Freundlich model assumes a multilayer adsorption and the surface of adsorbent contains a set of nearby sites. The linear form of the equation is:

$$\ln q_e = \ln K_f + \frac{1}{n_F} \ln C_e \quad (3)$$

Where  $K_f$  is an indicator of the adsorption capacity ( $(\text{mg g}^{-1}) (\text{L mg}^{-1})^{1/n}$ ) and  $\frac{1}{n_F}$  defines the adsorption intensity.

The Temkin model assumes the linear decrease of adsorption heat of all molecules in the layer with the coverage due to the adsorbent-adsorbate interaction. Moreover, the adsorption is characterized by a uniform distribution of the binding energies, up to some maximum binding energy. The linear form of the equation is:

$$q_e = B_1 \ln A + B_1 \ln C_e \quad (4)$$

Where  $A$  is the equilibrium binding constant ( $\text{L g}^{-1}$ ) and  $B_1$  is related to the heat of adsorption ( $\text{J mol}^{-1}$ ).

The Dubinin-Radushkevich model assumes that the adsorption occurs on a heterogeneous surface with a steric hindrance between adsorbed and incoming particles. The linear form of the equation is:

$$\ln(q_e) = \ln(q_s) - \beta \varepsilon^2 \quad (5)$$

$$\varepsilon = RT \ln\left(1 + \frac{1}{C_e}\right) \quad (6)$$

$$E = \frac{1}{-\sqrt{2\beta}} \quad (7)$$

Where  $E$  is related to free energy ( $\text{kJ mol}^{-1}$ ),  $\beta$  is the Dubinin-Radushkevich constant ( $\text{mol}^2 \text{J}^{-2}$ ),  $q_s$  is the adsorption capacity ( $\text{mg g}^{-1}$ ) and  $\varepsilon$  is the Polanyi potential.

The surface area covered by MB was calculated by using the following equation<sup>ii</sup>:

$$S_{MB} = q_e \cdot A_M \cdot 6.02 \cdot 10^{23} / M_{MB}$$

Where  $q_e$  is the adsorption capacity ( $\text{g g}^{-1}$ ),  $A_M$  is the molecular surface of MB ( $1.3 \text{ nm}^2$ ) and  $M_{MB}$  is the molecular weight of MB.

### *Thermodynamics of the process*

In order to evaluate the free energy of the process, the minimum temperature of spontaneity of the process and the driving force of the process, the thermodynamic study is required.

The adsorption capacity was determined for different temperature values (i.e. 273, 298 and 311 K) by adding 50 mL of MB solution (50 mg/L) to 10 mg of TPEG. The conical flask was placed on a magnetic stirrer and the solution was mixed at 650 rpm for 20 minutes. Each test was repeated in triplicate. The following relationships was used to evaluate the thermodynamics of the process [23]:

$$\Delta G^0 = -RT \ln \frac{q_e}{C_e} \quad (8)$$

$$\Delta G^0 = \Delta H^0 - T\Delta S^0 \quad (9)$$

Where  $\Delta G^0$  is the standard free energy,  $C_e$  is the concentration of adsorbate at equilibrium,  $q_e$  is the adsorption capacity,  $\Delta H^0$  is the standard enthalpy,  $\Delta S^0$  is the standard entropy and  $T$  is the temperature.

The following equation can be obtained from equations 5 and 6:

$$\ln \frac{q_e}{C_e} = -\Delta H^0/RT + \Delta S^0/R \quad (10)$$

Therefore, in order to evaluate the driving force of the process, enthalpy and entropy of the process were evaluated by plotting  $\ln \frac{q_e}{C_e}$  versus  $1/T$ .

### **2.6 Regeneration and reuse of TPEG**

The reuse of TPEG after a regeneration process is important to obtain subsequent technical and economic advantages and confer it a big competitiveness with already used technology. The thermo treatment was performed by regenerating TPEG samples in an oven at firstly  $105^\circ \text{C}$  for 2 hours and then at  $200^\circ \text{C}$  for 4 hours. Before the thermo-treatment, the material was separated from MB solution by aspirating the liquid phase with a pipette.

The regenerated TPEG was reused to perform 4 cycles of thermo-treatment, so 5 cycles of use as adsorbent material. Particularly, 10 mg of TPEG were added to 50 mL of MB solution (50



mg/L, pH 9) and mixed at 650 rpm for 20 minutes on a magnetic stirrer. The MB residual was evaluated and the TPEG was placed in the oven. After the thermo-treatment, TPEG was mixed again with a new MB solution and the cycle of adsorption was repeated. The thermo-treatment was repeated and so on, until 4 cycle of regeneration was reached. Each test was repeated in triplicate.

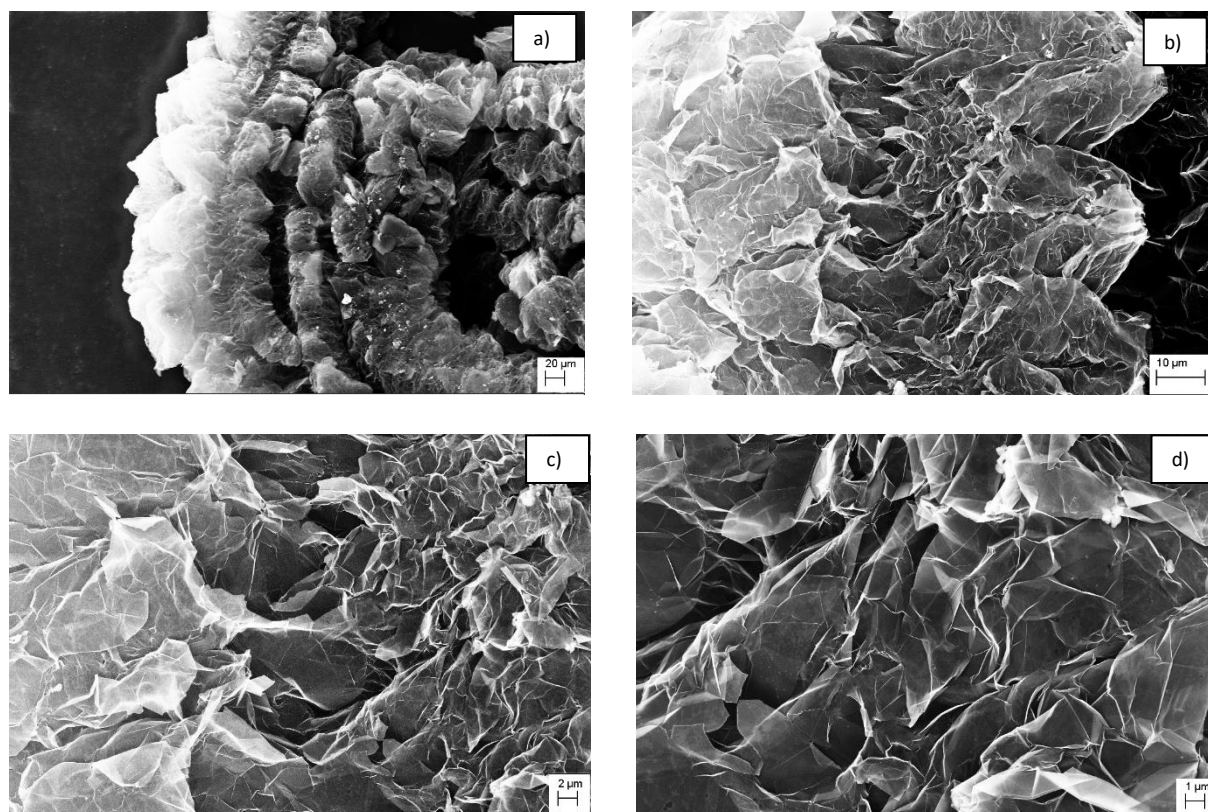
The performance of regenerated TPEG was evaluated by comparing the adsorption capacity using pure and regenerated material, as following (Equation 8):

$$\text{Relative } q_e = \frac{\text{MB adsorbed at specific cycle (mg)}}{\text{MB adsorbed at first use (mg)}} \times 100 \quad (11)$$

### 3. Results and discussion

#### 3.1 Material characterization

In the figure 27 and 28, the SEM and TEM images with different magnification of the material are reported.



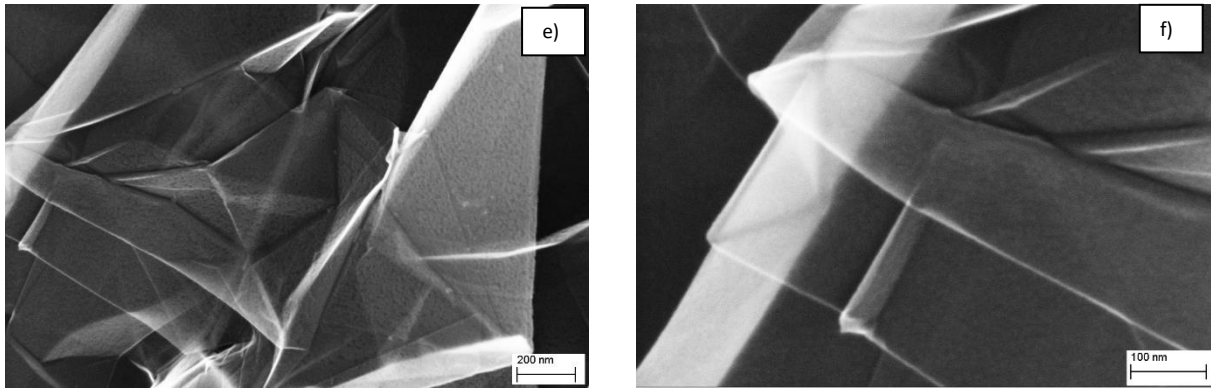


**Fig. 27 SEM images of the TPEG with different magnification (a: 500 X, b: 2500 X, c: 5000 X, d: 10000, e: 150000 X, f: 390400 X)**

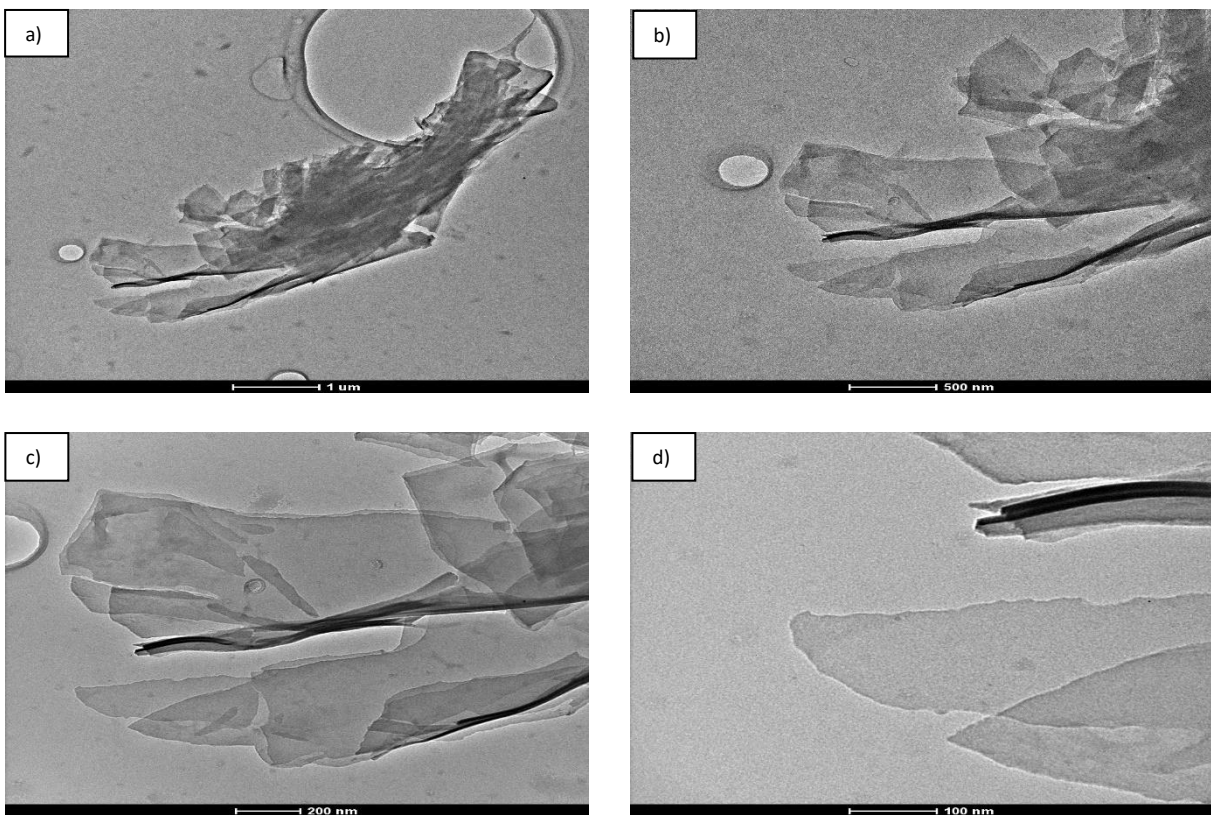


**Fig.28 TEM images of TPEG. The different scales of the images are reported to evidence the different magnifications.**

By observing SEM images of the material, it is clear the presence of different sheet of graphene packaged together to form a series of layers of sheet of graphene that form a fibrous macrostructure. It is possible to observe a crumple-like structure which is common in graphene. TEM images confirm the presence of multilayer of graphene. Thin stacked of various size and shape with a multilayered structure are present. X-ray diffraction and Raman analysis confirmed the packing of different sheet of graphene (number of layers > 5), because the typical

diffractogram of graphite (position and broad of peaks) and a typical Raman spectrum of graphite or sheet of graphene packed ( $n > 5$ ) were obtained<sup>36</sup> (ratio of the intensity of the peak  $I_D/I_G$  of about  $\frac{1}{2}$ , where  $I_D$  is the peak at about  $2679 \text{ cm}^{-1}$  and the  $I_G$  is the peak at about  $1577 \text{ cm}^{-1}$ ). From XRD and Raman analysis results, it is possible to conclude that the layers of graphene stacked are minimum 5<sup>36</sup>. In the figure 29, the diffractogram and Raman spectrum of TPEG are showed.

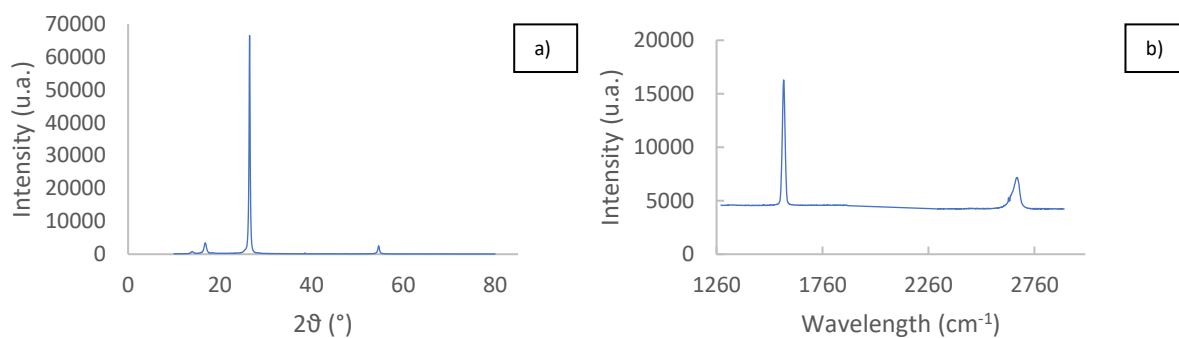


**Fig. 29 a) diffractogramm of TPEG, b) Raman spectrum of TPEG.**

The typical peaks of graphite at about  $26.5^\circ$  and  $55^\circ$  were obtained and the dimension of crystallites (stacking of graphite's sheets) and d-spacing were calculated from the shape and position of the peak at  $26.5^\circ$  by using the Scherrer and Bragg equation. The dimension of  $24.02 \text{ nm}$  was calculated as crystallite dimension, while  $0.374 \text{ nm}$  was obtained as d-spacing. The relative intensity of the peak, G and D, present in Raman spectrum (about  $1577$  and  $2679 \text{ cm}^{-1}$ ) obtained and the position and the shape of the peak D are typical for a graphitic system or packed graphene's sheet ( $n > 5$ ) that has a broad D peak. Therefore, the material presents a series of sheets ( $n > 5$ ) of graphene packed to form an ordered structure. The BET analysis reveals an important information about the structure of material, mesopores and micropores are present and the specific surface area of the mesopores is about  $18 \text{ m}^2 \text{ g}^{-1}$ , while the total surface area of the TPEG is about  $45 \text{ m}^2 \text{ g}^{-1}$ . Therefore, the surface area of micropores is  $27 \text{ m}^2 \text{ g}^{-1}$ .

In the figure 30 the FT-IR spectrum is reported. No peaks associated to functional groups are present, TPEG results inactive to the IR photons. The low peak at about  $3400 \text{ cm}^{-1}$  associated to OH stretching vibration is due to humidity presence caused by KBr used [24], confirmed by the absence of the peak associated to C-OH stretching vibration.

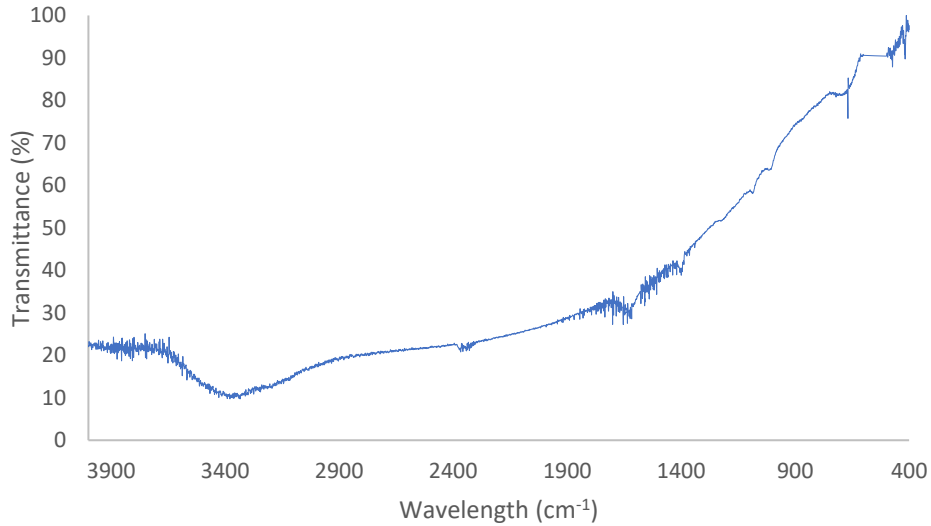


**Fig. 30 FT-IR spectrum of TPEG.**

### **3.2 pH influence on the adsorption capacity**

pH has an important parameter on the adsorption interaction due its capacity to protonate both the adsorbent and adsorbate, if they have some acid/basic group. For this reason, the optimal pH of adsorption was determined. Figure 31 shows the results obtained.

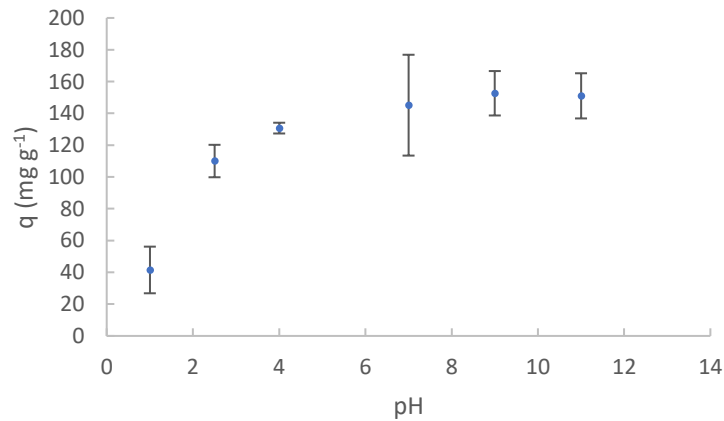


**Fig. 31 Effect of pH on MB removal by TPEG.  $C_0 = 50 \text{ mg L}^{-1}$ , contact time = 20 minutes, solution volume = 50 mL, mass of adsorbent = 10 mg, stirring speed = 650 rpm. Standard deviation of each experimental data is reported.**

The adsorption capacity increases by increasing the pH of the solution, in particular, it is about  $50 \text{ mg g}^{-1}$  at very acid condition (pH 1) and about  $150 \text{ mg g}^{-1}$  at alkaline condition. It can be caused by negatively charge formed on the adsorbent surface that can interact with cation dye [25]. At low value of pH the surface of TPEG could be protonated and electrostatic repulsion between TPEG and MB blocks the adsorption. The lower adsorption capacity at pH 1 could be also

attributed to the protonation of amino groups and higher solubility of the dye, even if this hypothesis requires further investigation.  $\pi$ - $\pi$  interaction as principal mechanism of interaction can be excluded because the number of  $\pi$  electron of MB and TPEG do not change by changing the pH, therefore, it implies no change of adsorption capacity by changing pH.

### 3.3 MB initial concentration influence

In fig.32 is reported the influence of initial concentration of MB on adsorption capacity. Standard deviation of adsorption capacity is also reported.

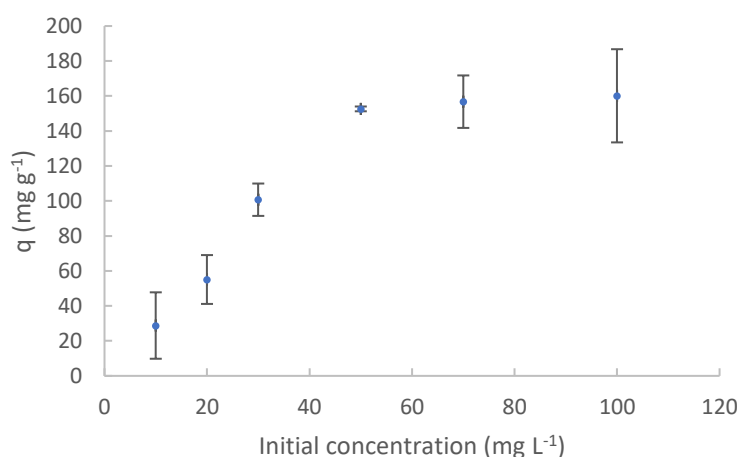


**Fig. 32 Adsorption capacity for different value of MB initial concentration.  $C_0= 100, 70, 50, 30, 20$  and  $10 \text{ mg L}^{-1}$ ,  $10 \text{ mg}$  of adsorbent material, stirring speed= $650 \text{ rpm}$ , contact time= $20$  minutes,  $\text{pH}=9$ .**

An initial rapid increase of adsorption capacity was observed by increasing the initial concentration of MB, after the initial increase a plateau was reached at initial concentration of about  $50 \text{ mg L}^{-1}$ . Therefore, when the concentration of  $50 \text{ mg L}^{-1}$  is reached, no further adsorption are observed and the adsorbent dosage increase are required maintaining the ratio solute/adsorbent of 0.25 to have an increase of adsorption capacity or removal efficiency.

### 3.4 Adsorption kinetics

The study of kinetics allows to understand the parameters that influence on the velocity of the process and it can be useful to ensure the best performance of the process in industrial use. The influence of the contact time on the adsorption capacity and the model that fit in the best way the experimental data were determined to have information on kinetic of the process. The figure 33 shows the obtained results.

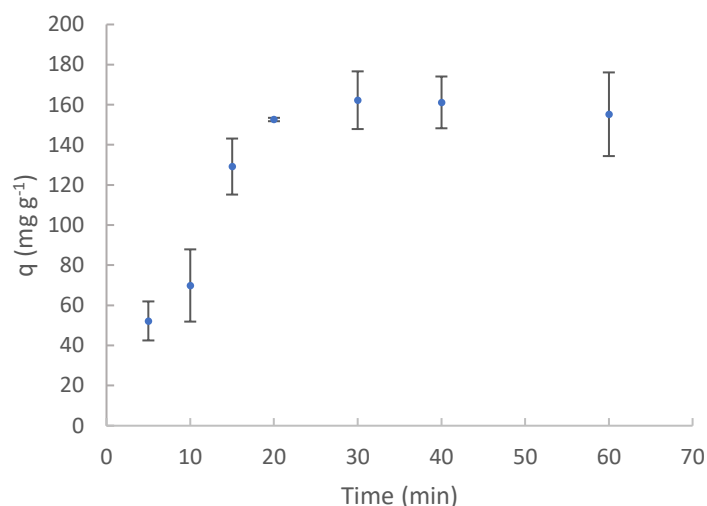


**Fig. 33 Adsorption capacity of TPEG for different contact time.  $C_0=50\text{ mg L}^{-1}$ , Solution volume= 50 mL, pH=9, mass of adsorbent= 10 mg, stirring speed= 650 rpm. Standard deviation of each data is reported.**

The adsorption capacity increase by increasing the contact time between TPEG and MB until to reach the equilibrium after about 20 minutes of contact. The shape is the classical shape of the adsorption process and it agreed with experiments reported in literature [2, 4, 5, 6, 7, 8, 27, 28, 29], even if other adsorbent materials were used. The equilibrium adsorption capacity results to be about  $150\text{ mg g}^{-1}$ . The experimental adsorption capacity was compared with theoretical equilibrium adsorption obtained by fitting the experimental data with different kinetics models. In the table 8, the linear correlation coefficient ( $R^2$ ) obtained for each model was reported.

**Table 8 Fitting of different kinetic models for adsorption of MB on TPEG.**

Model	Equation	$R^2$ ; $\chi^2$	Parameters
Pseudo-first order	$y = -0.0236x + 1.8474$	0.5016; 5	$K_1 = -2.36 \cdot 10^{-2}\text{ min}^{-1}$ $q_e = 70.37\text{ mg g}^{-1}$
Pseudo-second order	$y = 0.0051x + 0.055$	0.9384; 0.10	$q_e = 196\text{ mg g}^{-1}$ $k_2 = 4.7 \cdot 10^{-4}\text{ g mg}^{-1}\text{ min}^{-1}$
Elovich	$y = 48.811x - 18.955$	0.8117; 2.3	$\beta = 2.0 \cdot 10^{-2}\text{ mg g}^{-1}\text{ min}^{-1}$ $\alpha = 73.8\text{ g mg}^{-1}$
Liquid film diffusion	$y = -0.0543x - 0.8522$	0.5016; 3.8	$K_{fd} = 0.0543\text{ min}^{-1}$
Intraparticle diffusion	$y = 20.015x + 30.893$	0.6827; 2.8	$K_{dif} = 20.015\text{ mg g}^{-1}\text{ min}^{-1/2}$ $C = 30.893$

The best fit was obtained by using the pseudo-second order model, in agreement with our previous study<sup>n</sup>, in which the TPEG followed the pseudo-second order kinetics, even if a different adsorbate was investigated. Also, in this case, the velocity of the process quadruplicate when the concentration of MB duplicate. The kinetic constant of the process results to be  $4.7 \cdot 10^{-4} \text{ g mg}^{-1} \text{ min}^{-1}$  and the theoretical equilibrium adsorption capacity agreed with experimental parameters,  $196 \text{ mg g}^{-1}$  and  $150 \text{ mg g}^{-1}$  respectively. Both the value of adsorption capacity were comparable with the value of other materials reported in other study [2, 4, 5, 6, 7, 8, 27, 28, 29].

### 3.5 Adsorption isotherms

To characterize the adsorbent material and the process of adsorption in exam, the adsorption isotherms study results to be useful. The results obtained are showed in the figure 34.

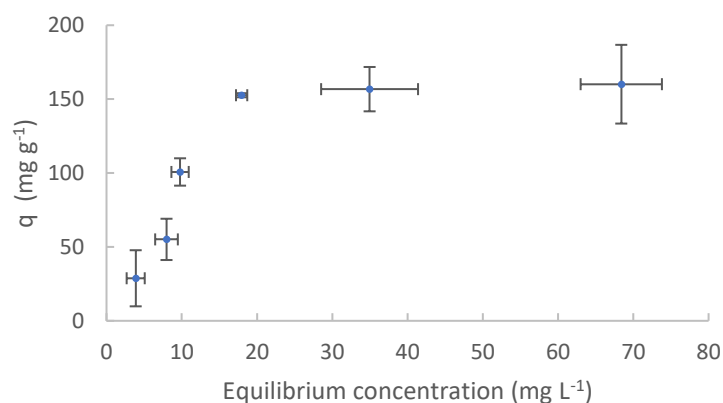


**Fig. 34** Equilibrium adsorption of MB on TPEG.  $C_0=10, 20, 30, 50, 70$  and  $100 \text{ mg L}^{-1}$ , pH 9, 10 mg of adsorbent material, stirring speed=650 rpm, contact time=20 minutes. Standard deviation of each experimental data is reported.

The adsorption capacity increase with the increase of the equilibrium concentration of MB until to reach an equilibrium value of about  $156 \text{ mg g}^{-1}$  at the equilibrium concentration of  $20 \text{ mg L}^{-1}$ . The shape of the isotherm is the typical shape of favorable adsorption process. In order to evaluate the mechanism of interaction and the theoretical equilibrium adsorption capacity, the experimental data were fitted with different isotherm models and the equation and the coefficient of linear regression ( $R^2$ ) are reported in the table 9.

**Table 9** Fit of adsorption isotherm data by using Langmuir, Freundlich, Temkin and Dubinin-Radushkevich models.

Model	Equation	R <sup>2</sup> ; $\chi^2$
Langmuir	y=0.0048x + 0.0752	0.9198; 0.12
Freundlich	y=0.5931x + 2.9046	0.7788; 1.5
Temkin	y=49.775x – 26.833	0.8357; 0.88
Dubinin-Radushkevich	y=-5·10 <sup>-6</sup> x + 4.9604	0.8711; 1.1

The Langmuir model was the best model to fit the experimental data, therefore, a monolayer of MB is adsorbed on the TPEG surface, that results to be a homogeneous surface. The theoretical maximum adsorption capacity results to be 208.33 mg g<sup>-1</sup>, value in agreement with experimental value and equilibrium adsorption capacity obtained from kinetic study (196 mg g<sup>-1</sup>) and comparable with value reported in literature [1, 2, 4, 5, 6, 7, 8, 27, 28, 29],. The value obtained for the Langmuir constant was 6.38·10<sup>-2</sup> L g<sup>-1</sup>. The surface area covered by MB calculated from adsorption isotherm studies results to be 574.08 m<sup>2</sup> g<sup>-1</sup>, while results to be 540.10 m<sup>2</sup> g<sup>-1</sup> from kinetics studies. R<sub>L</sub> was between 0 and 1, therefore, the process results to be favorable.

### 3.6 Thermodynamics study

The effect of the temperature on the process was evaluated and some thermodynamic parameters, such as free energy, enthalpy and entropy were determined. The plot of  $\ln \frac{q_e}{C_e}$  versus 1/T was done and the linear equation that is the best fit of the data obtained was obtained by the linear regression method. A coefficient of linear correlation of 0.9992 was obtained and from the best linear fit and the equation 7, the thermodynamic parameters were calculated. The enthalpy of the process, the entropy, the minimum temperature of spontaneity of the process and the free energy at 298 K were reported in the table 10.

**Tab. 10 Thermodynamics parameters of the MB adsorption on TPEG.**

$\Delta H^\circ$ (kJ mol <sup>-1</sup> )	$\Delta S^\circ$ (J mol <sup>-1</sup> K <sup>-1</sup> )	T <sub>min</sub> (K)	$\Delta G^\circ$ (kJ mol <sup>-1</sup> )
28.27	112.45	251.40	-5.24

The value of free energy obtained demonstrate that the physio-adsorption happens and the value is comparable with other reported in literature [2, 4, 8, 27, 30]. The driving force of the process results to be the increase of randomness associated to the high disorder to the liquid-solid interface. The process results to be endothermic but temperature above about -20° C ensure the



spontaneity of the process. The value of free energy obtained demonstrate that physical adsorption is involved.

In the table 10a the comparison between experimental data and theoretical data was reported to show the best fit between theoretical value and experimental data that confirms the agreement between experimental and theoretical data.

**Tab. 10a Equilibrium constant and free energy obtained from experimental and theoretical data. Experimental data obtained for MB solution of 500 mg<sup>-1</sup>L, 10 mg of adsorbent material, pH 9, stirring speed= 650 rpm and contact time= 20 minutes.**

Temperature (K)	$\frac{q_e}{c_e}$ experimental (mg L)	$\frac{q_e}{c_e}$ theoretical (mg L)	$\Delta G^0$ experimental (kJ mol <sup>-1</sup> )	$\Delta G^0$ theoretical (kJ mol <sup>-1</sup> )
273	3.93	1.07	-1.21	-2.43
298	8.50	9.80	-5.30	-5.24
323	16.81	16.16	-7.57	-8.05

### 3.7 Regeneration and reuse of TPEG

The possibility to reuse the adsorbent material and the results obtained is reported in the figure 35.

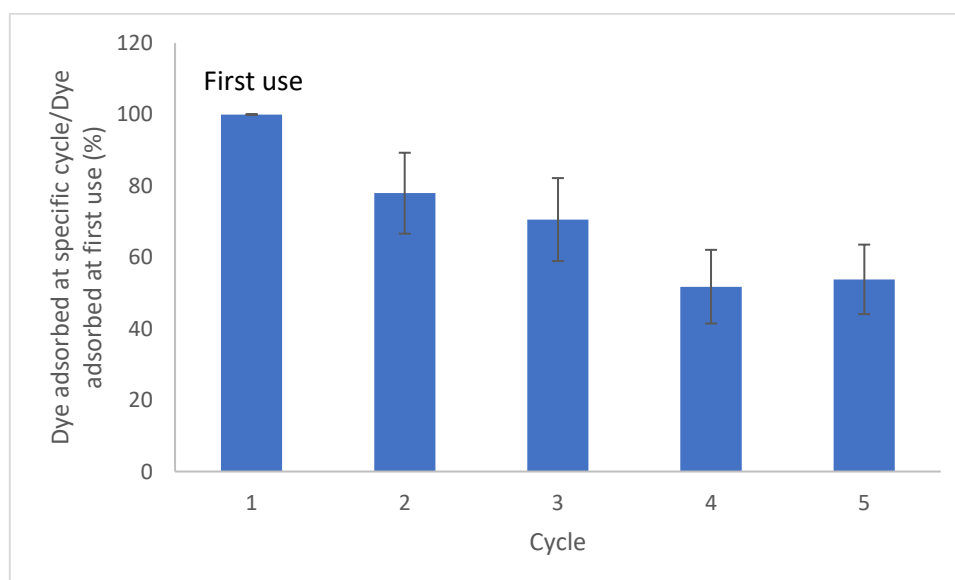


**Fig. 35 Performance of material after recovery treatment. Recovery performed by thermo treatment at 105°C for 2 hours and 200°C for 4 hours. Adsorption step was done by using**

*MB 50 mg/L, pH 9, stirring speed of 650 rpm, contact time of 20 minutes and 10 mg of adsorbent material.*

The thermo-treatment ensures a recovery of the performance of the material between about 80 and 50 % after 4 cycles of thermo-recovery. It can be very useful in a industrial process because after each use of the material, it requires only a limited amount of new material as integration to work again at the same adsorption capacity. The recovery of the performance results to be incomplete and it could be caused by strong interaction between MB and TPEG. The same shape is reported in literature and the recovery of the performance is comparable with other recover reported [7, 28, 31, 32].

#### **4. Conclusions**

In this study, TPEG was proposed as a good adsorbent material for MB adsorption and it results to be a valid alternative to already available adsorbent material, both in terms of adsorption capacity and reusability, for the removal of MB from water. The process follows a pseudo-second order kinetics and the Langmuir isotherm, furthermore, its driving force is the increase of entropy. The thermodynamics of the process indicates that a physio-adsorption is involved. The results obtained are in accordance with previous and recent studies. The adsorption capacity of the material is comparable with values reported in literature and it can be reuse as the other technology proposed. The mechanism of interaction involves hydrophobic interaction and probably electrostatic interaction. The deep characterization of morphology and the determination of functional groups present on surface can be useful to determine the interaction between adsorbate and adsorbent. Further studies can be conducted on this material, in particular, its oxidation, magnetization or transformation in graphene and then the evaluation of its adsorption capacity, the kinetics and the thermodynamics of the process of adsorption of the same contaminants or the investigation on the possibility to adsorb new contaminants. It could be interesting a different experimental setup for the adsorption of contaminants, such as the filtration.

#### **5. References**

- [1] Sharma, Y.C., Uma, Sinha, A.S.K., Upadhyay, S.N., 2010, Characterization and Adsorption Studies of Cocos Nucifera L. Activated Carbon for the Removal of Methylene Blue from Aqueous Solution, *Journal of Chemical and Engineering Data*, 55, 2662-2667.

- [2] Haque, E., Jun, J.W., Jhung, S.H., 2011, Adsorptive removal of methyl orange and methylene blue from aqueous solution with a metal-organic framework material, iron terephthalate (MOF-235), *Journal of Hazardous Materials*, 185, 507-511.
- [3] Garg, V.K., Amita, M., Kumar, R., Gupta, R., 2004, Basic dye (methylene blue) removal from simulated wastewater by adsorption by using Indian Rosewood sawdust: a timber industry waste, *Dyes and Pigments*, 63, 243-250.
- [4] El-Sayed, G., 2011, Removal of methylene blue and crystal violet from aqueous solution by palm kernel fiber, *Water, Air and Soil Pollution*, 272, 225-232.
- [5] Weng, C.H., Lin, Y.T., Tzeng, T.W., 2009, Removal of methylene blue from aqueous solution by adsorption onto pineapple leaf powder, *Journal of Hazardous Materials*, 170, 417-424.
- [6] Altenor, S., Carene, B., Emmanuel, E., Lambert, J., Ehrhardt, J.J., Gaspard, S., 2009, Adsorption studies of methylene blue and phenol onto vetiver roots activated carbon prepared by chemical activation, *Journal of Hazardous Materials*, 165, 1029-1039.
- [7] Madrakiana, T., Afkhami, A., Ahmadi, M., Bagheri, H., 2011, Removal of some cationic dyes from aqueous solution using magnetic-modified multi-walled carbon nanotubes, *Journal of Hazardous Materials*, 196, 109-114.
- [8] Liu, T., Li, Y., Du, Q., Sun, J., Jiao, Y., Yang, G., Wang, Z., Xia, Y., Zhang, W., Wang, K., Zhu, H., Wu, D., 2012, Adsorption of methylene blue from aqueous solution by graphene, *Colloids and Surface A*, 90, 197-203.
- [9] Yang, T., Chen, S., Chang, Y., Cao, A., Liu, Y., Wang, H., 2011, Removal of methylene blue from aqueous solution by graphene oxide, *Journal of Colloid and Interface Science*, 2011, 359, 24-29.
- [10] Pyrzynska, K., 2011, Carbon nanotubes as sorbent in the analysis of pesticides, *Chemosphere*, 83, 1407-1413.
- [11] Masi, S., Calace, S., Mazzone, G., Caivano, M., Buchicchio, A., Pascale, S., Bianco, G., Caniani, D., Lab-scale investigation on remediation of sediments contaminated with hydrocarbons by using super-expanded graphite, 15th International Conference on Environmental Science and Technology Rhodes, Greece, 31 August to 2 September 2017.

- [12] Caniani, D., Caivano, M., Calace, S., Mazzone, G., Pascale, R., Mancini, I.M., Masi, S., Remediation of water samples contaminated by BTEX using super-expanded graphite as innovative carbon-based adsorbent material, IWA World Water Congress & Exhibition, 16-21 September 2018, Tokyo, Japan.
- [15] Qiu, H., Lv, L., Pan, B.-, Zhang, Q.-j., Zhang, W.-m., Zhang, Q.-x., 2009, Critical review in adsorption kinetic models, Journal of Zhejiang University SCIENCE A, 10(5), 716-724.
- [16] Ho, Y.S., McKay, G., 1999, Pseudo-second order model for sorption process, Process Biochemistry, 34, 451-465.
- [17] Low, M.J.D., 1960, Kinetics of chemisorption of gases on solids, Chemical Reviews, 60(3), 267-312.
- [18] Langmuir, I., 1918. The adsorption of gases on plane surfaces of glass, mica and platinum, J. Am. Chem. Soc., 1918, 1361-1402.
- [19] Freundlich, H. M. F., 1906. Over the adsorption in solution, Journal of Physical Chemistry, 57, 385-471.
- [20] Temkin, M.I., Pyzhev, V., 1940. Kinetics of ammonia synthesis on promoted iron catalyst, Acta Physical Chemistry USSR, 12. 327-357.
- [21] Dubinin, M.M., Radushkevich, L.V., 1947. The equation of characteristic curve of the activated charcoal, Proceedings of the Academy of Science of the USSR Physical Chemistry Section, 55, 331-337.
- [22] Baghdadi, M., Ghaffari, E., Aminzadeh, B., 2016. Removal of carbamazepine from municipal wastewater effluent using optimally synthesized magnetic activated carbon: Adsorption and sedimentation kinetic studies, J. Environ. Chem. Eng., 4, 3309-3321.
- [24] Bourlinos, A.B., Gournis, D., Petridis, D., Szabo, T., Szeri, A., Dékani, I., 2003, Graphite Oxide: Chemical Reduction to Graphite and Surface Modification with Primary Aliphatic Amines and Amino Acids, Langmuir, 19, 6050-6055
- [25] Al Qada, E.M., Allen, S.J., Walker, G.M., 2006, Adsorption of Methylene Blue onto activated carbon produced from steam activated bituminous coal: A study of equilibrium adsorption isotherm, Chemical Engineering Journal, 124, 103-110.

- [26] Li, Y., Du, Q., Liu, T., Peng, X., Wang, J., Sun, J., Wang, Y., Wu, S., Wang, Z., Xia, Y., Xia, L., 2013 Comparative study of methylene blue dye adsorption onto activated carbon, graphene oxide and carbon nanotubes, *Chemical Engineering Research and Design*, 91, 361-368.
- [27] Liu, T., Li, Y., Du, Q., Su, J., Jiao, Y., Yang, G., Wang, Z., Xia, Y., Zhang, W., Wang, K., Zhu, H., Wu, D., 2012, Adsorption of methylene blue from aqueous solution by graphene, *Colloids and Surface B: Biointerfaces*, 90, 197-203.
- [28] Chen, L., Ramadan, A., Lu, L., Shao, W., Luo, F., Chen, J., 2011, Biosorption of Methylene Blue from Aqueous Solution Using Lawny Grass Modified with Citric Acid, *Journal of Chemical and Engineering Data*, 56, 3392-3399.
- [30] Sharma, P., Das, M.R., 2013, Removal of a Cationic Dye from Aqueous Solution Using Graphene Oxide Nanosheets: Investigation of Adsorption Parameters, *Journal of Chemical and Engineering data*, 58, 151-158.
- [31] Wang, P., Cao, M., Wang, C., Ao, Y., Hou, J., Qian, J., 2014, Kinetics and thermodynamics of adsorption of methylene blue by a magnetic graphene-carbon nanotube composite, *Applied Surface Science*, 290, 116-124.
- [32] Auta, M., Hameed, B.H., 2014, Chitosan-clay composite as highly effective and low cost adsorbent for batch and fixed-bed adsorption of methylene blue, *Chemical Engineering Journal*, 237, 352-361.

## **2.2 Removal of diclofenac from aqueous solutions using a thermo-plasma expanded graphite: material characterization, adsorption mechanism and material reuse**

### **Abstract**

The adsorption of diclofenac sodium on thermo-plasma expanded graphite (a commercial product) from water solutions was investigated. The adsorbent material was characterized by SEM, TEM, BET, Raman and X-ray diffraction analyses. Typical diffractogram and Raman spectrum of graphitic material were observed, dimension of 24.02 nm as crystallite dimension and a surface area of 47 m<sup>2</sup> g<sup>-1</sup> were calculated. The effect of pH on the adsorption capacity was evaluated in the range 1-7 and the adsorption mechanism was described by kinetic and isothermal studies. Pseudo-first order, pseudo-second order, intraparticle diffusion, liquid film diffusion and Elovich models were used to fit the kinetic experimental data, whereas the

isothermal experimental data were fitted by using Langmuir, Freundlich, Temkin and Dubinin-Radushkevich models. Pseudo-second order and Dubinin-Radushkevich models agreed with theoretical values of adsorption capacity (i.e. 400 and 433 mg g<sup>-1</sup>, respectively), thus resulting the best fit for experimental data. The thermodynamics of the process was evaluated by plotting the adsorption capacity/concentration ratio at the equilibrium as a function of different values of the multiplicative inverse of temperature. Moreover, the adsorbent regeneration was also investigated, comparing two different remediation techniques. Solvent washing was performed by adding the exhausted material to 50 mL of NaOH 0.2 M and mixing it for 3 hours. The thermo-treatment was carried out by heating in an oven at 105°C for 2 hours, firstly, and then at 200°C for 4 hours. The thermo-treatment was the best technique to regenerate the adsorbent, ensuring same performance after 4 cycles of use and regeneration.

### **Keywords**

Adsorption, contaminated water, diclofenac, thermo-plasma expanded graphite

### **1. Introduction**

Surface water contamination is a growing concern and different kinds of contaminants and remediation techniques have been widely investigated in literature. Pharmaceuticals and Personal Care Products (PPCPs) have increasingly been found in surface water and, even though they are normally present at very low concentrations, several scientific studies [1, 2, 3, 4] have proved their negative impact on aquatic life. Conventional wastewater treatment plants cannot completely remove PPCPs because of their high polarity and solubility in water [5, 6, 7, 8]). These characteristics represent the main challenge for the removal of PPCPs from water solution. Different methods, such as photodegradation [9] , coagulation-flocculation [10] , biodegradation [11] , chlorination [12] and ozonation [13], have been used to remove PPCPs by trapping or degradation. Coagulation-flocculation methods usually present a removal percentage from nil to 50%, whereas oxidative processes and photodegradation present almost total removal, but toxic by-products can be produced. For these reasons, the adsorption process has become a popular method for the removal of organic contaminants (i.e. PPCPs, petroleum derivates and dyes) from aqueous matrices. The strength of adsorption processes is their inexpensiveness and simplicity [14]. Activated carbons have largely been used as adsorbent material due to their hydrophobicity, surface functionality, pore structure and high surface area [15, 16]. Other carbon-based materials, such as multi-walled carbon nanotubes [17, 18] and

graphene/graphite [19, 20] compounds, have already been used as adsorbent material, showing high efficiency in removing (closed to 100%) PPCPs from water.

Diclofenac sodium (DCF) is an analgesic drug included in the class of PPCPs, generally prescribed to treat inflammatory disorders because of its nonsteroidal anti-inflammatory potential. The DCF neutral form presents free acid groups (-COOH), whereas the anionic form presents deprotonated acid groups (-COO<sup>-</sup>). Chronic exposure to DCF generates hemodynamic changes and thyroid tumors in Humans [2]. Furthermore, negative effects have been observed on natural ecosystems, causing the death of several animal species. Particularly, Oaks et al. 2004 investigated on the death of a popular specie of vultures in South Asia, proving that eating carcasses of animals nursed with DCF may cause visceral gout in vultures, mainly due to the crystallization of their internal organs. DCF has largely been detected in both natural water and wastewater worldwide because of its common use in large quantities [21]. Therefore, its removal by using adsorption process has attracted the attention of the research community. In this study, the thermo-plasma expanded graphite (TPEG) was used to remove DFC from aqueous solutions. Expanded graphite consists of laminated two-dimensional nanoparticles bound to each other by van der Waals forces only, and it is produced by the expansion of natural graphite. This process confers excellent physic-chemical properties to TPEG, for example an apparent density [22] in the range 2.3 to 9 g L<sup>-1</sup>, that makes it an excellent adsorbent material. Furthermore, it has a typical fibrous morphology and overlapping of graphene layers can be evidenced by SEM analysis. Packing of more than five graphene layers are the basic structure of TPEG with presence of mesopores and micropores. TPEG was used as an adsorbent material and its interaction with DCF was investigated. TPEG was chosen as adsorbent material because it is produced by an industrial process that ensures a significative increase of surface area of the starting material promising good potential adsorbent properties. The industrial process of the production is covered by industrial secret but basic information are available and it is known that the process involves a first step of chemical intercalation of natural graphite and a second step of very fast expansion conducted by a plasma thermal heating. Due to its industrial production that ensures a not very expensive cost, promising improvement of mechanical characteristic, increase of surface area and changing in the apparent density, TPEG resulted to be an interesting material to investigate for environmental remediation purpose. Therefore, experimental studies about the mechanisms of interaction between TPEG and DCF, the kinetics and the thermodynamics of the process, pH influence and the reuse of the adsorbent material, were conducted.

## **2. Materials and methods**

### ***2.1 Materials***

TPEG was obtained from Innograf (Potenza, Italy). The initial pH of the solutions was adjusted by adding NaOH and HCl purchased from Carlo Erba reagents (Carlo Erba, Rodano, Milano, Italy) and Diclofenac sodium salt was supplied from Sigma Aldrich (Sigma-Aldrich, Schnelldorf, Germany, purity: 99.9%). The stock solution of DCF was prepared in distilled water at a concentration of 100 mg/L. All reagents were of extra pure grade and used without further purification.

TPEG is obtained from natural graphite by means of chemical intercalation followed by the thermal plasma expansion at high temperatures. Different methods, such as chemical vapor deposition and chemical intercalation, are available to expand the natural graphite. TPEG used in this study is produced by means of an innovative process consisting in the chemical intercalation of natural graphite followed by high temperature thermal plasma expansion. This process separates graphite in different layers, with a volume expansion of up to 300 units, compared to an average of 200 units obtainable by other standard methods. TPEG has good structural properties, such as mechanical strength of about 1 TPa, a thermal conductivity of about 500 W mK<sup>-1</sup> and a diameter between 60 and 300 μm [22].

### ***2.2 Material characterization***

The characterization of the material was not conducted in that specific case because the material used was the same of the previous experimental work described.

### ***2.3 Experimental setup***

In order to investigate the influence of pH on the adsorption process, experimental batch adsorption tests were performed by adding 10 mg of TPEG to 50 mL of DCF solution (100 mg L<sup>-1</sup>) in a conical flask. The initial pH was adjusted at different values (i.e., 1, 2, 3, 5 and 7) by adding NaOH and HCl and monitored by an Orion 420A pH meter (ThermoFisher Scientific, Waltham, Massachusetts, USA). The conical flask was placed on a magnetic stirrer (IKA RH digital) and was mixed at 650 rates per minute (rpm) at room temperature for 22 hours to ensure contact between TPEG and the contaminated matrix. After treatment, the supernatant was aspirated to remove TPEG and the amount of residual DFC was measured. Therefore, the adsorption capacity was evaluated at different pH values, as follows:



$$q = \frac{\text{mass of DCF adsorbed (mg)}}{\text{mass of adsorbent (g)}} \quad (12)$$

$$q = (c_i - c_f) \frac{V}{m} \quad (13)$$

where  $c_i$  and  $c_f$  ( $\text{mg L}^{-1}$ ) are the DFC concentrations at the beginning and after each adsorption experiment,  $V$  is the initial solution volume (L), and  $m$  is the adsorbent weight (g).

Removal was also evaluated by the ratio between mass of adsorbed DCF and initial DCF present in the solution.

#### ***2.4 Analytical methods***

DCF residual concentrations were estimated by UV-vis spectrometry at 271 nm (Dr. Lange Cadas 200 spectrophotometer) with the calibration line method. The absorbance of DCF solution was measured at pH 3.3

All the tests were repeated three times to obtain the mean value.

#### ***2.5 Initial concentration influence***

The influence of initial concentration of the pollutant on the adsorption capacity of TPEG was also evaluated. 50 mL of DCF's solution at different initial concentration (250, 200, 100, 40, 20, 10  $\text{mg L}^{-1}$ ) at pH 1 was mixed with 10 mg of TPEG and stirred at 650 rpm for 10 minutes. Then, the residual concentration of DCF was evaluated and the adsorption capacity calculated. Each test was repeated three times.

#### ***2.6 Adsorption kinetics models***

The kinetics models investigate the velocity of the process, providing the relationship between contact time and adsorption capacity. In order to study the kinetic of the process, experimental tests were executed by mixing 10 mg of TPEG with a 50 mL sample of contaminated water with a DFC concentration of 100  $\text{mg L}^{-1}$ , at 650 rpm as the stirring speed and 1 as the initial pH. Using different contact times, i.e. 3, 5, 7, 10, 15, 20, 30 and 40 minutes, the adsorption capacity was determined. The obtained data were plotted to evaluate the correlation between contact time and adsorption capacity. In order to evaluate the real mechanism of DFC adsorption on TPEG, the experimental data were fitted to five kinetic mathematical models, i.e. pseudo-first order, pseudo-second order, intraparticle diffusion, Elovich and liquid film diffusion models. The best fitting was identified through the calculation of the  $R^2$  coefficient.

All tests were replicated three times to obtain the mean value. In the section 2.1 the equation of the models used are specified.

### ***2.7 Adsorption isotherms***

The analysis of the adsorption isotherms is important to identify the interaction between the residual concentration of pollutant in water samples and the adsorption capacity of the adsorbent. Therefore, adsorption capacity was evaluated for different DCF concentrations (i.e. 10, 20, 40, 100, 200 and 250 mg L<sup>-1</sup>). 10 mg of adsorbent were mixed with 50 mL of DCF solution, stirred for 10 minutes at 650 rpm at pH 1 (optimal pH) and the obtained experimental data were fitted using Langmuir [26], Freundlich [27, 28] Temkin [29] and Dubinin-Radushkevich [30] isotherm models. All the tests were repeated in triplicate. In order to evaluate the best fit of the isotherms to the experimental data, the coefficient of linear regression (R<sup>2</sup>) was calculated. In the previous section the equations of the models are specified.

### ***2.8 Thermodynamics of the process***

The thermodynamic study allows an understanding of the relationship between spontaneity, free energy, and temperature during the process. Moreover, it gives information about the temperature at which the process is at equilibrium under standard conditions.

In order to evaluate the thermodynamics of the process, the adsorption capacity was determined for different temperature values (i.e. 293, 299 and 311 K) by adding 10 mg of adsorbent to 50 ml of DCF solution (100 mg/L). The conical flask was placed on a magnetic stirrer and was mixed at 650 rpm for 10 minutes. Each test was repeated in triplicate. In the previous chapter the equations that regulates the thermodynamics are reported.

### ***2.9 Regeneration and reuse of TPEG***

The possible reuse of TPEG after a regeneration process is important to obtain subsequent technical and economic advantages. Two different regeneration processes were tested to recover the material for subsequent remediation tests. Solvent washing was carried out in a glass beaker by adding exhausted TPEG to 50 mL of NaOH (0.2 M). The solution was posed on a magnetic stirrer and mixed at 800 rpm for 3 hours.

The thermo treatment was performed by regenerating TPEG samples in an oven at firstly 105° C for 2 hours and then at 200° C for 4 hours. Before the treatment, the material was separated from DCF solution by aspirating the liquid phase with a pipette.

The regenerated TPEG was reused to perform 2 and 4 cycles of treatment after solvent washing and thermo-recovery, respectively. Particularly, 10 mg of TPEG were added to 50 mL of DCF solution (20 mg/L, pH 1) and mixed at 650 rpm for 10 minutes on a magnetic stirrer. Each test was repeated in triplicate.

The performance of regenerated TPEG was evaluated by comparing the adsorption capacity using pure and regenerated material, as following (Equation 14):

$$Relative\ q_e = \frac{DCF\ adsorbed\ at\ specific\ cycle\ (mg)}{DCF\ adsorbed\ at\ first\ use\ (mg)} \times 100 \quad (14)$$

### 3. Results and discussion

#### 3.1 pH influence on the adsorption capacity

Figure 36 shows the variation of TPEG adsorption capacity and removal by varying the pH in the range 1-7. Some value of removal and adsorption capacity are overlapped but this scale of removal is used in agreed with the next figures.

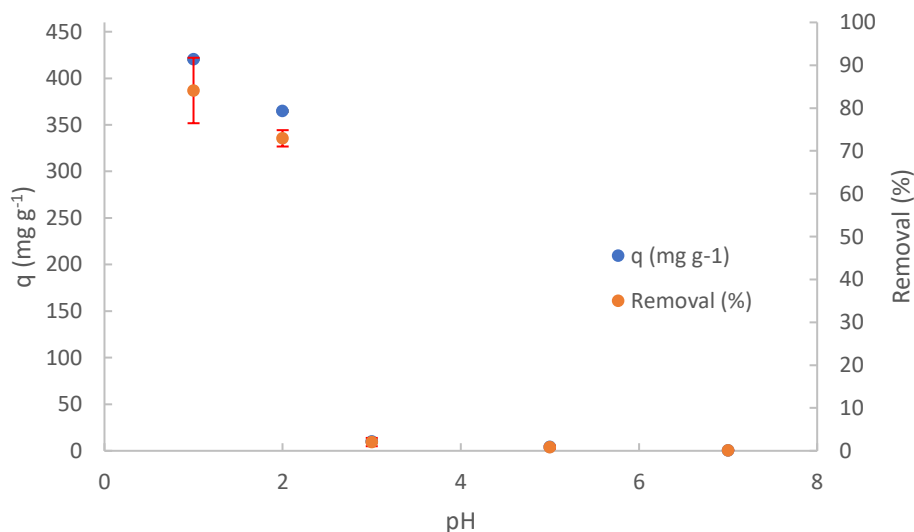


**Fig. 36 Effect of pH on DFC removal by TPEG and its adsorption capacity.  $C_o = 100\text{ mg L}^{-1}$ , contact time = 22 hours, Solution volume= 50 mL, mass of adsorbent= 10 mg, stirring speed= 650 rpm. Standard deviation is also reported for each experimental data.**

Adsorption capacity is maximum ( $420.5\text{ mg g}^{-1}$ ) at pH 1 and 2, i.e. at values higher than pKa. Adsorption capacity decreases with increasing pH, reaching the minimum (closed to 0) at pH 3, i.e. at values close to pKa. The reason for this is probably that DFC solubility decreases<sup>37</sup> at low pH values due to the presence of DCF in the neutral form, resulting in a better adsorption

capacity. Therefore, the optimal value of pH for this study is 1. The figure 36 illustrates the dissociation equilibrium of DCF to better understand the influence of pH on its grade of dissociation and therefore on its solubility. As can be observed, DCF has a carboxylic acid group able to react with water (acid-base reaction) to form the conjugate anion of DCF and hydroxonium. Because of DCF, as all organic acid, is a weak acid, the reaction of dissociation is an equilibrium dissociation and it is influenced by the external presence of  $\text{H}_3\text{O}^+$  or  $\text{OH}^-$ . In detail, when the pH is acid ( $[\text{H}_3\text{O}^+] > 10^{-7} \text{ M}$ ) the equilibrium moves to reagents of the reaction reported in the figure 37 because the presence of  $\text{H}_3\text{O}^+$ , therefore DCF is present in solution in its undissociated form. When the pH is basic ( $[\text{OH}^-] > 10^{-7} \text{ M}$ ) the equilibrium moves to the product of the reaction because  $\text{H}_3\text{O}^+$  reacts with  $\text{OH}^-$  present in the solution, therefore DCF is largely present in its dissociated form. The amino group of DCF can also react with water, as reported in the figure 4, to form the conjugate cation of DCF and hydroxide ion. The pH has the same reverse effect described for the carboxylic group. Therefore, the form of DCF in the solution depends on the pH of the solution and it is neutral for pH values less than its pKa (4.2) [31, 32]. The  $\text{pH}_{\text{ZPC}}$  of the TPEG was 12, therefore in the range of the pH considered, the charge of the TPEG was positively and electrostatic interaction between undissociated/dissociated form of DCF and TPEG is not affected by the change of the TPEG charge surface. It confirms that the increase of adsorption capacity by decreasing the pH is mainly related to the solubility of DCF decrease, for the value upper than 4.2 the increase of negatively charge of DCF does not compensate the increase of solubility and no further increase of adsorption capacity was observed.

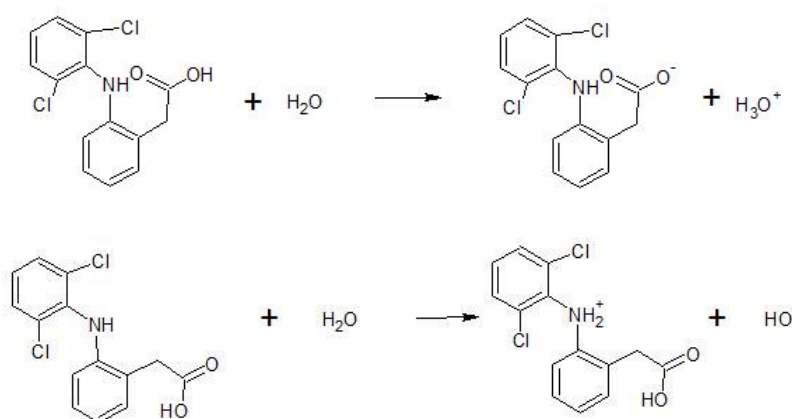


**Fig. 37 Equilibrium dissociation of DCF.**

By considering the results observed,  $\pi$ - $\pi$  interactions can be excluded because the number of DCF (Bhadra et al. 2016) and TPEG  $\pi$ -electrons do not change by changing the pH. Therefore, adsorption capacity is not influenced by pH in the case of these interactions as principal

adsorption mechanisms. Even if the value of pH of 1 is not normally detected in real application, the evaluation of best pH condition can be useful to have information on the trend of adsorption capacity by changing the pH and little pH variations can be managed in real application.

### 3.2 Initial concentration influence

The figure 38 shows the influence of initial concentration of MB on adsorption capacity and removal. Their standard deviations are also reported.

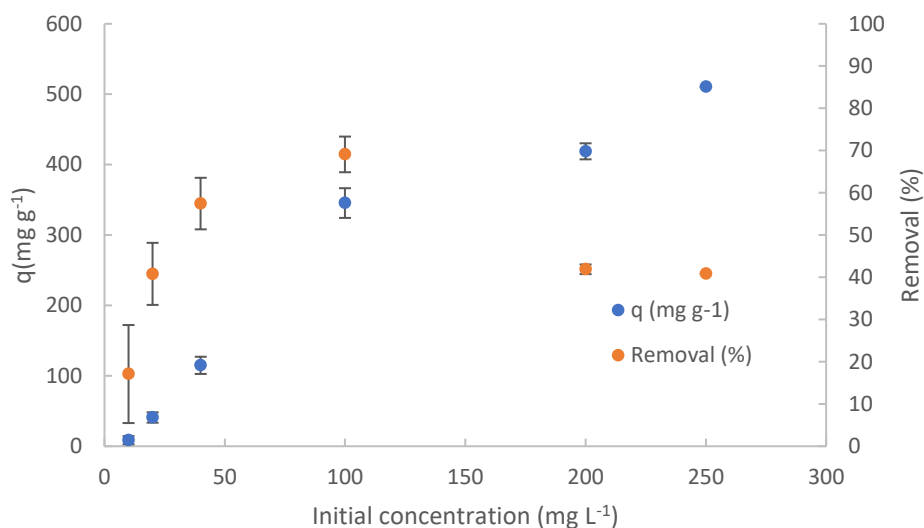


**Fig. 38 Adsorption capacity and removal for different Initial concentration of DCF.  $C_0=10, 20, 40, 100, 200$  and  $250 \text{ mg L}^{-1}$ , pH 1, 10 mg of adsorbent material, stirring speed=650 rpm, contact time=10 minutes.**

A rapid increase of adsorption capacity was observed at the initial increase of initial concentration of MB, followed by a slow increase of adsorption capacity for initial concentration higher than  $100 \text{ mg L}^{-1}$  probably caused by the saturation of the material. The observed behavior is the typical behavior observed in adsorption processes caused by the occupation of the TPEG adsorption sites involved into the interaction with adsorbate (DCF). When all the adsorption sites are occupied no further adsorption can be observed and the increase of concentration of adsorbate cannot involve other interaction with adsorbent. When that equilibrium is reached, increase of dosage of adsorbent is necessary to have further adsorption. The same behavior was observed for the removal, but for the initial concentration higher than  $100 \text{ mg L}^{-1}$  a decrease of removal was observed because the increase of concentration are not proportional to the increase of number of active sites occupied by the adsorbate (DCF). The values of 200 was evidenced as the ratio  $[DCF]/[TPEG]$  of maximum

removal observed, therefore for values of initial concentration of DCF higher than  $100 \text{ mg L}^{-1}$  an increase of TPEG are necessary to maintain the ratio at 200 and ensure the maximum removal reached (69%). For that described reason, in the scale up of the process it is necessary to decide what parameters would be maximized for value of initial concentration higher than  $100 \text{ mg L}^{-1}$ . In order to maximize the removal, more than 10 mg of TPEG are required but a decrease of adsorption capacity will be observed because of more adsorbent material will be used.

### 3.3 Adsorption kinetics

Figure 39 shows the study of kinetics adsorption by varying the contact time in the range 3 - 40 minutes. Removal and adsorption capacity observed at different time of contact are reported.

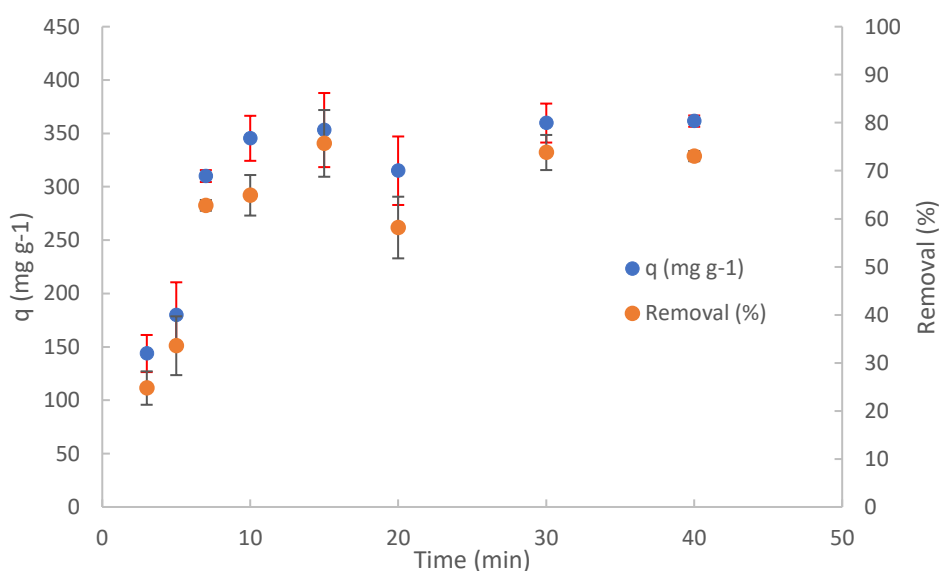


**Fig. 39** Kinetic trend and standard deviation of experimental data of adsorption capacity and removal with contact time.  $C_0= 100 \text{ mg L}^{-1}$ , Solution volume= 50 mL, pH=1, mass of adsorbent= 10 mg, stirring speed= 650 rpm. Some values of standard deviation are lower than surface area of indicators.

An increase of adsorption capacity with the increase of contact time can be observed in the first 10 minutes of treatment, then a plateau is reached. Therefore, the optimum contact time is 10 minutes, corresponding to the maximum adsorption capacity of about  $350 \text{ mg g}^{-1}$ . Table 11 summarizes the kinetic parameters and the coefficient of correlation obtained by fitting experimental data with the previous cited kinetic models.

**Tab. 11.** Fitting of experimental data with theoretical kinetics models

Model	$R^2; \chi^2$	Parameters
Pseudo-first order	0.5519; 18	$K_1=3.44 \cdot 10^{-2} \text{ min}^{-1}$ $q_e= 10^5 \text{ mg g}^{-1}$
Pseudo-second order	0.9818; 0.16	$q_e= 400 \text{ mg g}^{-1}$ $k_2=6.6 \cdot 10^{-4} \text{ g mg}^{-1} \text{ min}^{-1}$
Elovich	0.7222; 1.8	$\beta=1.2 \cdot 10^{-2} \text{ mg g}^{-1} \text{ min}^{-1}$ $\alpha=267.5 \text{ g mg}^{-1}$
Liquid film diffusion	0.5519; 5	$K_{fd}=0.0334 \text{ min}^{-1}$
Intraparticle diffusion	0.5873; 4.3	$K_{dif}=40.812 \text{ mg g}^{-1} \text{ min}^{-1/2}$ $C=143.43$

The results show that the pseudo-second order model is the best fitting of the experimental data. Particularly, the adsorption capacity obtained from the pseudo-second order kinetic model ( $400 \text{ mg g}^{-1}$ ) is close to the experimental data obtained for long contact time (i.e. 22 hours,  $420.5 \text{ mg g}^{-1}$ ). The value of kinetic constant ( $k_2:6.6 \cdot 10^{-4} \text{ g mg}^{-1} \text{ min}^{-1}$ , at room temperature) is comparable with that obtained in literature (i.e.  $10^{-2}/10^{-3}$ ) (Jodeh et al. 2015; Bhadra et al. 2016). Because of the pseudo second order model regulates the process, it is possible to conclude that by increasing two times the concentration of DCF an increase of four times of the rate of the process are observed. By considering that the kinetics model that regulate the process is the pseudo-second order model, we can conclude that the slowly step of the process resulted to be the interaction (the formation of the bond) between adsorbate and adsorbent active sites. By the pseudo-second order model is not possible to distinguish between physical adsorption, such as electrostatic interaction, and chemical adsorption, such as amide formation. To evaluate about the type of the interaction, thermodynamics evaluation, by considering the free energy, is necessary and for this reason were conducted and reported in section 3.6. To resume here the results obtained, physical-adsorption can be designed as mechanism of adsorption of DCF on TPEG because of the free energy value lower of  $30 \text{ kJ mol}^{-1}$ . Van der Waals force and other hydrophobic interactions can be designed as main interactions involved into the adsorption process. As expected, liquid film diffusion rate step was increased by the agitation of the solution and it was not the limiting step of the process. The intraparticle diffusion step was not

the limiting step probably due the dimension of pores that ensures fast diffusion of the molecules of DCF into the pores and reaching and approaching the active surface of the adsorbent (dimension of pores  $\gg$  dimension of DCF). Elovich and pseudo-first order model also involve as limiting step the interaction between adsorbate and adsorbent active sites but they differ from pseudo-second order model because the adsorbent site are heterogeneous for Elovich model and the rate of the process increase two times if an increase of two times of adsorbate (DCF) is observed. By considering that, to improve the rate of the process modification of the surface of the material must been conducted. Amino functionalization of the surface could improve the reactivity of the material for the adsorption of DCF, because the presence of the amino group could interact with acid group of DCF and form amide bond. If amino functionalization will be conducted, the addition of substance in the solution or adsorbed on TPEG surface with the capacity of catalyze the amide bond could further improve the rate of the process. By considering the kinetics studies, it is possible to conclude that diffusion of DCF into the mesopores and micropores of TPEG to approach the surface of it, where are involved physical interactions able to “entrap” the molecules of DCF. The same shape of the adsorption capacity was observed obviously for the removal. By increasing the time of contact an increase of removal until to reach the maximum removal of about 73%. The maximum removal was almost reached after ten minutes of contact. The value of adsorption capacity calculated from the pseudo-first order is an unrealistic value and it confirms that model as no adequate to describe the process.

### ***3.4 Adsorption isotherms***

Figure 40 shows the obtained results for the removal and adsorption capacity for different value of equilibrium concentration of DCF in the solution. As expected, the adsorption capacity increases with the increase of the pollutant concentration, reaching the adsorbent saturation represented by the plateau. The removal of DCF reach a maximum value and then it decreased because the increase of molecules of DCF is not proportional to the increase of the number of active sites occupied.



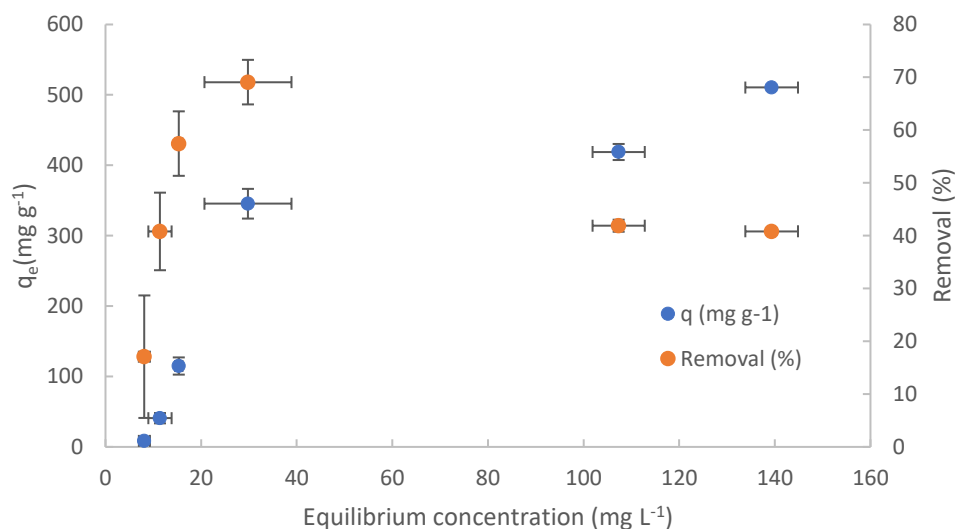


**Fig. 40** Equilibrium adsorption of DCF on TPEG.  $C_0=10, 20, 40, 100, 200$  and  $250 \text{ mg L}^{-1}$ ,  $\text{pH } 1$ ,  $10 \text{ mg}$  of adsorbent material, stirring speed= $650 \text{ rpm}$ , contact time= $10$  minutes. Standard deviation for adsorption capacity and equilibrium concentration are also reported (some values are lower than the indicator surface).

The results of experimentations demonstrate that the best fitting was obtained with the Dubinin-Radushkevich model with  $R^2 = 0.9903$  and  $\chi^2=0.15$ , proving that the adsorption occurs on a heterogeneous surface with steric hindrance between adsorbed and incoming particles. For the Langmuir model, Freundlich model and Temkin model values of  $R^2$  of 0.058, 0.7596 and 0.9372 and  $\chi^2$  of 18, 2.1 and 0.98 were obtained, respectively. Values of  $433.29 \text{ mg g}^{-1}$ ,  $5 \cdot 10^{-5} \text{ mol}^2 \text{ J}^2$  and  $-0.1 \text{ kJ mol}^{-1}$  were observed for adsorption capacity, constant of Dubinin-Radushkevich and free energy, respectively, calculated from the model. Particularly, the value of adsorption capacity calculated from this model ( $433.29 \text{ mg g}^{-1}$ ) is in good accordance with the value calculated from kinetic study ( $400 \text{ mg g}^{-1}$ ). The Dubinin-Radushkevich model are typical of process of adsorption that involve a formation of multilayers. Normally, multilayer adsorption involves two or more plateau of adsorption capacity because of a multilayer of adsorbate can be formed after the totally covering of adsorbent surface. In the figure 40, just one plateau can be observed, probably because the first one could be observed for equilibrium concentration lower than that investigated in this work. Furthermore, to prevent the steric hindrance between adsorbed molecules and incoming ones, can be useful to increase the surface area of TPEG to delay that hindrance as much as possible and increase the adsorption capacity and formation of more layer of adsorbate. Furthermore, the adsorption isotherm shape seems to have the typical shape of adsorption isotherm of type IV, characteristic of system that present mesopores and phenomena of pore blocking caused by the steric hindrance. Another

consideration useful that can be deduced by the isothermal fitting is the best correlation with model that assume heterogeneous surface of the adsorbent material (Temkin, Dubinin-Radushkevich).

The comparison between our results and those obtained in literature using other adsorbent materials is reported in Table 12, demonstrating the excellent adsorbent properties of TPEG. In some cases, the higher adsorption capacity observed cannot be related to the surface area of the material ( $47 \text{ m}^2 \text{ g}^{-1}$ ) because it is not higher than the values observed for some materials listed in the table for the comparison, such as CNT/ $\text{Al}_2\text{O}_3$  ( $237 \text{ m}^2 \text{ g}^{-1}$ ), UiO-66 ( $1710 \text{ m}^2 \text{ g}^{-1}$ ) and zeolite modified with cetylpyridiumchloride ( $712 \text{ m}^2 \text{ g}^{-1}$ ). In that cases the higher adsorption capacity can be related to the stronger interaction between DCF and TPEG. For the comparison with grape bagasse, higher surface area was observed for TPEG ( $47 \text{ vs } 2 \text{ m}^2 \text{ g}^{-1}$ ) and the higher adsorption capacity of TPEG could be also related to the higher surface of TPEG.

**Tab. 12. Comparative data of adsorbent material for removal of DCF**

Adsorbent material	Adsorption capacity (mg $\text{g}^{-1}$ )	Interaction	Reference
Thermo-plasma expanded graphite	433.29 (from isotherm) 400 (from kinetics)	Hydrophobic and heterogeneous carbon surface	This work
Grape bagasse	77	Electrostatic	33
CNT/ $\text{HNO}_3$	24	-	17
CNT/ $\text{Al}_2\text{O}_3$	27	$\pi$ - $\pi$ and van der Waals force	18
Expanded graphite	330	Hydrophobicity and energetically uniform carbon surface	34
GO	500	Hydrophobic and $\pi$ - $\pi$	34
UiO-66	189	Electrostatic	35

OAC (2.0)	487	Electrostatic and H-bonding	32
Commercial AC	76	Electrostatic	32
Zeolite modified with cetylpyridiumchloride	160	Electrostatic and hydrophobic	36

### 3.5 Thermodynamic study

The best fit is represented by Equation 15 with  $R^2 = 0.9992$ .

$$y = -4665.3x + 17.173 \quad (15)$$

Therefore, the value of enthalpy and entropy obtained are  $38.70 \text{ kJ mol}^{-1}$  and  $142.77 \text{ J mol}^{-1} \text{ K}^{-1}$ , respectively. The driving force of the process is represented by the increase of entropy, associated to the increase in randomness at solid/solution interface during the adsorption process. The process is endothermic and a temperature above  $271 \text{ K}$  is required to ensure spontaneity of the process. Table 13 shows both the experimental and theoretical values of equilibrium constant ( $\frac{q_e}{c_e}$ ) and free energy obtained from enthalpy and entropy values after the fitting. Experimental and theoretical data are comparable, confirming the fitting accuracy. Furthermore, the negative value of free energy confirms the spontaneity of the process.

**Tab. 13. Thermodynamics evaluation of the adsorption process.**

Temperature (K)	$\frac{q_e}{c_e}$ experimental (mg L)	$\frac{q_e}{c_e}$ theoretical (mg L)	$\Delta G^0$ experimental (kJ mol <sup>-1</sup> )	$\Delta G^0$ theoretical (kJ mol <sup>-1</sup> )
293	3.58	3.64	-3.10	-3.14
299	5.04	4.97	-4.18	-4.14
311	9.02	9.05	-5.46	-5.47

The standard free energy is comparable with values reported in literature and indicates a physical adsorption of DCF on TPEG. The endothermicity of the process guarantees the possibility to improve the performance of the process by increasing the temperature of the batch. It indicates that the interaction between particles of DCF with itself is strongly than the interaction between DCF and TPEG surface and it can also explain the formation of multilayer of DCF on the surface of the TPEG. The major disorder caused by the breaking of bonding

between of particles of DCF that were blocked casually on the surface of the TPEG is the driving force of the process. The comparison with other free energy of the adsorption of DCF on other material reported in literature demonstrated that the free energy of the adsorption on TPEG is one of the higher (considering the absolute value), therefore the process of adsorption is favored (higher free energy means higher equilibrium constant). The free energy calculated for the adsorption of DCF on TPEG was  $-4.18 \text{ KJ mol}^{-1}$ , while values of  $-4.30$ ,  $3.97$  and  $-0.99 \text{ KJ mol}^{-1}$  are reported in literature for adsorption on CNT/ $\text{HNO}_3$  [18], grape bagasse [33] and Zeolite modified with cetylpyridiumchloride [36], respectively.

### 3.6 Regeneration and reuse of TPEG

Figure 41 shows TPEG performance after the regeneration process.

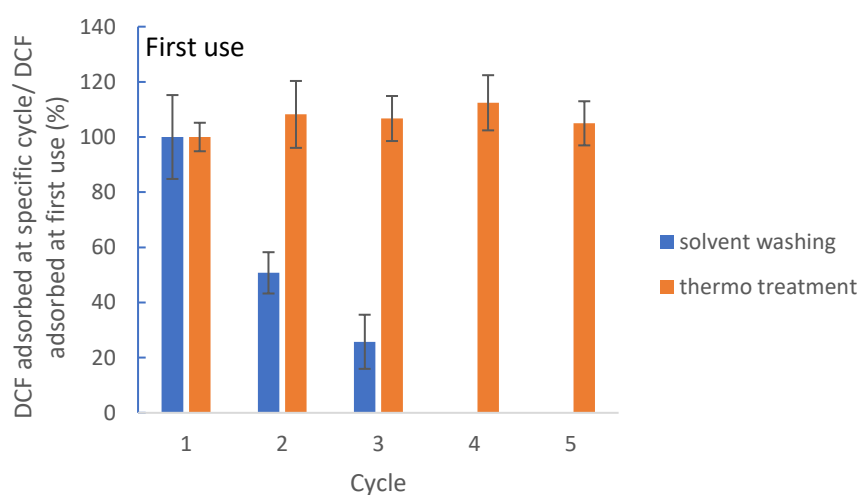


**Fig. 41 Performance of material after recovery treatment. Recovery performed by solvent washing with  $\text{NaOH}$  0,2 M for 3 hours at stirring speed of 800 rpm and thermo treatment at  $105^\circ\text{C}$  for 2 hours and  $200^\circ\text{C}$  for 4 hours. Adsorption step was done by using DCF 20 mg/L, pH 1, stirring speed of 650 rpm, contact time of 10 minutes and 10 mg of adsorbent material. Standard deviation of each experimental data is also reported.**

The thermo recovery results to be the best way to recover TPEG because the amount of adsorbed DCF after each cycle is comparable to that of pure TPEG. After four cycles of thermo treatment the relative adsorption capacity results to be about 100%, proving that by heating the material all the DCF adsorbed on it is released and all the sites available for the adsorption interact with other molecules. The solvent washing is not a good way to recover the material because the high solubility of DCF in basic solutions is not enough to desorb DCF from TPEG. The relative  $q_e$  is about 50% and 25% after the first and second treatment, respectively. The

reduction of relative  $q_e$  by using solvent washing is also justified by the loss of material during the separation water-TPEG. There is a technical limit due to the impossibility to do the filtration because the powder of the adsorbent material remains on the filter paper.

#### 4. Conclusions

In this study, TPEG was proposed as a good adsorbent material for DCF adsorption and removal from water. The morphological and structural analysis of TPEG demonstrates the presence of layers of sheet ( $n > 5$ ) of graphene packed together, dimension of 24.02 nm of the crystallite and a surface area of about  $47 \text{ m}^2 \text{ g}^{-1}$ . The point of strength of this material seems to be the possibility to reuse it without decreasing its adsorption performance by using a regeneration process not economically expensive (thermo-treatment). The adsorption results to be endothermic ( $38.70 \text{ kJ mol}^{-1}$ ) and the driving force of the process is the increase of entropy ( $142.77 \text{ J mol}^{-1} \text{ K}^{-1}$ ) at the surface of the material caused by the increasing of disorder generated after the breaking of the interaction between the particles of DCF and their casual disposition on the surface of TPEG. The thermodynamics studies (free energy observed,  $\Delta G^0$ :  $-4.18 \text{ kJ mol}^{-1}$ ) suggest that physio-adsorption is involved. Pseudo-second order model regulates the kinetics of the process and Dubinin-Radushkevich model regulates the isotherm adsorption, therefore multilayer adsorption can be deduced as mechanism of adsorption. Values of adsorption capacity of about  $400 \text{ mg g}^{-1}$  was obtained by both the kinetics and isotherm experiments. The diffusion of DCF in the solution and into the pores of the material are faster than the “bonding” formation between DCF and active sites of TPEG. Even if the diffusion is faster than interaction on the active sites of TPEG, steric hindrance is involved caused by the formation of multilayer of DCF on the surface of TPEG. The pH influence on the adsorption process demonstrates that solubility of DCF deeply affects the adsorption process. Furthermore, the effect of initial concentration of DCF on adsorption capacity and the removal was evaluated and the ratio of 200 of  $[\text{DCF}]/[\text{TPEG}]$  was evidenced as the optimum ratio of maximum removal. By considering the experiments conducted in this work, it is possible to conclude that increase of surface area of TPEG and functionalization of TPEG surface can be useful to improve the rate of the process by increasing the rate of the interaction between DCF and active sites and to delay the pore blocking and increase the adsorption capacity. Further studies can be conducted on this material, in particular, its oxidation, magnetization or transformation of its morphology and then the evaluation of its adsorption capacity, the kinetics and the thermodynamics of the process of adsorption of same or new contaminants. Another useful study could be the use of

TPEG as a filter to adsorb the same contaminant, so that the separation of treated water and TPEG is easier.

## 5. Reference

- [1] Heberer, T., 2002. Occurrence, fate and removal of pharmaceutical residues in the aquatic environment: a review of recent research data, *Toxicol. Lett.*, 131, 5-17.
- [2] Dutta, K., Lee, M.Y., Lai, W.W.P., Lee, C.H., Lin, A.Y.C., Lin, C.F., Lin, J.G., 2014. Removal of pharmaceuticals and organic matters from municipal wastewater using two-stage anaerobic fluidized membrane bioreactor, *Bioresour. Technol.*, 165, 42-49.
- [3] Zhou, J.I., Zhang, Z.I., Banks, E., Grover, D., Jiang, J.Q., 2009. Pharmaceuticals residues in wastewater treatment works effluents and their impacts on receiving river water, *J. Hazard. Mater.*, 166, 655-661.
- [4] Luo, Y., Guo, W., Ngo, H.H., Nghiem, L.D., Hai, F.I., Zhang, J., Liang, S., Wang, X.C., 2014. A review on the occurrence on micropollutant in the aquatic environment and their fate and removal during wastewater treatment, *Sci. Total Environ.*, 473-474, 619-641.
- [5] Evgenidou, E.N., Konstantinou, I.K., Lambropoulou, D.A., 2015. Occurrence and removal of transformation products of PPCPs and illicit drugs in wastewater: a review, *Sci. Total Environ.*, 505, 905-926.
- [6] Zhang, D., Gersberg, R.M., Ng, W.J., Tan, S.K., 2014. Removal of pharmaceuticals and personal care products in aquatic plants-based systems: a review, *Environ. Pollut.*, 184, 620-639.
- [7] Villaescusa, I., Fiol, N., Poch, J., Bianchi, A., Bazzicalupi, C., 2011. Mechanism of paracetamol removal by vegetable wastes: the contribution of  $\pi$ - $\pi$  interactions, hydrogen bonding and hydrophobic effect, *Desalination*, 270, 135-142.
- [8] Dominguez, J.R., Gonzalez, T., Palo, P.E., Cuerda-Correa, M., 2011. Removal of common pharmaceuticals present in surface waters by Amberlite XAD-7 acrylic -esterresin: influence of pH and presence of other drugs, *Desalination*, 269, 231-238.
- [9] Busar, H.R., Poiger, T., Muller, M.D., 1998. Occurrence and fate of pharmaceutical drug diclofenac in surface waters: rapid biodegradation in a lake, *Environ. Sci. Technol.*, 32, 3449-3556.

- [10] Boyda, G.R., Reemtsma, H., Grimmb, D.A., Mitrac, S., 2003. Pharmaceuticals and personal care products (PPCPs) in surface and treated waters of Louisiana; USA and Ontario, Canada, *Sci. Total Environ.*, 311, 135-149.
- [11] Joss, A., Zabczynski, S., Gobel, A., Hoffmann, B., Loffler, D., McArdell, C.S., Ternes, T.A., Thomsen, A., Siegrist, H., 2006. Biological degradation of pharmaceuticals in municipal wastewater treatment: proposing a classification scheme, *Water Res.*, 40, 1686-1696.
- [12] Boyd, G.R., Zhang, S., Grimm, D.A., 2005. Naproxen removal from water by chlorination and biofilm processes, *Water Res.*, 39, 668-676.
- [13] Esplugas, S., Bila, D.M., Gustavo, L., Krause, T., Dezotti, M., 2007. Ozonation and advanced oxidation technologies to remove endocrine disrupting chemicals (EDCs) and pharmaceuticals and personal care products (PPCPs) in water effluents, *J. Hazard. Mater.*, 149, 631-642.
- [14] Sotelo, J.L., Ovejero, G., Rodriguez, A., Alvarez, S., Galan, J., Garcia, J., 2014. Competitive adsorption studies of caffeine and diclofenac aqueous solutions by activated carbon, *Chem. Eng. J.*, 240, 443-453.
- [15] Yu, Z., Peldszus, S., Huck, P.M., 2008. Adsorption characteristic of selected pharmaceuticals and an endocrine disrupting compound-naproxen, carbamazepine and nonylphenol-on activated carbon, *Water Res.*, 42, 2873-2882.
- [16] Bhadra, B.N., Cho, K.H., Khan, N.A., Hong, D.Y., Jung, S.H., 2015 Liquid-phase adsorption of aromatics over a metal-organicframework and activated carbon: effects of hydrophobicity /hydrophilicity of adsorbent and solvent polarity, *J. Phys. Chem. Lett.*, 119, 26620-26627.
- [17] Hu, X., Cheng, Z., 2015. Removal of diclofenac from aqueous solution with multi-walled carbon nanotubes modified by nitric acid, *Chin. J. Chem. Eng.*, 23, 1551-1556.
- [18] Wei, H., Deng, S., Huang, Q., Nie, Y., Wang, B., Huang, J., Yu, G., 2013. Regenerable granular carbon nanotubes/alumina hybrid adsorbent for diclofenac sodium and carbamazepine removal from aqueous solution, *Water Res.*, 47, 4139-4147.
- [19] Nam, S.W., Jung, C., Li, H., Yu, M., Flora, J.R.V., Boateng, L.K., Her, N., Zoh, K.D., Yoon, Y., 2015. Adsorption characteristic of diclofenac and sulphamethoxazole to graphene oxide in aqueous solution, *Chemosphere*, 136, 20-26.

- [20] Jaurius, I.M., Matos, C.F., Saucier, C., Lima, E.C., Zarbin, A.J.G., Fagan, S.B., Machado, F.M., Zanella, I., 2016. Adsorption of sodium diclofenac on graphene: a combined experimental and theoretical study, *Phys. Chem. Chem. Phys.*, 18, 1526-1536.
- [21] Boyda, G.R., Reemtsma, H., Grimmb, D.A., Mitrac, S., 2003. Pharmaceuticals and personal care products (PPCPs) in surface and treated waters of Louisiana; USA and Ontario, Canada, *Sci. Total Environ.*, 311, 135-149.
- [22] Masi, S., Calace, S., Mazzone, G., Caivano, M., Buchicchio, A., Pascale, S., Bianco, G., Caniani, D. Lab-scale investigation on remediation of sediments contaminated with hydrocarbons by using super-expanded graphite, 15th International Conference on Environmental Science and Technology Rhodes, Greece, 31 August to 2 September 2017.
- [23] Qiu, H., Lv, L., B.-cPan, Zhang, Q.-j., Zhang, W-m., Zhang, Q.-x., 2009. Critical review in adsorption kinetic models, *Journal of Zhejiang University SCIENCE A*, 10(5), 716-724.
- [24] Ho, Y.S., McKay, G., 1999. Pseudo-second order model for sorption process, *Process Biochem*, 34, 451-465.
- [25] Low, M.J.D., 1960. Kinetics of chemisorption of gases on solids, *Chem. Rev.*, 60(3), 267-312.
- [26] Langmuir, I., 1918. The adsorption of gases on plane surfaces of glass, mica and platinum, *J. Am. Chem. Soc.*, 1918, 1361-1402.
- [27] Freundlich, H. M. F., 1906. Over the adsorption in solution, *Journal of Physical Chemistry*, 57, 385-471.
- [28] Temkin, M.I., Pyzhev, V., 1940. Kinetics of ammonia synthesis on promoted iron catalyst, *Acta Physical Chemistry USSR*, 12. 327-357.
- [29] Dubinin, M.M., Radushkevich, L.V., 1947. The equation of characteristic curve of the activated charcoal, *Proceedings of the Academy of Science of the USSR Physical Chemistry Section*, 55, 331-337.
- [30] Baghdadi, M., Ghaffari, E., Aminzadeh, B., 2016. Removal of carbamazepine from municipal wastewater effluent using optimally synthesized magnetic activated carbon: Adsorption and sedimentation kinetic studies, *J. Environ. Chem. Eng.*, 4, 3309-3321.



- [31] Jodeh, S., Abdelwahab, F., Jaradat, N., Warad, I., Jodeh, W., 2015. Adsorption of Diclofenac from aqueous solution using Cyclamen persicum tubers based activated carbon (CTAC). *J Assoc Arab Univ Basic Appl Sci*.
- [32] Bhadra, B.N., Seo, P.W., Jhung, S.H., 2016 Adsorption of diclofenac sodium from water using oxidized activated carbon, *Chem. Eng. J.*, 301, 27-34
- [33] Antunes, M., Esteves, V.I., Guégan, R., Crespo, J.S., Fernandes, A.N., Giovanela, M., 2012. Removal of diclofenac sodium from aqueous solution by Isabel grape bagasse, *Chem. Eng. J.*, 192, 114-121.
- [34] Vedenyapina, M.D., Borisova, D.A., Simakova, A.P., Proshina, L.P., Aedenyapin, A.A., 2013. Adsorption of diclofenac sodium from aqueous solution on expanded graphite, *Solid Fuel Chemistry*, 47, 59-63.
- [35] Lin, K.Y.A., Yang, H, Lee, W.D., 2015. Enhanced removal of diclofenac from water using a zeolitic imidazole framework functionalized with cetyltrimethylammonium bromide (CTAB), *RSC advanced*, 5, 81330-81340.
- [36] Suriyanon, N., Punyapalakul, P., Ngamacharussrivichai, C., 2013. Mechanistic study of diclofenac and carbamazepine adsorption on functionalized silica-based porous materials, *Chem. Eng. J.*, 208-218.

### **2.3 “Hydro-soluble” thermo-plasma expanded graphite: preparation, low pressure injectable permeable reactive barrier and adsorption of BTEX study**

#### **Abstract**

Nowadays, public interest about environmental pollution has increased and many researches are focused on the groundwater remediation. Benzene, toluene, ethylbenzene and xylenes (BTEX) are the typical molecules associated to gasoline pollution, caused by accidental leakage of petrol or diesel. They are designed as pollutants of primary importance and the maximum permissible concentrations of benzene, toluene, ethylbenzene and xylene in drinking water are respectively 0.01, 0.7, 0.3 and 0.5mg L<sup>-1</sup>. Different methods of BTEX remediation are available, such as chemical oxidation, biological degradation and air stripping, but the adsorption process seems to be more favored for its low-cost technology and absence of metabolites. Adsorption process for groundwater remediation requires excavation of the soil and installation of permeable reactive barrier (PRBs), but a new technology is developing by

academic world: low pressure injectable permeable reactive barrier. This technology allows to install PRBs without excavation of the soil. In order to achieve this aim, a “hydro-soluble” thermo-plasma expanded graphite (TPEG) was synthesized and its adsorption properties were evaluated. Furthermore, its injectability and adsorption after the injection was evaluated. Values of adsorption capacity of 18.91, 16.54, 22.24 and 19.81 mg g<sup>-1</sup> was obtained respectively for toluene, ethylbenzene, *m,p*-xylenes and *o*-xylene and different kinetics models were followed by varying the initial concentration of pollutants. Mono-layer adsorption was observed for toluene and multi-layer adsorption was observed for the other compound. Humic acid enhances the adsorption capacity until to reach value of adsorption capacity of about 400 mg g<sup>-1</sup> for ethylbenzene and about 150 mg g<sup>-1</sup> for the other molecules, while values of pH > 7 promote the process. The influence of the pressure on the injection step was evaluated and was observed that the “hydro-soluble” TPEG was able to act as permeable reactive barrier when injected into water-saturated soil with pollutants removal of about 90%.

## **1.Introduction**

In recent years, public concern has increased considerably due to environmental pollution, which is becoming an increasingly widespread problem that affects both the environment and human health. Among the main consequences of pollution there is the destruction of natural resources such as water, air and soil and the onset of new diseases, some of which cause malfunctions of the respiratory system, heart disease, skin and allergies. There are many sources of contamination: industrial activities, urban traffic, waste, and the effluents that come from agriculture. One of the most important sources of contamination is the leakage of petrol and diesel from underground tanks. Once this release occurs, the gasoline, which is a mixture of volatile and semi-volatile hydrocarbons, including benzene, toluene, ethylbenzene and xylene (BTEX), contaminates the soil and can move inside and contaminate the water underground [1]. The ever-increasing pollution has pushed towards the search for new technologies capable of controlling or removing VOCs (volatile organic compounds), including BTEX. The USEPA (Environmental Protection Agency of the United States) has classified BTEX as pollutants of primary importance and whose concentration must be significantly reduced both in wastewater and in soil. According to the guidelines of the WHO (World Health Organization), the maximum permissible concentrations of benzene, toluene, ethylbenzene and xylene in drinking water are respectively 0.01, 0.7, 0.3 and 0.5mg L<sup>-1</sup>. Some treatment methods such as chemical oxidation [2,3,4], biological treatments [5,6,7] and air stripping [8] have shown excellent results for the removal of BTEX from water but, among the innovative treatments, the adsorption

process is one of the best for the removal of these contaminants from aqueous solutions because is a low-cost technology, characterized by operational simplicity, and no metabolites are produced and no new chemical species are introduced into the treated water [9,10,11]. Furthermore, in the last years, innovative technologies are developing in the branch of permeable reactive barrier (PRBs) for in-situ groundwater remediation. The classic method PRBs is normally used for groundwater remediation [12,13,14], but it involves expensive and long-time work of installation because of excavation of soil, preparation of a vessel for reactive material and filling of the vessel are required. Several research teams are focusing their attention on the production of reactive materials that don't require excavation and vessel preparation for their installation. This objective was reached by preparing hydro-soluble reactive material and some example are reported in literature [15,16], as particular mineral phase of calcium phosphate and innocuous vegetable oil. The hydro-soluble material can inject into groundwater without excavation step. The purpose of this work consists of to produce a new material, which can be injected at low pressure into a groundwater, that is able to remove the BTEX through a characterized adsorption process. In order to achieve this goal, the thermo-plasma expanded graphite [17,18,19] (TPEG) was transformed in a "hydro-soluble" material (in the commercial form it floats on water and is therefore not injectable). Sonication was chosen and tested as method to transform insoluble TPEG in "hydrosoluble" TPEG. Mechanical exfoliation is involved with the sonication, indeed, bubbles which collapsing on the surface of the graphite, generate compression waves, leading to the exfoliation. A secondary process can also occur as a lateral compression wave can be generated which is able to separate two adjacent layers of graphite with a cutting effect or through a "wedge" effect. The cutting effect could reduce the dimension of the particle of graphite until dimension that allows the formation of colloids or dispersion [20]. The described process is reported in schematic form in the figure 42.

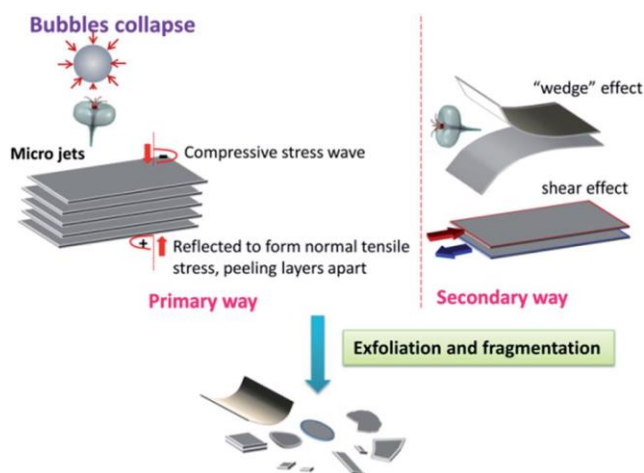


***Fig. 42 Schematic representation of exfoliation and fragmentation involved in the sonication process***

After the transformation of TPEG, the adsorption process of BTEX in aqueous solution on “hydro-soluble” TPEG surface was investigated. Kinetics, isotherm, influence of initial concentration of pollutants, co-presence of pollutants, pH and presence of humic acid was investigated. The injectability and the eventually leaching of the new form of the material was also investigated before to evaluate if adsorption properties were preserved when injected in a water-saturated soil.

## **2. Materials and Methods**

### ***2.1 Materials and Chemicals***

TPEG was obtained from Innograf, that produced it from natural graphite, intercalated with chemical compound and expanded by the thermal plasma expansion. This process ensures the exfoliation of graphite, with a volume expansion of up to 300 units, compared to an average of 200 units obtainable by other standard methods. TPEG has good structural properties, such as mechanical strength of about 1 TPa, a thermal conductivity of about 500 W mK<sup>-1</sup>, a diameter between 60 and 300 μm and high apparent density that could be associated with high surface area, property that can confer high adsorption capacity.

Toluene, ethylbenzene, *o*, *m*, *p*-xylenes, methanol, humic acid, HCl and NaOH were supplied from Carlo Erba reagents (Carlo Erba, Rodano, Milano, Italy). The stock solutions of all the aromatic compounds were prepared in methanol at a concentration of 2 g L<sup>-1</sup>. Solutions of all aromatic compounds used for adsorption experiment were prepared in distilled water with 1% of MeOH. All reagents were of extra pure grade and used without further purification. Sandy soil was used, and it was sieved between 2 mm and 62.5 μm to eliminate particles with dimension different from sand. 37.28 % of particles had a diameter between 1 and 2 mm, 60.82 % had a diameter between 500 μm and 1 mm, 0.67 % had a diameter between 250 and 500 μm, 1.04 % had a diameter between 125 and 250 μm, 0.16 % had a diameter between 75 and 125 μm and 0.01 % had a diameter between 62.5 and 75 μm. The porosity resulted to be 34 %.

For the sonication step a SONOREX ultrasonic bath RK 52 was used with a frequency of 35 kHz.

For injection step test a peristaltic pump PLP 380 of Labor-Technik with a pump head PPH 103. Tubes with internal diameter of 7.94 mm of TYGON (formulation E-LFL). These tubes ensure a flow rate between 0.4 and 138 mL min<sup>-1</sup>.

## ***2.2 Methods***

### ***2.2.1 Sonication of TPEG***

In order to reduce the particle dimension of TPEG, ultrasonication method was used. 0.2 g of TPEG was added to 400 mL of distilled water in a beaker of 1 L and the solution was putted in the ultrasonic bath for about 50 hours.

### ***2.2.2 Adsorption test in liquid solution***

#### ***2.2.2.1 Kinetics studies***

To evaluate the kinetics of the process, different volume of stock solution of toluene or ethylbenzene or xylenes were added to 36 mL of “hydro-soluble” TPEG (0.02 g) at 1% MeOH to obtain an initial concentration of 5, 10 and 20 mg L<sup>-1</sup> (when referred to xylenes, 20 mg L<sup>-1</sup> was the sum of the three types) and the residual concentration was evaluated at the different time. The value of adsorption capacity at different time was plotted. The equations used for the kinetics studies are the same reported in the chapter 2.1.

#### ***2.2.2.2 Isotherm adsorption evaluation***

The adsorption isotherm of the process was evaluated for each compound one by one. For this reason, different volume of stock solution of toluene or ethylbenzene or xylenes were added to 36 mL of “hydro-soluble” TPEG (0.02 g) at 1% MeOH in a sealed vials (to avoid volatilization loss) to obtain different initial concentration (range of 2.5-180 mg L<sup>-1</sup>) and the residual concentration was evaluated after 6 hours of contact. The value of the adsorption capacity at different residual concentration was plotted for each compound. The different models used to evaluate the adsorption isotherm are that reported in the chapter 2.1.

#### ***2.2.2.3 Influence of initial concentration***

The initial concentration of adsorbate influences the adsorption capacity and the evaluation of its influence is an important variable to know when an industrial interview is projected. For this reason, different volume of stock solution of toluene or ethylbenzene or xylenes were added to 36 mL of “hydro-soluble” TPEG (0.02 g) at 1% MeOH in a sealed vials (to avoid volatilization loss) to obtain different initial concentration (from 2.5 at 40 mg L<sup>-1</sup> for ethylbenzene, from 5 to

60 mg L<sup>-1</sup> for toluene and from 5 to 80 mg L<sup>-1</sup> for xylenes) and the residual concentration was evaluated after 20 hours of contact. The plot of adsorption capacity for the different initial concentration was done.

#### ***2.2.2.4 Influence of co-presence of each contaminant on adsorption capacity***

When more component can be adsorbed on the surface of adsorbent different condition can be observed. If the adsorbates don't compete for the same active sites, the adsorption capacity isn't affected by co-presence of adsorbate, while if they can compete for the same active sites and the adsorption capacity of each compound results to be lower than when only one component is present. When competition happens, the compound with high affinity and/or faster process is adsorbed in major amount and only the adsorption capacity of the other compounds is affected. In some cases of no-competition, the adsorption capacity of some compounds can be affected by the steric hindrance caused by faster adsorbed molecules of other contaminants that could impede the entrance in the pores of adsorbent material. In order to evaluate the effect of co-presence of all the compound examined in this study, different volume of stock solution of toluene, ethylbenzene and xylenes were added to 36 mL of "hydro-soluble" TPEG (0.02 g) at 1% MeOH in a sealed vials (to avoid volatilization loss) to obtain different initial concentration (5, 10 and 20 mg L<sup>-1</sup> of each compound) and the residual concentrations were evaluated after 20 hours of contact. The adsorption capacity obtained were compared with the value obtained when single-compound solutions were used to evaluate the adsorption capacity. This step was very useful because normally BTEX are present together in polluted water.

#### ***2.2.2.5 Influence of presence of humic acid on adsorption capacity***

Humic acid can be adsorbed on graphitic surface [30,31] and itself can adsorb molecules of BTEX<sup>32,33</sup>, therefore it is clear that it can influence the adsorption capacity of BTEX on TPEG. Humic acid is one major component of soil, therefore it is present in groundwater and its influence on adsorption capacity of BTEX resulted to be fundamental as parameter to investigate in this work. For this reason, 36 mL of "hydro-soluble" TPEG (0.02 g) at 1% MeOH in a sealed vials (to avoid volatilization loss) with concentration of toluene, ethylbenzene and xylenes at 20 mg L<sup>-1</sup> for each compound was added humic acid to obtain different concentration (12.5, 25, 50 and 100 mg L<sup>-1</sup>). The residual concentrations were evaluated after 20 hours of contact and all the obtained adsorption capacity were compared with values obtained when humic acid was not present.

#### ***2.2.2.6 Influence of pH***

The pH of solution can influence the adsorption capacity of “hydrosoluble” TPEG because the sonication could be partially oxidizing its surface. To verify it, the adsorption capacity was evaluated at different initial value of pH (3.8, 7.6, 10). The initial concentration of each contaminants was fixed at  $20 \text{ mg L}^{-1}$  and the residual concentrations were evaluated after 20 hours of contact. The values obtained were compared to verify the influence of the pH. The initial pH was modified by adding concentrated HCl and NaOH and controlling it by pHmeter.

### 2.2.3 Injection and leaching test

To verify the possibility to inject the “hydro-soluble” form of TPEG in a groundwater, several experiment at laboratory scale were done. A burette of 10 mL was filled with water-saturated soil and connected to a reservoir tank of solution of “hydro-soluble” TPEG that was pumped in the soil chamber by the peristaltic pump. The set-up of the experiment is reported in the figure 44.

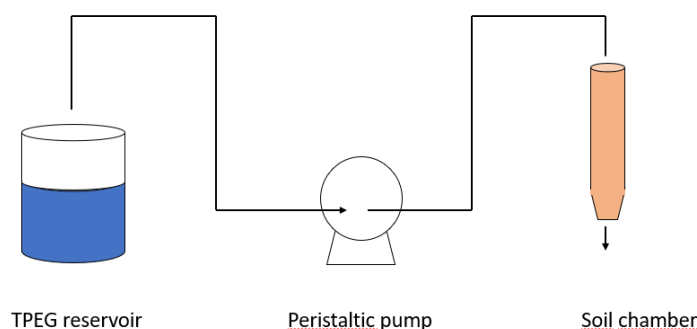


**Fig. 44 Schematic diagram of TPEG injection test.**

The solution contained the TPEG ( $0.25 \text{ g L}^{-1}$ ) was pumped and injected in the soil chamber at different flow rate (5, 22, 35 and  $45 \text{ mL min}^{-1}$ ). The time necessary to fill the same height of soil with TPEG at different flow rate was evaluated. Furthermore, the volume of TPEG solution used to fill the same height of soil at different flow rate was evaluated. After the filling of the soil with TPEG, 20 L of distilled water was pumped for 2 hours through the soil chamber to verify possible leaching of TPEG.

### 2.2.4 Adsorption of TPEG-soil system

After the verification of the possibility to inject “hydro-soluble” TPEG in the groundwater, the adsorption capacity of the system TPEG-soil was evaluated. The TPEG was injected by flowing the TPEG solution at  $45 \text{ mL min}^{-1}$  for about 2 minutes by using the setup described in the figure

44 . After the injection of TPEG, the burette filled with TPEG-soil (soil was previously water-saturated) system was connected with a reservoir tank of solution of toluene, ethylbenzene and xylenes at concentration of 20 mg L<sup>-1</sup> for each compound. To avoid loss of BTEX for volatilization the reservoir tank was sealed but anyway, the concentration of inner solution was controlled during the experiment. The solution of BTEX was pumped at 18 mL min<sup>-1</sup> through the TPEG-soil system for 6 hours, with the same setup used for the injection of TPEG, and the residual concentration of each compound was evaluated. The breakthrough curve was constructed and compared with the curve of a system constituted by only water-saturated soil. The flow of 18 mL min<sup>-1</sup> was choose because it was the value observed for groundwater that flows through the vertical soil chamber filled with water-saturated soil. It is the maximum flow of groundwater through the soil used in this work because the vertical setup represents the maximum hydraulic gradient.

### 2.2.5 Evaluation of experimental data: statistical analysis

In order to evaluate the fitting of the isotherm and kinetics models with experimental data, the coefficient of linear determination (R<sup>2</sup>) and other error functions including the sum of the squares of the errors (SSE), the residual root mean square error (RMSE) and the chi-square test ( $\chi^2$ ) were employed [34], expressed as the equation 16, 17, 18 and 19:

$$R^2 = \frac{1 - \sum_{n=1}^n (q_{e,n} - q_{m,n})^2}{\sum_{n=1}^n (q_{e,n} - q_{m,n})^2} \quad (16)$$

$$SSE = \sum_{n=1}^n (q_{m,n} - q_{e,n})^2 \quad (17)$$

$$RMSE = \sqrt{\frac{1}{n-1} \sum_{n=1}^n (q_{e,n} - q_{m,n})^2} \quad (18)$$

$$\chi^2 = \sum_{n=1}^n \frac{(q_{e,n} - q_{m,n})^2}{q_{e,n}} \quad (19)$$

Where  $q_e$  and  $q_m$  are the adsorption capacity at equilibrium and the calculated value at equilibrium from the model, respectively and  $n$  is the number of the observation. SSE and RMSE were calculated because R<sup>2</sup> and  $\chi^2$  were very similar for some fitting and was not enough to choose the best model.

### 2.2.6 Chemical analysis

A static headspace extraction coupled to gas chromatography-barrier ionization discharge detection method for the determination of residual concentration of BTEX was used, as described in literature [35]. BTEX's solution was opportunely diluted in 20 mL of distilled



water (1 % MeOH) and transferred in a 40 mL vial tightly sealed with polytetrafluoroethylene silicone septa (Supelco; Milano, Italy) and the vial was placed on a stirrer hot plate at 80°C and 200 rpm for 30 minutes. Headspace gaseous phase sampling was performed with syringe for gas (25 mL gas-tight syringe) and injected in GC through 500 µL sample loop at 70°C. A Shimadzu system (Kyoto, Japan) consisting of barrier ionization discharge (BID) detector equipped with a 2010 Plus Tracer gas chromatograph (GC) with a split/splitless injector was used for TCE quantification. The pressure drop was kept constant by using a 10-100 cc/min scale RMA-150-BV rotameter (Rometec, Roma, Italy), to improve the sample precision of manual injection. The injector port was maintained at 200°C and a 500 µL of headspace was injected in split mode (split ratio 90:10). A Restek Rtx-624 fused silica capillary column was employed with He 6.0 (SIAD Corporation, Bergamo, Italy) as the carrier gas at flow rate of 1 mL/min. The column temperature was programmed as follows: constant 30°C for 1 minute, increasing at 10°C/min to 70°C and holding for 10 minutes, increasing at 15°C/min to 200°C and holding for 5 minutes. The effluent from the GC was transferred by 50 mL/min discharge gas/flow into the BID detector at 250°C. For the data acquisition, LabSolution software was used (Shimadzu, Kyoto, Japan).

### **3.Results and discussion**

#### ***3.1 Sonication step***

As described in the previous section, the sonication step was conducted in distilled water without addition of emulsifier to doesn't affect the natural composition of the soil object of permeable reactive barrier installation. Clearly, possible implementation of sonication step could be projected and evaluated if it is necessary for an industrial application. 50 hours of sonication results to be the minimum time necessary to obtain a homogeneous TPEG dispersion in the water. Before of 50 hours were observed the formation of little particles of “hydro-soluble” TPEG. As reported in literature [36], dispersion of graphitic substance by sonication can be obtained (it is a step of graphite's exfoliation). The figure 45 shows the pictures of TPEG in the water before the treatment and after 50 hours of treatment.



**Fig. 45** Picture of TPEG in the water before sonication treatment (on the left) and after 50 hours of sonication treatment (on the right).

### 3.2 Kinetics studies

Kinetics studies were conducted to have further information about the adsorption process of BTEX on “hydro-soluble” TPEG. The variation of adsorption capacity by varying the time are gathered for adsorption process of toluene, ethylbenzene and xylenes at the concentration of 5, 10 and 20 mg L<sup>-1</sup>. The figures 46, 47, 48 and 49 report all the evaluation done on the influence of the time on the adsorption capacity.

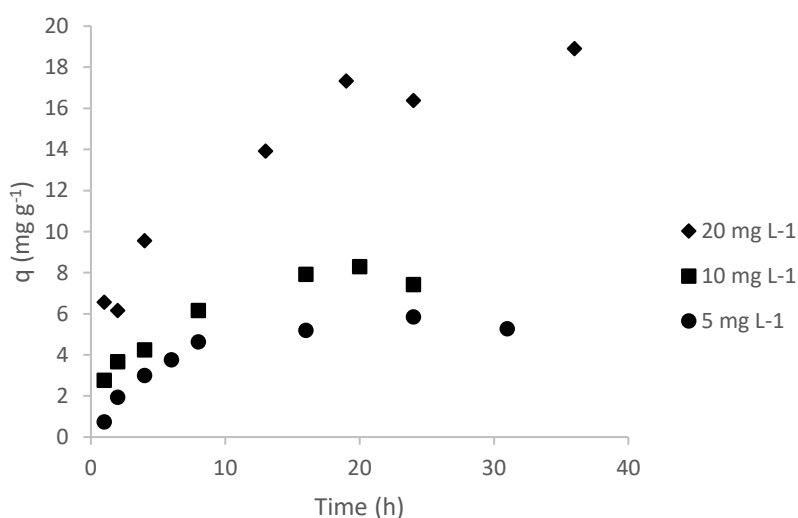


**Fig. 46** Time influence on adsorption capacity of toluene on “hydro-soluble” TPEG. Different initial concentration was investigated: 20 mg L<sup>-1</sup> (♦), 10 mg L<sup>-1</sup> (■) and 5 mg L<sup>-1</sup> (●). 0.02 g of TPEG used as adsorbent and the solution stirred at 800 rpm.

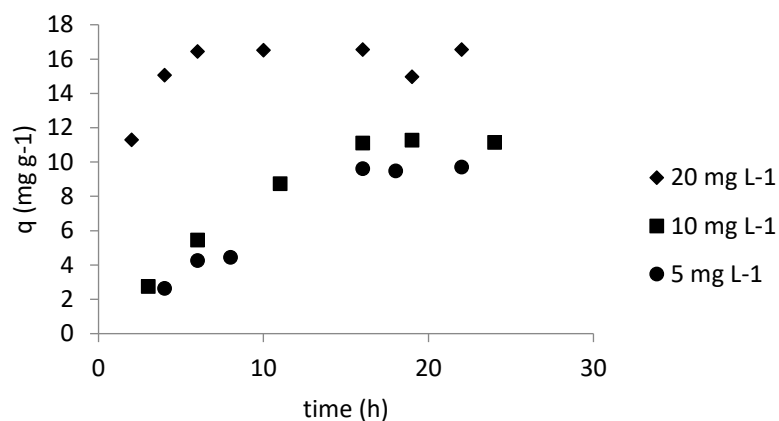


**Fig. 47** Time influence on adsorption capacity of ethylbenzene on “hydro-soluble” TPEG. Different initial concentration was investigated: 20 mg L<sup>-1</sup> (◆), 10 mg L<sup>-1</sup> (■) and 5 mg L<sup>-1</sup> (●). 0.02 g of TPEG used as adsorbent and the solution stirred at 800 rpm.

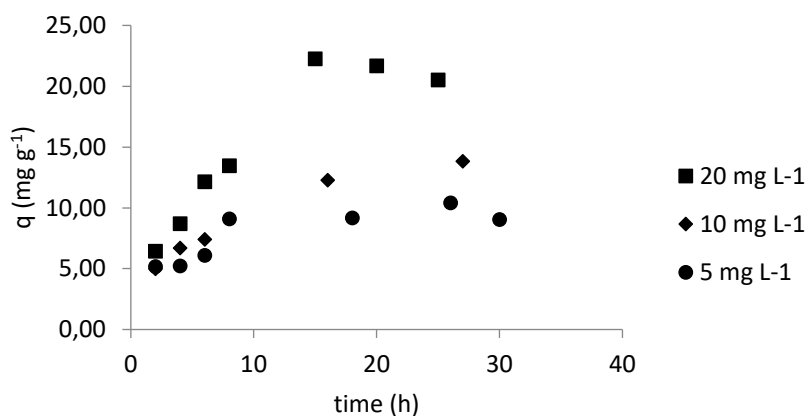


**Fig. 48** Time influence on adsorption capacity of m, p-xylenes on “hydro-soluble” TPEG. Different initial concentration was investigated: 20 mg L<sup>-1</sup> (■), 10 mg L<sup>-1</sup> (◆) and 5 mg L<sup>-1</sup> (●). 0.02 g of TPEG used as adsorbent and the solution stirred at 800 rpm.

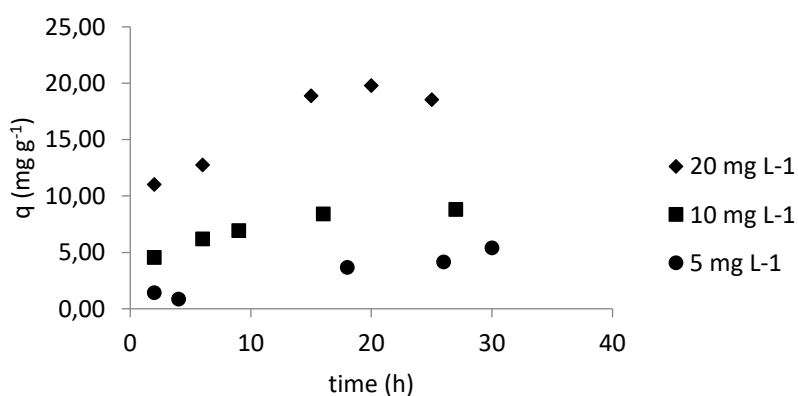


**Fig. 49 Time influence on adsorption capacity of *o*-xylene on “hydro-soluble” TPEG. Different initial concentration was investigated: 20 mg L<sup>-1</sup> (◆), 10 mg L<sup>-1</sup> (■) and 5 mg L<sup>-1</sup> (●). 0.02 g of TPEG used as adsorbent and the solution stirred at 800 rpm.**

By analyzing the data obtained, about 20 hours was the time to reach the saturation of the TPEG for all the compound at all the value of concentration examined. The maximum adsorption capacity was about the same for all the compound (with equal concentration) and it was influenced by the initial concentration of the contaminants, its reduction involves reduction of adsorption capacity. In the table 14 was reported the values of maximum adsorption capacity observed for each compound at all the value of concentrations examined to synthetize the results. The “hydro-soluble” TPEG had a capacity to remove these compounds comparable to other adsorbent material reported in the literature [37,38,39,40,41,42,43].

**Tab. 14 Maximum adsorption capacity observed of toluene, ethylbenzene, *m, p*-xylenes and *o*-xylene at concentration of 5, 10 and 20 mg L<sup>-1</sup> on “hydro-soluble” TPEG.**

Initial concentration (mg L <sup>-1</sup> )	q (mg g <sup>-1</sup> )
<b>Toluene</b>	
20	18.9
10	8.3
5	5.8
<b>Ethylbenzene</b>	
20	16.5
10	11.3
5	9.7
<b><i>m, p</i>-xylenes</b>	
20	22.2
10	13.8
5	10.4
<b><i>o</i>-xylene</b>	
20	19.8
10	8.8
5	5.4

As previous described, the data obtained for the kinetics study were fitted with different kinetics models (pseudo-first order, pseudo-second order, Elovich, intraparticle diffusion and liquid film diffusion) to determine the slower step of the adsorption process and to calculate the theoretical maximum adsorption capacity and the kinetics constant of the process. The statistical parameters of the analysis are reported in the table 15.

**Tab. 15 Statistical parameters obtained from data analysis of kinetics studies.**

Model	Parameter	Toluene Concentration (mg L <sup>-1</sup> )			Ethylbenzene Concentration (mg L <sup>-1</sup> )			<i>m, p</i> -xylenes Concentration (mg L <sup>-1</sup> )			<i>o</i> -xylene Concentration (mg L <sup>-1</sup> )		
		20	10	5	20	10	5	20	10	5	20	10	5
Pseudo-first order	R <sup>2</sup>	0.89	0.73	0.68	0.28	0.88	0.95	0.44	0.96	0.50	0.62	0.99	0.70
	RMSE	2.20	0.52	0.74	1.85	0.65	1.29	3.38	6.49	1.04	2.76	3.75	1.09
	SSE	29.19	1.62	3.87	20.69	2.13	8.33	68.44	168.3	6.52	45.68	5.42	4.75
	χ <sup>2</sup>	8.69	0.31	1.47	1.32	0.28	5.64	4.88	12.27	0.85	3.92	1.22	n.d.
Pseudo-second order	R <sup>2</sup>	0.99	0.98	0.97	0.99	0.90	0.70	0.95	0.99	0.98	0.91	0.99	0.64
	RMSE	1.37	0.55	0.35	1.27	0.73	0.69	1.67	0.63	0.96	2.69	0.42	0.55
	SSE	11.34	1.83	0.87	9.76	2.66	2.41	16.72	1.60	5.56	43.33	0.71	1.20
	χ <sup>2</sup>	2.08	0.38	0.28	0.68	0.29	0.31	0.98	0.27	0.80	5.39	0.15	1.01
Elovich	R <sup>2</sup>	0.95	0.95	0.95	0.53	0.97	0.96	0.92	0.98	0.80	0.72	0.98	0.87
	RMSE	1.12	0.51	0.39	1.31	0.61	0.68	1.82	0.60	0.97	2.54	3.48	0.70
	SSE	7.59	1.56	1.07	10.36	1.85	2.35	19.92	1.42	5.69	38.63	48.56	1.95
	χ <sup>2</sup>	0.97	0.26	0.27	0.71	0.18	0.38	1.31	0.20	0.76	3.44	4.13	1.27
Liquid film diffusion	R <sup>2</sup>	0.89	0.73	0.68	0.28	0.88	0.93	0.44	0.96	0.65	0.62	0.99	0.89
	RMSE	2.21	0.52	17.83	1.86	0.65	48.21	3.38	1.60	39.34	2.76	0.37	20.34
	SSE	29.21	1.62	2225	20.70	2.12	1162	68.50	10.31	9287	45.65	0.54	1655
	χ <sup>2</sup>	8.70	0.31	n.d.	1.33	0.28	n.d.	4.88	4.10	n.d.	3.92	0.12	n.d.
Intraparticle diffusion	R <sup>2</sup>	0.96	0.92	0.83	0.39	0.93	0.95	0.90	0.98	0.75	0.78	0.94	0.93
	RMSE	1.08	0.60	0.74	1.50	0.94	0.70	2.10	0.52	1.59	2.24	0.40	0.51
	SSE	7.04	2.20	3.88	13.46	4.40	2.46	26.22	1.09	15.18	30.10	0.66	1.04
	χ <sup>2</sup>	0.58	0.31	1.27	0.92	0.51	0.32	1.40	0.10	1.61	2.46	0.09	0.66

By analyzing the statistical parameters, it could be deduced the kinetics aspect of the adsorption process. For the toluene, the model that best fits the data at 20 mg L<sup>-1</sup> results to be the intraparticle diffusion, while at concentration of 10 and 5 mg L<sup>-1</sup> the best models result to be Elovich and pseudo-second order respectively. At higher level of concentration, the diffusion of the molecules across the pores of TPEG results to be the slower step and a “funnel effect” could explain that. By reducing the concentration, there is no “traffic” in the pores of the TPEG and the slower step results to be the chemical adsorption, due to lower number of molecules

that have to arrive on the surface of TPEG. For the ethylbenzene, by varying the initial concentration no change in slower step was observed and the chemical adsorption is the limiting process step. The best model changed from pseudo-second order at 20 mg L<sup>-1</sup> to Elovich model at 10 and 5 mg L<sup>-1</sup>, therefore only a change from homogeneous to heterogeneous surface of TPEG that adsorb the molecules. For *m, p*-xylenes, the best model to fit experimental data were pseudo-second order at 20 and 5 mg L<sup>-1</sup> and intraparticle diffusion at 10 mg L<sup>-1</sup>. At higher and lower value of concentration, the chemical adsorption results to be the slower step of the process, while at the value of concentration intermediate the slower step results to be the diffusion in the pores of TPEG. It seems to demonstrate that when high number of molecules are present, the effective adsorption step is slow because of the number of active sites could be lower or comparable than the number of molecules and the chemical bonding is slow, while when the concentration is low the chemical adsorption results to be the slower step because of it is made on two step, the diffusion on the proximity of the active site and the bonding to the active sites. At 5 mg L<sup>-1</sup> it is possible to deduce that the diffusion on the proximity of the active site is the limiting kinetic step. Anyway, for concentration lower than 20 mg L<sup>-1</sup>, a step that involves diffusion limits the velocity of the process. For the *o*-xylene, the best model to fit experimental data were pseudo-second order at 10 and 20 mg L<sup>-1</sup> and intraparticle diffusion at 5 mg L<sup>-1</sup>. Also, in this case, with the reduction of the concentration, the limiting kinetic step become a diffusion step. The different behavior of xylenes and toluene probably could be associated to the different mechanism of adsorption, that is multilayer and monolayer respectively as after described. The monolayer mechanism requires bonding between adsorbate and adsorbent and when high number of molecules are present, they have difficult to find and reach a free active site and diffusion step limiting the process. By decreasing the concentration there are no problem to find and reach free active sites and the limiting step become the chemical (or physical) bonding (normally chemical processes are slower than diffusion process). Vice versa, the multilayer mechanism doesn't require to all the molecules to find free active sites and the number of adsorbate molecules higher (or similar) than number of active sites is not affect the kinetics of the process and the slower step remains chemical adsorption, as normal happens for reaction in liquid phase. At lower value of concentration, the slower step could be to reach the active surface, caused by the lower gradient of concentration as usually happens.

From the models that best fit the experimental kinetics data of each compound, parameters as maximum adsorption capacity and kinetic constant of the process was calculated for all the

compound at the different concentration investigated. In the table 16, the results obtained are gathered.

**Tab.16 Kinetics parameters of adsorption process on TPEG and some theoretical maximum adsorption capacity for toluene, ethylbenzene and xylenes at different initial concentration.**

	20 mg L <sup>-1</sup>	10 mg L <sup>-1</sup>	5 mg L <sup>-1</sup>
Toluene	$k_{dif}: 2.70 \text{ mg g}^{-1} \text{ h}^{-1/2}$	$\alpha: 7.23 \text{ mg g}^{-1} \text{ h}^{-1}$ $\beta: 0.56 \text{ g mg}^{-1}$	$k_2: 0.031 \text{ g mg}^{-1} \text{ h}^{-1}$ $q_e: 6.54 \text{ mg g}^{-1}$
Ethylbenzene	$k_2: 0.17 \text{ g mg}^{-1} \text{ h}^{-1}$ $q_e: 16.39 \text{ mg g}^{-1}$	$\alpha: 2.75 \text{ mg g}^{-1} \text{ h}^{-1}$ $\beta: 0.22 \text{ g mg}^{-1}$	$\alpha: 1.89 \text{ mg g}^{-1} \text{ h}^{-1}$ $\beta: 0.21 \text{ g mg}^{-1}$
<i>m, p</i> -xylenes	$k_2: 0.004 \text{ g mg}^{-1} \text{ h}^{-1}$ $q_e: 28.81 \text{ mg g}^{-1}$	$k_{dif}: 2.42 \text{ mg g}^{-1} \text{ h}^{-1/2}$	$k_2: 0.033 \text{ g mg}^{-1} \text{ h}^{-1}$ $q_e: 10.58 \text{ mg g}^{-1}$
<i>o</i> -xylenes	$k_2: 0.007 \text{ g mg}^{-1} \text{ h}^{-1}$ $q_e: 23.81 \text{ mg g}^{-1}$	$k_2: 0.034 \text{ g mg}^{-1} \text{ h}^{-1}$ $q_e: 9.77 \text{ mg g}^{-1}$	$k_{dif}: 1.00 \text{ mg g}^{-1} \text{ h}^{-1/2}$

The parameters obtained from the kinetics studies allow to evaluate the velocity of the process and compare the different velocity of adsorption process for the different compound and the different concentration. For the concentration of 20 and 10 mg L<sup>-1</sup> the toluene has the higher kinetic constant. At 20 mg L<sup>-1</sup>, the adsorption process of toluene is 10-1000 times faster than the adsorption of the other compound. At 10 mg L<sup>-1</sup>, the values of kinetics constant are comparable with one another. At 5 mg L<sup>-1</sup>, the adsorption of ethylbenzene and *o*-xylene seems to be the faster process. The velocity of the process (also the affinity) can influence the adsorption capacity when all the compounds are present in the solution to treat. Kinetics constant obtained are comparable with the values reported in literature [40, 41, 44]. The value of theoretical adsorption capacity obtained from the kinetics model are comparable with experimental data and that confirms the good agreement between experimental data and the models used. For example, for the ethylbenzene at 20 mg L<sup>-1</sup> the maximum adsorption capacity observed was 16.54 mg g<sup>-1</sup> and the theoretical value obtained from kinetics model was 16.39 mg g<sup>-1</sup>. The order of adsorption capacity was influenced by the solubility [42], indeed it increases by decreasing the solubility. The decrease of adsorption capacity by decreasing the initial concentration involves that a bigger adsorbent dosage is required to have the same

absolute removal of pollutants. The lower value of kinetics constant involves that saturation of the material and maximum removal is reached at bigger time of contact.

### 3.3 Isotherm adsorption studies

Isotherm adsorption evaluation was done for each compound (toluene, ethylbenzene and xylenes) to determine the mechanism of adsorption. Monolayer and multilayer adsorption can be recognized, and the type of isotherm determined. The fitting of experimental data with the previous described models allow to choose the best model that represents the system and to calculate some parameters like the affinity adsorbate/adsorbent, intensity of the adsorption or bonding energy (from Dubinin- Radushkevich). The isotherm curves obtained from experimental data and the model curves are gathered in the figures 50, 51, 52 and 53.

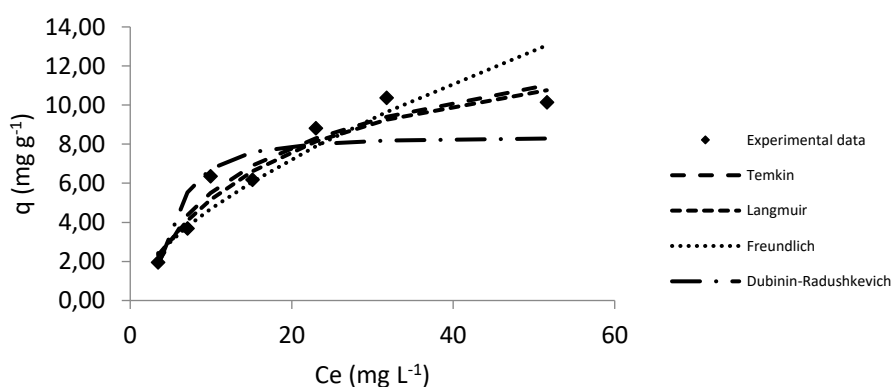


**Fig. 50 Isotherm adsorption of toluene. Solution with different concentration was mixed with about 0.02 g of “hydro-soluble” TPEG for 6 hours at 800 rpm.**

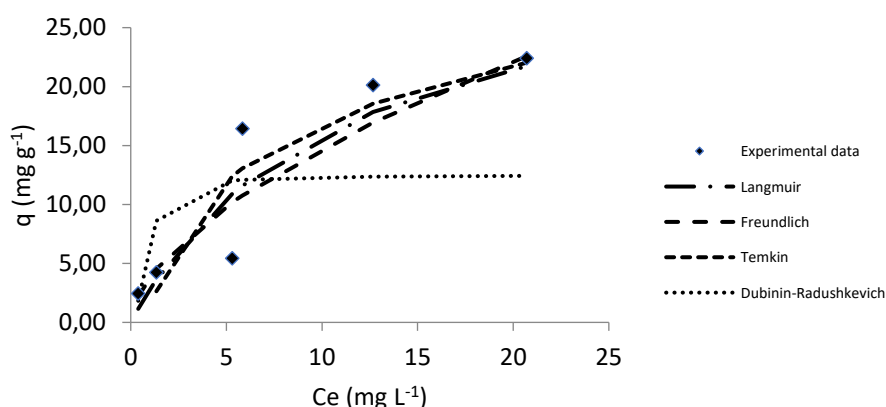


**Fig. 51 Isotherm adsorption of ethylbenzene. Solution with different concentration was mixed with about 0.02 g of “hydro-soluble” TPEG for 6 hours at 800 rpm.**



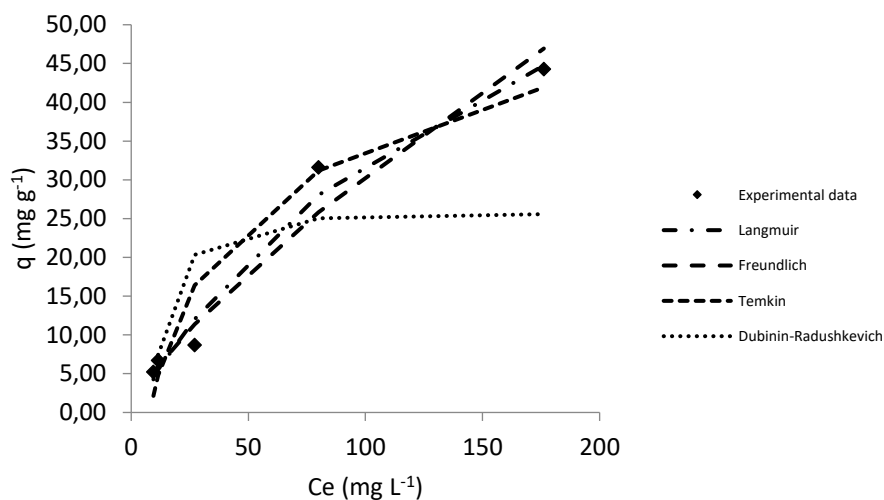


**Fig. 52 Isotherm adsorption of *m,p*-xylenes. Solution with different concentration was mixed with about 0.02 g of “hydro-soluble” TPEG for 6 hours at 800 rpm.**

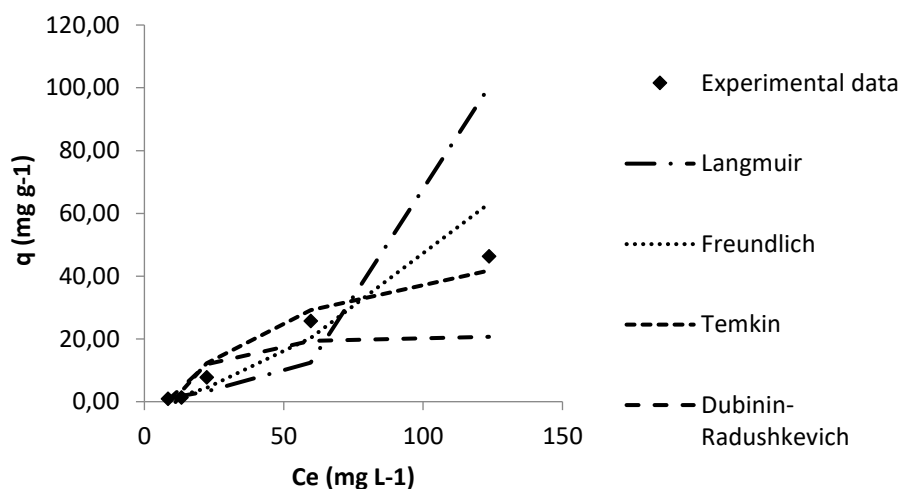


**Fig. 53 Isotherm adsorption of *o*-xylenes. Solution with different concentration was mixed with about 0.02 g of “hydro-soluble” TPEG for 6 hours at 800 rpm.**

From the experimental data obtained by isothermal study it is possible to classify the curve by BDDT classification. For the toluene, the isotherm curve seems to be of the type I, type IV for the ethylbenzene and *m,p*-xylenes, type V for *o*-xylenes. These classifications imply a monolayer adsorption for the toluene and multilayer adsorption for the other compounds. This different behavior could be explained by different solubility in water of studied compounds (toluene > ethylbenzene > xylenes), indeed the decrease of the solubility involves a higher aggregation of the molecules. The different behavior is also evidenced by the observed value of adsorption capacity that is higher for ethylbenzene and xylenes than toluene, as can be

observed by the figure 50, 51, 52 and 53. In the kinetics section little difference of  $q$  were observed because lower initial concentration was used. As previous described, the data obtained for the isothermal study were fitted with different models (Langmuir, Freundlich, Temkin and Dubinin-Radushkevich) and the statistical parameters of the analysis are reported in the table 17.

**Tab. 17 Statistical parameters obtained from data analysis of isothermal studies.**

Model	Parameter	Toluene	Ethylbenzene	m, p-xylenes	o-xylenes
Langmuir	R <sup>2</sup>	0.94	0.47	0.71	0.44
	RMSE	0.82	3.49	2.53	27.88
	SSE	4.05	60.83	25.70	3109.75
	X <sup>2</sup>	0.64	6.62	1.70	49.36
Freundlich	R <sup>2</sup>	0.90	0.86	0.96	0.95
	RMSE	1.47	3.61	3.48	9.00
	SSE	13.01	65.00	48.52	324.38
	X <sup>2</sup>	1.51	5.85	2.18	8.76
Temkin	R <sup>2</sup>	0.94	0.77	0.94	0.94
	RMSE	0.79	4.03	4.43	4.65
	SSE	3.75	64.87	78.56	86.57
	X <sup>2</sup>	0.52	5.89	8.93	n.v.
Dubinin-Radushkevich	R <sup>2</sup>	0.85	0.57	0.70	0.78
	RMSE	1.55	6.95	11.51	13.45
	SSE	14.44	241.42	530.07	723.47
	X <sup>2</sup>	2.00	20.46	22.36	37.76

By the statistical analysis, best models that fit experimental data were Temkin for toluene and Freundlich for ethylbenzene and xylenes. These data confirm the mechanism obtained from previous BDDT classification. From the best model were calculated some typical parameters of adsorption process and are reported in the table 18.

**Tab.18 Isothermal parameters of adsorption process on TPEG for toluene, ethylbenzene and xylenes.**

	Toluene	Ethylbenzene	m,p-xylene	o-xylene
Parameters	B <sub>1</sub> :3.35 J mol <sup>-1</sup> A: 0.52 L g <sup>-1</sup>	K <sub>f</sub> : 3.83 (mg g <sup>-1</sup> )(L mg <sup>-1</sup> ) 1/n <sub>f</sub> : 0.58	K <sub>f</sub> : 0.94 (mg g <sup>-1</sup> )(L mg <sup>-1</sup> ) 1/n <sub>f</sub> : 0.76	K <sub>f</sub> : 0.03 (mg g <sup>-1</sup> )(L mg <sup>-1</sup> ) 1/n <sub>f</sub> : 1.56

By analyzing the data obtained from isothermal studies, consideration about the affinity adsorbate/adsorbent of ethylbenzene and xylenes. It is possible to conclude, from the reverse of the affinity, that ethylbenzene has a higher affinity than xylenes, probably due to the higher number of double bonding present on its molecules that can increase the available sites for  $\pi$ - $\pi$  bonding. The Freundlich constant reveals higher adsorption capacity for ethylbenzene than

xylenes. Kinetics experimental data already revealed it for ethylbenzene and *o*-xylene, while comparable values were obtained for *m,p*-xylenes. By the study of toluene's isothermal, a value of adsorption heat typical of secondary bonding was obtained and it could indicate  $\pi$ - $\pi$  bonding[45] as interaction between toluene and TPEG. The same type of interaction can be imagined for the other compound caused by the similar structure that they have.

### 3.4 Influence of initial concentration

The adsorption capacity of adsorbent materials depends on the initial concentration of the adsorbate and this parameter results to be fundamental to project an environmental remediation intervention and to have the information about the amount of adsorbent to use. In the figure 54 are gathered the influence of initial concentration on the adsorption capacity of each compound studied (ethylbenzene, toluene and xylenes) on TPEG.

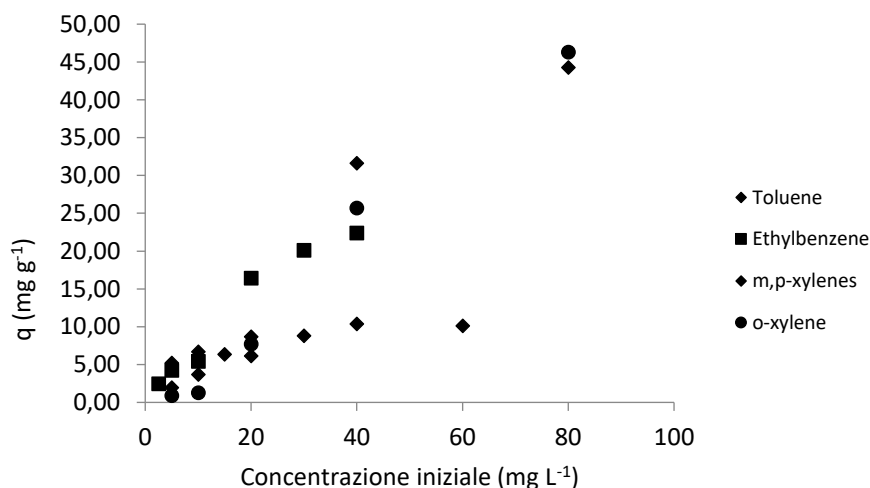


**Fig. 54 Influence of initial concentration on the adsorption capacity of BTEX on TPEG surface. The adsorption capacity was measured after 6 hours of contact, agitation speed of 800 rpm and initial concentration of each compound of 2.5, 5, 10, 20, 30, 40, 60 (for toluene and ethylbenzene) and 80 (for xylenes) mg L<sup>-1</sup>.**

As normal observed in literature, the adsorption capacity increases by increasing the initial concentration. The adsorption capacity of the toluene seems to reach a constant value of adsorption capacity by increasing the adsorption capacity, due to monolayer adsorption, while for the other compound a constant value of adsorption capacity was not reached by increasing the concentration ( in the investigated range) due to the multilayer adsorption mechanism. The adsorption capacity results to be about 1 mg g<sup>-1</sup> for toluene and *o*-xylene and about 5 mg g<sup>-1</sup> for ethylbenzene and *m,p*-xylenes at 2.5 mg L<sup>-1</sup> and it increase until about 40 mg g<sup>-1</sup> for xylenes at

80 mg L<sup>-1</sup>, about 20 mg g<sup>-1</sup> for ethylbenzene at 40 mg L<sup>-1</sup> and 10 mg g<sup>-1</sup> for toluene (value constant reached at plateau). 6 hours of contact was chosen as optimal time of contact to have a good compromise for an industrial use that requires fast processes.

### 3.5 Influence of co-presence of each contaminant on adsorption capacity

The previous paragraphs report the mechanism process, kinetics parameters and adsorption capacity of BTEX on “hydro-soluble” TPEG when in the solution is present one compound at a time. The previous studies were necessary for a deep investigation of the process. Normally, when a groundwater was polluted by hydrocarbon compounds, they are present in it as a mix of different molecules. Therefore, the investigation of adsorption capacity of BTEX on “hydro-soluble” TPEG when all the compounds are present is necessary to have useful information for an environmental remediation intervention. In the figure 55 the adsorption capacity for the initial concentration of contaminants of 20 mg L<sup>-1</sup> present together are gathered.

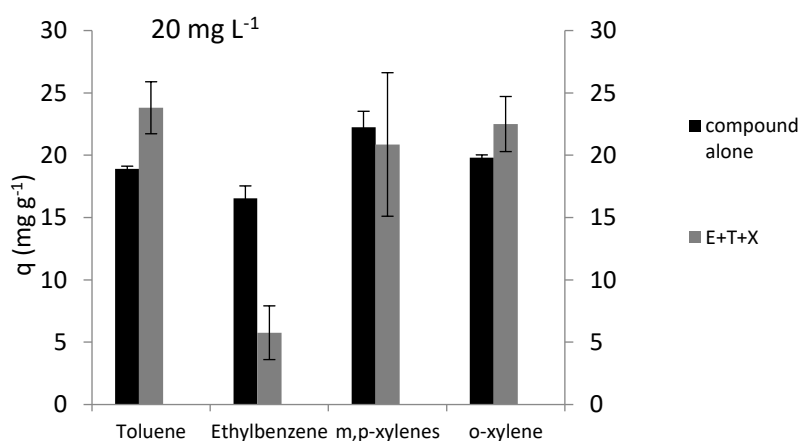


**Fig. 55 Adsorption capacity of BTEX on “hydro-soluble” TPEG. Initial concentration of 20 mg L<sup>-1</sup> of each compound was investigated. 0.02 g of TPEG was mixed at BTEX and stirred for 24 hours at 800 rpm. Black data are referred to the compound alone and the grey data are referred to co-presence of adsorbate. The bars of error were also reported.**

At 20 mg L<sup>-1</sup> of concentration of each compound, a reduction of the adsorption capacity was observed for ethylbenzene. It could be explained by evidencing that the kinetic of toluene (at 20 mg L<sup>-1</sup>) is the faster of all the investigated process, therefore the molecules of toluene are bonded to TPEG surface for first, then ethylbenzene molecules found some active site occupied. The adsorption capacity of xylenes is not affected probably due to the presence of available active sites for them that are not the same of the toluene. Further computational/experimental

investigation is necessary to confirm these hypotheses by evaluating the diameter of pores of TPEG and diameter of the molecules object of this work. In the figure 56 the adsorption capacity for the initial concentration of contaminants of  $10 \text{ mg L}^{-1}$  present together are gathered.

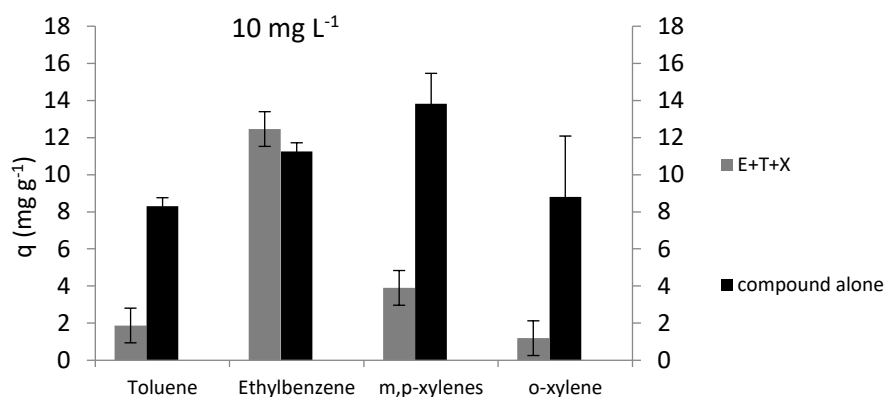


**Fig. 56 Adsorption capacity of BTEX on “hydro-soluble” TPEG. Initial concentration of  $10 \text{ mg L}^{-1}$  of each compound was investigated.  $0.02 \text{ g}$  of TPEG was mixed at BTEX and stirred for 24 hours at 800 rpm. Black data are referred to the compound alone and the grey data are referred to co-presence of adsorbate. The bars of error were also reported.**

At  $10 \text{ mg L}^{-1}$  different behavior was observed. At this initial concentration, only the adsorption capacity of ethylbenzene was preserved when the compounds are present in the solution together. From kinetics data it is possible to observe that the kinetic of the adsorption process of toluene and ethylbenzene are comparable the one with the other, therefore the higher affinity of ethylbenzene involves that it is the compound adsorbed in majority occupying the active sites. The kinetic of the process of adsorption of xylene is slower than ethylbenzene, especially for *o*-xylenes, therefore they could reach the surface of TPEG when the multilayer of ethylbenzene is already formed. The multilayer could act as steric hindrance and molecules of xylene have difficult to reach the active sites. Molecules of xylenes could be bonded to TPEG surface before the formation of multilayer of ethylbenzene and the adsorption capacity is limited by the number of these molecules. The lower adsorption capacity observed for *o*-xylene then *m,p*-xylenes, caused by lower kinetic, could confirm these hypothesis. Indeed, more molecules of *m,p*-xylenes than *o*-xylene reach the surface and are bonded on it (by kinetics consideration) before the formation of multilayer of ethylbenzene. In the figure 57 are gathered the behavior observed at  $5 \text{ mg L}^{-1}$ .

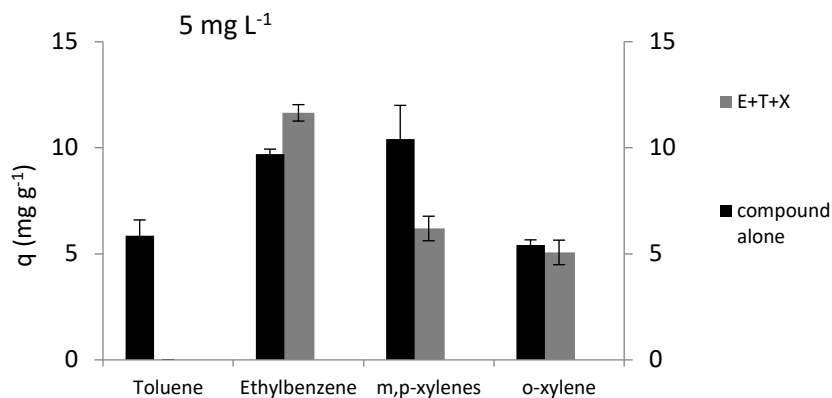


**Fig. 57 Adsorption capacity of BTEX on “hydro-soluble” TPEG. Initial concentration of 10 mg L<sup>-1</sup> of each compound was investigated. 0.02 g of TPEG was mixed at BTEX and stirred for 24 hours at 800 rpm. Black data are referred to the compound alone and the grey data are referred to co-presence of adsorbate. The bars of error were also reported.**

At 5 mg L<sup>-1</sup>, the same previous consideration could explain the behavior observed. The adsorption capacity of ethylbenzene and *o*-xylene are not affected by co-presence of all the compound because of they have the faster kinetic of adsorption. *o*-xylene adsorption seems not affected by the formation of multilayer of ethylbenzene, as previous observed, probably because of they have comparable kinetic. Capacity adsorption of toluene and *m,p*-xylenes decrease for the same reason described at 10 mg L<sup>-1</sup>.

### **3.6 Influence of presence of humic acid on adsorption capacity**

Because of the aim of this work is to obtain an injectable material in groundwater capable to adsorb BTEX, the influence of humic acid represents an important variable to analyze, because of it is one of the major component of soils and it is adsorbed on graphitic surface [30,31] and it is able to adsorb organic contaminant [32,33]. For these reasons, adsorption capacity of BTEX on TPEG in presence of different concentration (12.5, 25, 50, 100 and 150 mg L<sup>-1</sup>) of humic acid was evaluated. In the figure 58, adsorption capacity obtained in presence of 25 mg L<sup>-1</sup> of humic acid with initial concentration of 10 mg L<sup>-1</sup> of each compound are gathered as example and compared with the adsorption capacity observed without presence of humic acid when all the compound are alone and when they are all mixed in the solution.

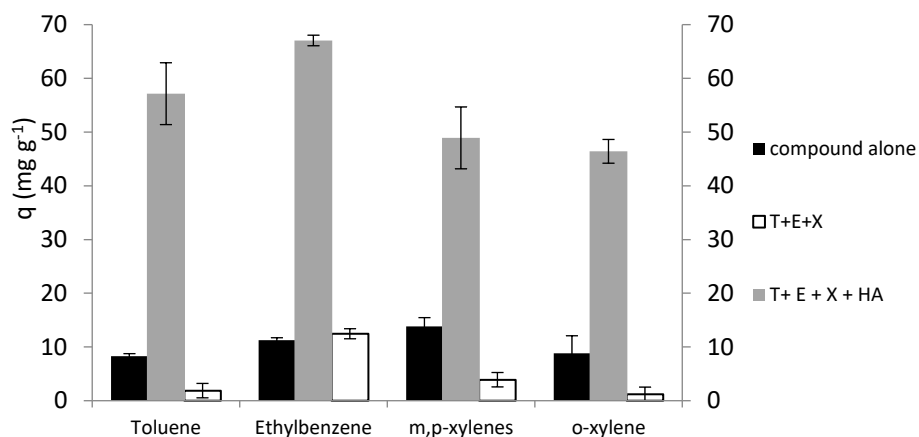


**Fig. 58 Comparison between adsorption capacity of BTEX observed at 10 mg L<sup>-1</sup> in presence of 12.5 mg L<sup>-1</sup> of humic acid. Adsorption capacity was evaluated after 24 hours of contact of BTEX with about 0.02 g of “hydro-soluble” TPEG in a solution with 25 mg L<sup>-1</sup> of humic acid. Adsorption capacity is reported for test with compound alone (black data), co-presence of all the contaminants (white data) and the co-presence of humic acid (grey data). The bars of error are also reported.**

In the figure 59 are reported the variation of adsorption capacity by varying the concentration of humic acid.

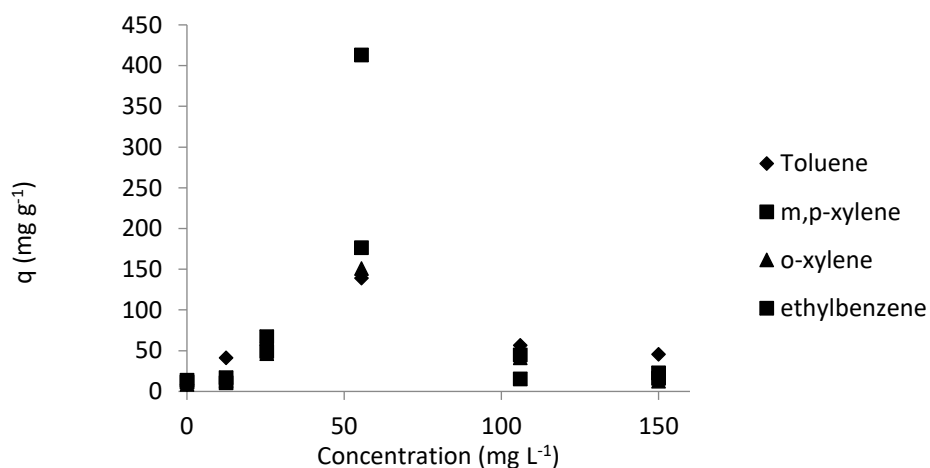


**Fig. 59 Adsorption capacity of BTEX on “hydro-soluble” TPEG for different concentration of humic acid. Adsorption capacity was measured after 24 hours of contact (stirred at 800rpm) between 0.02 g of TPEG and BTEX at 10 mg L<sup>-1</sup> in presence of different concentration of humic acid.**

From the experimental data, it is possible to observe that the presence of humic acid increases the adsorption capacity for value of concentration greater than 12.5 mg L<sup>-1</sup>. A peak of

adsorption capacity was observed at the concentration of about 50 mg L<sup>-1</sup> of humic acid. The increase of the adsorption capacity could be caused by the adsorption of humic acid that entraps/adsorb organic substance. A multilayer of BTEX on humic acid adsorbed on TPEG can be imagined. By increasing the concentration of humic acid an increase of adsorption capacity was observed because more humic acid able to entraps/adsorbs BTEX was present on TPEG's surface until to reach a peak, because of a further increase of concentration of humic acid involves a formation of multilayer of humic acid instead of the adsorption of BTEX on the first layer of humic acid. The adsorption of humic acid on TPEG surface involves an increase of free carboxylic group [31] that can bond BTEX through  $\pi$ - $\pi$  interactions<sup>46</sup>. Because in real application acid humic is often present in the water, the adsorption capacity of hydrosoluble TPEG will be positively affected.

### 3.7 Influence of initial pH on adsorption capacity

The variation of pH of the solution can influence the adsorption capacity of BTEX on “hydro-soluble” TPEG because of the sonication could partially oxidize the graphitic surface. In the figure 60 are gathered the adsorption capacity obtained for three different value of initial pH (3.8, 7.6 and 9.9). The obtained value was referred to a solution of BTEX (20 mg L<sup>-1</sup> of separated compound).

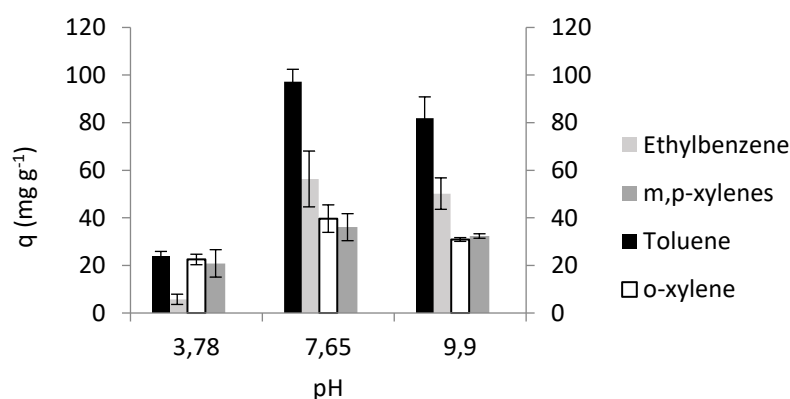


**Fig. 60** Adsorption capacity for different values of pH. Adsorption capacity was evaluated after 24 hours of contact between 0.02 g of TPEG and BTEX (20 mg L<sup>-1</sup>) stirred at 800 rpm. The data are available for toluene (black data), ethylbenzene (light grey data), m,p-xylene (grey data) and o-xylene (white data).

Study reported in literature [46], demonstrates the positively charge of BTEX in the investigated pH range. By increasing the pH of solution an increase of adsorption capacity was observed. It can be caused by the increase of interlayer separation [47] between the different sheet of



graphite that could involve increase of surface active area, caused by negative charge associate to dissociation of acid or hydroxyl group probably present on the surface of TPEG, and the increase of electrostatic interaction between positively charged BTEX molecules and negatively charged surface of adsorbent. By varying the pH from 7.6 to 9.9, a low reduction of adsorption capacity was observed probably caused by the increase of steric hindrance/competition of counter ions [48] ( $\text{Na}^+$ ).

### ***3.8 Injection and leaching test***

“Hydro-soluble” TPEG was obtained and its adsorbent properties were evaluated. The aim of the work was to obtain an adsorbent material easy to inject in groundwater, therefore a series of test to evaluate this property were done. First of all, a solution of “hydro-soluble” TPEG was pumped by peristaltic pump and injected in sand water-saturated soil, as described in material and methods description. Different flow rate was used to evaluate the effect on the time necessary to fill the soil with TPEG and the volume of solution used. In the figure 61 are reported picture of soil-chamber after the injection test conducted at different flow rate (5, 22, 35 and 45  $\text{mL min}^{-1}$ ).



***Fig. 61 Pictures of soil chamber after TPEG injection. “Hydro-soluble” TPEG’s solution was injected into soil-chamber at different flow rate (5, 22, 35 and 45  $\text{mL min}^{-1}$ ).***

In the figure 62 are reported the results obtained about the time and volume necessary to inject “hydro-soluble” TPEG in the water-saturated soil at different flow rate. Same height of soil was taken as reference to evaluate these parameters.

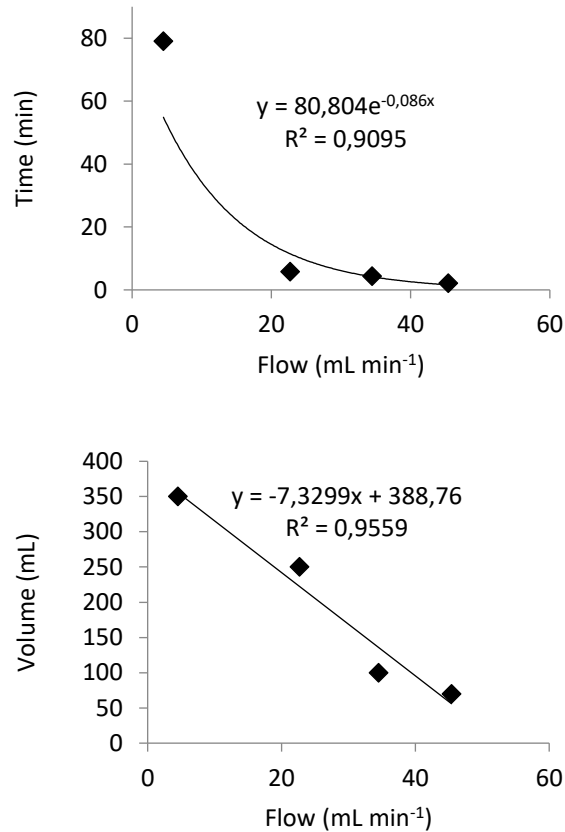


**Fig.62 Variation of time injection and volume of solution used of “hydro-soluble” TPEG at different flow.**

The results obtained demonstrate as the increase of the pressure of injection is associated to a decrease of time necessary to inject TPEG in the same fraction of soil. Anyway, the time of injection reaches a plateau at which is not useful to increase the pressure of injection. By varying the pressure of injection, a variation of volume of TPEG’s solution was observed and it is caused by the sedimentation of littler particle in the tube at low flow rate, associated to very quiet movement of the water. These observations allowed to have fundamental information about optimal parameter of injection. To verify the possible leaching of TPEG, 20 L of distilled water was pumped through the soil chamber for 2 hours. No visible leaching of TPEG was observed.

### **3.9 Adsorption of TPEG-soil system**

After the injection of “hydro-soluble” TPEG into the sand soil, its adsorbent properties were evaluated to verify if they are preserved during the operation. For this reason, the adsorption of soil and the system soil-TPEG was evaluated and the obtained results are gathered in the figure 63, 64, 65 and 66.

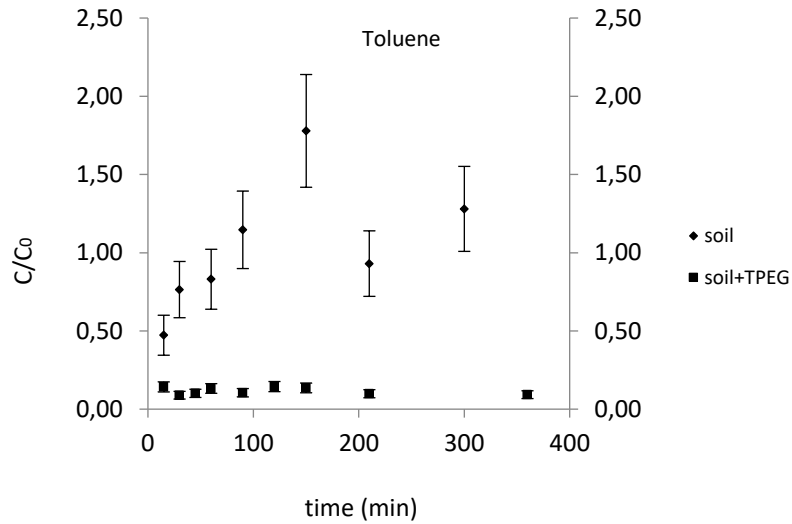


**Fig. 63 Breakthrough curves of toluene for the soil (◆) and the system soil-TPEG (■). Toluene's solution (20 mg L<sup>-1</sup>) was injected at 18 mL min<sup>-1</sup> for 6 hours. TPEG was injected at 45 mL min<sup>-1</sup> for 2 minutes. Bars of error are also reported.**

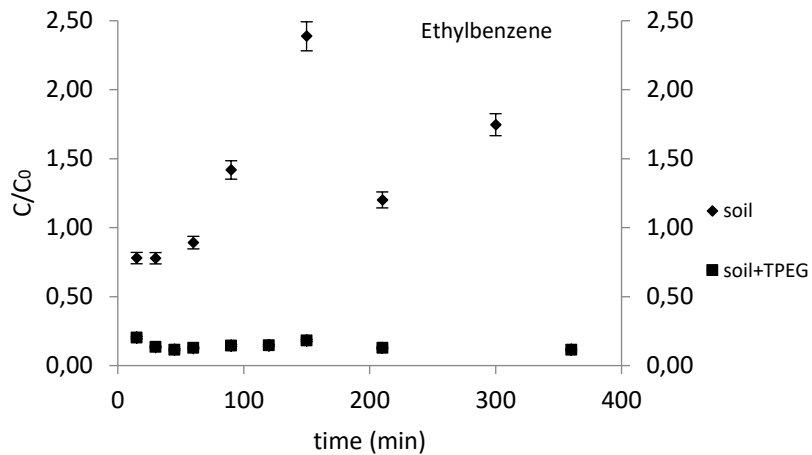


**Fig. 64 Breakthrough curves of ethylbenzene for the soil (◆) and the system soil-TPEG (■). Ethylbenzene's solution (20 mg L<sup>-1</sup>) was injected at 18 mL min<sup>-1</sup> for 6 hours. TPEG was injected at 45 mL min<sup>-1</sup> for 2 minutes. Bars of error are also reported.**

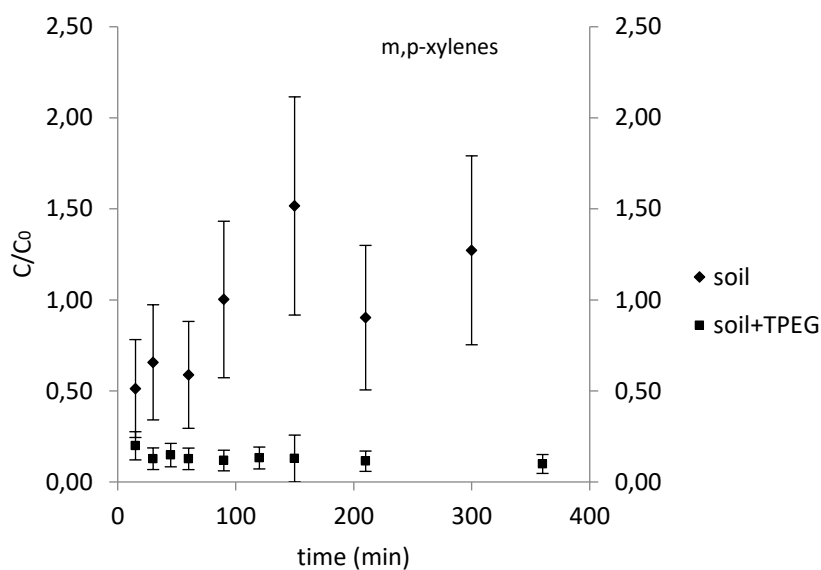


**Fig. 65 Breakthrough curves of *m,p*-xylenes for the soil (◆) and the system soil-TPEG (■). *m,p*-xylenes's solution ( $20 \text{ mg L}^{-1}$ ) was injected at  $18 \text{ mL min}^{-1}$  for 6 hours. TPEG was injected at  $45 \text{ mL min}^{-1}$  for 2 minutes. Bars of error are also reported.**

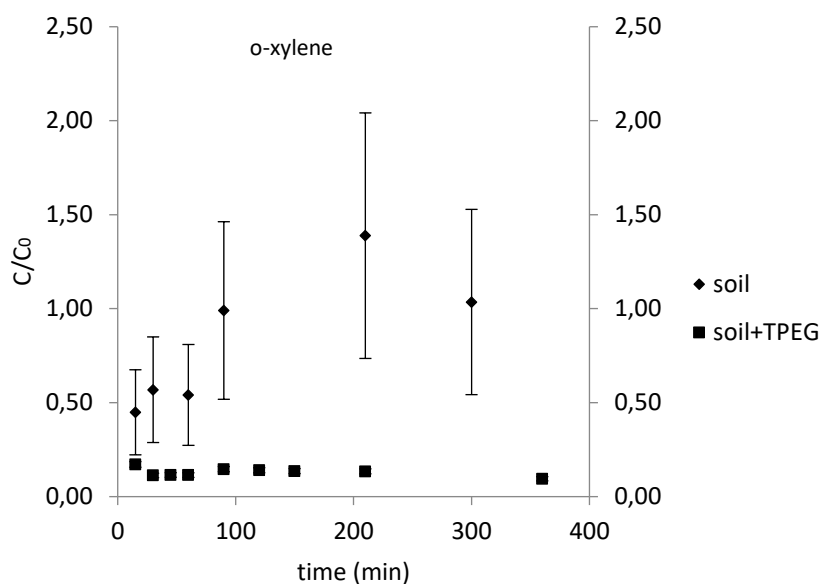


**Fig. 66 Breakthrough curves of *o*-xylenes for the soil (◆) and the system soil-TPEG (■). *o*-xylenes's solution ( $20 \text{ mg L}^{-1}$ ) was injected at  $18 \text{ mL min}^{-1}$  for 6 hours. TPEG was injected at  $45 \text{ mL min}^{-1}$  for 2 minutes. Bars of error are also reported.**

By analyzing the breakthrough curves obtained for the soil and the system soil-TPEG, it is possible to observe an increase of adsorption of the soil after the injection of “hydro-soluble” TPEG. Indeed, for the soil, in the range of time 0-360 min, is possible to observe the typical shape of a breakthrough curves of a system of filtration. At the initial moment, contaminants

were adsorbed into soil particle, until all the soil in the column was filled of contaminants. At this moment, the ratio  $C/C_0$  started to increase because the soil was saturated, and a plateau was reached (“treated” solution had same concentration of untreated solution) then groundwater kept for human use results polluted. For the system soil-TPEG, no plateau was reached into the range of time 0-360 minutes and the ratio  $C/C_0$  was lower than the ratio registered for the soil at all the time evaluated. It means that TPEG increase added to the soil can adsorb contaminants, therefore it could be used as permeable reactive barrier to remove BTEX from groundwater.

#### **4. Conclusion**

This study describes the simple preparation of a “hydro-soluble” form of thermo-plasma expanded graphite (TPEG). The “hydro-soluble” TPEG demonstrated to have good adsorbent properties for removal of toluene, ethylbenzene and xylenes from groundwater. The adsorption mechanism was dependent on the molecules in terms of mono-multilayer adsorption, kinetics of the process and affinity. The maximum adsorption capacity of BTEX on “hydro-soluble” TPEG registered was about  $20 \text{ mg g}^{-1}$  if are not present other organic substance in the water. The presence of humic acid increase the adsorption capacity until to reach values of  $400 \text{ mg g}^{-1}$  for ethylbenzene and  $150 \text{ mg g}^{-1}$  for the other compounds. Injection test in groundwater of this form of TPEG were done and promising results was obtained. The injection is possible and the effect of pressure of injection was evaluated on the time necessary of injection and on the volume of TPEG’s solution used. After the injection, “hydro-soluble” TPEG preserves its adsorption properties and it demonstrates the possibility to use this material as innovative permeable reactive barrier.

#### **Reference**

- [1] Daifullah, A.A.M., Girgis, B.S., 2003, Impact of surface characteristics of activated carbon on adsorption of BTEX, *Colloids and Surfaces A: Physicochemical Engineering Aspects*, 214, 181-193.
- [2] Crimi, M.L., Taylor, J., 2007, Experimental Evaluation of Catalyzed Hydrogen Peroxide and Sodium Persulfate for Destruction of BTEX Contaminants, *Soil and Sediment Contamination: An International Journal*, 16, 29-45
- [3] Liang, C., Huang, C.-F., Chen, Y.-J., 2008, Potential for activated persulfate degradation of BTEX contamination, *Water Research*, 42, 4091-4100.

- [4] Kang, N., Hua, I., 2015, Enhanced chemical oxidation of aromatic hydrocarbons in soil systems, *Chemosphere*, 61, 909-922
- [5] Christofolletti Mazzeo, D.E., Levy, C.E., de Franceschi de Angelis, D., Marin-Morales, M.A., 2010, BTEX biodegradation by bacteria from effluents of petroleum refinery, *Science of the Total Environment*, 408, 4334-4340
- [6] Lovanh, N., Hunt, C.S., Alvarez, P.J.J., 2002, BTEX biodegradation by bacteria from effluents of petroleum refinery, *Water Research*, 36, 3739-3746
- [7] Khoadei, K., Nassery, H.R., Asadi, M.M., Mohammadzadeh, H., Mahmoodlu, M.G., 2017, BTEX biodegradation in contaminated groundwater using a novel strain (*Pseudomonas* sp. BTEX-30), *International Biodeterioration and Biodegradation*, 116, 234-242
- [8] Caetano, M.O., Schneider, I.A.H., Gomes, L.P., Kieling, A.G., Miranda L.A.S., 2017, A compact remediation system for the treatment of groundwater contaminated with BTEX and TPH, *Environmental Technology*, 38, 1408-1420
- [9] Nourmoradi, H., Nikaeen, M., Khiadani, M., 2012, Removal of benzene, toluene, ethylbenzene and xylene (BTEX) from aqueous solutions by montmorillonite modified with nonionic surfactant: Equilibrium, kinetic and thermodynamic study, *Chemical Engineering Journal*, 191, 341– 348
- [10] Bandura, L., Kolodynska, D., Franus, W., 2017, Adsorption of BTX from aqueous solutions by Na-P1zeolite obtained from fly ash, *Process Safety and Environmental Protection*, 109, 214-223
- [11] Azizi, A., Torabian, A., Moniri E., Hassani, A.H., Panahi, H.A., 2016, Adsorption performance of modified graphene oxide nanoparticles for the removal of toluene, ethylbenzene, and xylenes from aqueous solution, *Desalination and Water Treatment*, 57, 28806-28821
- [12] Wang, Y., Pleasant, S., Jain, P., Powell, J., Townsend, T., 2016, Calcium carbonate-based permeable reactive barriers for iron and manganese groundwater remediation at landfills, *Waste Management*, 53, 128-135
- [13] Liu, Y., Mou, H., Chen, L., Mirza, Z.A., Liu, L., 2015, Cr(VI)-contaminated groundwater remediation with simulated permeable reactive barrier (PRB) filled with natural pyrite as

reactive material: Environmental factors and effectiveness, *Journal of Hazardous Materials*, 298, 83-90

[14] Zhao, X., Liu, W., Cai, Z., Han, B., Qian, T., Zhao, D., 2016, An overview of preparation and applications of stabilized zero-valent iron nanoparticles for soil and groundwater remediation, *Water Research*, 100, 245-266

[15] Vermeul V.R., Szecsody, J.E., Fritz, B.G., Williams, M.D., Moore, R.C., Fruchter, J.S., 2014, An Injectable Apatite Permeable Reactive Barrier for In Situ <sup>90</sup>Sr Immobilization, *Groundwater Monitoring and Remediation*, 34, 28-41

[16] Hunter, W.J., 2005, Injection of innocuous oils to create reactive barriers for bioremediation: Laboratory studies, *Journal of Contaminant Hydrology*, 80, 31-48

[17] Masi, S., Calace, S., Mazzone, G., Caivano, M., Buchicchio, A., Pascale, S., Bianco, G., and Caniani, D., Lab-scale investigation on remediation of sediments contaminated with hydrocarbons by using super-expanded graphite, 15th International Conference on Environmental Science and Technology Rhodes, Greece, 31 August to 2 September 2017

[18] Caniani, D., Caivano, M., Calace, S., Mazzone, G., Pascale, R., Mancini I.M., Masi S., Remediation of water samples contaminated by BTEX using super-expanded graphite as innovative carbon-based adsorbent material, IWA World Water Congress & Exhibition, 16-21 September 2018, Tokyo, Japan

[19] Caniani, D., Calace, S., Mazzone, G., Caivano, M., Mancini, I.M., Greco M., and Masi, S., Removal of Hydrocarbons from Contaminated Soils by Using a Thermally Expanded Graphite Sorbent, *Bulletin of Environmental Contamination and Toxicology*, 2018, [20] M. Yi, Z. Shen, A review on mechanical exfoliation for the scalable production of graphene, *Journal of Materials Chemistry A*, 2015, 3, 11700-11715

[21] Qiu, H., Lv, L., B.-cPan, Zhang, Q.-j., Zhang, W-m., Zhang, Q.-x., 2009. Critical review in adsorption kinetic models, *Journal of Zhejiang University SCIENCE A*, 10(5), 716-724.

[24] Ho, Y.S., McKay, G., 1999. Pseudo-second order model for sorption process, *Process Biochem*, 34, 451-465.

[25] Low, M.J.D., 1960. Kinetics of chemisorption of gases on solids, *Chem. Rev.*, 60(3), 267-312.

- [26] Langmuir, I., 1918. The adsorption of gases on plane surfaces of glass, mica and platinum, *J. Am. Chem. Soc.*, 1918, 1361-1402.
- [27] Freundlich, H. M. F., 1906. Over the adsorption in solution, *Journal of Physical Chemistry*, 57, 385-471.
- [28] Temkin, M.I., Pyzhev, V., 1940. Kinetics of ammonia synthesis on promoted iron catalyst, *Acta Physical Chemistry USSR*, 12, 327-357.
- [29] Dubinin, M.M., Radushkevich, L.V., 1947. The equation of characteristic curve of the activated charcoal, *Proceedings of the Academy of Science of the USSR Physical Chemistry Section*, 55, 331-337.
- [30] Yang, S., Hu, J., Chen, C., Shao, D., Wang, X., 2011, Mutual Effects of Pb(II) and Humic Acid Adsorption on Multiwalled Carbon Nanotubes/Polyacrylamide Composites from Aqueous Solutions, *Environmental Science and Technology*, 45, 3621-3627
- [31] Yang, S., Li, L., Pei, Z., Li, C., Shan, X.-Q., Wen, B., Zhang, S., Zheng, L., Zhang, J., Xie, Y., Huang, R., 2014, Effects of humic acid on copper adsorption onto few-layer reduced graphene oxide and few-layer graphene oxide, *Carbon*, 75, 227-235
- [32] Chang Chien, S.W., Chen, C.Y., Chang, J.H., Chen, S.H., Wang, M.C., Manneppalli, M.R., 2010, Sorption of toluene by humic acids derived from lake sediment and mountain soil at different pH, *Journal of Hazardous Materials*, 177, 1068-1076
- [33] Molson, J.W., Frind, E.O., Van Stempvoort, D.R., Lesage, S., 2002, Humic acid enhanced remediation of an emplaced diesel source in groundwater. 2. Numerical model development and application, *Journal of Contaminant Hydrology*, 54, 277-305
- [34] Jung, K.-W., Choi, B.H., Hwang, M.-J., Jeong, T.-U., Ahn, K.-H., 2016, Fabrication of granular activated carbons derived from spent coffee grounds by entrapment in calcium alginate beads for adsorption of acid orange 7 and methylene blue, *Bioresource Technology*, 219, 185-195
- [35] Pascale, R., Bianco, G., Calace, S., Masi, S., Mancini, I.M., Mazzone, G., Caniani, D., 2018, Method development and optimization for the determination of benzene, toluene, ethylbenzene and xylenes in water at trace levels by static headspace extraction coupled to gas chromatography–barrier ionization discharge detection, *Journal of Chromatography A*, 1548, 10-18



- [36] Hernandez, Y., Nicolosi, V., Lotya, M., Blighe, F.M., Sun, Z., De, S., McGovern, I.T., Holland, B., Byrne, M., Gun'Ko, Y.K., Boland, J.J., Niraj, P., Duesberg, G., Krishnamurthy, S., Goodhue, R., Hutchison, J., Scardaci, V., Ferrari A.C., and Coleman, J.N., 2008, High-yield production of graphene by liquid-phase exfoliation of graphite, *Nature Nanotechnology*, 3, 563–568
- [37] Li, B., Lei, Z., Huang, Z., 2009, Surface-Treated activated carbon for removal of aromatic compounds from water, *Chemical Engineering Technology*, 32, 763-770
- [38] Gueli Ulson de Souza, S.M.d.A., da Luz, A.D., da Silva, A., Ulson de Souza, A.N.A., 2012, Removal of mono and multi-component BTX compounds from effluents using activated carbon from coconut shell as the adsorbent, *Industrial and Engineering Chemistry Research*, 51, 6461-6469
- [39] Wibowo, N., Setyadi, L., Wibowo, D., Setiawan, J., Ismadji, S., 2007, Adsorption of benzene and toluene from aqueous solutions onto activated carbon and its acid and heat treated forms: Influence of surface chemistry on adsorption, *Journal of Hazardous Materials*, 146, 237-242
- [40] Nourmoradi, H., Nikaeen, M., Khiadani, M., 2012, Removal of benzene, toluene, ethylbenzene and xylene (BTEX) from aqueous solutions by montmorillonite modified with nonionic surfactant: Equilibrium, kinetic and thermodynamic study, *Chemical Engineering Journal*, 191, 341– 348
- [41] Anjum, H., Johari, K., Gnanasundaram, N., Murugesan, T., Decontamination of Benzene From Aqueous Solution by Green Functionalization of Activated Carbon, *IOP Conference* 2018,458, 012056
- [41] Konggidinata, M.I., Chao, B., Lian, Q., Subramaniam, R., Zappi, M., Gang, D.D., 2017, Equilibrium, kinetic and thermodynamic studies for adsorption of BTEX onto ordered mesoporous carbon (OMC), *Journal of Hazardous Materials*, 336, 249–259
- [42] Su, F.S., Lu, C.Y., Hu, S.K., 2010, Adsorption of benzene, toluene, ethylbenzene and p-xylene by NaOCl-oxidized carbon nanotubes, *Colloids Surface A: Physicochemical and Engineering Aspects*, 353, 83–91
- [43] Chin, C.J.M., Shih, L.C., Tsai, H.J., Liu, T.K., 2007, Adsorption of o-xylene and p-xylene from water by SWCNTs, *Carbon*, 45, 1254-1260

- [44] Anjum, H., Johari, K., Gnanasundaram, N., Appusamy, A., Thanabalan, M., 2019, Impact of surface modification on adsorptive removal of BTX onto activated carbon, *Journal of Molecular Liquids*, 280, 238-251
- [45] Tsuzuki, S., Honda, K., Uchamaru, T., Mikami, M., Tanabe, K., 2002, Origin of Attraction and Directionality of the  $\pi/\pi$  Interaction: Model Chemistry Calculations of Benzene Dimer Interaction, *Journal of American Chemical Society*, 124, 104-112
- [46] Lu, C., Su, F., Hu, S., 2008, Surface modification of carbon nanotubes for enhancing BTEX adsorption from aqueous solution, *Applied Surface Science*, 254, 7035-7041
- [47] Oh, Y., Armstrong, D.L., Finnerty, C., Zheng, S., Hu, M., Torrents, A., Mi, B., 2017, Understanding the pH-responsive behavior of graphene oxide membrane in removing ions and organic micropollutants, *Journal of Membrane Science*, 541, 235-243
- [48] Al Khateeb, L.A., Almotiry, S., Salam, M.A., 2014, Adsorption of pharmaceutical pollutants onto graphene nanoplatelets, *Chemical Engineering Journal*, 248, 191-199

## **2.4 Trichloroethylene adsorption from aqueous solution by thermo-plasma expanded graphite: investigation of mechanism process**

### **Abstract**

The adsorption of trichloroethylene (TCE) on thermo-plasma expanded graphite (TPEG) from water solution was investigated. The adsorbent material was characterized by SEM, TEM, BET, Raman and X-ray diffraction analysis. The influence of stirring speed on the adsorption capacity was evaluated by varying its value in the range 0-1500 rpm and the adsorption mechanism was determined by kinetic and isothermal studies for different initial concentration of TCE ( $1-25 \text{ mg L}^{-1}$ ) and different temperature ( $20-60^\circ\text{C}$ ). Pseudo-first order, pseudo-second order, intraparticle diffusion, liquid film diffusion and Elovich models were used to fit kinetics experimental data, whereas the isothermal experimental data were fitted by using Langmuir, Freundlich, Temkin and Dubinin-Radushkevich isotherms models. The results obtained demonstrates the influence of initial concentration of TCE and temperature on the mechanism process. Pseudo-second order model results to be the best fit in the range of concentration  $5-25 \text{ mg L}^{-1}$  while the Elovich model results to be the best fit for the concentration of TCE of  $1 \text{ mg L}^{-1}$ . Freundlich model results the best fit for the range temperature of  $20-45^\circ\text{C}$  while Langmuir

model is the best fit for the data obtained at the temperature of 60°C. The adsorption capacity is depending on the initial concentration of TCE and its value is respectively 1.51 mg g<sup>-1</sup> and 27.17 mg g<sup>-1</sup> at 1 mg L<sup>-1</sup> and 25 mg L<sup>-1</sup> of initial concentration of TCE. Furthermore, the influence of parameters, such as presence of cosolvent (methanol), height of headspace, adsorbent dosage on the process and the thermodynamics were investigated. The data obtained from test with methanol demonstrates that the Lundelius rule is respected. The investigation of the effect of stirring speed, temperature, adsorbent dosage and height of headspace demonstrate that the process could be separated into two consecutively steps, the stripping of TCE from solution (the first one) and the adsorption on the layer of TPEG.

## 1. Introduction

Trichloroethylene (TCE) has been widely used as solvent in different kind of industry and often was detected in surface/ground water, contaminated via direct discharge or leaching from disposal operation [1], furthermore, EPA identified TCE as a priority environmental pollutant [2] and set 5 ppb for the maximum level of contamination of TCE. TCE contamination is a great problem because of its high solubility in water (1100 mg L<sup>-1</sup> at 25°C) and high resistance to biological degradation, therefore contaminated water remains polluted for a long time. The agency for the Toxic Substance and Disease Registry has reported that 852 of 1430 National Priority List sites in 1997 present TCE [3]. An example of several contamination of groundwater by TCE was reported in Korea, at the industrial complex of Wonju, where the level of TCE was >50 times of limited indicated by Korean Ministry of Environment (0.06 mg L<sup>-1</sup> for industrial areas) [4]. Different technology for removal of TCE from soil or groundwater are available and they can be classified in biotic and abiotic process. Biotic removal of TCE involves the use of microorganisms to dechlorinate tetrachloroethylene (PCE) and TCE into less-chlorinated by products such as dichloroethylene (DCE) and vinyl chloride (VC) in aerobic or anaerobic system (normally O<sub>2</sub> is used at the begin of the process, then other acceptors of electron are used). Abiotic process includes chemical oxidation/reduction [5] of TCE like zero valent iron<sup>6</sup>, the physical adsorption using various adsorbent or the combination of adsorption and chemical oxidation/reduction [7,8]. The adsorption process is one of the most commonly used techniques for the purification of groundwater contaminated by TCE. Several adsorbents were investigated to mitigate the migration of TCE but the activated carbon results to be the most popular in both granular and powder form. Other available adsorbent materials for TCE were investigated and are nowadays investigated to found material with a higher capacity of adsorption or better mechanical characteristic than configure it as conventional adsorbent to use

for TCE removal. Example of adsorbent materials investigated are soils, peat moss [9], organo-clays [10,11], polymer adsorbent [12], zeolites [13], multiwalled carbon nanotubes [14], silica gels [15] and organic mulch [16]. Nowadays, accurate studies are conducting on the use of carbon materials like single/multiwalled carbon nanotubes, graphitic and graphenic materials due their higher surface area (if compared to typical activated carbon) that theoretically confers them a higher adsorption capacity. Their structural characteristic ensures strong interaction with organic molecules by mean of  $\pi$ - $\pi$  interactions, H-bonding, electrostatic forces, van der Waals forces and hydrophobic interactions [17,18]. Furthermore, mechanical characteristic of these materials, such as mechanical strength, confers them potential advantages in the conventional use as adsorbent instead of conventional activated carbon. For these reasons, in this work thermo-plasma expanded graphite (TPEG) was investigated as potential adsorbent for TCE removal and its performance in terms of adsorption capacity was evaluated. Furthermore, the kinetics, the adsorption isotherm, the thermodynamics of the process and the parameters that influence the adsorption process of TCE on TPEG was investigated. The complete study on the process of adsorption of TCE from water solution has not been diffuse in literature. TPEG used in this study is produced by means of an innovative process, that ensure a higher expansion than classical methods, consisting in the chemical intercalation of natural graphite followed by high temperature thermal plasma expansion. This process confers excellent physic-chemical properties to TPEG, i.e. apparent density [19] in the range 2.3 to 9 g L<sup>-1</sup>, that make it an excellent adsorbent material. TPEG is an innovative carbon-based material used to remove different kinds of hydrocarbons, like exhausted lubricating oil [20], BTEX [21] with a removal efficiency of more than 80%, both treating soil and water.

## **2. Materials and methods**

### ***2.1 Materials***

TPEG was obtained from Innograf, that produced it from natural graphite, intercalated with chemical compound and expanded by the thermal plasma expansion. This process ensures the exfoliation of graphite, with a volume expansion of up to 300 units, compared to an average of 200 units obtainable by other standard methods. TPEG has good structural properties, such as mechanical strength of about 1 TPa, a thermal conductivity of about 500 W mK<sup>-1</sup>, a diameter between 60 and 300  $\mu$ m and high apparent density that could be associated with high surface area, property that can confer high adsorption capacity.

The trichloroethylene and methanol were supplied from Carlo Erba reagents (Carlo Erba, Rodano, Milano, Italy). The stock solution of TCE was prepared in methanol at a concentration of 1000 mg/L. The solution of TCE used for adsorption experiment were prepared in water with 1% of MeOH. All reagents were of extra pure grade and used without further purification.

## **2.2 TPEG characterization**

TPEG characterization was already managed for the previous works.

## **2.3 Experimental setup and analytical method**

The adsorption experiments were conducted by adding different amount of TPEG to 36 ml of solution of different concentration of TCE. The mix of TPEG and TCE solution were maintained in closed vials [16,22], to avoid TCE loss by volatilization, and stirred for different times. The experimental parameters such as contact time, initial concentration of TCE, amount of TPEG, temperature and presence of cosolvent were varied to evaluate the influence of each parameters on adsorption capacity. At the end of the chosen contact time, TCE residual concentration was evaluated by GC-BID analysis by using headspace method [23]. 20 ml of TCE solution (in 30 mL vial closed with silicon septum bottom) at 1% of MeOH was stirred and heated at 80°C for 15 minutes and then the gas in headspace was collected with syringe for gas (25 mL gas-tight syringe) and injected in GC through 500  $\mu$ L sample loop at 70°C. The area of TCE peak was used to calculate the residual concentration by comparing it with calibration line obtained by analysis of TCE solution with known concentration. TCE solutions were opportunely diluted by considering that calibration line was obtained in the range 10-100 ppb (distilled water and 1% of MeOH).

A Shimadzu system (Kyoto, Japan) consisting of barrier ionization discharge (BID) detector equipped with a 2010 Plus Tracer gas chromatograph (GC) with a split/splitless injector was used for TCE quantification. The pressure drop was kept constant by using a 10-100 cc/min scale RMA-150-BV rotameter (Rometec, Roma, Italy), to improve the sample precision of manual injection. (inserire flusso usato). The injector port was maintained at 200°C and a 500  $\mu$ L of headspace was injected in split mode (split ratio 90:10). A Restek Rtx-624 fused silica capillary column was employed with He 6.0 (SIAD Corporation, Bergamo, Italy) as the carrier gas at flow rate of 1 mL/min. The column temperature was constant at 30°C for 1 min, increasing to 70°C at 10°C/min and holding for 3 minutes. The effluent of column was transferred via a 50 mL/min discharge gas flow into the BID detector at 250°C. LabSolution software (Shimadzu, Kyoto, Japan) was used to process the obtained data.

The adsorption capacity was calculated by using the following equation:

$$q = \frac{\text{mass of TCE adsorbed (mg)}}{\text{mass of adsorbent (g)}} \quad (20)$$

$$q = (c_i - c_f) \frac{V}{m} \quad (21)$$

where V is the initial solution volume (L), m is the adsorbent weight (g),  $c_i$  and  $c_f$  (mg L<sup>-1</sup>) are the TCE concentrations at the beginning and after each adsorption experiment. For each test the standard deviation was evaluated, and it always was below 5 % of main value. Test without TPEG was done to verify that no lack of TCE for volatilization was obtained.

#### **2.4 Effect of stirring speed**

The stirring speed could influence the adsorption capacity because it influences on stripping of TCE and agitation of TPEG phase that float on water surface. 20 mg of TPEG was mixed to 36 mL of TCE solution (10 mg/L, 1% MeOH), and stirred for 2 hours at room temperature. Different stirring speed was evaluated (0, 150, 300, 600 and 1500 rpm). The residual concentration of TCE was evaluated at the end of 2 hours of contact time.

#### **2.5 Effect of headspace**

To evaluate the possible effect of headspace on adsorption capacity a series of experiments were made. The headspace is correlated with the number of TCE molecules necessary to reach the value of pressure of gas phase on liquid phase that is regulated by Raoult law. More headspace is related with higher number of molecules of TCE that pass in gas phase through the layer of TPEG.

18, 27 and 36 mL of TCE solution (25 mg/L, 1% MeOH) was mixed with 20 mg of TPEG and stirred at 300 rpm for 2 hours and then the residual concentration of TCE was measured.

#### **2.6 Effect of adsorbent dosage**

Different amount of TPEG (5, 10, 20, 30, 40 and 50 mg) was mixed to 36 ml of TCE (25 mg/L, 1% MeOH) and stirred at 300 rpm for 2 hours. The residual TCE was then measured with analytical method already described. The adsorbent dosage could influence adsorption capacity due the different headspace associated with different amount of TPEG and different number of active sites that can adsorb TCE.

#### **2.7 Effect of cosolvent**

Normally, the presence of reagents that improve the solubility of adsorbate in liquid phase decrease the adsorption capacity (Lundelius rule), but exceptions were observed and reported in literature, therefore the influence of this parameter was evaluated. 20 mg of TPEG was mixed to 36 mL of TCE solutions (10 mg/L) with different amount of methanol (1, 5, 10, 20 and 30%) and stirred at 300 rpm for 2 hours and then TCE residual concentration was evaluated.

## **2.8 Adsorption kinetics**

The kinetics models investigate the velocity of the process, providing the relationship between contact time and adsorption capacity. Kinetics models give also information about the slowly step of the process and the mechanism of interaction between adsorbent and adsorbate. In order to evaluate the kinetics of the process, different experiments were conducted. The kinetic was evaluated at different concentration of TCE (1, 5, 10 and 25 mg/L) to evaluate also the effect of this parameter on the mechanism of the adsorption. Therefore, 36 mL of TCE solution (variable concentration, 1% MeOH) was mixed with 20 mg of TPEG and stirred at 300 rpm for different time (20 minutes-24 hours) and the residual TCE concentration measured. The obtained data were fitted to different kinetic models, i.e. pseudo-first order, pseudo-second order, intraparticle diffusion, Elovich and liquid film diffusion models, and the  $R^2$  coefficient of linear regression and  $\chi^2$  were calculated for each fitting. The equation of the models used are reported in the chapter 2.1.

## **2.9 Effect of initial concentration and temperature**

The influence of initial concentration and temperature on the adsorption capacity were evaluated by mixing 20 mg of TPEG with 36 mL of TCE solution with different initial concentration (1, 2.5, 5, 7.5, 15, 25 and 33 mg/L, 1% MeOH), stirred for 2 hours at 300 rpm at different temperature (r.t., 45°C and 60°C). The residual TCE concentration was then evaluated.

## **2.10 Thermodynamics**

Very important results to be to have information about the thermodynamics of the process. In this way is possible to know if the process is spontaneous in normal condition, the minimum temperature that ensure the spontaneity of the process and the exothermicity/endothermicity of the adsorption phenomena. This last parameter allows to know if the increase of temperature correspond to an increase of adsorption capacity. Therefore, the adsorption capacity was determinate at different temperature (0, 25, 45 and 60°C). 20 mg of TPEG was mixed with 36 mL of TCE (25 mg/L, 1% MeOH) and stirred at 300 rpm for 2 hours and residual TCE

concentration evaluated. The equations that regulates the thermodynamics and used are reported in the chapter 2.1.

## 2.11 Adsorption isotherms

The investigation of the isotherms of adsorption allows to know the mechanism of interaction between adsorbent and adsorbate. Different models were formulated but the most used are Langmuir, Freundlich, Temkin and Dubinin-Radushkevich isotherm models.

36 mL of TCE solution with different initial concentration (1% MeOH, 1, 2.5, 5, 7.5, 15, 25 and 33 mg/L) was mixed with 20 mg of TPEG and stirred at 300 rpm for 2 hours at different temperature (r.t., 45°C and 60°C). Then, the residual TCE concentration was evaluated. In this way, the mechanism of interaction was determinate and the effect of the temperature on the mechanism of the process was also evaluated. The equations of the models used are reported in the chapter 2.1.  $R^2$  and  $\chi^2$  were calculated.

## 3 Results and discussion

### 3.1 Effect of stirring speed

The effect of the stirring speed on the adsorption capacity was reported in the figure 68.

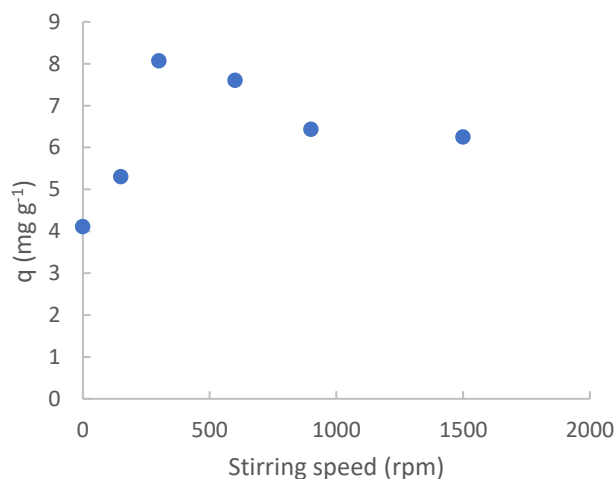


**Fig. 68** *The effect of the stirring speed on the adsorption capacity. 20 mg of TPEG was mixed to 36 mL of TCE (10 mg/L, 1% MeOH) and stirred for 2 hours at r.t.*

The increase of adsorption capacity with the increase of the stirring speed was observed until 300 rpm, further increase of stirring speed involves a decrease of adsorption capacity. From 0 to 300 rpm no dispersion of TPEG in water is observed, therefore it floats on the water, while from 600 to 1500 rpm the dispersion of TPEG in water was observed. Therefore, it means that the initial increase of adsorption capacity could be caused by increased stripping of TCE



molecules from liquid phase and they cross the TPEG floating on the water and adsorbed on it. The further increase is associated with an increase of stripping of TCE molecules, but they can't cross TPEG because it is dispersed in water and just a little amount of TPEG floating on water.

### 3.2 Effect of headspace height

The effect of the headspace was studied to verify if the number of molecules necessary to reach the value of the pressure regulated by Raoult law can influence the adsorption capacity. The hypothesis was that the increase number of molecules that go across the layer of TPEG increase the adsorption capacity. The results are gathered in the figure 69.

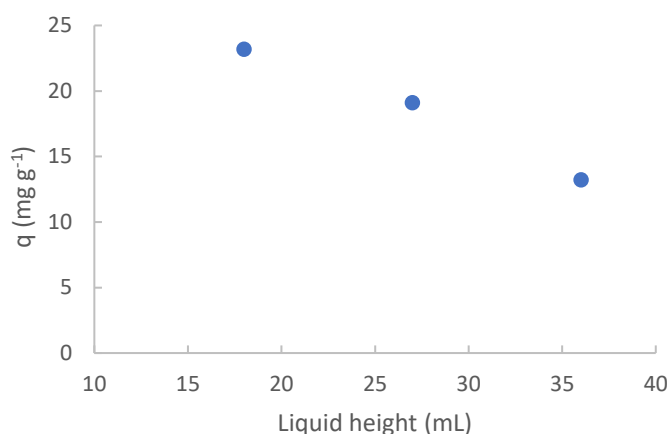


**Fig. 69** The effect of headspace height on the adsorption capacity. Adsorption capacity was measured after mixing 18, 27 and 36 mL of TCE solution (25 mg/L, 1%MeOH) with 20 mg of TPEG and stirred at 300 rpm for 2 hours.

The figure 70 represents schematically the setup of the experiment for a good comprehension of the experiment and the conclusion obtained.

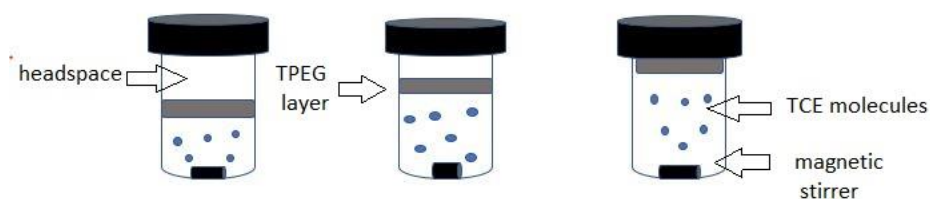


**Fig. 70** Schematic representation of setup experiment at 18, 27 and 36 mL respectively.

The decrease of adsorption capacity obtained with the decrease of headspace height could be explained by the lower number of molecules that go across the TPEG layer. Indeed, to reach the value of pressure regulated by Raoult law a lower number of TCE molecules is necessary.

### 3.3 Effect of adsorbent dosage

The optimum dosage of adsorbent could be a parameter that improves the cost benefits of the process because an overdosage of adsorbent can be obtained when the active sites is bigger than adsorbate molecules. For this reason, the influence of adsorbent dosage was investigated. In the figure 71 are shown the obtained results.

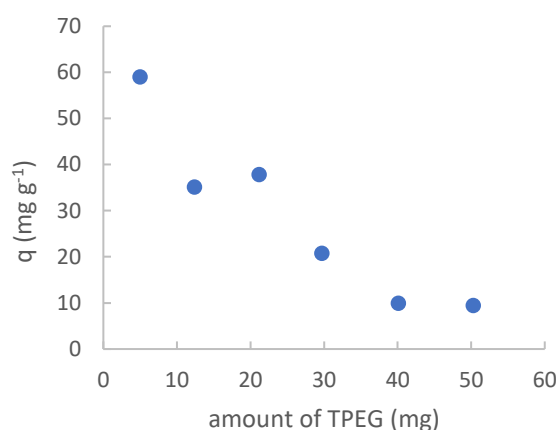


**Fig.71 Effect of amount of TPEG on adsorption capacity. 36 mL of TCE solution (25 mg/L, 1% MeOH) was mixed to different amount of TPEG (5, 10, 20, 30, 40 and 50 mg) and stirred at 300 rpm for 2 hours.**

The decrease of adsorption capacity with the increase of the amount of TPEG mixed to TCE solution was observed. Two reasons could explain this behavior, indeed the increase of the amount of TPEG corresponds to decrease of the headspace height, therefore lower number of TCE molecules go across the TPEG layer even if the number of active sites were increased. The decrease of adsorption capacity seems to reach a plateau that could be caused by a negligible decrease of headspace that no compensate the increase of active sites.

### 3.4 Effect of cosolvent

To verify if the Lundelius rule is valid also for the adsorption of TCE on TPEG, the adsorption capacity was evaluated by increasing the solubility of TCE in the solution by increasing the amount of methanol in the solution. The results obtained are reported in figure 72.

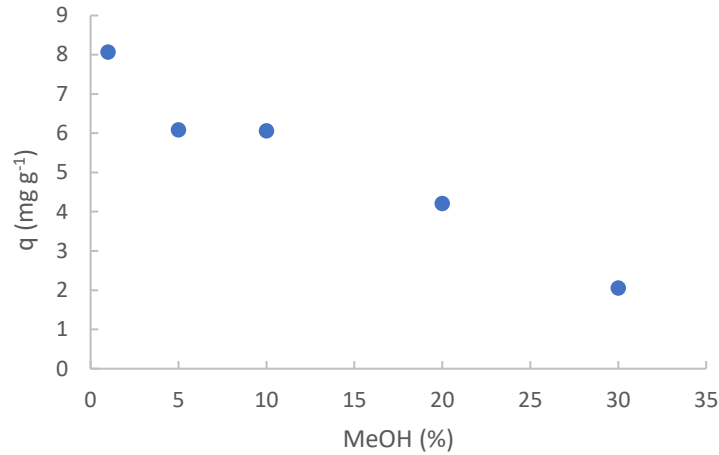


**Fig. 72** Effect of the amount of methanol on the adsorption capacity. 36 mL of TCE solution (10 mg/L) was mixed with 20 mg of TPEG and stirred at 300 rpm for 2 hours.

The increase of the amount of methanol corresponds to the increase of solubility of TCE and the decrease of the adsorption capacity was observed, therefore the Lundelius rule is respected for this adsorption process.

### 3.5 Adsorption kinetics

The evaluation of the kinetics of the process results to be another way to increase the benefit of the cost of the process because the time of saturation of the adsorbent can be determinate. It is useful because a contact time upper than saturation time doesn't involve an increase of adsorption and time is wasted and time means money. Furthermore, the study of the adsorption kinetics allows to know if there is a one specific step that slow down the process and work on it to develop the process. By the study of the kinetics of the process, the kinetic constant can be calculated. In the figure 73 are reported the results obtained.

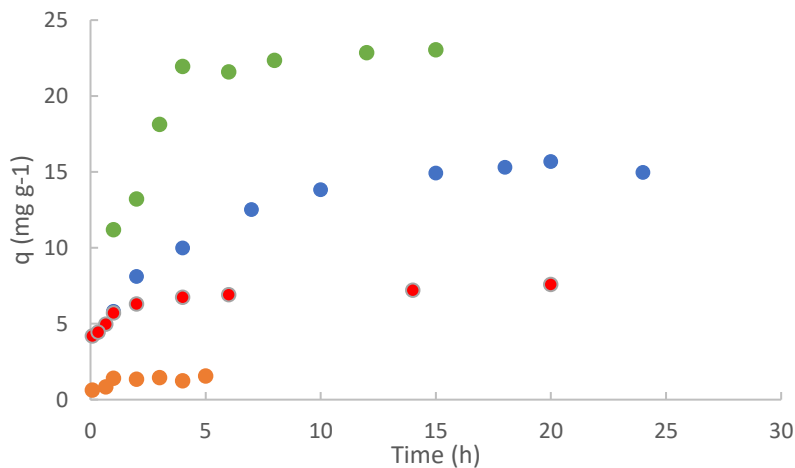


**Fig.73 Effect of the time on the adsorption capacity. 36 mL of TCE solution (1 mg/L: orange points, 5 mg/L: red points, 10 mg/L: blu points and 25 mg/L: green points) was mixed with 20 mg of TPEG and stirred at 300 rpm for variable times.**

The results obtained shows that the increase of the concentration corresponds with an increase of adsorption capacity but also with an increase of the time necessary to reach the equilibrium. The fit of experimental data with kinetics model (pseudo-first order, pseudo-second order, Elovich model, intraparticle diffusion model and liquid film diffusion model) was done and the linear correlation constant and the parameters obtained from the fit are reported in the table 19.

**Tab. 19 Parameters of the fit of experimental data with kinetics models.**

	1 mg/L		5 mg/L		10 mg/L		25 mg/L	
Pseudo-first order	R <sup>2</sup> 0.6088 X <sup>2</sup> -1.8	k: 0.4297 mg g <sup>-1</sup> q: 0.45 mg g <sup>-1</sup>	R <sup>2</sup> 0.9179 X <sup>2</sup> -1.3	k: 0.2012 mg g <sup>-1</sup> q: 10.20 mg g <sup>-1</sup>	R <sup>2</sup> 0.8549 X <sup>2</sup> -3.7	k: 0.2578 mg g <sup>-1</sup> q: 674.2 mg g <sup>-1</sup>	R <sup>2</sup> 0.9394 X <sup>2</sup> -11	k: 0.3696 mg g <sup>-1</sup> q: 408.50 mg g <sup>-1</sup>
Pseudo-second order	R <sup>2</sup> 0.9676 X <sup>2</sup> 0.15	q:1.51 mg g <sup>-1</sup> k : 2.55 g mg <sup>-1</sup> min <sup>-1</sup>	R <sup>2</sup> 0.9989 X <sup>2</sup> 0.08	q:7.57 mg g <sup>-1</sup> k : 3.74·10 <sup>-1</sup> g mg <sup>-1</sup> min <sup>-1</sup>	R <sup>2</sup> 0.9967 X <sup>2</sup> 0.008	q: 16.86 mg g <sup>-1</sup> k : 2.69·10 <sup>-2</sup> g mg <sup>-1</sup> min <sup>-1</sup>	R <sup>2</sup> 0.9785 X <sup>2</sup> 0.06	q: 27.17 mg g <sup>-1</sup> k: 2.35·10 <sup>-2</sup> g mg <sup>-1</sup> min <sup>-1</sup>
Elovich	R <sup>2</sup> 0.9895 X <sup>2</sup> 0.12	α: 2.88 g mg <sup>-1</sup> min <sup>-1</sup> β: 0.984 g mg <sup>-1</sup>	R <sup>2</sup> 0.9578 X <sup>2</sup> 0.10	α: 2617.12 g mg <sup>-1</sup> min <sup>-1</sup> β: 1.48 g mg <sup>-1</sup>	R <sup>2</sup> 0.9802 X <sup>2</sup> 0.14	α: 20.60 g mg <sup>-1</sup> min <sup>-1</sup> β: 0.314 g mg <sup>-1</sup>	R <sup>2</sup> 0.844 X <sup>2</sup> 0.23	α: 56.75 g mg <sup>-1</sup> min <sup>-1</sup> β: 0.204 g mg <sup>-1</sup>
Intraparticle diffusion	R <sup>2</sup> 0.6731 X <sup>2</sup> 0.85	K <sub>dif</sub> : 0.40 mg g <sup>-1</sup> min <sup>-1/2</sup>	R <sup>2</sup> 0.8253 X <sup>2</sup> 0.38	K <sub>dif</sub> : 0.77 mg g <sup>-1</sup> min <sup>-1/2</sup>	R <sup>2</sup> 0.9098 X <sup>2</sup> 0.88	K <sub>dif</sub> : 2.43 mg g <sup>-1</sup> min <sup>-1/2</sup>	R <sup>2</sup> 0.7034 X <sup>2</sup> 0.96	K <sub>dif</sub> : 4.17 mg g <sup>-1</sup> min <sup>-1/2</sup>
Liquid film diffusion	R <sup>2</sup> 0.6088 X <sup>2</sup> -18	K <sub>fd</sub> : 0.43 min <sup>-1</sup>	R <sup>2</sup> 0.9179 X <sup>2</sup> -15	K <sub>fd</sub> : 0.20 min <sup>-1</sup>	R <sup>2</sup> 0.8669 X <sup>2</sup> -19	K <sub>fd</sub> : 0.14 min <sup>-1</sup>	R <sup>2</sup> 0.9394 X <sup>2</sup> -8	K <sub>fd</sub> : 0.37 min <sup>-1</sup>

The pseudo-second order model results to be the best fit for the concentration of 5, 10 and 25 mg/L and it is symptomatic of chemisorption and quadratic relation between adsorbate concentration and velocity. At the value of concentration of 1 mg/L the best fit of experimental data results to be the Elovich model, therefore the surface of TPEG results to be heterogeneous, the affinity decreases with the increase of covered surface. The values of adsorption capacity obtained from the model result to be in optimum agree with experimental data, indeed 1.51 mg g<sup>-1</sup> (from pseudo-second order) vs about 1.5 mg g<sup>-1</sup> for 1 mg/L, 7.57 mg g<sup>-1</sup> vs about 7.2 mg g<sup>-1</sup> for 5 mg/L, 16.86 mg g<sup>-1</sup> vs 15.5 mg g<sup>-1</sup> for 10 mg/L and 27.17 mg g<sup>-1</sup> vs about 23 m g<sup>-1</sup> were obtained, respectively for theoretical and experimental data. By comparing the data obtained

about kinetic constant and adsorption capacity with data reported in literature<sup>Ahmad b,Wei</sup> is clear that the TPEG has performance in terms of velocity of adsorption and adsorption capacity in the range of best adsorbent. Furthermore, it is interesting to note the increase of kinetic constant with the decrease of the concentration of TCE solution. In the figure 74 is reported the trend of kinetic constant for different initial concentration and the equation that best fit the trend of experimental data.

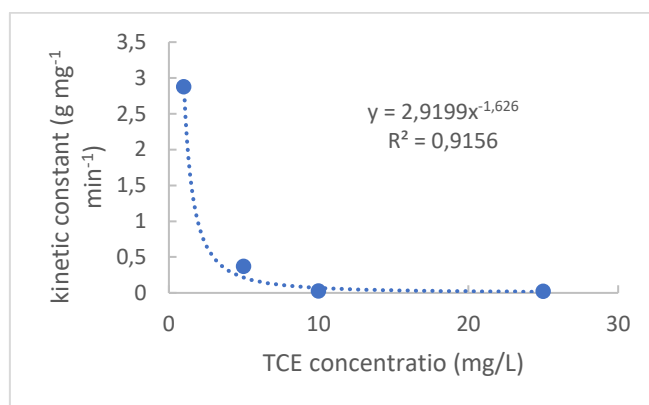


**Fig. 74 Influence of initial concentration on kinetic constant.**

### 3.6 Effect of initial concentration and temperature

The initial concentration has a big influence on the performance of adsorbent material. The influence that this parameter has on kinetic constant was already reported in the previous section. In this section the influence of initial concentration on adsorption capacity is investigated in a range of 1-33 mg/L. It is important to know the performance on different range of concentration because normally real sample have concentration that depends on the origin of it. Furthermore, the trend of the adsorption capacity with the change of temperature was also investigated and reported in this section. The figure 75 reported the experimental data obtained.

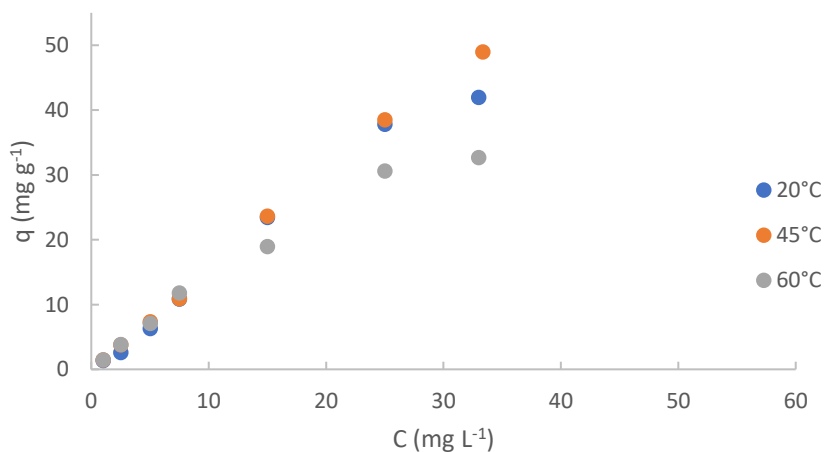


***Fig. 75 Effect of initial concentration for different temperature on adsorption capacity. 36 mL of TCE solutions at different concentration (1, 2.5, 5, 7.5, 15, 25 and 33 mg/L) were mixed with 20 mg of TPEG and stirred for 2 hours at different temperature (20, 45 and 60°C).***

The increase of adsorption capacity with the increase of TCE concentration was observed and the concentration of 33 mg/L seems to be the value of concentration to reach the plateau of adsorption capacity at 20°C and 60°C.

The temperature seems to have no influence for low value of concentration and little variations of adsorption capacity were observed until 7.5 mg/L of TCE. Upper to 7.5 mg/L, the temperature affects the adsorption capacity, indeed an increase of adsorption capacity was observed by comparing the adsorption capacity at 20°C and 45°C and a decrease of adsorption capacity was observed by comparing the adsorption capacity at 60°C and the value obtained at lower temperature. From the obtained results seems that a no clear trend is observed by increasing the temperature and it could be explained by considering two factor that are influenced by the increase of the temperature, the value of pressure of TCE gas phase on liquid phase and the thermodynamics of the process. The value of vapor pressure of pure TCE increase with the increase of the temperature, therefore the pressure of gas phase of TCE on liquid phase results increase and a bigger number of TCE molecules go across the layer of TPEG. The process could be exothermic, therefore, an increase of the temperature decreases the adsorption capacity. In conclusion, by increasing the temperature from 20 to 45°C an increase of adsorption capacity was observed because the increase of pressure of gas phase is not compensate by the exothermicity of the process, but the reverse happened with the further increase of the temperature until 60°C.

### *3.7 Thermodynamics*

The results showed in the previous section about the effect of the temperature push us to investigate on the thermodynamics of the process. Therefore, a test to determinate the thermodynamics of the process was done. As reported in the section of thermodynamics in materials and methods, the natural logarithm of the ratio of adsorption capacity and equilibrium concentration versus the reverse of the temperature was reported, for four different values of temperature (8, 20, 45 and 60°C). The results obtained are gathered in the figure 76.

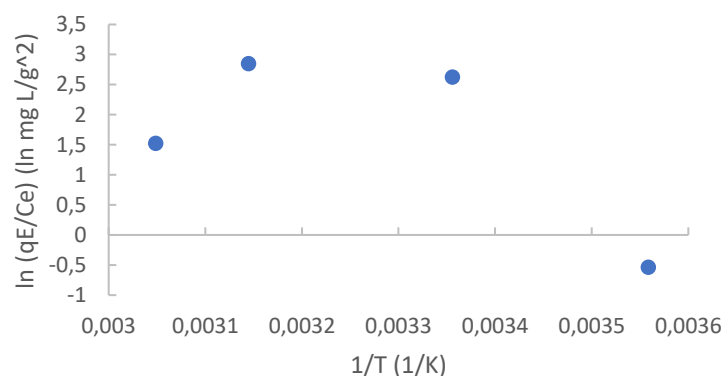


**Fig. 76 Effect of the temperature on the natural logarithm of equilibrium constant. 36 mL of TCE solution (25 mg/L, 1% MeOH) was mixed with 20 mg of TPEG and stirred for 2 hours at 300 rpm at different temperatures (8, 20, 45 and 60°C).**

The further investigation on the temperature effect on the process seems to confirm the previous hypothesis. The increase of the temperature from 8°C to 40°C was associated with an increase of equilibrium constant, while the increase until 60°C from 40°C or 20°C was associate with a decrease of equilibrium constant. It is possible to conclude that the process is exothermic but the increase of the pressure of TCE molecules in gas phase on liquid phase associated with the increase of the temperature favors the increase of adsorption capacity in a specific range of temperature (until 40°C).

#### *Adsorption isotherms*

In order to investigate the mechanism of interaction between adsorbate and adsorbent the adsorption isotherms of the process were evaluated at different temperature (20, 45 and 60°C). The experimental data were fitted with Langmuir, Freundlich, Temkin and Dubinin-Radushkevich models and the classification of each isotherm obtained with BDDT classification was done. The results obtained are showed in the figure 77.

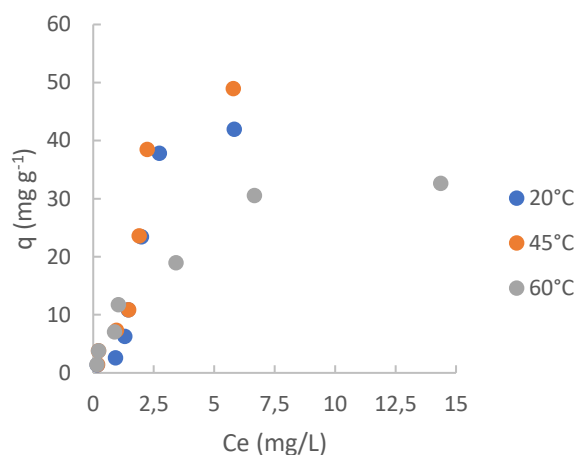


**Fig. 77 Adsorption isotherms at different temperatures (20, 45 and 60°C). 36 mL of TCE solution at variable concentration was mixed with 20 mg of TPEG and stirred at 300 rpm for 2 hours.**

By observing the isotherms obtained is possible to classify them by using the BDDT classification. The isotherm at 20 and 45°C results to be an isotherm of type V and it results to be of the type I at 60°C. In the table 20 are reported the square linear correlation coefficient and parameters obtained from the fit of experimental data with the previous cited isotherm models.

**Tab. 20 Overview on the fit of experimental data with some isotherm models. The square of linear correlation coefficient and parameters of the models are reported.**

	20°C		45°C		60°C	
Langmuir	R <sup>2</sup> 0.085 X <sup>2</sup> n.a.	q: negative value (no logic) k : negative value (no logic)	R <sup>2</sup> 0.004 X <sup>2</sup> 25	q: 769.23 mg g <sup>-1</sup> k <sub>L</sub> : 1.3·10 <sup>-2</sup>	R <sup>2</sup> 0.966 X <sup>2</sup> 0.02	q: 40.98 mg g <sup>-1</sup> k <sub>L</sub> : 0.30 L mg <sup>-1</sup>
Freundlich	R <sup>2</sup> 0.845 X <sup>2</sup> 12	K <sub>F</sub> : 6.84 ((mg g <sup>-1</sup> ) (L mg <sup>-1</sup> ) <sup>1/n</sup> ) 1/n <sub>F</sub> : 1.16	R <sup>2</sup> 0.912 X <sup>2</sup> 0.85	K <sub>F</sub> : 10.38 ((mg g <sup>-1</sup> ) (L mg <sup>-1</sup> ) <sup>1/n</sup> ) 1/n <sub>F</sub> : 0.98	R <sup>2</sup> 0.925 X <sup>2</sup> 0.16	K <sub>F</sub> : 7.84 ((mg g <sup>-1</sup> ) (L mg <sup>-1</sup> ) <sup>1/n</sup> ) 1/n <sub>F</sub> : 0.65
Temkin	R <sup>2</sup> 0.679 X <sup>2</sup> 5.8	B <sub>1</sub> : 12.63 J mol <sup>-1</sup> A : 2.95 L g <sup>-1</sup>	R <sup>2</sup> 0.764 X <sup>2</sup> 2.1	B <sub>1</sub> : 12.92 J mol <sup>-1</sup> A : 4.19 L g <sup>-1</sup>	R <sup>2</sup> 0.941 X <sup>2</sup> 0.3	B <sub>1</sub> : 7.23 J mol <sup>-1</sup> A : 5.81 L g <sup>-1</sup>
Dubinin-Radushkevich	R <sup>2</sup> 0.557 X <sup>2</sup> 16	q : 16.94 mg g <sup>-1</sup> β : 1·10 <sup>-7</sup> mol <sup>2</sup> J <sup>-2</sup>	R <sup>2</sup> 0.796 X <sup>2</sup> 0.86	q : 55.64 mg g <sup>-1</sup> β : 1·10 <sup>-7</sup> mol <sup>2</sup> J <sup>-2</sup>	R <sup>2</sup> 0.875 X <sup>2</sup> 0.16	q : 20.91 mg g <sup>-1</sup> β : 1·10 <sup>-7</sup> mol <sup>2</sup> J <sup>-2</sup>



The results obtained demonstrates that the temperature influence the mechanism of the adsorption process. In particular, the same type of isotherm was obtained at 20 and 45°C (type V) while isotherm of type I was observed at 60°C. The fit with isotherms model confirms this trend, indeed the Freundlich model results to be the best fit for isotherm at 20 and 45°C while the Langmuir model results to be the best fit for isotherm at 60°C. It means that a monolayer of TCE on homogeneous surface of TPEG is adsorbed at 60°C while a multilayer of TCE is adsorbed on homogeneous surface of TPEG at 20 and 45°C. This change of the mechanism of the interaction could be also related to the change in the trend of adsorption capacity with the increase of temperature observed at 60°C reported in the section of effect of initial concentration and temperature and thermodynamics. The multilayer adsorption observed at 20 and 45°C could explain the bigger adsorption capacity observed at 60°C (monolayer adsorption). The theoretical value of  $q$  obtained at 60°C by the Langmuir model (40.98 mg g<sup>-1</sup>) was in good agreement with experimental value (about 30 mg g<sup>-1</sup>). By analyzing the parameters of Freundlich isotherm obtained at 20 and 45°C is possible to observe the decrease of the intensity of interaction ( $1/n_F$ ) between adsorbate and adsorbent by increasing the temperature in this range and the increase of adsorption capacity ( $k_F$ : parameter associated to adsorption capacity). The comparison with data reported in literature shows different mechanism of interaction between TCE and TPEG from other investigated adsorbent materials but the adsorption capacity evaluated by isotherm adsorption is comparable with the value reported in literature [24, 25, 26, 27].

#### **4. Conclusions**

The adsorption of TCE on TPEG was investigated and characterized in this work. The process seems to be divided in two steps, the stripping of TCE molecules in the liquid phase that tend to go in gas phase and the adsorption of these molecules on TPEG when they go across the TPEG layer. The parameters that favors the stripping of TCE molecules, like the height of headspace, stirring speed and temperature increase the adsorption capacity. The increase of adsorption capacity with the increase of stirring speed and temperature is observed in a specific range. The increase of stirring speed upper 300 rpm is associated with a decrease of adsorption capacity caused by dispersion of TPEG in liquid phase and TCE molecules go across a thinner layer of TPEG. The increase of temperature upper 45°C involves a decrease of adsorption capacity probably due the exothermicity of the adsorption process. Commonly to the typical adsorption process, the adsorption capacity results to be decreased by the increase of methanol in solution (methanol used as model molecules that increase the solubility of TCE) while it is

increased by the increase of initial concentration of TCE. Furthermore, the kinetic constant of adsorption rate depends on the concentration of TCE and it increase with the decrease of the concentration and the mechanism of the interaction between TCE and TPEG is depending on the temperature. This work demonstrates the potentiality of TPEG to adsorb TCE from water, therefore it results to be a good adsorbent comparable to conventional adsorbent typically used for TCE removal. Further study could be interesting to develop the TPEG to remove TCE from groundwater by injecting, at low pressure, adsorbent material in contaminated plume. For this reason, TPEG needs a functionalization or a morphological transformation and study on it will be conducted.

## 5. References

- [1] Chiu, W.A., Caldwell, J.C., Keshava N., and Scott, C.S., 2006, Key Scientific Issues in the Health Risk Assessment of Trichloroethylene, *Environmental Health Perspectives*, 114, 1445-1449
- [2] Klasson, K.T., L.Wartelle, L.H., Lima, I.M., Marshall, W.E., Akin, D.E., 2009, Activated carbons from flax shive and cotton gin waste as environmental adsorbents for the chlorinated hydrocarbon trichloroethylene, *Bioresource Technology*, 100, 5045-5050
- [3] Doherty, R.E., 2000, A History of the Production and Use of Carbon Tetrachloride, Tetrachloroethylene, Trichloroethylene and 1,1,1-Trichloroethane in the United States: Part 2—Trichloroethylene and 1,1,1-Trichloroethane, *Journal of Environmental Forensics*, 1, 83-93
- [4] Jo, Y.-J., Lee, J.-Y., Yi, M.-J., Kim, H.-S., Lee, K.-K., 2010, Soil contamination with TCE in an industrial complex: contamination levels and implication for groundwater contamination, *Geoscience Journal*, 14, 313-320
- [5] Gotpagar, J., Grulke, E., Tsang T., and Bhaitacharyya, D., 1997, Reductive Dehalogenation of Trichloroethylene Using Zero-Valent Iron, *Environmental Progress*, 16, 137-143
- [6] Sun, Y., Li, J., Huang, T., and Guan, X., 2016, The influences of iron characteristics, operating conditions and solution chemistry on contaminants removal by zero-valent iron: A review, *Water Research*, 100, 277-295
- [7] Yan, J., Han, L., Gao, W., Xue, S., and Chen, M., 2015, Biochar supported nanoscale zerovalent iron composite used as persulfate activator for removing trichloroethylene, *Bioresource Technology*, 175, 269-274

- [8] Tseng, H.-H., Su J.-C., and Liang, C., 2011, Synthesis of granular activated carbon/zero valent iron composites for simultaneous adsorption/dechlorination of trichloroethylene, *Journal of Hazardous Materials*, 192, 500-506
- [9] Zytner, R.G., 1992, Adsorption-desorption of trichloroethylene in granular media, *Water, Air and Soil Pollution*, 65, 245-255
- [10] Sheng, G., Wang, X., Wu, S., and Boyd, S.A., 1998, Enhanced Sorption of Organic Contaminants by Smectitic Soils Modified with a Cationic Surfactant, *Journal of Environmental Quality*, 27, 806-814
- [11] Zhao, H., and Vance, G.F., 1998, Sorption of trichloroethylene by organo-clays in the presence of humic substances, *Water Research*, 32, 3710-3716
- [12] P. Liu, C. Long, Q. Li, H. Qian, A. Li and Q. Zhang, Adsorption of trichloroethylene and benzene vapors onto hypercrosslinked polymeric resin, *Journal of Hazardous Materials*, 2009, 166, 46-51
- [13] L. Pasti, A. Martucci, M. Nassi, A. Cavazzini, A. Alberti and R. Bagatin, The role of water in DCE adsorption from aqueous solutions onto hydrophobic zeolites, *Microporous and Mesoporous Materials*, 2003, 59, 205-214
- [14] Naghizadeh, A., Nasser S., and Nazmara, S., 2011, Removal of trichloroethylene from water by adsorption on to multiwall carbon nanotubes, *Iranian Journal of Environmental Health Science and Engineering*, 8, 317-324
- [15] Farrell, J., Hauck, B., and Jones, M., 1999, Thermodynamic investigation of Trichloroethylene adsorption in water-saturated microporous adsorbent, *Environmental Toxicology and Chemistry*, 18, 1637-1642
- [16] Wei, Z. S., eo, Y., 2010, Trichloroethylene (TCE) adsorption using sustainable organic mulch, *Journal of Hazardous Materials*, 181, 147-153
- [17] Yang, S.T., Chen, S., Chang, Y., Cao, A., Liu, Y., and Wang, H., 2011, Removal of methylene blue from aqueous solution by graphene oxide, *Journal of Colloid and Interface Science*, 359, 24-29
- [18] Pyrzynska, K., 2011, Carbon nanotubes as sorbent in the analysis of pesticides, *Chemosphere*, 83, 1407-1413

- [19] Masi, S., Calace, S., Mazzone, G., Caivano, M., Buchicchio, A., Pascale, S., Bianco, G., and Caniani, D., Lab-scale investigation on remediation of sediments contaminated with hydrocarbons by using super-expanded graphite, 15th International Conference on Environmental Science and Technology Rhodes, Greece, 31 August to 2 September 2017
- [20] Caniani, D., Caivano, M., Calace, S., Mazzone, G., Pascale, R., Mancini I.M., Masi S., Remediation of water samples contaminated by BTEX using super-expanded graphite as innovative carbon-based adsorbent material, IWA World Water Congress & Exhibition, 16-21 September 2018, Tokyo, Japan
- [21] Caniani, D., Calace, S., Mazzone, G., Caivano, M., Mancini, I.M., Greco M., and Masi, S., Removal of Hydrocarbons from Contaminated Soils by Using a Thermally Expanded Graphite Sorbent, *Bulletin of Environmental Contamination and Toxicology*, 2018, [20] M. Yi, Z. Shen, A review on mechanical exfoliation for the scalable production of graphene, *Journal of Materials Chemistry A*, 2015, 3, 11700-11715
- [22] M. Ahmad, M., S.S. Lee, S.S., A.U. Rajapaksha, A.U., Vithanage, M., Zhang, M., Cho, J.S., Lee, S.-E., and Ok, Y.S., 2013, Trichloroethylene adsorption by pine needle biochars produced at various pyrolysis temperatures, *Bioresource Technology*, 143, 615-622
- [23] Pascale, R., Bianco, G., Calace, S., Masi, S., Mancini, I.M., Mazzone, G., Caniani, D., 2018, Method development and optimization for the determination of benzene, toluene, ethylbenzene and xylenes in water at trace levels by static headspace extraction coupled to gas chromatography–barrier ionization discharge detection, *Journal of Chromatography A*, 1548, 10-18
- [24] Bourlinos, A.B., Gournis, D., Petridis, D., Szabo, T., Szeri, A., Dékani, I., 2003, Graphite Oxide: Chemical Reduction to Graphite and Surface Modification with Primary Aliphatic Amines and Amino Acids, *Langmuir*, 19, 6050-6055
- [25] Ahmad, M., Lee, S.S., Oh, S.E., Mohan, D., Moon, D.H., Lee, Y.H., and Ok, Y.S., 2013, Modeling adsorption kinetics of trichloroethylene onto biochars derived from soybean stover and peanut shell wastes, *Environmental Science and Pollution Research*, 20, 8364-8373
- [26] Ahmad, M., Lee, S.S., Dou, X., Mohan, D., Sung, J.K., Yang, J.E., and Ok, Y.S., 2012, Effects of pyrolysis temperature on soybean stover- and peanut shell-derived biochar properties and TCE adsorption in water, *Bioresource Technology*, 118, 536-544

[27] L. Huang, Z. Yang, B. Li, J. Hu, W. Zhang and W.-C. Ying, Granular activated carbon adsorption process for removing trichloroethylene from groundwater, *American Institute of Chemical Engineering Journal*, 2011, 57, 542-550

[28] Qiu, H., Lv, L., B.-cPan, Zhang, Q.-j., Zhang, W.-m., Zhang, Q.-x., 2009. Critical review in adsorption kinetic models, *Journal of Zhejiang University SCIENCE A*, 10(5), 716-724.

[29] Ho, Y.S., McKay, G., 1999. Pseudo-second order model for sorption process, *Process Biochem*, 34, 451-465.

[30] Low, M.J.D., 1960. Kinetics of chemisorption of gases on solids, *Chem. Rev.*, 60(3), 267-312.

## **2.5 Removal of organic micropollutants from water by adsorption on fixed-bed of thermo-plasma expanded graphite encapsulated into calcium alginate**

### **Abstract**

Nowadays, public concern is focused on the degradation of water quality. For this reason, the development of innovative technologies for water treatment in view of (micro)pollutant removal is important. Indeed, organic (micro)pollutants, such as pharmaceuticals, herbicides, pesticides and plasticizers at concentration levels of  $\mu\text{g L}^{-1}$  or even  $\text{ng L}^{-1}$  are hardly removed during conventional wastewater treatment. In view of this, thermo-plasma expanded graphite, a light-weight innovative material in the form of a powder, was encapsulated into calcium alginate to obtain a granular form useful as filtration and adsorption material for removal of different pollutants. The produced material was used to remove atrazine, bisphenol-A, 17- $\alpha$ -ethinylestradiol and carbamazepine (at concentration levels of 125, 250 and 500  $\mu\text{g L}^{-1}$ ) by top-down filtration. The effect of flow rate, bed depth and adsorbent composition was evaluated based on breakthrough curves. The experimental data was analysed with the Adams-Bohart model in view of scale-up. Under optimal conditions, removal and adsorption capacity of respectively about 21%, 21%, 38%, 42%, 43  $\mu\text{g g}^{-1}$ , 44  $\mu\text{g g}^{-1}$ , 37  $\mu\text{g g}^{-1}$  and 87  $\mu\text{g g}^{-1}$  were obtained for atrazine, bisphenol, 17- $\alpha$  ethinylestradiol and carbamazepine when using 0.12 g of thermo-plasma expanded graphite to treat 200 mL at 500  $\mu\text{g L}^{-1}$  (for each compound) of solution obtaining at contact time of 20 minutes.

### **1. Introduction**

Water is a precious resource used in households, industry and agriculture. Freshwater on the Earth is very rare and only 0.2% of the total water is directly accessible for human consumption [1] and about 36% of that is actually used [2] -Its distribution in the world is unequal and some countries, where accounting for 30% of the total world population, face freshwater scarcity. The future increase of world population expected in the next years will even increase the problem associated to the freshwater scarcity [3]. In this context, the source of freshwater (groundwater and surface water) needs protection and intensive treatment and reuse of wastewater should be aimed for [4]. Wastewater cannot be directly discharged into surface water because normally it contains several hazardous substances that can affect its quality. Nevertheless, globally 80% of the produced wastewater is discharged in surface water without treatment [5]. For this reason an increase of wastewater treatment plans (WWTP) is required to preserve the quality of the water, although this alone will not be enough as a typical WWTP is not able to remove emerging pollutants such as herbicides, plasticizers, pesticides and pharmaceutical products that are still detected in WWTP effluent [6,7,8,9].

Indeed, innovative treatment needs to be introduced to remove these pollutants. To achieve this goal, operational aspects of the conventional activate sludge process were looked upon, such as increasing the hydraulic retention time [10] or sludge retention time [11] even if it involves an increase of operation cost. Alternative biological treatment technologies, such as a membrane bioreactor [12] and a biofilter [13], were investigated and good results were obtained. Also technologies for tertiary treatment such as advanced oxidation process, adsorption and membrane filtration were tested [14,15, 16]. With respect to adsorption, commercial available activated carbon is the most common used adsorbent [14], although several innovative adsorbents, such as biochar [17, 18, 19], activated carbon from waste [20, 21], carbon nanotubes [22, 23], natural polymers [24, 25] and graphitic or graphenic substances [26, 27, 28] are being investigated or used.

In this work, thermo-plasma expanded graphite (TPEG) produced by an innovative process was used as adsorbent material to remove different types of organic micropollutants from water by adsorption. Due to its light-weight characteristics it floats on the water and as such TPEG was entrapped into calcium alginate polymers by in-situ cross-linking. The method used was inspired by physical entrapment of enzyme for biosensor's production [29, 30] and already used in water treatment[31, 32, 33]. Recently, the method is used to prepare adsorptive material that can be used in filtration systems [34, 35, 36]. The entrapment process was optimized to produce a granular TPEG (GTPEG) heavier than water and the material obtained was characterized by

SEM, FT-IR and BET analysis. The adsorption process was then characterized to evaluate the removal of carbamazepine, atrazine, 17- $\alpha$  ethinylestradiol and bisphenol A. Carbamazepine and 17- $\alpha$  ethinylestradiol are pharmaceuticals, while bisphenol-A is a plasticizers and atrazine a herbicide. All four micropollutants have hazardous effect on human life. The effect of the flow rate, bed depth, initial concentration, GTPEG composition was investigated as well as the long-term stability of the entrapped TPEG.

## **2. Materials and methods**

### **2.1 Materials**

Sodium alginate and calcium chloride were purchased from Carlo Erba reagents (<https://www.carloerbareagents.com/en/>). All chemicals were of analytical grade (purity > 98%) and used without further purification. TPEG was purchased from Innograf s.r.l. Atrazine, bisphenol-A, carbamazepine and 17- $\alpha$  ethinylestradiol standards were purchased from Sigma Aldrich (<https://www.sigmaaldrich.com/italy.html>). All solutions were prepared in deionised water (electrical conductivity below 5  $\mu\text{S cm}^{-1}$ ). A saturated solution of the individuals micropollutants was prepared by adding an amount that equals three times the solubility of the compound to 1 liter of deionised water. This saturated solution was vigorously stirred for three hours. The solution was then filtered on Rotilabo type 601 cellulose filter (Carl Roth, 5-13  $\mu\text{m}$  of retention range) to remove undissolved particles. Then, individual solutions were diluted with water to obtain a stock solution of 1 mg L<sup>-1</sup> and stored at 4°C to avoid degradation. Every two weeks working solutions were renewed. Before each experiment, working solutions were mixed and diluted to obtain the required concentration.

### **2.2 Preparation of granular thermo-plasma expanded graphite**

To prepare granular thermo-plasma expanded graphite, 20 g of sodium alginate was added to 1 liter of distilled water and stirred until a homogeneous gelatinous solution was obtained. Then, TPEG was added to the solution and stirred for 24 hours to obtain a homogeneous solution. Different amounts of TPEG (2.5%, 5%, 7.5% and 10%, amount expressed as function of total weight of sodium alginate) were added to the solution to test the effect of the composition of adsorbent material on the filtration operation and estimate the optimal amount. When the homogeneous solution was obtained, it was gradually transferred into a 250 mL separating funnel and dripped into 1 liter of solution of CaCl<sub>2</sub> (2%) which was gently stirred. The presence of Ca<sup>2+</sup> ions results in cross-linking of the alginate chains and formation of insoluble spheres where TPEG is entrapped. The spheres were then recovered by filtration and dried in the oven

at 105°C for 24 hours. The granular thermo-plasma expanded graphite (GTPEG) obtained was used as adsorbent material for further testing. The GTPEG prepared by adding 7.5% and 10% of TPEG were not useful for filtration because of its low density which resulted in floatation during the water treatment tests. As such, 5% of TPEG was estimated as the maximal amount that can be added to 1 litre of water to obtain a suitable water treatment material. GTPEG obtained by different relative amount of TPEG were denominated GTPEG 2.5%, GTPEG 5%, GTPEG 7.5% and GTPEG 10% respectively.

### **2.3 Characterization of granular thermo-plasma expanded graphite**

The GTPEG obtained were characterized by SEM and FT-IR analysis. SEM images was obtained by using a high-resolution field emission scanning electronic microscopy (HR-FESEM), Auriga Zeiss model, at CNIS laboratory of University of Sapienza (Rome, Italy). FT-IR spectrum was obtained in the range 400-4000  $\text{cm}^{-1}$  (16  $\text{cm}^{-1}$  of resolution) by using a ThermoNicolet 5700 FT-IR spectrophotometer (Thermo Fischer Scientific, <https://www.thermofisher.com/be/en/home.html>). For the FT-IR analysis, GTPEG 2.5%, 5%, 7.5% and 10% samples were analyzed to compare these samples with each other and with individual alginate and TPEG spectrum. All the sample was measured in the form of KBr pellet, prepared by mixing 0.2 g of sample to 20 g of KBr (stored in the oven at 105°C to eliminate trace of humidity), crushed by hand in a mortar and pressed at 9 tons  $\text{cm}^{-2}$ . The characterization of material was done consistent with literature information [36, 37, 38, 39]

### **2.4 Labscale experiments**

#### ***Fixed bed column adsorption test for system optimisation***

A 50 cm long glass burette of 1 cm of diameter was used as the column for all adsorption tests. A cotton filter was added to the bottom of the column as a support to avoid loss of adsorbent material. Prior of each experiment, the column was filled with wetted GTPEG and deionized water was passed through the column to avoid the formation of air bubbles. The micropollutants solution was pumped through the column by a peristaltic pump connected by silicones tubes to the column and the flow was controlled by the valve at the bottom of the burette. For all the experiments a top-down flow was imposed and 200 mL of effluent collected every 10 mL for analysis. In the figure 78 is reported the schematization of experimental scheme.



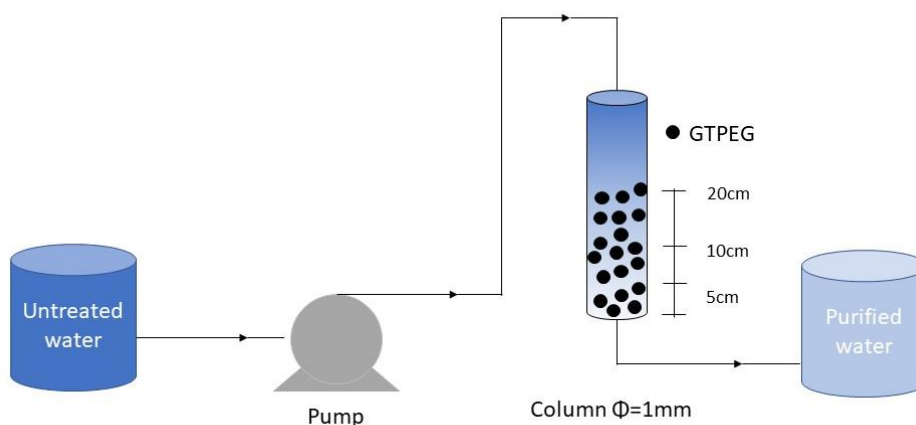


***Fig.78 Schematic representation of lab-scale filtration plant***

The effect of the flow rate on the removal and/or breakthrough was evaluated by using 500  $\mu\text{g L}^{-1}$  solutions of atrazine, bisphenol, 17- $\alpha$  ethinylestradiol and carbamazepine which were introduced at flow rates of 0.2, 1 and 2.7  $\text{mL min}^{-1}$  to a 5 cm GTPEG 5% (2.4g, therefore 0.12g of TPEG) column. These flow rates correspond to contact times of 25 min, 5 min and 1.8 minutes respectively.

The effect of the bed depth on the removal and/or breakthrough was evaluated by using 500  $\mu\text{g L}^{-1}$  solutions of atrazine, bisphenol, 17- $\alpha$  ethinylestradiol and carbamazepine which were introduced at flow rate of 1  $\text{mL min}^{-1}$  to columns of 5 cm (2.4g of GTPEG5% = 0.12g of TPEG), 10 cm (4.8g of GTPEG5% = 0.24g of TPEG) and 20 cm (9.6g of GTPEG5% = 0.48g of TPEG). These conditions ensured a contact time of 5, 10 and 20 minutes respectively. For these test GTPEG 5% was used.

The effect of the initial concentration of micropollutants on the removal and/or breakthrough was evaluated in order to have information on the minimal concentration that can be treated by GTPEG. The evaluation was performed by using different initial concentrations of atrazine, bisphenol, 17- $\alpha$  ethinylestradiol and carbamazepine (125, 250 and 500  $\mu\text{g L}^{-1}$ ) at a flow rate of 1  $\text{mL min}^{-1}$ . A column height of 10 cm (4.8g of GTPEG5% = 0.24g of TPEG) was used to ensure a contact time of 10 minutes and linear velocity of 1  $\text{cm min}^{-1}$ . For all these test GTPEG 5% was used.

In order to have information about the influence of the composition of GTPEG, some tests were performed at a concentration level of 500  $\mu\text{g L}^{-1}$  with a column height of 10 cm (4.8g of GTPEG5% = 0.24g of TPEG, 4.8g of GTPEG2,5% = 0.12g of TPEG) at a flow rate of 1 mL

min<sup>-1</sup> to ensure a contact time of 10 minutes. Granular alginate without TPEG was compared with GTPEG2.5% and GTPEG5%.

### ***Leaching test***

To verify that TPEG did not leach from the prepared granular material and the adsorption performance is not affected, a leaching test was performed with the material. The column was filled with 10 cm of GTPEG 5% and 5 liters of deionized water was pumped through it at a flow rate of 100 mL min<sup>-1</sup> and linear velocity of 10 cm min<sup>-1</sup>, an higher velocity of the tested condition that can carry on particles of TPEG if it were not entrapped very well into the alginate and on its surface. After water pumping, 200 mL of micropollutants solution at initial concentration of 500 µg L<sup>-1</sup> was treated by pumping it through the above reported column at the flow rate of 1 mL min<sup>-1</sup> (contact time 10 minutes and linear velocity of 1 cm min<sup>-1</sup>). Breakthrough curve, removal and adsorption capacity were evaluated and compared with that observed were no leaching test was applied.

## **2.5 Data analysis of fixed bed column adsorption data**

### ***Removal efficiency and adsorption capacity***

For all the test considered, breakthrough was reached after filtration of maximal 200 mL of micropollutant solution. To evaluate the time of the filtration, the equation 22 can be used:

$$T = \frac{V}{Q} \quad (22)$$

Where T is the time of filtration (min), V is the volume of effluent (mL) and Q is the flow rate (mL min<sup>-1</sup>). The removal efficiency (R) for each compound was calculated based on the breakthrough curve, plotting the ratio of the concentration in the effluent (C<sub>eff</sub>) and influent (C<sub>inf</sub>) versus the treated volume (V). The removal efficiency was calculated as follows (considering that the maximal treated volume (V<sub>max</sub>) in this study is 200 ml):

$$R = \frac{\int_0^{V_{max}} (1 - C_{eff}/C_{inf}) dV}{\int_0^{V_{max}} dV} \quad (23)$$

The amount of each pollutants that is adsorbed (W) was calculated by equation 24:

$$W = R \times (C_{influent} \times V_{max}) \quad (24)$$

The adsorption capacity (q) was calculated by equation 25:

$$q = \frac{W}{m} \quad (25)$$

Where m was the mass of the adsorbent material. In this work, the adsorption capacity was calculated by considering both the amount of TPEG into the GTPEG (because this is the actual adsorbent material) and the total amount of GTPEG used. All the data obtained were processed by using Microsoft Excel software.

### ***Adams-Bohart model and Thomas model fitting***

The experimental data obtained were further analysed with the Adams-Bohart model and Thomas model to have a fundamental understanding of the adsorption process in view of scale-up of the process [40, 41]. The Adams-Bohart model assumes that the adsorption rate is proportional to the residual capacity and the concentration of adsorbed micropollutants. Normally, this model can be applied well in the first stage of the adsorption when  $C_{eff}/C_{inf} < 0.15$ . The Adams-Bohart model used for the description of the initial part of the breakthrough curve is expressed by equation 26:

$$\frac{C_{eff}}{C_{inf}} = e^{(KC_{inf}t - KN_0\frac{Z}{F})} \quad (26)$$

Where K is the kinetic constant ( L  $\mu\text{g}^{-1} \text{min}^{-1}$ ), t is the time (min),  $N_0$  is the saturation concentration (mass of adsorbate adsorbed for unit of volume of bed,  $\mu\text{g L}^{-1}$ ), Z is the bed depth of the column (cm) and F is the linear velocity (cm  $\text{min}^{-1}$ ). By plotting the natural logarithm of  $C_{eff}/C_{inf}$  versus the time is possible to obtain the value of the kinetic constant and saturation concentration when bed depth and column section area are already known. After the determination of K and  $N_0$ , evaluation of reactor dimension when done. Equation 26 can be transformed in equation 27:

$$\ln \frac{C_{eff}}{C_{inf}} = KC_{inf}t - KN_0\frac{Z}{F} \quad (27)$$

If the breakthrough point is reached, the value of dependent variable of the equation 6 is zero, therefore equation 27 can be arranged in equation 28:

$$KN_0\frac{Z}{F} = KC_{inf}t \quad (28)$$

Equation can be rearranged in equation 29:

$$\frac{Z}{tF} = \frac{C_{inf}}{N_0} \quad (29)$$

By programming an excel sheet, it is possible evaluate one of variable Z, t or F by fixing all the other parameters. In this work, F was evaluated by fixing Z (10 m of GTPEG5%) for  $C_{inf}$  of 500 and 250  $\mu\text{g L}^{-1}$  and assuming to reach the breakthrough in one day by treating 10000 liter of contaminated water (flow rate 10000 liter for day). After evaluation of F, surface area of the reactor was calculated by the equation (30):

$$\text{surface area reactor (s)} = \frac{\text{flow rate}}{F} \quad (30)$$

By assuming to use a circular reactor, diameter of it was calculated by using the equation to calculate surface of circle. Dimension of reactor was calculated for all the micropollutants considered at initial concentration of 500 and 250  $\mu\text{g L}^{-1}$ . From the volume of the reactor, the mass of GTPEG necessary to fill the reactor was also calculated by considering the density of GTPEG (480  $\text{g dm}^{-3}$ ).

The Thomas model is one of the most general and used methods in column performance theory. The model assumes Langmuir kinetics of adsorption–desorption and no axial dispersion is derived with the adsorption that the rate driving force obeys second-order reversible reaction kinetics. By using this model, it is possible to evaluate the adsorption capacity of the system. The linear form of the model is regulated by the equation 31.

$$\ln\left(\frac{C_{inf}}{C_{eff}} - 1\right) = k_{Th} \cdot q_e \cdot \frac{x}{v} - k_{Th} \cdot C_{inf} \cdot t \quad (31)$$

Where  $k_{Th}$  is the Thomas constant rate ( $\mu\text{g}^{-1} \text{L min}^{-1}$ ),  $q_e$  is the adsorption capacity of the system ( $\mu\text{g g}^{-1}$ ),  $x$  is the amount of the adsorbent material (g) and  $v$  is the flow rate ( $\text{L min}^{-1}$ ). From the Thomas model, after the calculation of kinetics constant and theoretical adsorption capacity, the necessary amount of adsorbent material was estimated by considering to treat contaminated water with initial concentration of 500 and 250  $\mu\text{g L}^{-1}$  at the flow rate of 10000 liter for day. From the amount of GTPEG necessary for the treatment considered, volume and diameter of reactor was calculated by considering the density of GTPEG and a bed depth of 10 meters.

## 2.6 Analytical procedure

In order to quantify the concentration in the effluent of considered micropollutants (carbamazepine, bisphenol A, atrazine and 17- $\alpha$  ethinylestradiol) micro-liquid extraction was performed to transfer analytes from water to organic solvent, then GC-MS analysis was conducted. Therefore, 1 mL of dichloromethane was added to 20 mL of water sample and vigorously handly-shaken for 10 minutes. After the extraction, 500  $\mu\text{L}$  of the organic phase was

taken and transferred into a GC-MS vial. An aliquot of 1  $\mu\text{L}$  of the sample was injected in the splitless mode by an Agilent 7683 Series autosampler. The temperature of injection was set on  $250^{\circ}\text{C}$  and helium gas was used at mobile phase at flow rate of  $13.9\text{ mL min}^{-1}$ . The chromatographical separation was performed on a fused silica capillary (5% phenyl)-methyl polysiloxane HP-5MS column (30 m length, 0.25 mm I.D. and  $0.25\text{ }\mu\text{m}$  film thickness). The initial column temperature was programmed at  $100^{\circ}\text{C}$  and hold for 1 minute, then raised to  $270^{\circ}\text{C}$  with temperature rate of  $10^{\circ}\text{C min}^{-1}$ . The mass spectrometer was operated in negative electron-impact ionization (EI) mode at 70 eV. A solvent delay of 2.0 min was used to preserve the ion source. The MS transfer line temperature was set at  $200^{\circ}\text{C}$ , while the MS source temperature was maintained at  $230^{\circ}\text{C}$ . MS spectra were acquired in SIM mode using one target ion that were 200 for atrazine, 213 for bisphenol, 193 for carbamazepine and 296 for 17- $\alpha$  ethinylestradiol. The total run time of the analysis was about 10 min.

### 3. Results and discussion

#### 3.1 Characterization of GTPEG

In the figure 79, SEM images obtained for GTPEG 5% are reported. By the SEM analysis is possible to observe the fibrous and rough structure of GTPEG and the presence of pores useful for the adsorption process. Shape and pore size on the GTPEG surface seem to be heterogeneous and not uniform and it is a good indicator of presence of surface porosity, useful to react with adsorbate, as reported in literature [42]

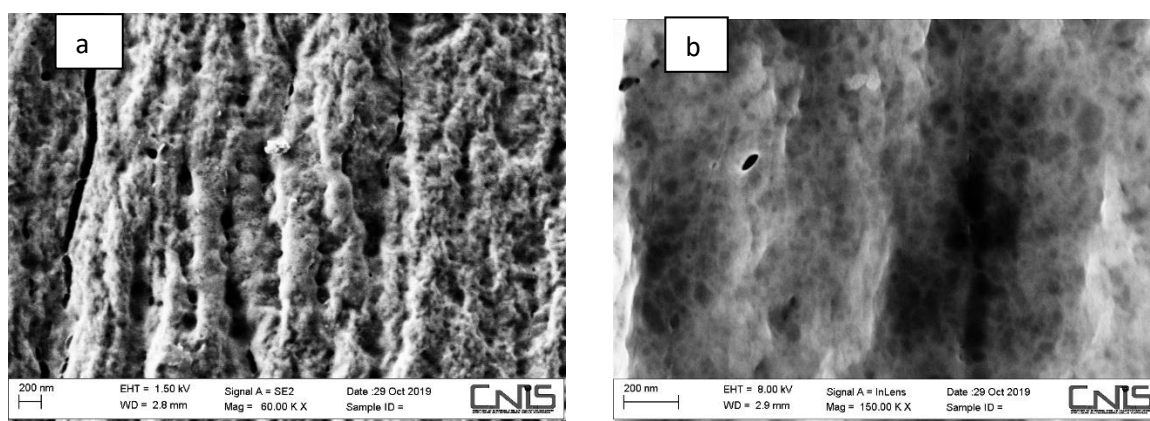


**Fig.79 SEM images of GTPEG 5% at different magnification a) 60KX and b) 150 KX.**

In the figure 80, the FT-IR spectrum obtained for granular alginate, TPEG, GTPEG 2.5%, 5%, 7.5% and 10% is reported. In the FT-IR spectrum the typical peaks associated with the carboxylic group of alginate at about  $1000\text{ cm}^{-1}$ ,  $1400\text{ cm}^{-1}$  and  $1600\text{ cm}^{-1}$  [43, 44]. By increasing the amount of TPEG in GTPEG a decrease of the intensity of these peak is observed,

proving that a higher relative amount of TPEG is entrapped into the alginate (note that into the spectrum of TPEG no peaks can be observed because it does not have functional group).

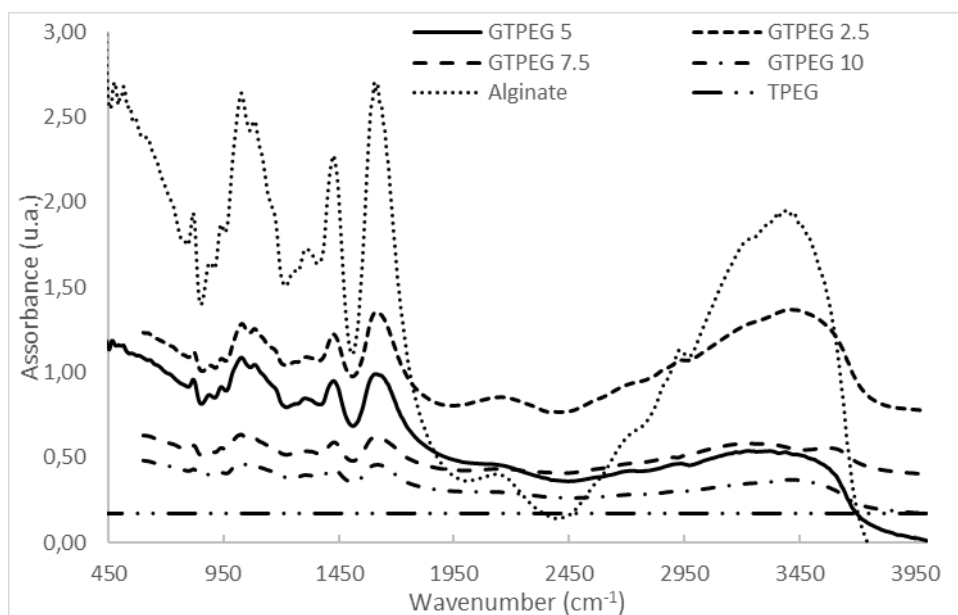


**Fig.80 FT-IR spectrum acquired in the range 400-4000  $\text{cm}^{-1}$  and resolution of 16  $\text{cm}^{-1}$ .**

### 3.2 Effect of flow rate

In the figure 81, the breakthrough curves of the carbamazepine for the three different flow rates (0.2, 1 and 2.7  $\text{mL min}^{-1}$ ) are demonstrated. By decreasing the flow rate the exponential increase of the ratio  $C_{\text{eff}}/C_{\text{inf}}$  was observed at higher breakthrough volume. For 0.2  $\text{mL min}^{-1}$  it was observed at about 180 mL, about 90 mL for 1  $\text{mL min}^{-1}$  and 2.7  $\text{mL min}^{-1}$ .

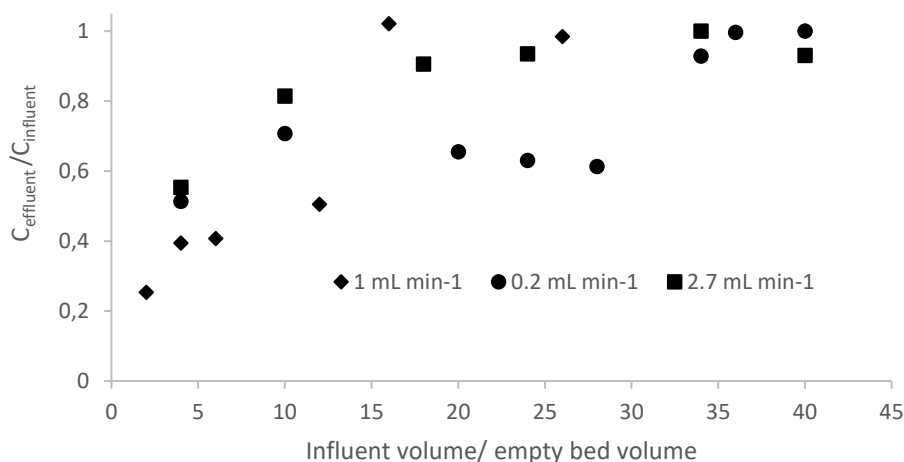


**Fig.81 Breakthrough curves of carbamazepine at the flow rate of 0.2  $\text{mL min}^{-1}$  (●), 1  $\text{mL min}^{-1}$  (◆) and 2.7  $\text{mL min}^{-1}$  (■).**

In the table 21 the typical parameter of adsorption on filtration bed are gathered for all the four compounds at the all experimented flow rate. . Breakthrough volume is considered as the volume when y axis reaches the value of about 1.

**Tab. 21 Typical parameters of adsorption of considered micropollutants (initial concentration of 500  $\mu\text{g L}^{-1}$ ) on 5 cm of filtration bed of GTPEG 5%.**

Flow rate ( $\text{mL min}^{-1}$ )	q ( $\mu\text{g g}^{-1}$ GTPEG)	Removal (%)	Breakthrough volume (mL)
<b>Atrazine</b>			
0.2	186	22	180
1	127	15	110
2.7	106	13	100
<b>Bisphenol A</b>			
0.2	208	25	180
1	133	16	110
2.7	92	11	90
<b>17-<math>\alpha</math> ethinylestradiol</b>			
0.2	292	35	180
1	128	15	110
2.7	111	13	80
<b>Carbamazepine</b>			
0.2	290	35	180
1	184	22	80
2.7	168	20	90

From Table 1 it becomes clear that by decreasing the flow rate an increase of adsorption capacity and removal is obtained as is also reported in literature [34, 35, 36, 40, 41, 44, 45, 46, 47, 48]. For example, for atrazine the adsorption capacity increased from 106  $\mu\text{g g}^{-1}$  to 195  $\mu\text{g g}^{-1}$  and the removal increase from 13% to 22%. The same effect was observed for the other micropollutants: for 17- $\alpha$  ethinylestradiol the removal efficiency even tripled (compared to a doubling for the other micropollutants). By changing the flow rate also different breakthrough volumes were observed. Carbamazepine is the molecules with the highest affinity for GTPEG.

### 3.3 Effect of bed depth

In figure 82, the breakthrough curves of 17- $\alpha$  ethinylestradiol are presented as example of the effect of bed depth on the adsorption. By increasing the bed depth an increase of breakthrough volume was observed and the adsorption at the initial stage of the filtration increased. In the case of 17- $\alpha$  ethinylestradiol, a breakthrough volume of 200 mL was obtained for 20 cm and 10 cm bed height while a volume of 110 mL was obtained for 5 cm bed depth. By increasing the

depth also a decrease of initial value of the ratio  $C_{\text{eff}}/C_{\text{inf}}$  (increase of initial removal) was observed.

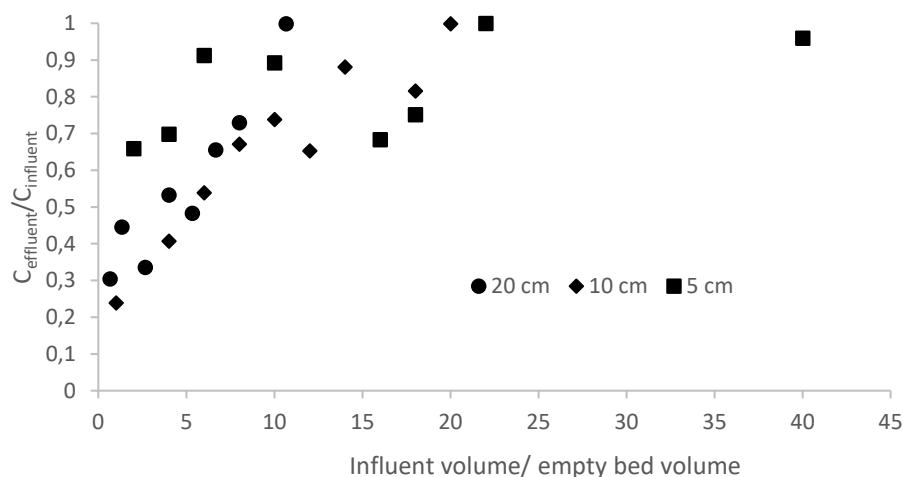


**Fig. 82 Breakthrough curves of 17- $\alpha$  ethinylestradiol (initial concentration of 500  $\mu\text{g L}^{-1}$ ) at the flow rate of 1 mL min $^{-1}$  filtered through a bed depth of 5 (■), 10 (◆) and 20 cm (●) of GTPEG 5%.**

In the table 22 the typical parameter of adsorption on filtration bed are gathered for all the four compounds at all the experimented bed depth tested to evidence the effect of this parameter.

**Tab. 22 Typical parameters of adsorption of considered micropollutants (initial concentration of 500  $\mu\text{g L}^{-1}$ ) filtered through different bed depth of GTPEG 5% at 1 mL min $^{-1}$ .**

Bed depth (cm)	q ( $\mu\text{g g}^{-1}$ GTPEG)	Removal (%)	Breakthrough volume (mL)
<b>Atrazine</b>			
5	127	15	110
10	65	16	140
20	43	21	160
<b>Bisphenol A</b>			
5	133	16	110
10	96	23	140
20	44	21	160
<b>17-<math>\alpha</math> ethinylestradiol</b>			
5	128	15	110
10	152	37	200
20	78	38	200
<b>Carbamazepine</b>			
5	184	22	80



10	175	42	200
20	87	42	200

From Table 22 it can be seen that the increase of the bed height is the increase of the removal and breakthrough volume, as reported in literature [34, 36, 40, 41, 44, 47, 48] due to the higher amount of adsorbent material. The adsorption capacity increases when the increase of removal balances the increase of amount of adsorbent material. The bed depth of 20 cm ensures a contact time of 20 minutes that is the almost the same of the experiments conducted at 0.2 mL min<sup>-1</sup> on a column of 5 cm (25 minutes) and the results obtained confirms it. Therefore, a bed depth of 20 cm at 1 mL min<sup>-1</sup> had the same performance of the filtration on 5 cm at 0.2 mL min<sup>-1</sup> but the adsorption capacity is lower because more material is used and the denominator of adsorption capacity is higher. Because of the removal obtained at 1 mL min<sup>-1</sup> with 20 cm of bed depth was the same of that one obtained at 0.2 mL min<sup>-1</sup> and 5 cm of bed depth, bigger amount of water can be treated in the same time with same removal efficient. This solution can be used to face emergency situations and wasting of GTPEG is not the priority. by increasing the bed depth and flow rate. By the analysis of the effect of the bed depth on the adsorption, another interesting observation can be deduced. For bisphenol, 17- $\alpha$  ethynylestradiol and carbamazepine the same breakthrough volume and/or removal is observed by increasing the bed depth from 10 cm to 20 cm. This means that for contact times higher than 10 minutes, the contact time is not the limiting step of the adsorption process. Therefore the adsorption capacity does not increase and the removal is not affected. In the figure 83 the removal efficiency obtained at different contact time (includes the results obtained at different flow rate) are reported.

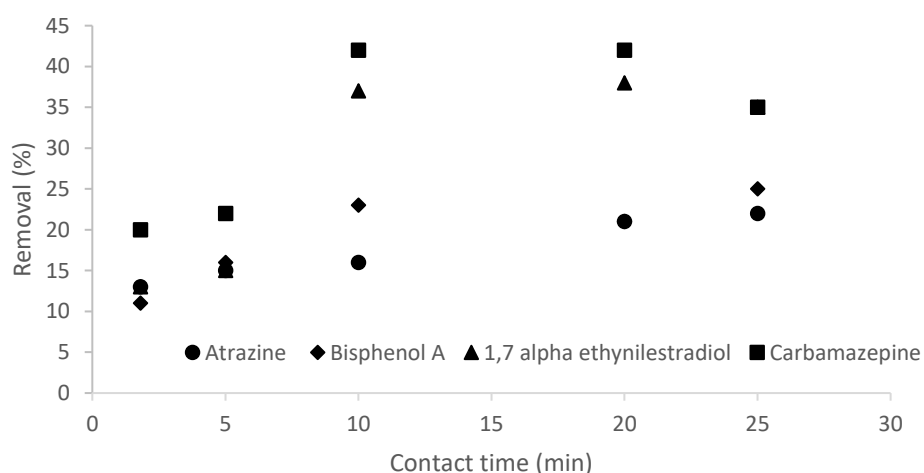


**Fig. 83** Effect of contact time on removal observed in the previous experiments.

The affinity of each compound for the GTPEG is as follows: atrazine > bisphenol > 17- $\alpha$  ethinylestradiol > carbamazepine. . Carbamazepine is the molecules with the highest affinity for GTPEG probably due to the higher number of aromatic rings compared to the other molecules. These aromatic rings can interact with the  $sp^2$  bonds of graphite. Atrazine has a lower affinity for GTPEG probably due to its lower number of aromatic rings and molecular weight, while 17- $\alpha$  ethinylestradiol could be more affine than bisphenol due its higher molecular weight, lower polarity and solubility.

### 3.4 Effect of initial concentration

In figure 84, the breakthrough curves of bisphenol-A obtained at different initial concentrations (500, 250 and 125  $\mu\text{g L}^{-1}$ ) using a column of 10 cm with GTPEG 5% at 1  $\text{mL min}^{-1}$  are demonstrated. The decrease of initial concentration affects the breakthrough curves. At a concentration of 125  $\mu\text{g L}^{-1}$  the influent and effluent concentrations are almost equal, even in the initial phase of the experiment. This means that little adsorption occurs at these low concentrations. adsorb at lower value of concentration. The other general considerations for the behavior observed at the value of 500 and 250  $\mu\text{g L}^{-1}$  are reported in the next part of the test.

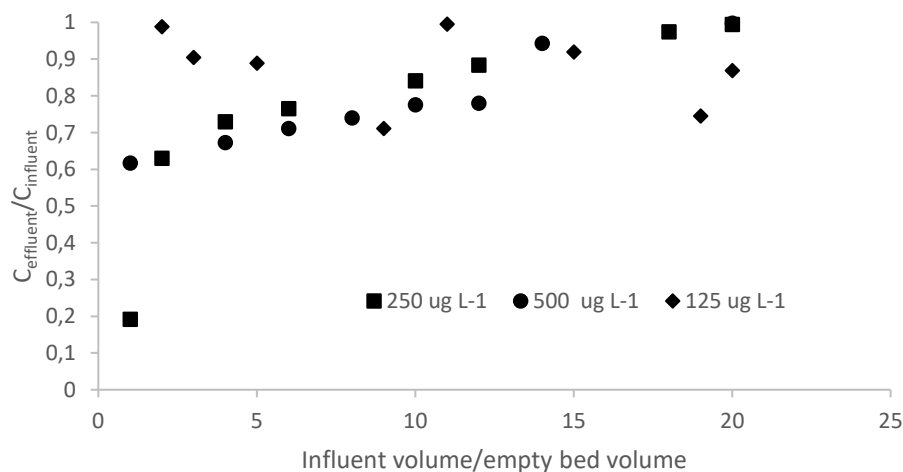


**Fig. 84 Breakthrough curves of bisphenol filtered on 10 cm of GTPEG 5% at the flow rate of 1  $\text{mL min}^{-1}$ . The initial concentration of the solution filtered were 125 ( $\blacklozenge$ ), 250 ( $\blacksquare$ ) and 500  $\mu\text{g L}^{-1}$  ( $\bullet$ ).**

In the table 23 the typical parameter of adsorption on filtration bed are gathered for all the four compounds at the all initial concentration tested to evidence the effect of this parameter.

**Tab. 23 Typical parameters of adsorption of investigated micropollutants at different initial concentration filtered through 10 cm of GTPEG 5% at 1 mL min<sup>-1</sup>.**

Initial concentration (µg L <sup>-1</sup> )	q (µg g <sup>-1</sup> GTPEG)	Removal (%)	Breakthrough volume (mL)
<b>Atrazine</b>			
125	28	7	10
250	74	18	190
500	65	16	140
<b>Bisphenol A</b>			
125	55	13	10
250	89	21	200
500	96	23	140
<b>17-α ethinylestradiol</b>			
125	56	14	10
250	139	33	200
500	153	37	200
<b>Carbamazepine</b>			
125	78	19	10
250	148	36	200
500	175	42	200

As normal observed in literature [34, 36, 40, 44, 45, 47, 49], by decreasing the initial concentration a decrease of the adsorption capacity was observed for all the compounds considered. In the case of atrazine and bisphenol-A an elongation of breakthrough was observed due to the lower gradient of concentration at lower initial concentration. By decreasing the initial concentration to 250 µg L<sup>-1</sup> from 500 µg L<sup>-1</sup> no big variation in terms of removal was observed. It is a good indication to project a multi-filter system on series where an influent of initial concentration of about 500 µg L<sup>-1</sup> for each compounds is filtered through the first filter and the resulting effluent is filtered through a second filter. In this way, by considering the removal observed in the previous experiments and reported in the previous table an influent of initial concentration of 500 µg L<sup>-1</sup> could be transformed in an effluent of 347, 303, 211 and 187 µg L<sup>-1</sup> for atrazine, bisphenol, 17-α ethinylestradiol and carbamazepine respectively. By adding another filter, an effluent of the concentration of 285, 238.5, 141 and 152 µg L<sup>-1</sup> for atrazine, bisphenol, 17-α ethinylestradiol and carbamazepine respectively. A system of four filter could allow to reach a effluent of concentration of 238.5, 234, 122 and 124 µg L<sup>-1</sup> for atrazine, bisphenol, 17-α ethinylestradiol and carbamazepine respectively.

From the analysis of breakthrough curves, lower value of the ratio  $C_{\text{eff}}/C_{\text{inf}}$  (higher adsorption) were observed at the initial stage of the filtration because the adsorbent material has all its active sites free and the same amount of particles can be adsorbed for both the concentration of 500 and 250  $\mu\text{g L}^{-1}$  and it means that in relative values the adsorption at 250  $\mu\text{g L}^{-1}$  is higher at initial stage. After this initial stage, the value of the ratio  $C_{\text{eff}}/C_{\text{inf}}$  is lower for the concentration of 500  $\mu\text{g L}^{-1}$  because of higher gradient of concentration ensures higher adsorption. This behavior was observed for all the compounds tested.

### 3.5 Effect of GTPEG composition

In the figure 85, the breakthrough curves of 17- $\alpha$  ethinylestradiol observed for different composition of GTPEG are shown. By increasing the concentration of TPEG into GTPEG an increase of adsorption was observed and as a consequence, higher breakthrough volumes were obtained. As previous reported, GTPEG 5% contains the higher amount of TPEG that can be added to obtain a material heavier than water (TPEG is light powder that float on water). Alginate contributes to the adsorption but, as next reported, its contribution to the adsorption capacity of GTPEG 5% was negligible.

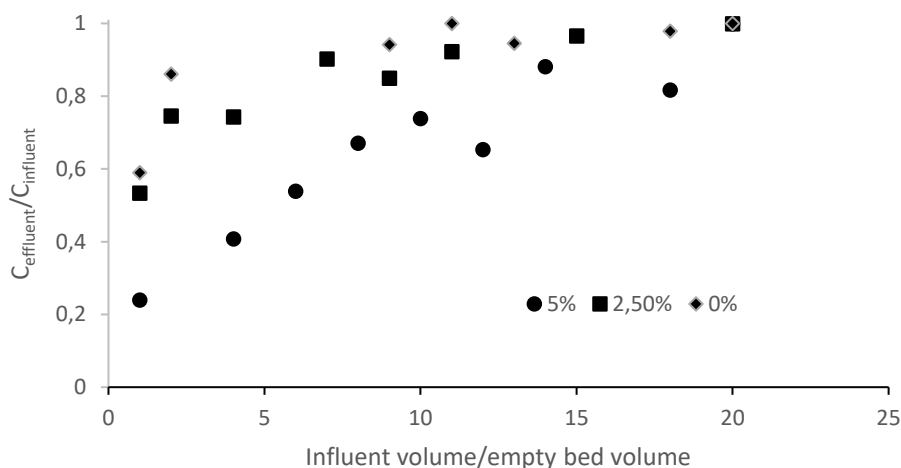


**Fig. 85 Breakthrough curves of 17- $\alpha$  ethinylestradiol (initial concentration 500  $\mu\text{g L}^{-1}$ ) filtered on 10 cm of GTPEG 5% (●), GTPEG 2.5% (■) and GTPEG 0% (◆) at the flow rate of 1 mL min<sup>-1</sup>.**

In the table 24 the adsorption results when using different concentrations of TPEG are summarized. In this case, also the value of the adsorption capacity calculated by considering only the adsorbent material (TPEG) is given.

**Tab. 24 Typical parameters of adsorption for considered micropollutants for an adsorption column containing 10 cm of GTPEG with difference compositions operated with an influent concentration of 500  $\mu\text{g L}^{-1}$  and an influent flow rate of 1  $\text{mL min}^{-1}$**

GTPEG content (%)	$q^*$ ( $\mu\text{g g}^{-1}$ GTPEG)	$q$ ( $\mu\text{g g}^{-1}$ TPEG)	Removal (%)	Breakthrough volume (mL)
<b>Atrazine</b>				
0%	0.9	-	3	10
2.5%	1.1	25	3	10
5%	3	65	16	140
<b>Bisphenol A</b>				
0%	3	-	8	20
2.5%	4	92	11	70
5%	5	96	23	140
<b>17-<math>\alpha</math> ethinylestradiol</b>				
0%	3	-	9	90
2.5%	5	133	16	150
5%	8	152	37	200
<b>Carbamazepine</b>				
0%	2	-	8	90
2.5%	7	175	21	200
5%	18	175	42	200

As logically expected, by decreasing the amount of TPEG used to produce GTPEG, a decrease of the removal and adsorption capacity were observed because lower amount of adsorbent material was present. The alginate can contribute to the adsorption because of its specific functional groups, detected in FT-IR conducted analysis, as reported in literature [34] but its contribute in terms of the adsorption capacity to the adsorption of GTPEG 5% is low. It was also negligible in the case of GTPEG 2.5% for the adsorption of 17- $\alpha$  ethinylestradiol and carbamazepine due to their higher affinity. The results obtained offer a new perspective for future studies: to find a different substrate to entrap TPEG heavier than calcium alginate to increase the amount of TPEG entrapped without affect the precipitation in the water.

### 3.6 Leaching test

In the figure 86, the breakthrough curves of atrazine (initial concentration of 500  $\mu\text{g L}^{-1}$ ) obtained with a bed height of 10 cm of GTPEG 5% at a flow rate of 1  $\text{mL min}^{-1}$  before and after passing 5 l (500 times the bed volume) of water through the column (at a flow rate of 100  $\text{mL min}^{-1}$ ). It is clear that no decrease of adsorption capacity or removal caused by leaching is observed and that as such it can be assumed that little leaching occurred. Therefore, it can be

concluded that the method used to entrap the TPEG is a good choice although limited amount of it can be entrapped without affect precipitation in the water.

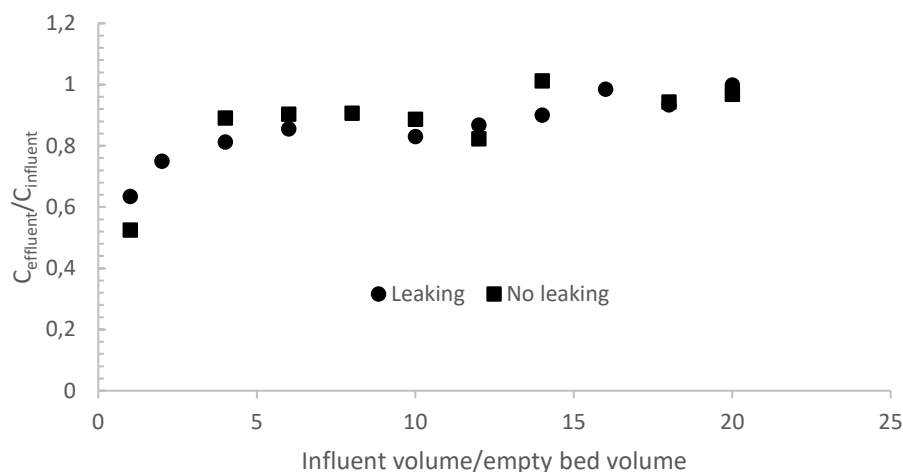


Fig. 86 Breakthrough curves of atrazine (initial concentration  $500 \mu\text{g L}^{-1}$ ) filtered on 10 cm of GTPEG 5% at the flow rate of  $1 \text{ mL min}^{-1}$  before (■) and after (●) leaking test.

In the table 25 the typical parameter of adsorption on filtration bed are demonstrated for all the four compounds at the all initial concentration tested to evidence the effect of this parameter.

**Tab. 25 Typical parameters of adsorption of considered micropollutants at initial concentration of  $500 \mu\text{g L}^{-1}$  filtered through 10 cm of GTPEG 5% at  $1 \text{ mL min}^{-1}$ , before and after the leaking test.**

Leaking test	q ( $\mu\text{g g}^{-1}$ GTPEG)	Removal (%)	Breakthrough volume (mL)
<b>Atrazine</b>			
Before	65	16	140
After	73	18	160
<b>Bisphenol A</b>			
Before	96	23	140
After	79	19	140
<b>17-<math>\alpha</math> ethinylestradiol</b>			
Before	152	37	200
After	139	33	160
<b>Carbamazepine</b>			
Before	175	42	200
After	195	47	200

The results obtained from the leaking test demonstrate that no leak of TPEG happened and the adsorption capacity of the system is not affected, therefore the method used to entrap it results to be a good choice.

### 3.7 Models fitting

The experimental data was further assessed with the Adams-Bohart model. With this model it is possible to have information about the kinetics of the process and the saturation concentration of the system. These parameters are useful to scale-up the system. In the tables 26, 27, 28, 29 and 30 the correlation parameters of regression, kinetics constant and concentration of saturation obtained for all the compound at the different parameters tested are reported to compare the effect of their variations. Sometimes not excellent correlation was observed but it can be used as first analysis to have a confirm of general trend observed in experimental tests.

**Tab. 26 Correlation parameter of regression, kinetics constant and saturation concentration (theoretical and experimental) obtained by the Adams-Bohart fitting of experimental data obtained for atrazine at the different conditions tested.**

Initial concentration ( $\mu\text{g L}^{-1}$ )	Bed depth (cm)	Flow rate ( $\text{mL min}^{-1}$ )	GTPEG%	Leaching test	K ( $\text{L min}^{-1} \mu\text{g}^{-1}$ )	$N_0$ ( $\mu\text{g L}^{-1}$ )	$N_{0\text{exp}}$ ( $\mu\text{g L}^{-1}$ )	$R^2; \chi^2$
Atrazine								
500	5	1	5	No	$4 \cdot 10^{-6}$	15000	3040	0.42; 8
500	5	0.2	5	No	$5 \cdot 10^{-7}$	20800	4400	0.60; 1.2
500	5	2.7	5	No	/	/	2600	0.02; 22
500	10	1	5	No	$4 \cdot 10^{-6}$	8900	1600	0.42; 6
500	20	1	5	No	$2.8 \cdot 10^{-6}$	5900	1000	0.63; 0.9
500	10	1	2.5	No	/	/	300	0.01; 25
500	10	1	5	Yes	$3.6 \cdot 10^{-6}$	9600	1800	0.80; 0.28
250	10	1	5	No	$4.8 \cdot 10^{-6}$	9300	900	0.46; 5
125	10	1	5	No	/	/	200	0

**Tab. 27 Correlation parameter of regression, kinetics constant and saturation concentration (theoretical and experimental) obtained by the Adams-Bohart fitting of experimental data obtained for bisphenol at the different conditions tested.**

Initial concentration ( $\mu\text{g L}^{-1}$ )	Bed depth (cm)	Flow rate ( $\text{mL min}^{-1}$ )	GTPEG%	Leaching test	K ( $\text{L min}^{-1} \mu\text{g}^{-1}$ )	$N_0$ ( $\mu\text{g L}^{-1}$ )	$N_{0\text{exp}}$ ( $\mu\text{g L}^{-1}$ )	$R^2; \chi^2$
Bisphenol A								
500	5	1	5	No	$5.8 \cdot 10^{-6}$	11900	3200	0.93; 0.2
500	5	0.2	5	No	$2.6 \cdot 10^{-6}$	3700	500	0.79; 0.8
500	5	2.7	5	No	/	/	2200	0.04; 25
500	10	1	5	No	$5.8 \cdot 10^{-6}$	9500	2300	0.93; 0.18
500	20	1	5	No	$5.6 \cdot 10^{-6}$	9200	1000	0.81; 0.98
500	10	1	2.5	No	/	/	300	0.01; 29
500	10	1	5	Yes	$1.8 \cdot 10^{-5}$	8100	1900	0.89; 0.5
250	10	1	5	No	$1 \cdot 10^{-5}$	4400	1100	0.47; 6
125	10	1	5	No	/	/	300	0

**Tab. 28 Correlation parameter of regression, kinetics constant and saturation concentration (theoretical and experimental) obtained by the Adams-Bohart fitting of experimental data obtained for 17- $\alpha$  ethinylestradiol at the different conditions tested.**

Initial concentration ( $\mu\text{g L}^{-1}$ )	Bed depth (cm)	Flow rate ( $\text{mL min}^{-1}$ )	GTPEG %	Leaching test	K ( $\text{L min}^{-1} \mu\text{g}^{-1}$ )	$N_0$ ( $\mu\text{g L}^{-1}$ )	$N_{0\text{exp}}$ ( $\mu\text{g L}^{-1}$ )	$R^2, \chi^2$
17- $\alpha$ ethinylestradiol								
500	5	1	5	No	$1.3 \cdot 10^{-5}$	21400	3100	0.80; 0.3
500	5	0.2	5	No	$2.4 \cdot 10^{-6}$	7400	7000	0.31; 14
500	5	2.7	5	No	$5.6 \cdot 10^{-6}$	21500	2600	0.6; 3



500	10	1	5	No	$1.3 \cdot 10^{-5}$	8700	3700	0.80; 1.3
500	20	1	5	No	$1.2 \cdot 10^{-5}$	4600	1900	0.89; 0.92
500	10	1	2.5	No	$5.2 \cdot 10^{-5}$	8100	1600	0.68; 2
500	10	1	5	Yes	$2.4 \cdot 10^{-5}$	8600	3300	0.90; 0.98
250	10	1	5	No	$1.5 \cdot 10^{-5}$	8400	1600	0.65; 1.5
125	10	1	5	No	/	/	400	0

**Tab. 29 Correlation parameter of regression, kinetics constant and saturation concentration (theoretical and experimental) obtained by the Adams-Bohart fitting of experimental data obtained for carbamazepine at the different conditions tested.**

Initial concentration ( $\mu\text{g L}^{-1}$ )	Bed depth (cm)	Flow rate ( $\text{mL min}^{-1}$ )	GTPEG %	Leaching test	K ( $\text{L min}^{-1} \mu\text{g}^{-1}$ )	$N_0$ ( $\mu\text{g L}^{-1}$ )	$N_{0\text{exp}}$ ( $\mu\text{g L}^{-1}$ )	$R^2$ ; $\chi^2$
Carbamazepine								
500	5	1	5	No	$1.5 \cdot 10^{-5}$	15600	4420	0.96; 0.03
500	5	0.2	5	No	$1.4 \cdot 10^{-6}$	20200	7000	0.68; 0.5
500	5	2.7	5	No	$1.3 \cdot 10^{-5}$	14200	4000	0.62; 0.7
500	10	1	5	No	$1.5 \cdot 10^{-5}$	9200	4200	0.96; 0.09
500	20	1	5	No	$1.1 \cdot 10^{-5}$	5500	2100	0.60; 1.2
500	10	1	2.5	No	$3.4 \cdot 10^{-6}$	10000	2100	0.84; 0.6
500	10	1	5	Yes	$2.4 \cdot 10^{-5}$	8600	4700	0.90; 0.2
250	10	1	5	No	$9.4 \cdot 10^{-6}$	9900	1800	0.65; 1.8
125	10	1	5	No	/	/	500	0

By the kinetic constants and saturation concentrations obtained from the Adams-Bohart model, general trends can be noticed. By increasing the flow rate, an increase of kinetic constant and a decrease of saturation concentration (except from calculated value of bisphenol and 17- $\alpha$

ethinylestradiol probably due to the model used) was observed for all the compound. This confirms that breakthrough is reached faster and lower amount of adsorbate saturates the system. By increasing the bed depth, a decrease of kinetics constant and adsorption capacity is observed, therefore the breakthrough is reached later as observed in experimental test. The decrease of saturation concentration can be explained by increase of amount of adsorbent used. The trend of saturation concentration is the same of the experimental observed. The decrease of initial concentration involves an increase of the kinetics of the process (except for carbamazepine). The saturation concentration decrease by decreasing the initial concentration of the influent (exception was observed for theoretical value of carbamazepine). As observed in the experimental section effect of initial concentration, by decreasing the concentration an elongation of breakthrough was observed but it does not involve a decrease of kinetics constant because of at the initial stage the removal was higher due to increase of relative numbers of active site respect pollutants molecules then the slope of the curve increases. The general trend observed in this work agrees with that already reported in literature [36,40]. By decreasing the amount of the TPEG entrapped, a decrease of the kinetics constant and saturation concentration was observed for 17- $\alpha$  ethinylestradiol but not for carbamazepine (from theoretical value). After the leaching test a small increase of the kinetic constant and small variations of the saturation concentration is noticed probably higher grade of hydration of the adsorbent material. As expected, the values of saturation concentration are not very close to experimental ones because of the model can be well adapted at the first stage of the breakthrough curves, but in this work we use it just for an estimations of the values of saturation concentration and kinetics that can be then compared with the values obtained from Thomas model, widely used for adsorption on fixed-bed. In the table 23 the dimension of the reactor estimated by assuming to treat 10000 liters of contaminated water for day in a reactor of a bed depth of 10 meters of GTPEG5%. Results evidence that a reactor of diameter of 8.3 and 8.5 m is necessary to treat water and remove carbamazepine, 17- $\alpha$  ethinylestradiol, bisphenol A and atrazine at initial concentration of 500 and 250  $\mu\text{g L}^{-1}$  respectively at the flow rate of 10  $\text{m}^3 \text{day}^{-1}$  and bed depth of 10 m.

**Tab. 3 Reactor diameter and volume and mass of GTPEG estimation for treatment of 10  $\text{m}^3 \text{d}^{-1}$  to remove carbamazepine, 17- $\alpha$  ethinylestradiol, bisphenol A and atrazine by adsorption on column of bed depth of 10 m of GTPEG5%.**

Initial concentration ( $\mu\text{g L}^{-1}$ )	Diameter of the reactor (m)	Volume of the reactor ( $\text{m}^3$ )	Mass of GTPEG (tons)
Atrazine			
250	5.7	255	130

500	8.3	540	268
Bisphenol A			
250	8.3	540	268
500	8.2	528	253
17- $\alpha$ ethinylestradiol			
250	6.1	292	142
500	8.5	567	275
Carbamazepine			
250	5.6	250	129
500	8.3	543	268

In the table 31, 32, 33 and 34 the correlation parameters of regression, kinetics constant and adsorption capacity obtained from the fit of experimental data with the Thomas model for all the compound at the different parameters tested are reported to compare the effect of their variations. Furthermore, the experimental adsorption capacity is also reported to compare.

**Tab. 31 Correlation parameter of regression, kinetics constant and adsorption capacity (theoretical and experimental) obtained by the Thomas fitting of experimental data for atrazine at the different conditions tested.**

Initial concentration ( $\mu\text{g L}^{-1}$ )	Bed depth (cm)	Flow rate ( $\text{mL min}^{-1}$ )	GTPEG %	Leaching test	K ( $\text{L min}^{-1} \mu\text{g}^{-1}$ )	q ( $\mu\text{g g}^{-1}$ )	q <sub>exp</sub> ( $\mu\text{g g}^{-1}$ )	R <sup>2</sup> ; $\chi^2$
Atrazine								
500	5	1	5	No	$3.8 \cdot 10^{-5}$	66	127	0.92; 0.08
500	5	0.2	5	No	$4.8 \cdot 10^{-6}$	363	186	0.63; 0.98
500	5	2.7	5	No	$1.6 \cdot 10^{-4}$	190	106	0.51; 1.8
500	10	1	5	No	$2.3 \cdot 10^{-5}$	171	65	0.60; 1.9
500	20	1	5	No	$2.0 \cdot 10^{-5}$	75	43	0.61; 1.3
500	10	1	2.5	No	$2.4 \cdot 10^{-5}$	1146	25	0.34; 9
500	10	1	5	Yes	$4.2 \cdot 10^{-5}$	23	73	0.80; 0.19
250	10	1	5	No	$7.7 \cdot 10^{-5}$	13	74	0.67; 1.2
125	10	1	5	No	/	/	28	0.2; 15

**Tab. 32 Correlation parameter of regression, kinetics constant and adsorption capacity (theoretical and experimental) obtained by the Thomas fitting of experimental data for bisphenol A at the different conditions tested.**

Initial concentration ( $\mu\text{g L}^{-1}$ )	Bed depth (cm)	Flow rate ( $\text{mL min}^{-1}$ )	GTPEG %	Leaching test	K ( $\text{L min}^{-1} \mu\text{g}^{-1}$ )	q ( $\mu\text{g g}^{-1}$ )	q <sub>exp</sub> ( $\mu\text{g g}^{-1}$ )	R <sup>2</sup> ; $\chi^2$
Bisphenol A								
500	5	1	5	No	$3.1 \cdot 10^{-5}$	103	133	0.89; 0.14
500	5	0.2	5	No	$6.8 \cdot 10^{-6}$	76	208	0.47; 4
500	5	2.7	5	No	$1.2 \cdot 10^{-4}$	40	92	0.54; 3.6
500	10	1	5	No	$5.6 \cdot 10^{-5}$	62	96	0.80; 0.45
500	20	1	5	No	$5.8 \cdot 10^{-5}$	18	44	0.81; 0.14
500	10	1	2.5	No	$4.1 \cdot 10^{-5}$	257	92	0.77; 0.89
500	10	1	5	Yes	$5.9 \cdot 10^{-5}$	40	79	0.82; 0.95
250	10	1	5	No	$1.1 \cdot 10^{-4}$	27	89	0.90; 0.13
125	10	1	5	No	/	/	55	0.02; 16

**Tab. 33 Correlation parameter of regression, kinetics constant and adsorption capacity (theoretical and experimental) obtained by the Thomas fitting of experimental data for 17- $\alpha$  ethinylestradiol at the different conditions tested.**

Initial concentration ( $\mu\text{g L}^{-1}$ )	Bed depth (cm)	Flow rate ( $\text{mL min}^{-1}$ )	GTPEG%	Leaching test	K ( $\text{L min}^{-1} \mu\text{g}^{-1}$ )	q ( $\mu\text{g g}^{-1}$ )	q <sub>exp</sub> ( $\mu\text{g g}^{-1}$ )	R <sup>2</sup> ; $\chi^2$
17- $\alpha$ ethinylestradiol								
500	5	1	5	No	$2.3 \cdot 10^{-5}$	206	128	0.51; 12
500	5	0.2	5	No	/	/	292	0.02; 18
500	5	2.7	5	No	$1.2 \cdot 10^{-6}$	185	111	0.63; 6.7

500	10	1	5	No	$5.5 \cdot 10^{-5}$	62	152	0.69; 3.6
500	20	1	5	No	$6.6 \cdot 10^{-5}$	60	78	0.75; 1.2
500	10	1	2.5	No	$6.1 \cdot 10^{-5}$	32	133	0.87; 0.88
500	10	1	5	Yes	$9.1 \cdot 10^{-5}$	120	139	0.87; 0.6
250	10	1	5	No	$1.3 \cdot 10^{-4}$	55	139	0.88; 0.5
125	10	1	5	No	$9.3 \cdot 10^{-5}$	44	56	0.54; 9

**Tab. 34 Correlation parameter of regression, kinetics constant and adsorption capacity (theoretical and experimental) obtained by the Thomas fitting of experimental data for carbamazepine at the different conditions tested.**

Initial concentration ( $\mu\text{g L}^{-1}$ )	Bed depth (cm)	Flow rate ( $\text{mL min}^{-1}$ )	GTPEG %	Leaching test	K ( $\text{L min}^{-1} \mu\text{g}^{-1}$ )	q ( $\mu\text{g g}^{-1}$ )	q <sub>exp</sub> ( $\mu\text{g g}^{-1}$ )	R <sup>2</sup> ; $\chi^2$
Carbamazepine								
500	5	1	5	No	$9.5 \cdot 10^{-5}$	163	184	0.98; 0.02
500	5	0.2	5	No	$1.5 \cdot 10^{-5}$	236	290	0.57; 9.8
500	5	2.7	5	No	$6.6 \cdot 10^{-5}$	127	168	0.68; 6.7
500	10	1	5	No	$9.9 \cdot 10^{-5}$	136	175	0.77; 7.8
500	20	1	5	No	$7.8 \cdot 10^{-5}$	62	87	0.74; 8.9
500	10	1	2.5	No	$5.9 \cdot 10^{-4}$	48	175	0.61; 12
500	10	1	5	Yes	$8.7 \cdot 10^{-5}$	160	195	0.90; 0.09
250	10	1	5	No	$1.1 \cdot 10^{-4}$	51	148	0.62; 3.6
125	10	1	5	No	$1.3 \cdot 10^{-4}$	44	78	0.32; 14

By analyzing the data obtained by the Thomas model can be observed that the value of experimental and theoretical adsorption capacity are close as expected because this model is widely used for all fixed-bed adsorption test. As observed by the Adams-Bohart model, by increasing the flow rate an increase of kinetic constant and decrease of adsorption capacity is

observed. By increasing the bed depth, variation of kinetics constant is observed but the trend is different for each compound (decrease for atrazine and carbamazepine and increase for bisphenol A and 17- $\alpha$  ethinylestradiol). The adsorption capacity decrease by increasing the bed depth because the increase of removal does not balance the increase of amount of adsorbent material. By decreasing the initial concentration of the influent and amount of TPEG into adsorbent material a decrease of adsorption capacity and increase of kinetics constant is observed. Leaching test involves variation of kinetics constant and adsorption capacity due to the probably higher grade of hydration of adsorbent material, but as can be observed from experimental data, not loss of performance can be deduced. Also the general trend observed in this case agrees with that already reported in literature [36,40]. In the table 35 the dimension of the reactor estimated by assuming to treat 10000 liters of contaminated water for day in a reactor of a bed depth of 10 meters of GTPEG5%. Results evidence that a reactor of diameter of 0.6 and 0.7 m is necessary to treat water and remove carbamazepine, 17- $\alpha$  ethinylestradiol, bisphenol A and atrazine at initial concentration of 500 and 250  $\mu\text{g L}^{-1}$  respectively at the flow rate of 10  $\text{m}^3 \text{day}^{-1}$  and bed depth of 10 m. As expected, results are different from Adams-Bohart model because it is a good model for all fixed-bed system while Adams-Bohart model can be used just for the initial step of breakthrough curves and also because Thomas model can be used to estimate reactor dimension by assuming  $C_{\text{inf}}/C_{\text{eff}} = 2$ . The better agreement between experimental and theoretical data predicted by Thomas model than Adams-Bohart suggests to consider the Thomas model as reference to scale-up of this system.

**Tab. 35 Reactor volume and diameter and mass of GTPEG estimation for treatment of 10  $\text{m}^3 \text{d}^{-1}$  to remove carbamazepine, 17- $\alpha$  ethinylestradiol, bisphenol A and atrazine by adsorption on column of bed depth of 10 m of GTPEG5%.**

Initial concentration ( $\mu\text{g L}^{-1}$ )	Mass of GTPEG (kg)	Volume of the reactor ( $\text{m}^3$ )	Diameter of the reactor (m)
Atrazine			
500	584	1.2	0.4
250	3800	8.0	1
Bisphenol A			
500	1611	3.3	0.6
250	1800	3.8	0.7
17- $\alpha$ ethinylestradiol			
500	1611	3.3	0.6
250	908	1.9	0.5
Carbamazepine			
500	734	1.5	0.4

250	979	2.0	0.5
-----	-----	-----	-----

In the table 36, values obtained from Adams-Bohart, Thomas model and experimental of carbamazepine are reported for a fast comparison but as already mentioned, Thomas model is more indicated model for this system than Adams-Bohart. The value of saturation concentration was transformed into adsorption capacity by considering the density of GTPEG (480 g dm<sup>3</sup>).

**Tab. 36 Comparison of the typical parameters of Adams-Bohart and Thomas model obtained for carbamazepine.**

Initial concentration (μg L <sup>-1</sup> )	Bed depth (cm)	Flow rate (mL min <sup>-1</sup> )	GTPEG %	Leaching test	K <sub>AB</sub> (L min <sup>-1</sup> μg <sup>-1</sup> )	K <sub>Th</sub> (L min <sup>-1</sup> μg <sup>-1</sup> )	q <sub>AB</sub> (μg g <sup>-1</sup> )	q <sub>Th</sub> (μg g <sup>-1</sup> )
Carbamazepine								
500	5	1	5	No	1.5·10 <sup>-5</sup>	9.5·10 <sup>-5</sup>	650	163
500	5	0.2	5	No	1.4·10 <sup>-6</sup>	1.5·10 <sup>-5</sup>	841	236
500	5	2.7	5	No	1.3·10 <sup>-5</sup>	6.6·10 <sup>-5</sup>	592	127
500	10	1	5	No	1.5·10 <sup>-5</sup>	9.9·10 <sup>-5</sup>	383	136
500	20	1	5	No	1.1·10 <sup>-5</sup>	7.8·10 <sup>-5</sup>	229	62
500	10	1	2.5	No	3.4·10 <sup>-6</sup>	5.9·10 <sup>-4</sup>	832	48
500	10	1	5	Yes	2.4·10 <sup>-5</sup>	8.7·10 <sup>-5</sup>	358	160
250	10	1	5	No	9.4·10 <sup>-6</sup>	1.1·10 <sup>-4</sup>	412	51
125	10	1	5	No	/	1.3·10 <sup>-4</sup>	/	44

### 3.8 Literature comparison

In the table 37, relevant results obtained by adsorption of carbamazepine, 17- $\alpha$  ethinylestradiol, bisphenol A and atrazine on fixed bed are reported to have a faster comparison with results of this work. When comparison is done, it is important to remember the very low of amount of TPEG (adsorbent material) used to prepare the fixed bed in this work ( 0.24 g for 20 cm of bed depth represents the higher amount used) and the four pollutants are present in the same solution. Very few data in literature are available by considering a mix of these kind of pollutants in the same solution. Normally the conditions used in every work are different, but

we can consider the results that we obtained comparable with that present in literature and it encourages us to continue to investigate on way to improve the use of this material.

**Tab. 37 Literature overview on removal of carbamazepine, 17- $\alpha$  ethinylestradiol, bisphenol A and atrazine by adsorption on fixed bed of different adsorbent material. Reference which consider a mix of pollutants in the same solution are evidenced by \*.**

Reference	Adsorbent material	Initial conditions	Adsorption capacity, removal	K, N <sub>0</sub>	K <sub>Th</sub> , adsorption capacity (Thomas model)
<b>Carbamazepine</b>					
50	Activated carbon	C <sub>inf</sub> : 2.5 mg L <sup>-1</sup> Bed depth: 8 cm=0.8g Flow rate: 2 mL min <sup>-1</sup>	227 mg g <sup>-1</sup> 45%	Not available	K <sub>Th</sub> : 2.8·10 <sup>-8</sup> m <sup>3</sup> μg <sup>-1</sup> min <sup>-1</sup> q: 277·10 <sup>3</sup> μg g <sup>-1</sup>
51*	Mesoporous silica	C <sub>inf</sub> : 10 μg L <sup>-1</sup> Bed depth: 10 cm Flow rate: 1.5 mL min <sup>-1</sup>	0.72 μg g <sup>-1</sup>	Not available	Not available
	Cu-Amino grafted mesoporous silica	C <sub>inf</sub> : 10 μg L <sup>-1</sup> Bed depth: 10 cm Flow rate: 1.5 mL min <sup>-1</sup>	0 μg g <sup>-1</sup>	Not available	Not available
This work	GTPEG	C <sub>inf</sub> : 500 μg L <sup>-1</sup> Bed depth: 10 cm Flow rate: 1 mL min <sup>-1</sup>	175 μg g <sup>-1</sup> 42%	K: 1.5·10 <sup>-5</sup> m <sup>3</sup> μg <sup>-1</sup> min <sup>-1</sup> N <sub>0</sub> : 92.3 mg L <sup>1</sup>	K <sub>Th</sub> : 9.9·10 <sup>-5</sup> m <sup>3</sup> μg <sup>-1</sup> min <sup>-1</sup> q: 136 μg g <sup>-1</sup>
<b>Bisphenol A</b>					
52*	Activated carbon	C <sub>inf</sub> : 2 μg L <sup>-1</sup> Bed depth: 4 cm=173g Linear velocity: 3 m h <sup>-1</sup>	6·10 <sup>-2</sup> μg g <sup>-1</sup> 50%	K: 9.8·10 <sup>-8</sup> m <sup>3</sup> μg <sup>-1</sup> min <sup>-1</sup> N <sub>0</sub> : 22.7·10 <sup>3</sup> mg L <sup>-1</sup>	Not available



This work	GTPEG	$C_{inf}$ : 500 $\mu\text{g L}^{-1}$ Bed depth: 10 cm Flow rate: 1 $\text{mL min}^{-1}$	96 $\mu\text{g g}^{-1}$ 23%	$K$ : $5.8 \cdot 10^{-6}$ $\text{m}^3 \mu\text{g}^{-1} \text{min}^{-1}$ $N_0$ : 92.3 $\text{mg L}^{-1}$	$K_{Th}$ : $5.6 \cdot 10^{-5}$ $\text{m}^3 \mu\text{g}^{-1} \text{min}^{-1}$ $q$ : 62 $\mu\text{g g}^{-1}$
17- $\alpha$ ethinylestradiol					
53	Aliphatic polyamides	$C_{inf}$ : 300 $\mu\text{g L}^{-1}$ Bed depth: 2.9 cm=1g Contact time: 1 min	4470 $\mu\text{g g}^{-1}$	Not available	Not available
54	Activated carbon	$C_{inf}$ : 14 $\mu\text{g L}^{-1}$ Flow rate: 20 $\text{mL min}^{-1}$	55 $\mu\text{g g}^{-1}$	Not available	Not available
	Manganese oxide	$C_{inf}$ : 14 $\mu\text{g L}^{-1}$ Flow rate: 20 $\text{mL min}^{-1}$	2 $\mu\text{g g}^{-1}$	Not available	Not available
This work	GTPEG	$C_{inf}$ : 500 $\mu\text{g L}^{-1}$ Bed depth: 10 cm Flow rate: 1 $\text{mL min}^{-1}$	152 $\mu\text{g g}^{-1}$ 37%	$K$ : $1.3 \cdot 10^{-5}$ $\text{m}^3 \mu\text{g}^{-1} \text{min}^{-1}$ $N_0$ : 87.4 $\text{mg L}^{-1}$	$K_{Th}$ : $5.5 \cdot 10^{-5}$ $\text{m}^3 \mu\text{g}^{-1} \text{min}^{-1}$ $q$ : 62 $\mu\text{g g}^{-1}$
Atrazine					
55	Activated carbon	$C_{inf}$ : 20 $\mu\text{g L}^{-1}$ Contact time: 1 min	104 $\mu\text{g g}^{-1}$	Not available	Not available
This work	GTPEG	$C_{inf}$ : 500 $\mu\text{g L}^{-1}$ Bed depth: 10 cm Flow rate: 1 $\text{mL min}^{-1}$	65 $\mu\text{g g}^{-1}$ 16%	$K$ : $4 \cdot 10^{-6}$ $\text{m}^3 \mu\text{g}^{-1} \text{min}^{-1}$ $N_0$ : 89.3 $\text{mg L}^{-1}$	$K_{Th}$ : $2.3 \cdot 10^{-5}$ $\text{m}^3 \mu\text{g}^{-1} \text{min}^{-1}$ $q$ : 171 $\mu\text{g g}^{-1}$

#### 4. Conclusion

In this work a method to entrap an innovative adsorbent material (TPEG) was optimized and demonstrated. The granular form of TPEG obtained (GTPEG) results to have a good adsorbent property for the removal of carbamazepine, atrazine, bisphenol A and 17- $\alpha$  ethinylestradiol from water at concentration levels between 250 and 500  $\mu\text{g L}^{-1}$ . Good removal, about 40 % for carbamazepine and 17- $\alpha$  ethinylestradiol and about 20 % for atrazine and bisphenol A, was obtained by using a very low amount of TPEG (5% as weight relative to total alginate weight, GTPEG5%) and a low contact time (10 minutes). Furthermore, in the work it was demonstrated that experimental parameters such as flow rate, bed depth and composition of TPEG can be optimized to increase the removal and adsorption capacity. A systematic investigation was done to give information about the influence of the experimental parameters on the process and theoretical models (Thomas and Adams-Bohart) were used to confirm the influence observed and to estimate the dimension of the reactor for a scale-up of the process. These promising results confirm the adsorbent properties of TPEG and push-up us to investigate on its application and improve of its performance. To use an entrapping agent heavier than alginate can be useful to increase the amount of TPEG entrapped and to be sure to obtain a granular form of TPEG heavier than water and useful as fixed-bed adsorbent material.

## 5. Reference

- [1] Oki, T., Kanae, S. (2006). *Global hydrological cycles and world water resources*. *Freshwater Resources*, 313 (5790), 1068-1072.
- [2] Gude, V. G. (2017). *Desalination and water reuse to address global water scarcity*. *Reviews in Environmental Science and Bio/Technology*, 16, 591-609.
- [3] WWAP (United Nations World Water Assessment Program)/UN-water, The United Nations World Water Development Report 2018: Nature-Based Solutions for Water, UNESCO (United Nations Educational Scientific and Cultural Organization) Paris (France) 2018.
- [4] Food and Agriculture Organisation of the United Nations (2019). *Aquastat* [on line]. <http://www.fao.org/nr/water/aquastat/data/query/index.html>
- [5] UNEP (2010). *Sick Water: The central role of wastewater management in sustainable development*. Internal report, United Nations Environment Programme/GRID-Arendal, 4p.
- [6] Deblonde, T., Cossu-Leguille, C., Hartemann, P. (2011). *Emerging pollutants in wastewater: A review of the literature*. *International Journal of Hygiene and Environmental Health*, 214, 442-448.

- [7] Verlicchi, P., Al Aukidy, M., Zambello, E. (2012). *Occurrence of pharmaceutical compounds in urban wastewater: Removal, mass load and environmental risk after a secondary treatment-A review*. Science of the Total Environment, 429, 123-155.
- [8] Deeb, A. A., Stephan, S., Schmidt, O. J., Schmidt, T. C. (2017). *Suspect screening of micropollutants and their transformation products in advanced wastewater treatment*. Science of the Total Environment, 601-602, 1247-1253.
- [9] Tiedeken, E. J., Tahar, A., McHugh, B., Rowan, N. J. (2017). *Monitoring, sources, receptors and control measures from three European Union watch list substance of emerging concern in receiving waters- A 20 systematic review*. Science of the Total Environment, 574, 1140-1163.
- [10] Gros, M., Petrovic, M., Ginebreda, A., Barcelo, D. (2010). *Removal of pharmaceuticals during wastewater treatment and environmental risk assessment during hazard indexes*. Environment International, 36(1), 15-26.
- [11] Clara, M., Kreuzinger, N., Strenn, B., Gans, O., Kroiss, H. (2005). *The solids retention time – A suitable design parameter to evaluate the capacity of wastewater treatment plants to remove micropollutants*. Water research, 39(1), 97-106.
- [12] Cirja, M., Ivashechkin, P., Schäffer, A., Corvini, P. F. X. (2008). *Factors affecting the removal of organic micropollutants from wastewater in conventional treatment plants (CTP) and membrane bioreactors (MBR)*. Reviews in Environmental Science and (Bio)Technology, 7, 61-78.
- [13] Hai, F. I., Tessmer, K., Nguyen, L. N., Kang, J., Price, W. E., Nghiem, L. D. (2011). *Removal of micropollutants by membrane bioreactor under temperature variation*. Journal of Membrane Science, 383, 144-151.
- [14] Rizzo, L., Malato, S., Antakyali, D., Beretsou, V. G., Dolic, M. B., Gernjak, W., Heath, E., Ivancev-Tumbas, I., Karaolia, P., Ribeiro, A. R. L., Mascolo, G., McArdell, C.S., Schaar, H., Silva, A. M. T., Fatta-Kassinos, D. (2019). *Consolidated vs new advanced treatment methods for the removal of contaminants of emerging concern from urban wastewater*. Science of the Total Environment, 655, 986-1008.
- [15] Wardenier, N., Vanraes, P., Nikiforov, A., Van Hulle, S. W. H., Leys, C. (2019). *Removal of micropollutants from water in a continuous-flow electrical discharge reactor*. Journal of Hazardous Materials, 362, 228-245.

- [16] Liu, Z., Wardenier, N., Hosseinzadeh, S., Verheust, Y., De Buyck, P.-J., Chys, M., Nikiforov, A., Leys, C., Van Hulle, S. (2018). *Degradation of bisphenol A by combining ozone with UV and H<sub>2</sub>O<sub>2</sub>*. *Clean Technology and Environmental Policy*, 20, 2109-2118
- [17] Li, S., Wang, Z., Zhao, X., Yang, X., Liang, G., Xie, X. (2019). *Insight into enhanced carbamazepine photodegradation over biochar-based magnetic photocatalyst Fe<sub>3</sub>O<sub>4</sub>/BiOBr/BC under visible LED light irradiation*. *Chemical Engineering Journal*, 360, 600-611.
- [18] Chen, D., Xie, S., Chen, C., Quan, H., Hua, L., Luo, X., Guo, L. (2017). *Activated biochar derived from pomelo peel as a high-capacity sorbent for removal of carbamazepine from aqueous solution*. *Royal Society of Chemistry*, 7, 54969-54979.
- [19] Shan, D., Deng, S., Zhao, T., Wang, B., Wang, Y., Huang J., Yu, G., Winglee, J., Wiesner, M. R. (2016). *Preparation of ultrafine magnetic biochar and activated carbon for pharmaceutical adsorption and subsequent degradation by ball milling*. *Journal of Hazardous Materials*, 305, 156-163
- [20] Calisto, V., Ferreira, C. I. A., Oliveira, J. A. B. P., Otero M., Esteves, V. I. (2015). *Adsorptive removal of pharmaceuticals from water by commercial and waste-based carbons*. *Journal of Environmental Management*, 152, 83-90.
- [21] Baccar, R., Sarrà, M., Bouzid, J., Feki, M., Blanquez, P. (2012). *Removal of pharmaceutical compounds by activated carbon prepared from agricultural by-product*. *Chemical Engineering Journal*, 211-212, 310-317
- [22] Jung, C., Son, A., Her, N., Zoh, K.-D., Cho, J., Yoon, Y. (2015) *Removal of endocrine disrupting compounds, pharmaceuticals, and personal care products in water using carbon nanotubes: A review*. *Journal of Industrial and Engineering Chemistry*, 27, 1-11.
- [23] Ji, L., Shao, Y., Xu, Z., Zheng, S., Zhu, D., (2010) *Adsorption of Monoaromatic Compounds and Pharmaceutical Antibiotics on Carbon Nanotubes Activated by KOH Etching*. *Environmental Science and Technology*, 44 (16), 6429-6436.
- [24] Moulahcene, L., Skiba, M., Senhadji, O., Milon, N., Benamor, M., Lahiani-Skiba, M. (2015) *Inclusion and removal of pharmaceutical residues from aqueous solution using water-insoluble cyclodextrin polymers*. *Chemical Engineering Research and Design*, 97, 145-158
- [25] Alsbaiee, A., Smith, B. J., Xiao, L., Ling, Y., Helbling, D. E., Dichtel, W. R. (2016) *Rapid removal of organic micropollutants from water by a porous  $\beta$ -cyclodextrin polymer*. *Nature*, 529, 190-194

- [26] Al-Khateeb, L.A., Almotiry, S., Salam, M. A. (2014) *Adsorption of pharmaceutical pollutants onto graphene nanoplatelets*. Chemical Engineering Journal, 248, 191-199
- [27] Yu, F., Bi, D. (2015) *Enhanced adsorptive removal of selected pharmaceutical antibiotics from aqueous solution by activated graphene*. Environmental Science and Pollution Research, 22, 4715-4724
- [28] D. Caniani, M. Caivano, S. Calace, G. Mazzone, R. Pascale, I.M. Mancini and S. Masi. *Remediation of water samples contaminated by BTEX using super-expanded graphite as innovative carbon-based adsorbent material*. IWA World Water Congress & Exhibition, 16-21 September 2018, Tokyo, Japan
- [29] Sassolas, A., Blum, L. J., Leca-Bouvier, B. D. (2012) *Immobilization strategies to develop enzymatic biosensors*. Biotechnology Advances, 30(3), 489-511
- [30] El-Maiss, J., Cuccarese, M., Maerten, C., Lupattelli, P., Chiummineto, L., Funicello, M., Schaaf, P., Jierry, L., Boulmedais, F. (2018) *Mussel-Inspired Electro-Cross-Linking of Enzymes for the Development of Biosensors*. Applied Materials and Interfaces, 10, 22, 18574-18584.
- [31] Escudero, C., Fiol, N., Villaescusa, I., Bollinger, J.-C. (2009) *Arsenic removal by a waste metal (hydr)oxide entrapped into calcium alginate beads*. Journal of Hazardous Materials, 164(1-2), 533-541
- [32] Swain, S. K., Patnaik, T., Jha, U., Dey, R. K. (2013) *Development of new alginate entrapped Fe(III)-Zr(IV) binary mixed oxide for removal of fluoride from water bodies*. Chemical Engineering Journal, 215-216, 763-771
- [33] Haider, T., Husain, Q. (2007) *Calcium alginate entrapped preparation of Aspergillus oryzae  $\beta$  galactosidase: Its stability and application in the hydrolysis of lactose*. International Journal of Biological Macromolecules, 41(1), 72-80
- [34] Mohammed N., Grishkewich N., Waeijen H.A., Berry, R.M., Tam, K.C. (2016) *Continuous flow adsorption of methylene blue by cellulose nanocrystal-alginate hydrogels beads in fixed bed columns*. Carbohydrate Polymers, 136, 1194-1202
- [35] Jung K.-W., Choi, B.H., Hwang, M.J., Jeong, T.-U., Ahn, K.-H. (2016) *Fabrication of granular activated carbons derived from spent coffee grounds by entrapment in calcium alginate beads for adsorption of acid orange 7 and methylene blue*. Bioresource Technology, 219, 185-195

- [36] Jang, J., Lee, D.S. (2016) *Enhanced adsorption of cesium on PVA-alginate encapsulated Prussian blue-graphene oxide hydrogel-beads in a fixed-bed column system*. *Bioresource Technology*, 218, 294-300
- [37] Bhadra, B. N., Seo, P. W., Jhung, S. H. (2016) *Adsorption of diclofenac sodium from water using oxidized activated carbon*. *Chemical Engineering Journal*, 301, 27-34.
- [38] Cai, N., Larese-Casanova, P. (2016) *Application of positively-charged ethylenediamine-functionalized graphene for the sorption of anionic organic contaminants from water*. *Journal of Environmental Chemical Engineering*, 4, 2941-2951.
- [39] Zhu, J., Zhu, Z., Zhang, H., Lu, H., Zhang, W., Qiu, Y., Zhu, L., Koppers, S. (2018) *Calcined layered double hydroxides/reduced graphene oxide composites with improved photocatalytic degradation of paracetamol and efficient oxidation-adsorption of As(III)*. *Applied Catalysis B: Environmental*, 225, 550-562
- [40] Han, R., Ding, D., Xu, Y., Zou, W., Wang, Y., Li, Y., Zou, L. (2008) *Use of rice husk for the adsorption of congo red from aqueous solution in column mode*. *Bioresource Technology*, 99, 2938-2946
- [41] Han, R., Wang, Y., Zhao, X., Wang, Y., Xie, F., Cheng, J., Tang, M. (2009) *Adsorption of methylene blue by phoenix tree leaf powder in a fixed-bed column: experiments and prediction of breakthrough curves*. *Desalination*, 245, 284-297
- [42] Nure, J. F., Shibeshi, N. T., Asfaw, S. L., Audenaert, W., & Van Hulle, S. (2017). *COD and colour removal from molasses spent wash using activated carbon produced from bagasse fly ash of Matahara sugar factory, Oromiya region, Ethiopia*. *WATER SA*, 43(3), 470–479
- [43] Benouria, A., Azharul Islam, Md, Zaghouane-Boudiaf, H., Boutahala, M., Hameed, B.H. (2015) *Calcium alginate–bentonite–activated carbon composite beads as highly effective adsorbent for methylene blue*. *Chemical Engineering Journal*, 270, 621-630
- [44] Papageorgiou, S.K., Kouvelos, E.P., Favvas, E.P., Sapalidis, A.A., Romanos, G.E., Katsaros, F.K. (2010) *Metal-carboxylate interactions in metal-alginate complexes studied with FTIR spectroscopy*. *Carbohydrate Research*, 345, 469-473
- [45] Lezehari, M., Baudu, M., Bouras, O., Basly, J.-P. (2012) *Fixed-bed column studies of pentachlorophenol removal by use of alginate-encapsulated pillary clay microbeads*. *Journal of Colloid and Interface Science*, 379, 101-106.

- [46] Xu, D., Hein, S., Loo, S. L., Wang, K. (2008) *The Fixed-Bed study of Dye Removal on Chitosan Beads at High pH*. Industrial and Engineering Chemistry Research, 47(22), 8796-8800.
- [47] Kumar, A., Jena, H. M. (2016) *Removal of methylene blue and phenol onto prepared activated carbon from Fox nutshell by chemical activation in batch and fixed-bed column*. Journal of Cleaner Production, 137(20), 1246-1259.
- [48] Ahmed, M.J., Hameed, B.H. (2018) *Removal of emerging pharmaceutical contaminants by adsorption in a fixed-bed column: A review*. Ecotoxicology and Environmental Safety, 149, 257-266
- [49] Charumathi, D., Das, N. (2012) *Packed bed column studies for the removal of synthetic dyes from textile wastewater using immobilised dead C. tropicalis*. Desalination, 285, 22-30
- [50] Sotelo, J.L., Ovejero, G., Rodriguez, A., Alvarez, S., Garcia, J. (2013) *Adsorption of Carbamazepine in Fixed Bed Columns: Experimental and Modeling Studies*. Separation Science and Technology, 48, 2626-2637.
- [51] Ortiz-Martinez, K., Valentin, D.V., Hernandez-Maldonado, A.J. (2018) *Adsorption of Contaminants of Emerging Concern from Aqueous Solution using Cu Amino Grafted SBA-15 Mesoporous Silica: Multi-Component and Metabolites Adsorption*. Industrial and Engineering Chemistry Research, 57(18), 6426-6439
- [52] Katsigiannis, A., Noutsopolous, C., Mantziaras, J., Gioldasi, M. (2015) *Removal of emerging pollutants through granular activated carbon*. Chemical Engineering Journal, 280, 49-57.
- [53] Han, J., Qiu, W., Meng, S., Gao, W. (2012) *Removal of ethinylestradiol (EE2) from water via adsorption on aliphatic polyamides*. Water Research, 46, 5715-5724.
- [54] de Rudder, J., Van de Wiele, T., Dooghe, W., Comhaire, F., Verstraete, W. (2004) *Advanced water treatment with manganese oxide for the removal of 17- $\alpha$  ethinylestradiol (EE2)*. Water Research, 38, 184-192.
- [55] Jones, L.R., Owen, S.A., Horrell, P., Burns, R.G. (1998) *Bacterial inoculation of granular activated carbon filters for the removal of atrazine from surface water*. Water Research, 32(8), 2542-2549.

## **2.6 Removal of phtalathes plasticizers from water by adsorption on fixed-bed of thermo-plasma expanded graphite encapsulated into calcium alginate**

### **Abstract**

Plastic is currently one of the most practical and economical ways to hold food, sanitary products, cosmetics or other products. Chemical additives are added to their composition to increase their malleability, brilliance and workability. Among these additives, the most commonly used are plasticizers such as phtalathes. Microplastics have been increasingly found in freshwater ecosystems in recent years and growing concerns have been raised about their potential environmental health risks. That microplastic represent the vector of phtalathes into the freshwater, because they are released during the process of physical degradation of the microplastic by atmospheric agents. The removal of phtalathes from water was tested by adsorption on fixed-bed of thermo-plasma expanded graphite encapsulated into calcium alginate (GTPEG). Dimethyl, diethyl, dibuthyl and diisobuthyl phtalathes were filtered on fixed-bed of GTPEG and the effect of different bed depth (3, 10 and 20 cm), different flow rate (0.4, 1.2 and 2.4 mL min<sup>-1</sup>) and different initial concentration of phtalathes (10, 25 and 50 mg L<sup>-1</sup>) were tested. The breakthrough curve were evaluated to evaluate adsorption capacity and removal efficiency. The maximum value of removal efficiency observed was about 80% for the removal of the dibuthyl phtalathes. The removal efficiency decrease by decreasing the length of hydrocarburic chain and a removal efficiency of about 20% was observed for dimethyl phtalathes at the same condition. The experimental data were compared with Thomas and Adams-Bohart model to have a model to predict the system for an industrial scale up.

### **1. Introduction**

Plastic is currently one of the most practical and economical ways to hold food, sanitary products, cosmetics or other products. Chemical additives are added to their composition to increase their malleability, brilliance and workability. Among these additives, the most commonly used are plasticizers such as phtalathes. Phthalates (or phthalate esters, PAE) are compounds synthesized by the double esterification of 1,2 benzendicarboxylic acid (phthalic acid) with linear or branched alcohols, starting from methanol or ethanol (C1-C2), up to isotridecanol (C13). Plasticizer phthalates, which also include diisodecyl phthalate (DIDP), dimethyl phthalate (DMP), diethyl phthalate (DEP), dibutyl phthalate (DBP) and benzyl butyl phthalate (BBP), are used as intermolecular lubricants which confer hardness, flexibility, malleability and elasticity. Worldwide, up to 8 million tons of phthalates are produced annually,



of which over 2 million are DEHP only. PAEs are molecules that are not covalently linked to the matrix and show a tendency to migrate, especially in case of mechanical or thermal stress, so they can be dispersed in the environment during their production, use or after disposal [1, 2]. PAEs represent ubiquitous contaminants and decompose both with exposure to sunlight and with aerobic microbial activity; by affinity with the natural organic substance, they tend to absorb themselves to the soil, sediment and humus particles where they are also protected from sunlight. The accumulation of PAE in human tissues can cause chronic intoxication causing serious damage to the liver and / or reproductive system. The toxicity of phthalates is still under study, however it has been shown that many types of them, such as DEHP, DBP, BBzP and various phthalate metabolites, are carcinogenic to the liver of rodents and teratogenic to other animals [3]. Microplastics have been increasingly found in freshwater ecosystems in recent years and growing concerns have been raised about their potential risks to environmental health. Thanks to their lightness, durability, corrosion resistance and low electrical and thermal conductivity, the materials plastics have become universal materials [4, 5, 6]. Plastic debris is accumulating in both terrestrial and aquatic (marine and freshwater) systems globally [7, 8] and, given their slow degradation, they remain for much longer than that for which the product from which they derive was created [9, 10]. They have even been found in remote regions such as the Arctic (trapped in sea ice) and the deep sea [11]. They are then degraded into smaller and smaller pieces until they reach dimensions less than 1 mm, therefore such as to be considered "microplastic" [12]; conventionally, these are also defined as those having an upper limit of size 5 mm, to distinguish them from mesoplastics. They are divided into primaries, specially made to be microscopic in size, consisting mainly of pellets and microbeads ("beads") used in many products for daily hygiene (which are presented in flattened, cylindrical, spheroidal or discoid shapes), and secondary, deriving from the disintegration of larger, much more irregular waste and from the angular or rounded (depending on the degree of wear) and fibrous forms, which occur in the form of thin and elongated filaments. potential risks for organisms include inflammation of the digestive system [13], reduced nutrient absorption and reduced growth and reproduction [14]. Given their small size following degradation and fragmentation processes, they acquire a high specific surface which gives them a strong increase in adsorbing power, as in the case of microplastics deriving from PVC, capable of adsorbing varieties of organic and inorganic compounds (Teuten et al., 2007). A study carried out on phthalates, in particular diethyl phthalate (DEP) and dibutyl phthalate (DBP) [14] has shown how the latter can be adsorbed by polystyrene (PS) microplastics, polyethylene (PE) and polyvinyl chloride (PVC); the factors that favor the process are the high specific surface, hydrophobicity and conditions

of high salinity (making marine environments more risky). The same plastics contain additives such as phthalates, Bisphenol A and brominated flame retardants, which can enter the aquatic environment causing harmful effects to the endocrine, carcinogenic or mutagenic system in aquatic organisms. Phthalates are more commonly used as plasticizer additives for polyvinyl chloride which, among all types of plastic, requires the highest number of additives [15]. The breakdown of the polymer bonds and subsequent fractures on the surfaces of the microplastics due to strong atmospheric agents can lead to the migration of the additives from the inside towards the external surfaces of the microplastics [16, 17]. Since they are not chemically linked to the polymeric matrix, they can be easily released into the environment through leaching and emission by microplastics, especially deriving from PVC [18]. Ding et al., 2019 [19] evidenced the presence of phthalate esters (dimethylphthalate DMP, diethylphthalate DEP, diisobutyl phthalate DiBP, di-n-butyl phthalate DnBP and di-2-ethylhexyl phthalate DEHP) and phthalate monoesters (monomethyl phthalate MMP, monoethyl phthalate MEP, monoisobutyl phthalate MiBP, mono-n-butyl phthalate MnBP and mono-2-ethylhexyl phthalate MEHP) in 146 drinking water samples collected in 90 drinking water plants in 24 cities located throughout China. Liu et al. (2015) [20] identified PAEs in seven geographic areas of China, of which the prevalent were DBP and DEHP. The detection frequencies of DEP, DBP, DEHP and DMP were greater than 88% with concentrations of  $0.18 \pm 0.97 \mu\text{g} / \text{L}$ , while those of BBP and DnOP were between 45.4 and 50.7% with very low concentrations ( $0.001 \mu\text{g} / \text{L}$ ). Wastewater treatment plants contribute largely to the contribution of phthalates in surface water bodies. Salaudeen et al. (2018) [21] found the concentration of six PAEs (DMP, DEP, DBP, BBP, DEHP and DnOP) in the wastewater from three treatment plants that adopt activated sludge technology in the municipality of Amathole, in the Eastern Cape, in South Africa. They were found in all influents and in almost all effluents, where DBP was the most abundant followed by DEHP. The concentrations of DBP in the influent of the three plants varied between 2.7 and 2488 mg / L, while in the effluent it was between 4.9 and 8.88 mg / L. For these reason, it is necessary to develop process to treat freshwater and wastewater to remove plasticizers. Not several studies are reported in the literature on the topics, therefore that work would introduce the topic into the research community. Thermo-plasma expanded graphite encapsulated into calcium alginate (GTPEG) was tested as fixed-bed to treat water and remove dimethyl, diethyl, dibutyl and diisobutyl phthalates (DMP, DEP, DBP, DIBP) by the adsorption process. The effect of bed depth, flow rate and initial concentration of phthalates were evaluated to characterize the process. Furthermore, the experimental data were compared with Adams-Bohart and Thomas models to predict the system behavior for a industrial scale-up.

## **2. Materials and methods**

### *Materials*

Ethanol, dichloromethane, sodium alginate, calcium chloride, dimethyl, diethyl, dibutyl and diisobutyl phtalates were purchased from Carlo Erba Reagenti and used as commercial form. All the solution were prepared into deionized water with 5% of ethanol.

### *GTPEG preparation and characterization*

See the chapter 2.5.

### *Experimental setup*

A 30 cm long glass burette of 0.8 cm of diameter was used as the column for all adsorption tests. A cotton filter was added to the bottom of the column as a support to avoid loss of adsorbent material. Prior of each experiment, the column was filled with wetted GTPEG and deionized water was passed through the column to avoid the formation of air bubbles. The pollutants solution was pumped through the column by a peristaltic pump connected by Tygon R-3603 tubes to the column and the flow was controlled. For all the experiments a top-down flow was imposed and effluent collected regularly.

The effect of the flow rate on the removal and/or breakthrough was evaluated by using 50 mg L<sup>-1</sup> solutions of DMP, DEP, DBP, DIBP which were introduced at flow rates of 0.4, 1.2 and 2.4 mL min<sup>-1</sup> to a 20 cm GTPEG 5% column.

The effect of the bed depth on the removal and/or breakthrough was evaluated by using 50 mg L<sup>-1</sup> solutions of DMP, DEP, DBP, DIBP which were introduced at flow rate of 0.4 mL min<sup>-1</sup> to columns of 3 cm (0.5g of GTPEG5%), 10 cm (3.10g of GTPEG5%) and 20 cm (6.18g of GTPEG5%).

The effect of the initial concentration of micropollutants on the removal and/or breakthrough was evaluated in order to have information on the minimal concentration that can be treated by GTPEG. The evaluation was performed by using different initial concentrations of DMP, DEP, DBP, DIBP (10, 25 and 50 mg L<sup>-1</sup>) at a flow rate of of 0.4 mL min<sup>-1</sup>. A column height of 20 cm was used.

### **Data analysis of fixed bed column adsorption data**

#### *Removal efficiency and adsorption capacity*

### *Adams-Bohart model and Thomas model fitting*

See the chapter 2.5.

### **Analytical procedure**

In order to quantify the concentration in the effluent of considered pollutants solid-phase extraction on Supelclean ENVI-18 SPE 500 mg, 6 mL was performed to transfer analytes from water to organic solvent, then GC-BID analysis was conducted. Therefore, 5 mL of sample was added to the SPE filter and filtered on it. Then, 5 mL of petroleum ether was used to elute the DMP, DEP, DBP and DIBP retained on the SPE filter. After the extraction, 500  $\mu$ L of the organic phase was taken and injected into the GC. The temperature of injection was set on 250°C and helium gas was used at mobile phase at flow rate of 0.2 mL min<sup>-1</sup>. The chromatographical separation was performed on a fused silica capillary column (30 m length, 0.25 mm I.D. and 0.25  $\mu$ m film thickness). The initial column temperature was programmed at 120°C and hold for 2 minute, then raised to 250°C with temperature rate of 10°C min<sup>-1</sup>. The BID detector was maintained at 250°C to detect the analytes and reveal it. The calibration line method was used to evaluate the concentration of each phtalathes.

## **3. Results and discussion**

### **Effect of bed depth**

In figure 87, the breakthrough curves of DEP are presented as example of the effect of bed depth on the adsorption. By increasing the bed depth an increase of breakthrough volume was observed.

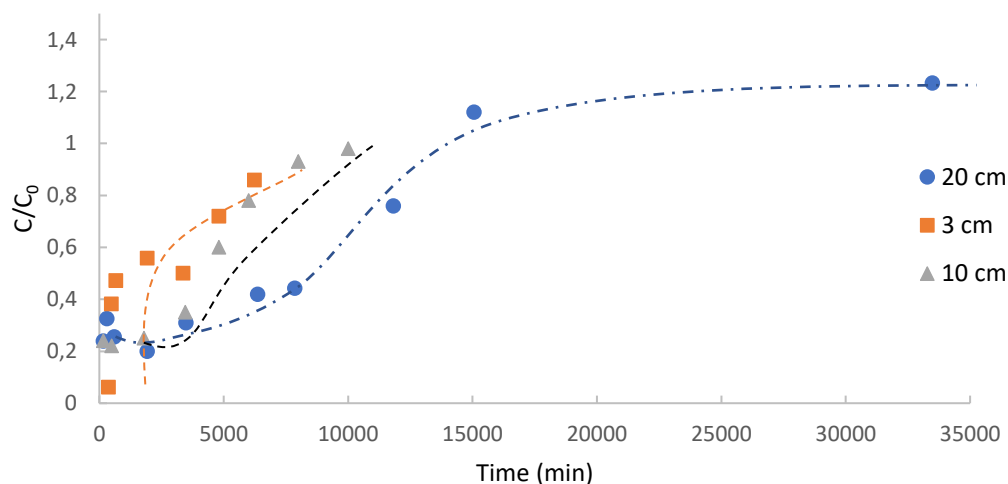


**Fig. 87 Breakthrough curves of DEP (initial concentration of 50 mg L<sup>-1</sup>) at the flow rate of 0.4 mL min<sup>-1</sup> filtered through a bed depth of 3, 10 and 20 cm of GTPEG 5%.**

In the table 38 the typical parameter of adsorption on filtration bed are gathered for all the four compounds at all the experimented bed depth tested to evidence the effect of this parameter.

**Tab. 38 Typical parameters of adsorption of considered micropollutants (initial concentration of 50 mg L<sup>-1</sup>) filtered through different bed depth of GTPEG 5% at 0.4 mL min<sup>-1</sup>.**

Bed depth (cm)	q (mg g <sup>-1</sup> GTPEG)	Removal (%)	Breakthrough volume (L)	Pollutant adsorbate (mg)
<b>DMP</b>				
3	850	23	1.9	22
10	173	26	2	26
20	85	21	2.5	26
<b>DEP</b>				
3	1998	42	2.5	52
10	1080	81	4	162
20	445	46	6	138
<b>DIBP</b>				
3	5114	45	6	135
10	5265	81	19.5	790
20	3143	83	23.2	963
<b>DBP</b>				
3	20180	38	27.9	530
10	3850	55	21	578
20	1963	52	23.2	603

By increasing the bed depth, the adsorption capacity decrease because the increase of adsorbate does not compensate the increase of the adsorbent material. The removal efficiency is affected by the bed depth and the best removal seems to be obtained for the bed depth of 10 cm, but in the last column can be observed that by increasing the bed depth an increase of pollutants adsorbate was obtained. However, it is possible to conclude that the bed depth of 10 cm is the optimal value of bed depth, because for higher bed depth probably the diffusion step from solution to adsorbent surface is not the slowest step of the process (interaction between adsorbate and adsorbent could start to be the limiting step for higher than 10 cm bed depth).

#### **Effect of the flow rate**

In figure 88, the breakthrough curves of DIBP are presented as example of the effect of the flow rate on the adsorption. By increasing the flow rate a decrease of breakthrough time was observed. More details will be reported in the next lines.

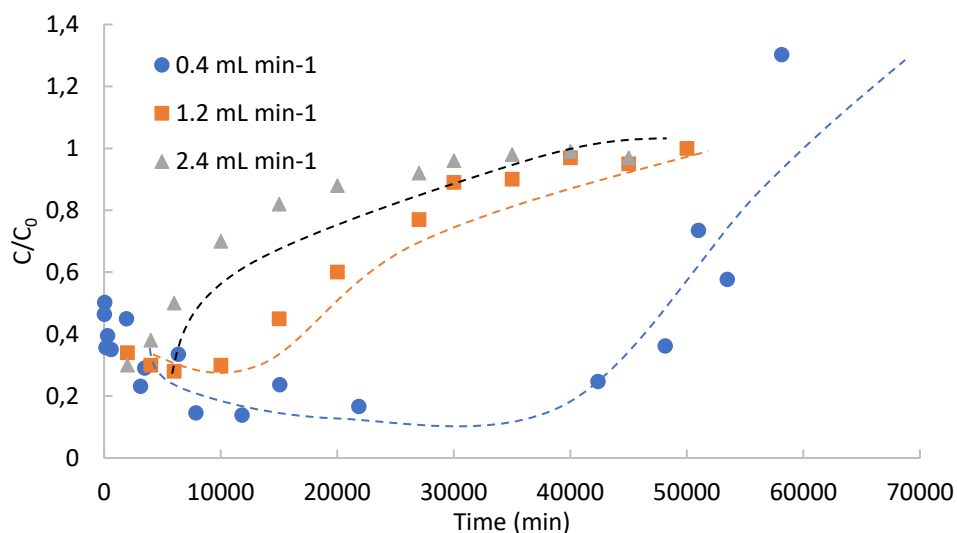


**Fig. 88 Breakthrough curves of DIBP (initial concentration of 50 mg L<sup>-1</sup>) at the flow rate of 0.4, 1.2 and 2.4 mL min<sup>-1</sup> filtered through a bed depth of 20 cm of GTPEG 5%.**

In the table 39 the typical parameter of adsorption on filtration bed are gathered for all the four compounds at all the flow rate tested to evidence the effect of this parameter.

**Tab. 39 Typical parameters of adsorption of considered pollutants (initial concentration of 50 mg L<sup>-1</sup>) filtered through 20 cm of GTPEG 5% at 0.4, 1.2 and 2.4 mL min<sup>-1</sup>.**

Flow rate (mL min <sup>-1</sup> )	q (mg g <sup>-1</sup> GTPEG)	Removal (%)	Breakthrough volume (L)	Pollutant adsorbate (mg)
<b>DMP</b>				
2.4	71	10	4.4	22
1.2	97	18	3.3	30
0.4	85	21	2.5	26
<b>DEP</b>				
2.4	387	24	10	120
1.2	484	38	7.9	150
0.4	445	46	6	138
<b>DIBP</b>				
2.4	3116	23	84	966
1.2	3290	34	60	1020
0.4	3143	83	23.2	963
<b>DBP</b>				
2.4	1871	20	58	580
1.2	1906	30	39	591
0.4	1963	52	23.2	603

The results obtained demonstrate that the condition used ensure the maximum adsorption capacity. Indeed, by increasing the flow rate almost the same adsorption capacity is obtained even if much solution needs to be filtrate to reach the saturation of the GTPEG. The higher breakthrough volume was reached after lower time of filtration because higher flow rate was used. It involves a decrease of removal efficiency and the effluents result to have higher concentration of pollutants after treatment at higher flow rate.

### Effect of the initial concentration

In figure 89, the breakthrough curves of DBP are presented as example of the effect of the initial concentration on the adsorption. By increasing the initial concentration an increase of breakthrough time was observed. More details will be reported in the next lines.

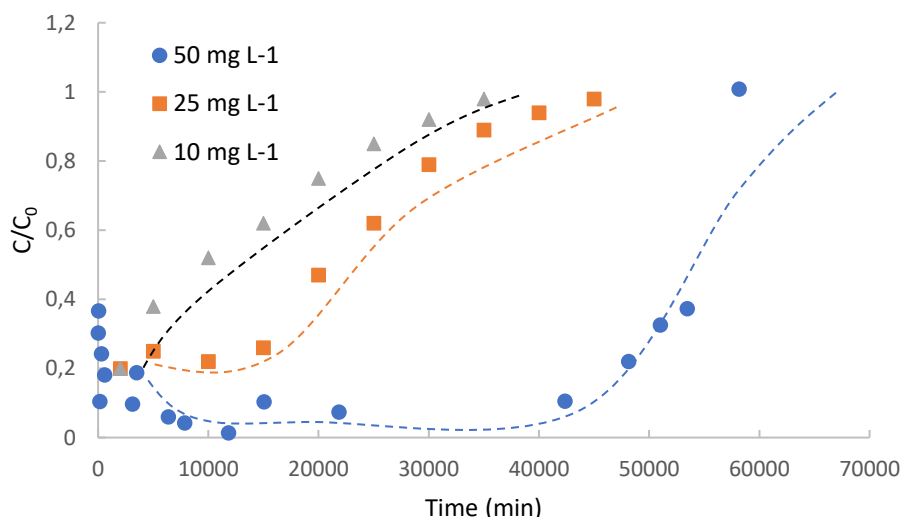


**Fig. 89 Breakthrough curves of DBP at the flow rate of  $0.4 \text{ mL min}^{-1}$  filtered through a bed depth of 20 cm of GTPEG 5%. Initial concentration of DBP of 10, 20 and 50 mg L<sup>-1</sup>.**

In the table 40 the typical parameter of adsorption on filtration bed are gathered for all the four compounds at all the initial concentration tested to evidence the effect of this parameter.

**Tab. 40 Typical parameters of adsorption of considered pollutants (initial concentration of 10, 25 and 50 mg L<sup>-1</sup>) filtered through 20 cm of GTPEG 5% at  $0.4 \text{ mL min}^{-1}$ .**

Initial concentration (mg L <sup>-1</sup> )	q (mg g <sup>-1</sup> GTPEG)	Removal (%)	Breakthrough volume (L)	Pollutant adsorbate (mg)
DMP				
10	7	10	1.7	2
25	22	14	2	7

50	85	21	2.5	26
DEP				
10	27	24	3.5	8.4
25	129	32	5	40
50	445	46	6	138
DIBP				
10	274	50	17	85
25	1400	79	22	434
50	3143	83	23.2	963
DBP				
10	163	35	14	49
25	653	45	18	202
50	1963	52	23.2	603

The results obtained demonstrate that the decrease of the initial concentration involves a decrease of the adsorption capacity and of the removal. It is probably due to lower gradient concentration between adsorbate surface and solution and equilibrium condition are reached for lower particle of adsorbate fixed on the surface of the adsorbent.

### Models fitting

The experimental data was further assessed with the Adams-Bohart model. With this model it is possible to have information about the kinetics of the process and the saturation concentration of the system. These parameters are useful to scale-up the system. In the tables 41, 42, 43 and 44 the correlation parameters of regression, kinetics constant and concentration of saturation obtained for all the compound at the different parameters tested are reported to compare the effect of their variations.

**Tab. 41 Correlation parameter of regression, kinetics constant and saturation concentration (theoretical and experimental) obtained by the Adams-Bohart and Thomas fitting of experimental data obtained for DMP at the different conditions tested.**

Initial concentration (mg L <sup>-1</sup> )	Bed depth (cm)	Flow rate (mL min <sup>-1</sup> )	K (L min <sup>-1</sup> mg <sup>-1</sup> )	N <sub>0</sub> (mg L <sup>-1</sup> )	R <sup>2</sup> ; $\chi^2$	K <sub>Th</sub> (L min <sup>-1</sup> mg <sup>-1</sup> )	q (mg g <sup>-1</sup> )	R <sup>2</sup> ; $\chi^2$
DMP								
50	20	0.4	2·10 <sup>-6</sup>	511	0.67; 6	6·10 <sup>-6</sup>	60	0.49; 5
50	20	1.2	5·10 <sup>-6</sup>	621	0.78; 2	8·10 <sup>-6</sup>	77	0.88; 0.92
50	20	2.4	8·10 <sup>-6</sup>	472	0.71; 3.1	1·10 <sup>-5</sup>	50	0.85; 0.91



50	10	0.4	$4 \cdot 10^{-6}$	725	0.76; 2.8	$1 \cdot 10^{-5}$	150	0.75; 2.1
50	3	0.4	$8 \cdot 10^{-5}$	1428	0.81; 1.1	$6 \cdot 10^{-5}$	700	0.83; 1.6
25	20	0.4	$5 \cdot 10^{-6}$	416	0.71; 4.1	$8 \cdot 10^{-5}$	32	0.88; 1.3
10	20	0.4	$7 \cdot 10^{-6}$	52	0.78	$9 \cdot 10^{-5}$	15	0.91

**Tab. 42 Correlation parameter of regression, kinetics constant and saturation concentration (theoretical and experimental) obtained by the Adams-Bohart fitting of experimental data obtained for DEP at the different conditions tested.**

Initial concentration ( $\mu\text{g L}^{-1}$ )	Bed depth (cm)	Flow rate ( $\text{mL min}^{-1}$ )	K ( $\text{L min}^{-1} \text{mg}^{-1}$ )	$N_0$ ( $\text{mg L}^{-1}$ )	$R^2; \chi^2$	$K_{Th}$ ( $\text{L min}^{-1} \text{mg}^{-1}$ )	q ( $\text{mg g}^{-1}$ )	$R^2; \chi^2$
DEP								
50	20	0.4	$2 \cdot 10^{-6}$	829	0.77; 1.8	$4 \cdot 10^{-6}$	400	0.91; 0.36
50	20	1.2	$5 \cdot 10^{-6}$	850	0.82; 1.3	$7 \cdot 10^{-6}$	500	0.86; 1.2
50	20	2.4	$9 \cdot 10^{-6}$	610	0.78; 1.9	$1 \cdot 10^{-5}$	360	0.85; 1.8
50	10	0.4	$7 \cdot 10^{-6}$	1024	0.72; 2.1	$9 \cdot 10^{-5}$	800	0.88; 1.2
50	3	0.4	$9 \cdot 10^{-6}$	1860	0.82; 1.1	$1 \cdot 10^{-5}$	1800	0.91; 0.52
25	20	0.4	$8 \cdot 10^{-6}$	510	0.76; 3	$2 \cdot 10^{-5}$	1025	0.79; 2.8
10	20	0.4	$8 \cdot 10^{-6}$	87	0.66; 6.8	$2 \cdot 10^{-5}$	521	0.67; 3.5

**Tab. 43 Correlation parameter of regression, kinetics constant and saturation concentration (theoretical and experimental) obtained by the Adams-Bohart and Thomas fitting of experimental data obtained for DIBP at the different conditions tested.**

Initial concentration ( $\mu\text{g L}^{-1}$ )	Bed depth (cm)	Flow rate ( $\text{mL min}^{-1}$ )	K ( $\text{L min}^{-1} \text{mg}^{-1}$ )	$N_0$ ( $\text{mg L}^{-1}$ )	$R^2; \chi^2$	$K_{Th}$ ( $\text{L min}^{-1} \text{mg}^{-1}$ )	q ( $\text{mg g}^{-1}$ )	$R^2; \chi^2$
DIBP								
50	20	0.4	$1 \cdot 10^{-6}$	5000	0.73; 2.8	$1 \cdot 10^{-6}$	5740	0.9; 0.23

50	20	1.2	$3 \cdot 10^{-6}$	4802	0.72; 3.1	$4 \cdot 10^{-6}$	5250	0.83; 0.62
50	20	2.4	$5 \cdot 10^{-6}$	5102	0.75; 2.2	$5 \cdot 10^{-6}$	5528	0.86; 0.52
50	10	0.4	$8 \cdot 10^{-6}$	7205	0.72; 1.8	$9 \cdot 10^{-6}$	7024	0.91; 0.18
50	3	0.4	$1 \cdot 10^{-5}$	1860	0.82; 0.55	$2 \cdot 10^{-5}$	7982	0.91; 0.26
25	20	0.4	$1 \cdot 10^{-5}$	1250	0.74; 3.8	$3 \cdot 10^{-5}$	3521	0.83; 1.3
10	20	0.4	$2 \cdot 10^{-5}$	600	0.78; 4.5	$3 \cdot 10^{-5}$	1728	0.85; 1.1

**Tab. 44 Correlation parameter of regression, kinetics constant and saturation concentration (theoretical and experimental) obtained by the Adams-Bohart and Thomas fitting of experimental data obtained for DBP at the different conditions tested.**

Initial concentration ( $\mu\text{g L}^{-1}$ )	Bed depth (cm)	Flow rate ( $\text{mL min}^{-1}$ )	K ( $\text{L min}^{-1} \text{mg}^{-1}$ )	$N_0$ ( $\text{mg L}^{-1}$ )	$R^2; \chi^2$	$K_{Th}$ ( $\text{L min}^{-1} \text{mg}^{-1}$ )	q ( $\text{mg g}^{-1}$ )	$R^2; \chi^2$
DBP								
50	20	0.4	$6 \cdot 10^{-7}$	4400	0.78; 5.6	$1 \cdot 10^{-6}$	3000	0.76; 4.8
50	20	1.2	$8 \cdot 10^{-7}$	4600	0.73; 6.2	$3 \cdot 10^{-6}$	3210	0.88; 1.1
50	20	2.4	$1 \cdot 10^{-6}$	4000	0.78; 4.3	$5 \cdot 10^{-6}$	2985	0.82; 1.5
50	10	0.4	$7 \cdot 10^{-7}$	7000	0.68; 9	$3 \cdot 10^{-6}$	5010	0.75; 2.8
50	3	0.4	$9 \cdot 10^{-7}$	14520	0.78; 4	$5 \cdot 10^{-6}$	12182	0.82; 1.3
25	20	0.4	$1 \cdot 10^{-6}$	1200	0.76; 4.5	$5 \cdot 10^{-6}$	1060	0.85; 0.8
10	20	0.4	$3 \cdot 10^{-6}$	628	0.85; 2.1	$6 \cdot 10^{-6}$	521	0.88; 0.48

By the kinetic constants and saturation concentrations obtained from the Adams-Bohart and Thomas model, general trends can be noticed. By increasing the flow rate, an increase of kinetic constant was observed for all the compound. This confirms that breakthrough is reached faster. No variations of adsorption capacity and saturation concentration were observed probably because the system had the time to reach the maximum saturation of the adsorbent and the diffusion step from solution to adsorbent surface was not the slowest step of the adsorption process. By increasing the bed depth, a decrease of kinetics constant and adsorption capacity is

observed, therefore the breakthrough is reached later as observed in experimental test. The decrease of saturation concentration can be explained by increase of amount of adsorbent used. The trend of saturation concentration is the same of the experimental observed. The decrease of initial concentration involves an increase of the kinetics of the process. The saturation concentration decrease by decreasing the initial concentration of the influent. The general trend observed in this work agrees with that already reported in literature.

In the table 45 the dimension of the reactor estimated with the Adams-Bohart model by assuming to treat 10000 liters of contaminated water for day in a reactor of a bed depth of 10 meters of GTPEG. The parameters obtained for the filtration on 20 cm of GTPEG at the the flow rate of 0.4 mL min<sup>-1</sup> and initial concentration of 50 mg L<sup>-1</sup> were used.

**Tab. 45 Reactor diameter and volume and mass of GTPEG estimation for treatment of 10 m<sup>3</sup> d<sup>-1</sup> to remove DMP, DEP, DIBP and DBP by adsorption on column of bed depth of 10 m of GTPEG.**

Initial concentration (mg L <sup>-1</sup> )	Diameter of the reactor (cm)	Volume of the reactor (m <sup>3</sup> )	Mass of GTPEG (kg)
DMP			
500	108	9	4425
DEP			
500	110	9.6	4608
DIBP			
500	57	2.6	1239
DBP			
500	40	1.3	609

In the table 46 the dimension of the reactor estimated with the Thomas model by assuming to treat 10000 liters of contaminated water for day in a reactor of a bed depth of 10 meters of GTPEG. The parameters obtained for the filtration on 20 cm of GTPEG at the the flow rate of 0.4 mL min<sup>-1</sup> and initial concentration of 50 mg L<sup>-1</sup> were used.

**Tab. 46 Reactor volume and diameter and mass of GTPEG estimation for treatment of 10 m<sup>3</sup> d<sup>-1</sup> to remove DMP, DEP, DIBP and DBP by adsorption on column of bed depth of 10 m of GTPEG.**

Initial concentration (µg L <sup>-1</sup> )	Mass of GTPEG (kg)	Volume of the reactor (m <sup>3</sup> )	Diameter of the reactor (m)
DMP			
250	8	0.017	1

DEP			
250	10	0.022	0.7
DIBP			
250	6.7	0.014	0.5
DBP			
250	0.5	0.001	0.5

#### 4. Conclusion

In this work the TPEG entrapped into calcium alginate was demonstrated useful also to remove plasticizers from the water by filtration on fixed-adsorbent bed. The granular form of TPEG obtained (GTPEG) results to have a good adsorbent property for the removal of DMP, DEP, DIBP and DBP from water at concentration levels between 10 and 50 mg L<sup>-1</sup>. Good removal, about 80% and 50% for DIBP and DBP was obtained by using a very low amount of TPEG (5% as weight relative to total alginate weight, GTPEG5%). Furthermore, it was demonstrated that experimental parameters such as flow rate and bed depth can be optimized to increase the removal and adsorption capacity. A systematic investigation was done to give information about the influence of the experimental parameters on the process and theoretical models (Thomas and Adams-Bohart) were used to confirm the influence observed and to estimate the dimension of the reactor for a scale-up of the process. These promising results confirm the adsorbent properties of TPEG and push-up us to investigate on its application and improve of its performance. To use an entrapping agent heavier than alginate can be useful to increase the amount of TPEG entrapped and to be sure to obtain a granular form of TPEG heavier than water and useful as fixed-bed adsorbent material.

#### 5. Reference

- [1] Abdel daiem MM, Rivera-Utrilla J, Ocampo-Pérez R, Méndez-Díaz JD, Sánchez-Polo M (2012) *Environmental impact of phthalic acid esters and their removal from water and sediments by different technologies - a review*. J Environ Manage vol.109; pp. 164–178.
- [2] Yang, M., Park, M.S., Lee, H., 2006. *Endocrine disrupting chemicals: human exposure and health risks*. J. Environ. Sci. Health, Part C vol. 24, pp. 183-224.
- [3] Silva, M.J., Barr, D.B., Reidy, J.A., Malek, N.A., Hodge, C.C., Caudill, S.P., Brock, J.W., Needham, L.L., Calafat, A.M., 2004. *Urinary levels of seven phthalate metabolites in the U.S. Population from the national Health and nutrition examination survey (NHANES) 1999-2000*. Environ. Health Perspect. Vol. 112 (3), pp. 331-338.

- [4] Rillig, M.C., 2012. *Microplastic in terrestrial ecosystems and the soil?* Environmental Science and Technologies, pp. 6453-6454.
- [5] Lambert, S., Sinclair, C., Boxall, A., 2014. *Occurrence, degradation, and effect of polymer based materials in the environment.* Reviews of Environmental Contamination and Toxicology, vol 227, pp. 1-53.
- [6] Wagner, M., Scherer, C., Alvarez-Muñoz, D., Brennholt, N., Bourrain, X., Buchinger, S., Fries, E., Grosbois, C., Klasmeier, J., Marti, T., Rodriguez-Mozaz, S., Urbatzka, R., Vethaak, A., Winther-Nielsen, M., Reifferscheid, G., 2014. *Microplastics in freshwater ecosystems: what we know and what we need to know.* Environmental Sciences Europe, vol 26, pp. 1-9.
- [7] Ivleva, N.P., Wiesheu, A.C., Niessner, R., 2017. *Microplastic in aquatic ecosystems.* Angewandte Chemie Int. Ed. Vol 56, pp. 1720-1739.
- [8] Lithner, D., Larsson, A., Dave, G., 2011. *Environmental and health hazard ranking and assessment of plastic polymers based on chemical composition.* Science of Total Environment, vol 409, pp. 3309-3324.
- [9] Wright, S.L., Kelly, F.J., 2017. *Plastic and human health: a micro issue?* Environmental Science and Technologies, vol. 51, pp. 6634-6647.
- [10] Hartmann, N.B., Huffer, T., Thompson, R.C., Hasselov, M., Verschoor, A., Daugaard, A.E., et al., 2019. *Are we speaking the same language? Recommendations for a definition and categorization framework for plastic debris.* Environmental Science and Technologies, vol 53, pp. 1039-1047.
- [11] Von Moos, N., Burkhardt-Holm, P., Kohler, A., 2012. *Uptake and effects of microplastics on cells and tissue of the blue mussel *Mytilus edulis* L. after an experimental exposure.* Environmental Science and Technologies, vol 46, pp. 11327-11335.
- [12] Hurley, R.R., Woodward, J.C., Rothwell, J.J., 2017. *Ingestion of microplastics by freshwater *Tubifex* worms.* Environmental Science and Technologies, vol. 51, pp. 12844-12851.
- [13] Sussarellu, R., Suquet, M., Thomas, Y., Lambert, C., Fabioux, C., Pernet, M.E.J., Le Goic, N., Quillien, V., Mingant, C., Epelboin, Y., Corporeau, C., Guyomarch, J., Robbens, J., Paul-Pont, I., Soudant, P., Huvet, A., 2016. *Oyster reproduction is affected by exposure to polystyrene microplastics.* Proceedings of the National Academy of Sciences of the United States of America. Vo [14] Fei-fei Liu, Guang-zhou Liu, Zhi-lin Zhu, Su-chun Wang, Fei-fei

Zhao, 2019. *Interactions between microplastics and phthalate esters as affected by microplastics characteristics and solution chemistry*, Chemosphere, Vol. 214, pp. 688-694. 113, pp. 2430-2435.

[15] Teuten, E.L., Saquing, J.M., Knappe, D.R.U., Barlaz, M.A., Jonsson, S., Bjorn, A., et al., 2009. *Transport and release of chemicals from plastics to the environment and to wildlife*. Philosophical Transactions of The Royal Society B. Vol 364, pp. 2027–2045.

[16] Calvert, P.D., Billingham, N.C., 1979. *Loss of additives from polymers: a theoretical model*. J. Appl. Polym. Sci. Vol. 24, pp. 357–370.

[17] Wensing, M., Uhde, E., Salthammer, T., 2005. *Plastics additives in the indoor environment - flame retardants and plasticizers*. Science of the Total Environment, vol. 339, pp. 19–40.

[18] Kovacic, T., Mrklic, Z., 2002. *The kinetic parameters for the evaporation of plasticizers from plasticized poly(vinyl chloride)*. Thermochemica Acta, vol. 381, pp. 49–60.

[19] Mengyu Ding, Qiyue Kang, Shiyi Zhang, Fanrong Zhao, Di Mu, Haifeng Zhang, Min Yang, Jianying Hu, 2019. *Contribution of phthalates and phthalate monoesters from drinking water to daily intakes for the general population*. Chemosphere, Vol 229, pp. 125-131.

[20] Xiaowei Liu, Jiangong Shi, Ting Bo, Huiyuan Li, John C. Crittenden, 2015. *Occurrence and risk assessment of selected phthalates in drinking water from waterworks in China*. Environ. Sci. Pollut. Res. vol. 22, pp. 10690-10698.

[21] Taofeek Salaudeen, Omobola Okoh, Foluso Agunbiade, Anthony Okoh, 2018. *Fate and impact of phthalates in activated sludge treated municipal wastewater on the water bodies in the Eastern Cape, South Africa*. Chemosphere, vol. 203, pp. 336-344.

## **2.7 Adsorbent material prepared by soft alkaline activation of spent ground coffee: characterization and adsorption mechanism of methylene blue from aqueous solution**

### **Abstract**

Ground coffee waste was used as precursor for the preparation of activated carbon by chemical activation using NaOH. Ground coffee was impregnated with NaOH and carbonized at 300°C for 3 hours. Its morphological and physical-chemical properties was determinate by SEM, X-ray diffraction, Raman spectroscopy and BET analysis. The performance of the treated ground coffee as adsorbent material for methylene blue (MB) was evaluated, by analyzing the effect of the initial pH and ionic strength of adsorption capacity and by evaluating the kinetics of the process and the mechanism of the process analyzing the adsorption isotherms. The effect of the

initial concentration ( $500 \text{ mg L}^{-1}$  and  $250 \text{ mg L}^{-1}$ ) of MB on the kinetic of the process and the effect of the initial pH (7.5, 6) on adsorption isotherm was evaluated. Pseudo-second order model results to be the model that control the process for both the initial concentration investigated and the adsorption capacity resulted to be  $142.8 \text{ mg L}^{-1}$  and  $113.64 \text{ mg L}^{-1}$ , respectively. The pH influences the adsorption isotherm model that regulates the process, in particular, Temkin's model regulates the process at pH of 7.5 and Langmuir's model regulates the process at pH 6. The surface covered by MB and the thermodynamics of the process were also determined.

## 1. Introduction

Activated carbons have found a wide range of use and application thanks to their porous structure, large availability and neutral effect on the environment. Japan and USA are the first consumer of these materials [1] and the increasing demand of activated carbons is caused by the use in all branch of industries in economically developed countries of new technology that use porous materials. Activated carbons result to be the cheaper porous materials available. The production of activated carbons is mainly based on the natural organic substrate like wood [2], sawdust [3], waste product as fruit stone [4, 5, 6, 7]. Other precursors were also used, like waste phenolic resins [8], phenol-formaldehyde resins [9] or other synthetic polymers, but they are a little bit more expensive than natural source. The morphological properties of activated carbons depend on the condition of the process of activation, as the temperature of pyrolysis and the presence of chemical activating agent. Normally, the surface area and porosity obtained by the simple pyrolysis are not enough use of activated carbons as adsorbent material or other application and chemical activation is required [10, 11, 12, 13]. Typical chemical activation is conducted by using phosphoric acid [14, 15] but an example of chemical activation with KOH by using pyrolysis conditions is reported [16, 17, 18]. A mechanism for alkaline activation was proposed in a study reported in literature<sup>Hu</sup>. When the starting material is mixed with a KOH solution, KOH or  $\text{K}^+$  cations are intercalated in the carbon matrix. After dehydration, the carbon layers expand in the presence of  $\text{K}_2\text{O}$  derived from KOH ( $300^\circ\text{C}$ ). Since carbon inside the sample is consumed, pores were formed in the carbon matrix. In the figure 90 the schematic representation of alkaline activation is reported.

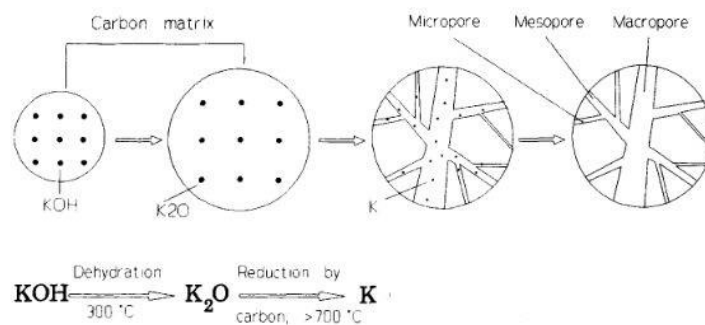


**Fig.90 Schematic representation of alkaline activation**

When the activation temperature exceeds 700°C, a considerable amount of metallic potassium is formed due to a reduction of K<sub>2</sub>O by carbon at high temperature. The effect of the use of KOH and NaOH as alkaline medium on morphological properties on the activated carbon is reported in literature [19]. NaOH results to confer bigger surface area and higher adsorption capacity to not pyrolyzed precursor than KOH, due to the higher expansion of carbon lamellae.

Many pollutants are present in water and sewage, like heavy metals, dyes and pigments. They are very difficult to remove, and different physical, biological, mechanical and chemical technologies were developed to solve this problem. The most used treatment to remove dye is the adsorption on activated carbon, because it is very cheap and easy to design, furthermore it is applicable with large range of concentration of pollutant. Activated carbons used as adsorbents can be functionalized to improve their properties, like surface area, selectivity or affinity, by introducing functional group like amine [20] or other chelating ligands [21], sulphide [22] and metals nanoparticle [23]. Other new carbonaceous material, like expanded graphite or nanotube, functionalized or not, are developed and increasingly used for the removal of different pollutants, like dyes [24, 25], PCPs [26] or BTEX [27]. These new materials have a higher surface area than activated carbons, but they are more expensive, therefore, they are not yet largely used in applied technology. In this study, we demonstrate the possibility to obtain an activate carbon by soft alkaline activation (300°C and NaOH as alkaline medium) of spent ground coffee and its ability to remove an organic dye, methylene blue (MB), with an adsorption capacity comparable with activated carbons obtained from ground coffee by acid or other activation and activated carbons obtained from other sources. The kinetics, isotherm adsorption, thermodynamics, pH and ionic strength influence on the process and material characterization studies were done. Several condition of pyrolysis, as inert atmosphere and high temperature are not necessary to obtain an activated carbon useful for adsorption use.

## 2. Materials and methods



## *Materials*

Ground coffee waste was obtained from the central cafeteria of the University and then treated as reported in methods section. The initial pH of the solutions was adjusted by adding NaOH and HCl purchased from Carlo Erba reagents (Carlo Erba, Rodano, Milano, Italy), MB was purchased from Carlo Erba reagents (Carlo Erba, Rodano, Milano, Italy). The stock solution of MB was prepared at 1000 mg/L. All reagents were of extra pure grade and used without further purification, and the solutions prepared in distilled water.

## *Ground coffee treatment*

13 g of ground coffee was washed with 1 L of NaOH 1 M, by mixing the two phase and stirring for 6 hours, to eliminate the soluble compounds present in the waste and impregnate with NaOH the ground coffee. After the wash treatment, the solid phase (very viscous slurry was obtained) was carbonized at 300°C in an oven overnight and a carbonaceous powder (11 g) was obtained.

## *Material characterization*

SEM images was obtained by using a high-resolution field emission scanning electronic microscopy (HR-FESEM), Auriga Zeiss model, at CNIS laboratory of University of Sapienza (Rome, Italy).

Micro-Raman analysis have been carried out using a Jobin-Yvon Horiba LabRam microRaman-spectrometer, equipped with a He-Ne laser ( $\lambda = 632.8$  nm), an edge filter and an Olympus microscope with  $10\times/50\times/100\times$  objectives. A spectral resolution of about  $5\text{ cm}^{-1}$  was obtained by a holographic grating with 600 grooves/mm. Spectra were acquired with an accumulation time of 60 s and laser power of 20mW.

FT-IR spectrum was obtained in the range  $400\text{-}4000\text{ cm}^{-1}$  ( $4\text{ cm}^{-1}$  of resolution) by using a JASCO FT-IR 460 Plus spectrophotometer. The sample was measured in the form of KBr pellet.

## *Adsorption test*

The influence of the pH, ionic strength and initial concentration of MB on the adsorption capacity were evaluated. 50 mL of MB solution (500 mg/L) was mixed at 100 mg of treated ground coffee in a conical flask of 100 mL and stirred at 400 rpm for 30 minutes. After 30 minutes of contact time, the liquid phase was aspirated and analyzed by UV-Vis spectrophotometer, to determinate the MB residue concentration. The adsorption capacity was measured by using the following equation:

$$q = \frac{\text{mass of DCF adsorbed (mg)}}{\text{mass of adsorbent (g)}} \quad (32)$$

$$q = (c_i - c_f) \frac{V}{m} \quad (33)$$

where  $c_i$  and  $c_f$  ( $\text{mg L}^{-1}$ ) are the MB concentrations at the beginning and after each adsorption experiment,  $V$  is the initial solution volume (L), and  $m$  is the adsorbent weight (g).

The initial pH (1, 3, 4.5, 6, 7.5, 9) of the MB solution was modified before the adsorption test by adding NaOH and HCl and monitoring the pH by using a pHmeter (Orion 420A, ThermoFisher Scientific, Waltham, Massachusetts, USA). The initial ionic strength (0, 0.25, 0.5, 0.75, 1 M) of the solution was modified by adding the useful amount of NaCl. The initial concentration of MB for the evaluation of its influence on the adsorption capacity were 500, 400, 250, 125, 100 and 25  $\text{mg L}^{-1}$  at pH 7.5 and 1000, 500, 350, 250, 100 and 50  $\text{mg L}^{-1}$  at pH 6. All the test was repeated two times.

#### *Kinetics studies*

In order to evaluate the velocity of the process and the relationship between contact time and adsorption capacity, the same experimental setup described below was used, but different contact time (5, 10, 15, 30, 40 and 60 min) was used. Therefore, 50 mL of MB solution (500 and 250  $\text{mg/L}$ ) was mixed at 100 mg of treated ground coffee and stirred at 400 rpm for different contact time, at pH 7.5 (optimal pH). Two different concentration of MB was used to verify the influence of initial concentration on the kinetic of the process. Adsorption capacity was evaluated and reported versus contact time. All tests were repeated three times to obtain the main value.

To interpret the mechanism of adsorption of MB on treated coffee ground and to evaluate the slowest step of the process, the experimental data were fitted to five kinetic mathematical models, i.e. pseudo-first order, pseudo-second order, intraparticle diffusion, Elovich and liquid film diffusion models. In the chapter 2.1 the equations of the used models are reported.

#### *Adsorption isotherm*

Further considerations on the mechanism of the process of adsorption were done by evaluating the adsorption isotherm of the MB on treated ground coffee. In particular, the influence of pH on the adsorption isotherm was also investigated. Therefore, 50 mL of MB solution at different initial concentration (1000, 500, 350, 250, 100, 50  $\text{mg/L}$ ) at pH 6 and 50 mL of MB solution at different initial concentration (500, 400, 250, 125, 100, 25  $\text{mg/L}$ ) at pH 7.5 was prepared. pH 6

and 7.5 were chosen because near the neutrality and no further process was required to reintroduce water in environment after the treatment. Each solution was mixed in a conical flask of 100 mL with 100 mg of treated ground coffee and stirred at 400 rpm for 30 minutes. After 30 minutes of contact time, the liquid phase was aspirated, and the residual concentration of MB was determined by UV-Vis spectrophotometer analysis and the adsorption capacity was calculated. All the tests were repeated two times. The data obtained were fitted with Langmuir [32], Freundlich [33, 34], Temkin [35] and Dubinin-Radushkevich [36] isotherm models. The equations of the models used are reported in the chapter 2.1.

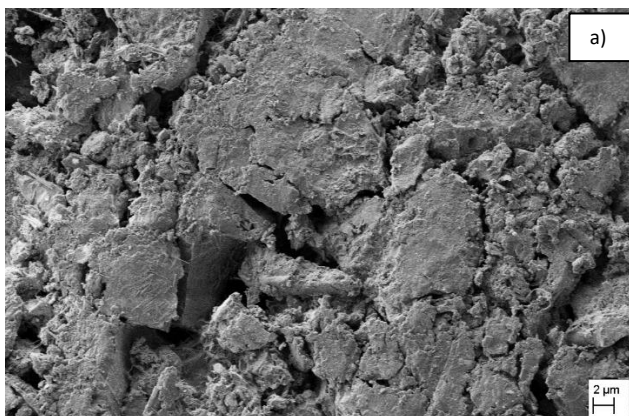
#### *Thermodynamics study*

The driving force, the free energy of the process and the minimum temperature that ensure the spontaneity of the process can be determined by evaluating the thermodynamic of the process. Therefore, 50 mL of MB solution (500 mg/L) at pH 7.5 was mixed at 100 mg of treated ground coffee and stirred at 400 rpm for 30 minutes. The adsorption capacity was evaluated at different temperature (293, 313 and 323 K), by controlling it with a magnetic stirred with heat control system. All the tests were repeated two times. In the chapter 2.1 the equation used for the thermodynamic studies are reported.

### **3.Results and discussions**

#### *Material characterization*

Textural properties of treated ground coffee were evaluated by SEM analysis. In the figure 91 are reported the SEM images acquired by using different magnification.



b)

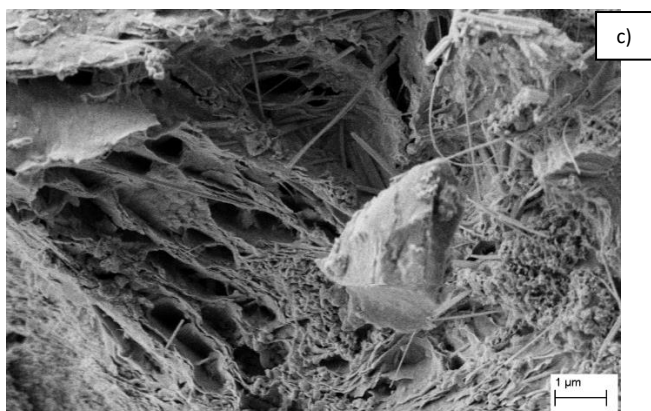
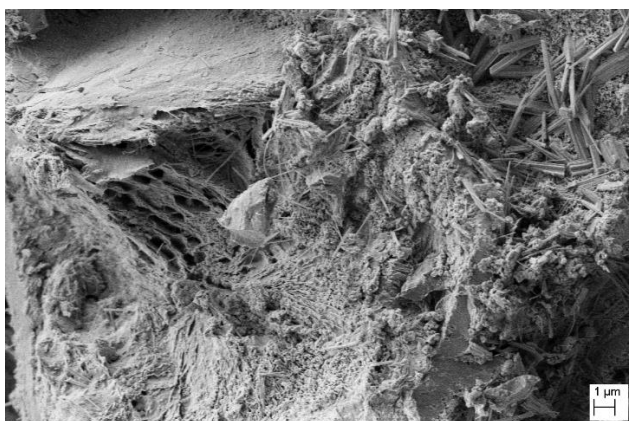


***Fig. 91 SEM images acquired with different magnification, (a: 5000 X, b: 10000 X, c: 25000 X).***

By analyzing the SEM images can be observed the roughly heterogeneous surface of the treated coffee (figure a). Probably on the surface were present residue of activating agent. By observing the images with higher magnification, the formation of pores can be observed. The typical honeycomb structure obtained with pyrolysis at about 700°C reported in literature [37, 38] can be observed, even if it is not extended on all the surface of the material. It confirms that the temperature used involves the dehydration of water that impregnate the ground coffee and a partial reduction of sodium oxides by carbon. As demonstrated subsequently, the porosity obtained was enough to obtain an adsorption capacity comparable with materials pyrolyzed at

higher temperature. In the figure 92 the Raman spectrum is gathered and the abroad peak at about  $1500\text{ cm}^{-1}$  confirms the carbonaceous amorphic structure of the treated ground coffee.

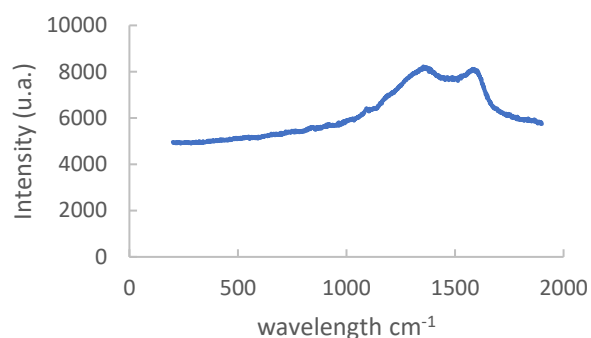


**Fig. 92 Raman spectrum of treated coffee ground.**

In the figure 93 the FT-IR spectrum in the range of  $400\text{-}4000\text{ cm}^{-1}$  obtained for the treated ground coffee is reported.

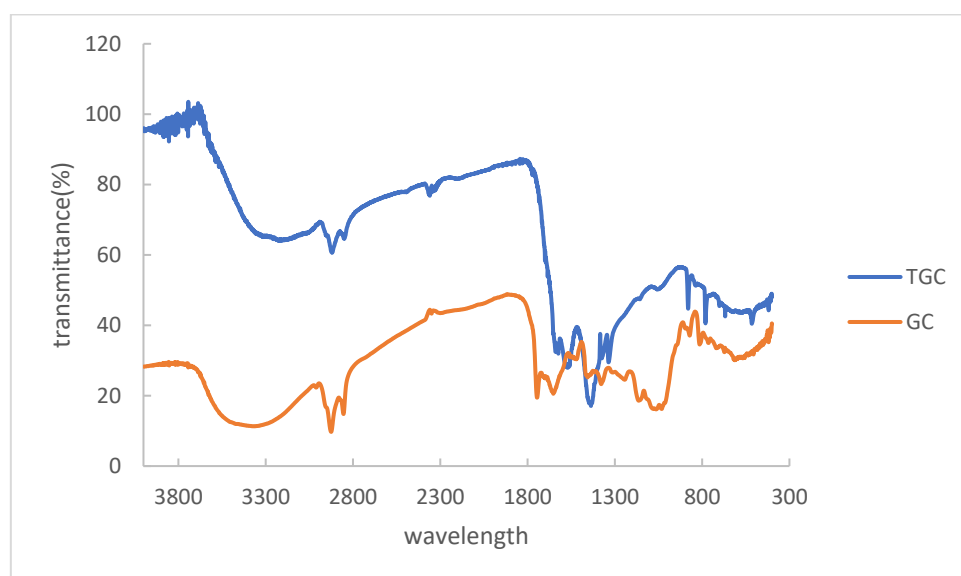


**Fig. 93 FT-IR spectrum of treated coffee ground (TGC) and coffe ground without treatment (GC).**

The broad peak at about  $3400\text{ cm}^{-1}$  is typically attributed to hydroxyl groups and it seems to be more intense in non-treated ground coffee, the band located at about  $2900\text{ cm}^{-1}$  corresponds to C-H stretching vibrations and it is more intense in non-treated ground coffee. The band at about  $2300\text{ cm}^{-1}$  can be attributed to the stretching of triple bond C-C and it is present only in treated ground coffee. The band at about  $1600\text{-}1400\text{ cm}^{-1}$  can be associated to stretching of double bond C-C of alkene compounds, C-H bending and also to the bending of N-H bond. This band is present in treated ground coffee while the peak at about  $1400\text{ cm}^{-1}$  is lower in non-treated

ground coffee and the peak at about  $1600\text{ cm}^{-1}$  is shifted at about  $1700\text{ cm}^{-1}$  in non-treated ground coffee and it could be associated to the stretching of C=O bond. The band at  $1000\text{ cm}^{-1}$  associated to alcohol groups is present in not treated ground coffee. The band in the range  $780\text{--}880\text{ cm}^{-1}$  about can be associated to rock of C-H aromatics bond and it is present only in treated ground coffee.

#### *pH influence*

In the figure 93 is reported the variation of adsorption capacity of treated ground coffee for MB at different values of pH. The standard deviation is also reported.

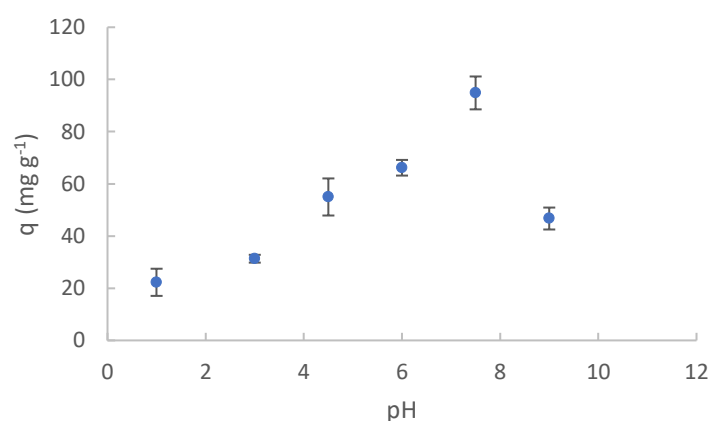


**Figure 93 Effect of pH on MB removal by treated ground coffee.  $C_o = 500\text{ mg L}^{-1}$ , contact time = 30 minutes, Solution volume = 50 mL, mass of adsorbent = 100 mg, stirring speed = 400 rpm.**

The decrease of the pH involves a decrease of adsorption capacity due the protonation of adsorbent's functional groups and/or surface and decrease of electrostatic interaction between adsorbate and adsorbent [39, 40, 41, 42] (MB is positively charged), while the large amount of  $\text{OH}^-$  influence negatively on the adsorption capacity due the possible neutralization of MB and decrease of electrostatic interaction. Therefore, an optimal value of pH was obtained when the two effect was balanced.

#### *Effect of ionic strength*

The figure 94 shows the influence of ionic strength on the adsorption capacity of treated ground coffee for the MB. The measurements of adsorption capacity were reported with their standard deviation.

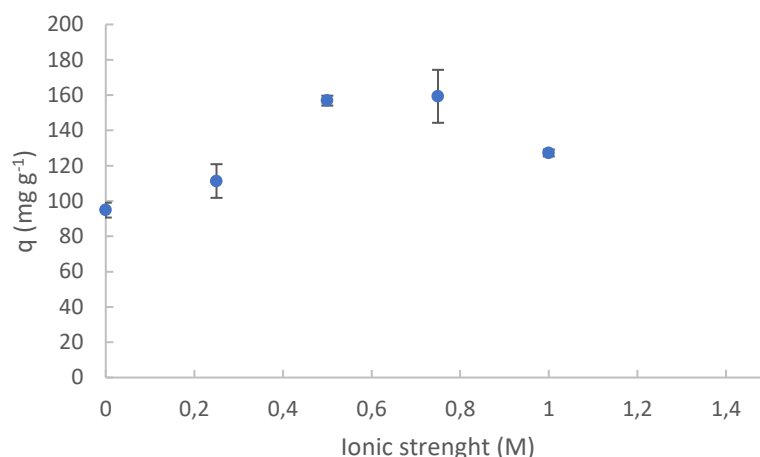


**Figure 94 Effect of ionic strength on MB removal by treated ground coffee.  $C_o= 500 \text{ mg L}^{-1}$ , contact time = 30 minutes, Solution volume= 50 mL, mass of adsorbent= 100 mg, stirring speed= 400 rpm, pH= 7.5.**

The increase of ionic strength is associated with an initially increase of adsorption capacity due probably to increase of solubility of the MB caused by salt effect. The same increase of adsorption capacity with the increase of ionic strength is reported in literature [43], even if the ionic strength used in this study was higher. After the initial increase of adsorption capacity with the increase of ionic strength, a decrease of adsorption capacity was revealed due the probably hindering effect caused by the high concentration of negatively charged sodium ions and/or by the competition between MB and positively charged ions added to the solution [44].

#### *Kinetics studies*

The influence of the contact time for different values of initial concentration of MB on the adsorption capacity was evaluated and reported in the figure 95. The standard deviation is also reported.

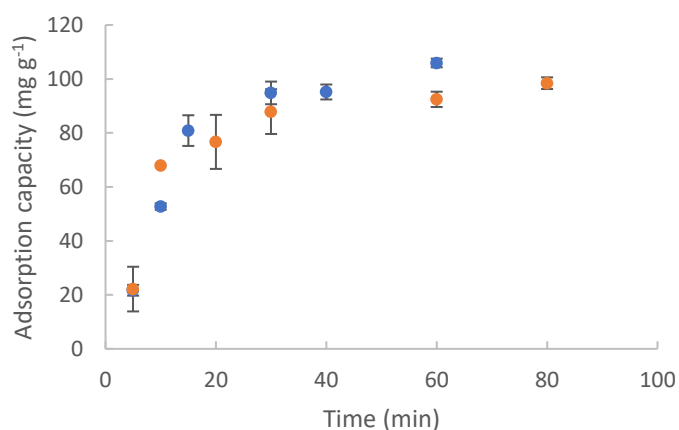


**Figure 95 Effect of contact time on MB removal by treated ground coffee.  $C_o= 500 \text{ mg L}^{-1}$  (blue circle),  $250 \text{ mg L}^{-1}$  (orange circle), contact time = 30 minutes, Solution volume= 50 mL, mass of adsorbent= 100 mg, stirring speed= 400 rpm, pH= 7.5.**

An increase of adsorption capacity with the increase of contact time can be observed in the first 30 minutes of treatment, then a plateau is reached. Therefore, the optimum contact time is 30 minutes, corresponding to the maximum adsorption capacity of about  $100 \text{ mg g}^{-1}$ . The trend is the typical present in the literature and it is interesting to note that the initial concentration of MB doesn't affect on the trend of the kinetic of the process. Table 47 summarizes the kinetic parameters and the coefficient of correlation calculated by fitting the experimental data with the already cited kinetic models.

**Tab. 47 Fitting of experimental data with kinetics models.**

	500 mg L <sup>-1</sup>		250 mg L <sup>-1</sup>	
Model	R <sup>2</sup> ; $\chi^2$	Parameters	R <sup>2</sup> ; $\chi^2$	Parameters
Pseudo-first order	0.861; 1.1	$K_1=1.15 \cdot 10^{-1} \text{ min}^{-1}$ $q_e \approx 10^5 \text{ mg g}^{-1}$	0.912; 0.67	$K_1=5.46 \cdot 10^{-2} \text{ min}^{-1}$ $q_e \approx 10^4 \text{ mg g}^{-1}$
Pseudo-second order	0.932; 0.23	$q_e= 142.8 \text{ mg g}^{-1}$ $k_2=3.7 \cdot 10^{-4} \text{ g mg}^{-1} \text{ min}^{-1}$	0.973; 0.14	$q_e= 113.64 \text{ mg g}^{-1}$ $k_2=7.3 \cdot 10^{-4} \text{ g mg}^{-1} \text{ min}^{-1}$
Elovich	0.829; 1.5	$\beta=3 \cdot 10^{-2} \text{ mg g}^{-1} \text{ min}^{-1}$ $\alpha=16.7 \text{ g mg}^{-1}$	0.715; 1.6	$\beta=4.1 \cdot 10^{-2} \text{ mg g}^{-1} \text{ min}^{-1}$ $\alpha=22.7 \text{ g mg}^{-1}$
Intraparticle diffusion	0.929; 0.35	$K_{dif}=14.04 \text{ mg g}^{-1} \text{ min}^{-1/2}$ $C=7.76$	0.852; 0.96	$K_{dif}=9.02 \text{ mg g}^{-1} \text{ min}^{-1/2}$ $C=26.10$
Liquid film diffusion	0.861; 0.89	$K_{fd}=1.15 \cdot 10^{-1} \text{ min}^{-1}$	0.912; 0.38	$K_{fd}=5.46 \cdot 10^{-2} \text{ min}^{-1}$

By analyzing the results of the fit of experimental data with kinetics model it is possible to note that the pseudo-second order model results to be the best model to fit the experimental data for MB concentration of  $500 \text{ mg L}^{-1}$  and  $250 \text{ mg L}^{-1}$ , therefore, the concentration doesn't affect on the kinetic of the process, and a chemisorption is observed. For the concentration of  $250 \text{ mg L}^{-1}$  of MB, the fit with the pseudo-second order model gives a value of  $113.64 \text{ mg g}^{-1}$  for the adsorption capacity (about  $100 \text{ mg g}^{-1}$  for the experimental data). For the concentration of  $500 \text{ mg L}^{-1}$  the intraparticle diffusion model results to have a R<sup>2</sup> coefficient higher than liquid film diffusion and the value obtained of R<sup>2</sup> allows to say that the intraparticle diffusion is the slow step (limiting for diffusion step) while for the concentration of  $250 \text{ mg L}^{-1}$  the slowly step of the adsorption is the liquid film diffusion. The value of  $142.8 \text{ mg g}^{-1}$  for  $q_e$  obtained from the



pseudo-second order model is higher than the value obtained for initial concentration of 250 mg L<sup>-1</sup> (113.64 mg g<sup>-1</sup>), that is very closed to the experimental data (about 100 mg g<sup>-1</sup>), confirms the best fit obtained for the data collected with the initial concentration of 250 mg L<sup>-1</sup>. The surface area covered by MB results to be 311,39 m<sup>2</sup> g<sup>-1</sup> for C<sub>0</sub>= 250 mg L<sup>-1</sup> and 393.50 m<sup>2</sup> g<sup>-1</sup> for C<sub>0</sub>= 500 mg L<sup>-1</sup>. The value of adsorption capacity obtained is higher or comparable with other reported in literature for pyrolyzed/activated coffee waste [45, 46] or coffee residues untreated [39, 45, 47]. In the table 48 a comparison with other activated carbon derived from different/same biosources was reported.

**Tab. 48 Comparison of adsorption capacity for different adsorbent material derived from different bioresources.**

Material	Adsorption capacity (mg g <sup>-1</sup> )	Reference
Ground coffee activated by alkaline medium at 300°C	113.64 (C <sub>0</sub> =250 mg L <sup>-1</sup> ) 142.80 (C <sub>0</sub> =500 mg L <sup>-1</sup> )	This work
Coffee ground activated by microwave heating (alkaline activation)	99.43	48
Coffee residues	6.76	46
Coffee ground pyrolyzed at 850°C	129.90	47
Coffee residues	4.68	40
Coffee ground activated by phosphoric acid at 450°C	367.00	31
Pine fruit shell	529.00	49
Black stone cherries	321.75	6
Walnut shell	315.00	50
Oil palm shell	243.90	51
Hazelnut husks	204.00	52
Plant leaf powder	61.22	53
Wood apple rind	40.00	54
Cherry stones	276.00	55
Rice husks	441.52	56

#### *Adsorption isotherm*

The adsorption isotherm obtained at initial pH of 6 and 7.5 are reported in the figure 96. The standard deviation of each data is also reported.

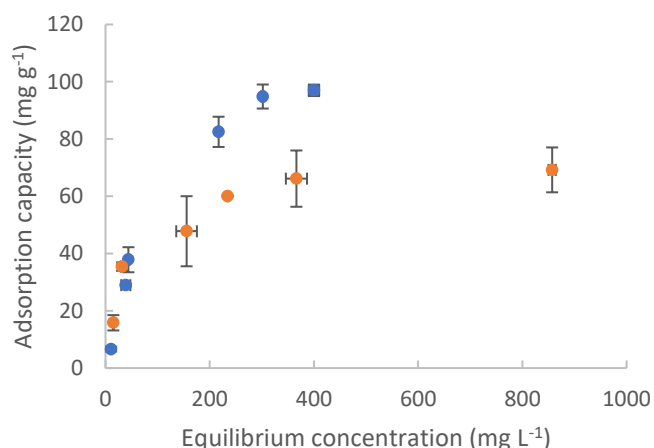


**Fig. 96 Isotherm adsorption at different value of pH (6 orange circle and 7.5 blue circle).  $C_0=500, 400, 250, 125, 100$  and  $25 \text{ mg L}^{-1}$  for pH 7.5,  $C_0=1000, 500, 350, 250, 100$  and  $50 \text{ mg L}^{-1}$  for pH 6, 100 mg of adsorbent material, stirring speed=400 rpm, contact time=30 minutes.**

As expected, the adsorption capacity increase with the increase of equilibrium concentration until to reach a plateau at  $300 \text{ mg L}^{-1}$  at pH 7.5 with a  $q_{\text{max}}$  of about  $100 \text{ mg g}^{-1}$  and  $400 \text{ mg L}^{-1}$  with a  $q_{\text{max}}$  of about  $60 \text{ mg g}^{-1}$  at pH 6. In the table 49 are reported the equation of linear regression and the linear regression coefficient of experimental data fitted with each models.

**Table 49 Fit of adsorption isotherm data by using Langmuir, Freundlich, Temkin and Dubinin-Radushkevich models.**

Model	pH 7.5		pH 6	
	$R^2; \chi^2$	Equation	$R^2; \chi^2$	Equation
Langmuir	0.922; 0.39	$y = 6.5 \cdot 10^{-3}x + 1.18$	0.983; 0.36	$y = 1.3 \cdot 10^{-2}x + 0.73$
Freundlich	0.934; 0.26	$y = 0.75x + 0.42$	0.896; 1.1	$y = 0.39x + 1.89$
Temkin	0.983; 0.08	$y = 26.98x - 62.68$	0.957; 0.51	$y = 14.42x - 20.08$
Dubinin-Radushkevich	0.841; 0.67	$y = -5 \cdot 10^{-5}x + 4.09$	0.938; 0.6	$y = -5 \cdot 10^{-5}x + 4.02$

By varying the pH, a change of mechanism of interaction happens. In particular, at pH 7.5 the model that best fits the experimental data results to be the Temkin model, while at pH 6 the Langmuir model was the best fit for experimental data. Therefore, at pH 7.5 the adsorbate

interact with a heterogeneous surface and a multilayer of adsorbate on adsorbent could be present, while at pH 6.5 the increase of  $H^+$  causes an adsorption of just one layer of MB due to the reduction of electrostatic interaction and the surface could result homogeneous because  $H^+$  was adsorbed on it. The  $q_{max}$  reported previously support these hypothesis ( $100 \text{ mg g}^{-1}$  at pH 7.5 vs  $60 \text{ mg g}^{-1}$  at pH 6). The value of Langmuir constant calculated was  $1.8 \cdot 10^{-2} \text{ L mg}^{-1}$  and the value of  $q_{max}$  calculated was  $76.92 \text{ mg g}^{-1}$ . The value of separation factor is between 0 and 1 for each value of initial concentration, therefore the process was favorable. The value of equilibrium binding constant calculated by Temkin model was  $0.099 \text{ L g}^{-1}$  and the value of  $B_1$  (related to the heat of adsorption) was  $26.98 \text{ J mol}^{-1}$ . The adsorption capacity evaluated by isotherm adsorption is comparable with values reported in literature [39, 44, 46].

#### *Influence of initial concentration*

In the figure 97 is reported the influence on the adsorption capacity of different initial concentration of MB for different value of pH.

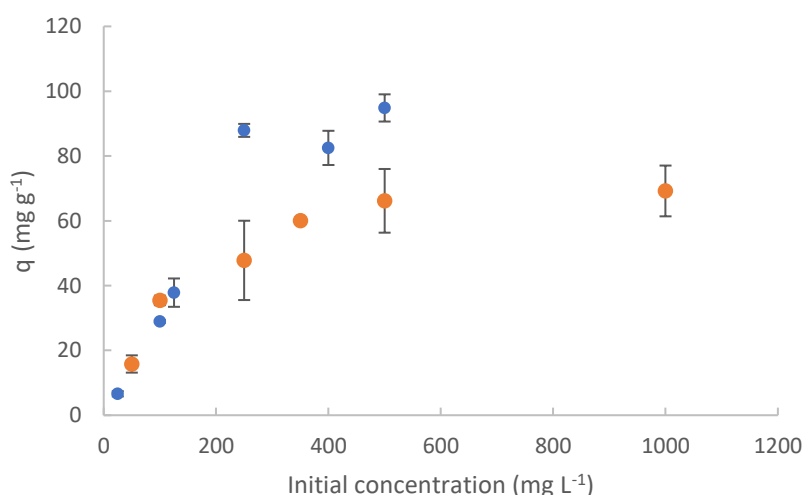


**Fig. 97 Adsorption capacity for different value of MB initial concentration.  $C_0=500, 400, 250, 125, 100$  and  $25 \text{ mg L}^{-1}$  for pH 7.5 (blue circle),  $C_0=1000, 500, 350, 250, 100$  and  $50 \text{ mg L}^{-1}$  for pH 6 (orange circle),  $100 \text{ mg}$  of adsorbent material, stirring speed= $400 \text{ rpm}$ , contact time= $30 \text{ minutes}$ .**

An initial rapid increase of adsorption capacity was observed by increasing the initial concentration of MB for both the value of pH, after the initial increase a plateau was reached at initial concentration of about  $250 \text{ mg L}^{-1}$  at pH 7.5 and about  $350 \text{ mg L}^{-1}$  at pH 6. The different minimum initial concentration required to reach the plateau is associated to a different adsorption capacity of the material at different condition of pH.

### Thermodynamics studies

The evaluation of the thermodynamic of the adsorption process of MB on treated ground coffee was conducted. In the table 50 are reported the values of each parameters calculated from this study (standard enthalpy, standard entropy, standard free energy and minimum temperature of spontaneity).

**Tab. 50 Thermodynamic parameters of adsorption process of MB on treated ground coffee.**

$\Delta H$ (kJ mol <sup>-1</sup> )	$\Delta S$ (J mol <sup>-1</sup> K <sup>-1</sup> )	$\Delta G^\circ$ (kJ mol <sup>-1</sup> )	T <sub>min</sub> (°C)
1.28	7.10	-0.84	-83

The increase of entropy due to the increase of randomness at interface liquid/solid results to be the driving force of the process. The process results to be endothermic, therefore the increase of temperature promote the process in terms of equilibrium position and velocity of process. The value of free energy obtained demonstrates that the physio adsorption happens. The value of free energy obtained and the physical adsorption observed were comparable with literature data [56, 57]. In the table 51 are showed the experimental and theoretical free energy and equilibrium constant of the process at different temperature. It is possible to note the perfect correlation between experimental and theoretical data.

**Tab. 52 Equilibrium constant and free energy obtained from experimental and theoretical data. Experimental data were obtained for adsorption test of MB solution of 500 mg<sup>-1</sup>L, 100 mg of adsorbent material, pH 7.5, stirring speed= 400 rpm and contact time= 30 minutes.**

Temperature (K)	$\frac{q_e}{C_e}$ experimental (mg L)	$\frac{q_e}{C_e}$ theoretical (mg L)	$\Delta G^0$ experimental (kJ mol <sup>-1</sup> )	$\Delta G^0$ theoretical (kJ mol <sup>-1</sup> )
293	1.39	1.39	-0.80	-0.80
313	1.43	1.45	-0.94	-0.94
323	1.46	1.46	-1.02	-1.01

### 4. Conclusions

The above presented and discussed results have proved that ground coffee can be treated and carbonized by soft alkaline activation. The performance of this activated carbon is comparable with that of other active carbon derived from other biosource and/or activated with different processes. No particular or hard condition are required to remove MB from aqueous solution, the very low minimum temperature of spontaneity of the process ensure the feasibility of the

process also during the winter if the process is conducted outdoor. The neutral pH required for the treatment allows to reintroduce the treated water in the natural cycle of water without further treatment. Furthermore, the ground coffee and the described process of activation result to be a good way to produce an adsorbent material useful for environmental safeguard and, further study can be conducted to examine the possibility to remove other pollutants and determinate the amount of it adsorbed by this material. This study demonstrates how a human waste can become a resource and offer a reflection on the recycle of waste product of agri-food industry.

## 5. Reference

- [1] Bansal, R.C., Goyal, M., 2005, Activated Carbon Adsorption, Taylor & Francis Group, Boca Raton
- [2] Wang, T., Tan, S., C. Liang, C., 2009, Preparation and characterization of activated carbon from wood via microwave-induced ZnCl<sub>2</sub> activation, Carbon, 47, 1867-1885
- [3] Pietrzak, R., 2010, Sawdust pellets from coniferous species as adsorbent for NO<sub>2</sub> removal, Bioresource Technology, 101, 907-913
- [4] Chen, X., Jeyaseelan, S., Graham, N., 2002 Physical and chemical properties studies of activated carbon made from sewage sludge, Waste Management, 22, 755-760
- [5] Dilek, 2014, Production and characterization of activated carbon from sour cherry stones by zinc chloride, Fuel, 115, 804-811
- [6] Rodriguez Arana, J.M.R., Mazzocco, R.R., 2010, Adsorption studies of methylene blue and phenol onto black stone cherries prepared by chemical activation, Journal of Hazardous Materials, 180, 656-661
- [7] Tennison, S.R., 1998, Phenolic-resin derived activated carbons, Applied Catalysis A: General, 173, 289-311
- [8] Teng, H., Wang, S.C., 2000, Preparation of porous carbons from phenol-formaldehyde resins with chemical and physical activation, Carbon, 38, 817-824
- [9] Fukuyama, H., Terai, S., 2008, Preparing and characterizing the active carbon produced by steam and carbon dioxide as a heavy oil hydrocracking catalyst support, Catalysis Today, 130, 382-388

- [10] Ariyadejwanich, P., Tanthapanichakoon, W., Nakagawa, K., Mukai, S.R., Tamon, H., 2003 Preparation and characterization of mesoporous activated carbon from waste tires, *Carbon*, 41, 157-164
- [11] Lee, W.H., Reucroft, P.J., 1999, Vapor adsorption on coal- and wood-based chemically activated carbons (II) adsorption of organic vapors, *Carbon*, 37, 15-20
- [12] Suzuki, R.M., Andrade, A.D., Sousa, J.C., Rollemberg, M.C., 2007 Preparation and characterization of activated carbon from rice bran, *Bioresource Technology*, 98, 1985-1991
- [13] Namane, A., Mekarzia, A., Benrachedi, K., Belhaneche-Bensemra, N., Hellal, A., 2005, Determination of the adsorption capacity of activated carbon made from coffee grounds by chemical activation with  $ZnCl_2$  and  $H_3PO_4$ , *Journal of Hazardous Materials B*, 119, 189-194
- [14] Teng, H., Yeh, T.S., Hsu, L.Y., 1998, Preparation of activated carbon from bituminous coal with phosphoric acid activation, *Carbon*, 36, 1389-1395
- [15] Evans, M.J.B., Halliop, E., MacDonald, J.A.F., 1999 The production of chemically-activated carbon, *Carbon*, 37, 269-274
- [16] Ubago-Perez, R., Carrasco-Marin, F., Fairen-Jimenez, D., Moreno-Castilla, C., 2006, Granular and monolithic activated carbons from KOH-activation of olive stones, *Microporous and Mesoporous Materials*, 92, 64-70
- [17] Carrott, P.J., Ribeiro Carrott, M.M.L., Mourao, P.A.M., 2006, Pore size control in activated carbons obtained by pyrolysis under different conditions of chemically impregnated cork, *Journal of Analytical and Applied Pyrolysis*, 75, 120-127
- [18] Hu, Z., Vansant, E.F., Synthesis and characterization of a controlled-micropore-size carbonaceous adsorbent produced from walnut shell, *Microporous Material*, 1195, 3, 603-612
- [19] Lillo-Rodenas, M.A., Marco-Lozar, J.P., Cazorla-Amoros, D., Linares-Solano, A., 2007, Activated carbons prepared by pyrolysis of mixture of carbon precursor alkaline/hydroxide, *Journal of Analytical and Applied Pyrolysis*, 80, 166-174
- [20] Wang, J., Zheng, S., Shao, Y., Liu, J., Xu, Z., Zhu, D., 2010 Amino-functionalized  $Fe_3O_4@SiO_2$  core-shell magnetic nanomaterial as a novel adsorbent for aqueous heavy metals removal, *Journal of Colloid and Interface Science*, 349, 293-299

- [21] Lee, B., Kim, Y., Lee, H., Yi, J., 2001, Synthesis of functionalized porous silicas via templating method as heavy metal ion adsorbents: the introduction of surface hydrophilicity onto the surface of adsorbents, *Microporous and Mesoporous Materials*, 50, 77-90
- [22] Roosta, M., Ghaedi, M., Daneshfar, A., Saharei, R., 2014, Experimental design based response surface methodology optimization of ultrasonic assisted adsorption of safranin O by tin sulfide nanoparticle loaded on activated carbon, *Spectrochimica Acta A*, 122, 223-231
- [23] Ghaedi, M., Heidarpour, Sh., Kokhdan, S.N., Sahraie, R., Daneshfar, A., Brazesh, B., 2012, Comparison of silver and palladium nanoparticle loaded on activated carbon for efficient removal of methylene blue: kinetics and isotherm study of removal process, *Powder Technology*, 228, 18-25
- [24] Fan, J., Shi, Z., Lian, M., Li, H., Yin, J., 2013, Mechanically strong graphene oxide/sodium alginate/polyacrylamide nanocomposite hydrogel with improved dye adsorption capacity, *Journal of Material Chemistry A*, 1, 7433-7443
- [25] Sharma, P., Das, M.R., 2013, Removal of a Cationic Dye from Aqueous Solution Using Graphene Oxide Nanosheets: Investigation of Adsorption Parameters, *Journal of Chemical and Engineering data*, 58, 151-158.
- [26] Cai, N., Larese-Casanova, P., 2014, Sorption of carbamazepine by commercial graphene oxides: A comparative study with granular activated carbon and multiwalled carbon nanotubes, *Journal of Colloid and Interface Science*, 426, 152-161
- [27] Caniani, D., Caivano, M., Calace, S., Mazzone, G., Pascale, R., Mancini, I.M., Masi, S., 2018 Remediation of water samples contaminated by BTEX using super-expanded graphite as innovative carbon-based adsorbent material, *IWA World Water Congress & Exhibition*, 16-21 September, Tokyo, Japan.
- [28] Qiu, H., Lv, L., Pan, Q.-j. Zhang, W.-m. Zhang, Q.-x. Zhang, Critical review in adsorption kinetic models, *Journal of Zhejiang University SCIENCE A*, 2009, 10(5), 716-724
- [29] Ho, Y.S., McKay, G., 1999, Pseudo-second order model for sorption process, *Process Biochemistry*, 34, 451-465
- [30] Low, M.J.D., 1960, Kinetics of chemisorption of gases on solids, *Chemical Reviews*, 60(3), 267-312

- [31] Reffas, A., V. Bernardet, B. David, L. Reinert, M.B. Lehocine, M. Dubois, N.Batiste, L. Duclaux, 2010, Carbons prepared from coffee grounds by  $H_3PO_4$  activation: Characterization and adsorption of methylene blue and Nylosan Red N-2RBL, *Journal of Hazardous Materials*, 175, 779-788
- [32] Langmuir, I., 1918, The adsorption of gases on plane surfaces of glass, mica and platinum, *Journal of the American Chemical society*, 1361-1402.
- [33] Freundlich, H.M.F., 1906, Over the adsorption in solution, *Journal of Physical Chemistry*, 57, 385-471.
- [34] Butler, J.A.V., and Ockrent, C., 1930, The surface tensions of solutions containing two surface-active solutes, *The Journal of Physical Chemistry*, 34, 2841-2859.
- [35] M.I. Temkin M.I., and V. Pyzhev, V., 1940, Kinetics of ammonia synthesis on promoted iron catalyst, *Acta Physical Chemistry USSR*, 12. 327-357.
- [36] Dubinin M.M., and Radushkevich, L.V., 1947, The equation of characteristic curve of the activated charcoal, *Proceedings of the Academy of Science of the USSR Physical Chemistry Section*, 55, 331-337
- [37] Baghdadi, M., Ghaffari, E., and Aminzadeh, B., 2016, Removal of carbamazepine from municipal wastewater effluent using optimally synthesized magnetic activated carbon: Adsorption and sedimentation kinetic studies, *Journal of Environmental Chemical Engineering*, 4, 3309-3321
- [38] Cazetta, A.L., Vargas, A.M.M., Nogami, E.M., Kunita, M.H., Guilherme, M.R., Martins, A.C., Silva, T.L., Moraes, J.C.G., Almeida, V.C., 2011, NaOH-activated carbon of high surface area produced from coconut shell: Kinetics and equilibrium studies from the methylene blue adsorption, *Chemical Engineering Journal*, 174, 117-125
- [39] Foo, K.Y., Hameed, B.H., 2011, Utilization of rice husk as a feedstock for preparation of activated carbon by microwave induced KOH and  $K_2CO_3$  activation, *Bioresource Technology*, 2011, 102, 9814-9817.
- [40] Nitayaphat, W., Jintakosol, J., Engkaseth, K., Wanrakakit, Y., 2015, Removal of Methylene Blue from Aqueous Solution by Coffee Residues, *Chiang Mai Journal of Science*, 42, 407,416



- [41] Hameed, B.H., Ahmad, A.A., 2009, Batch adsorption of methylene blue from aqueous solution by garlic peel, an agriculture waste biomass, *Journal of Hazardous Materials*, 164, 870-875
- [42] Kavitha, D., Namasivayam, 2007, Experimental and kinetic studies on methylene blue adsorption by coir pith carbon, *Bioresource Technology*, 98, 14-21
- [43] Pavan, F.A., Mazzocato A.C., Gushikem, Y., 2008, Removal of methylene blue dye from aqueous solutions by adsorption using yellow passion fruit peel as adsorbent, *Bioresource Technology*, 99, 3162-3165
- [44] Dogan, M., Abak, H., Alkan, M., 2009, Adsorption of methylene blue onto hazelnut shell: Kinetics, mechanism and activation parameters, *Journal of Hazardous Materials*, 164, 172–181
- [45] Al Khateeb, L.A., Almotiry, S., Salam, M.A., 2014 Adsorption of pharmaceutical pollutants onto graphene nanoplatelets, *Chemical Engineering Journal*, 248, 191-199
- [46] Orfanos, A., Manariotis, I.D., Karapanagioti, H.K., Sorption of Methylene Blue onto Food Industry Byproducts, *International Biochar Initiative*, Article ID 7046
- [47] Pavlovic, M.D., Nikolic, I.R., Milutinovic, M.D., Dimitrijevic-Brankovic, S.D., Siler-Marinkovic, S.S., Antonovic, D.G., 2015 Plant waste materials from restaurants as the adsorbent for dyes, *Hemijaska industrija*, 69, 667-677
- [48] Hirata, M., Kawasaki, N., Nakamura, T., Matsumoto, K., Kabayama, M., Tamura, T., Tanada, S., 2002, Adsorption of Dyes onto Carbonaceous Materials Produced from Coffee Grounds by Microwave Treatment, *Journal of Colloid and Interface Science*, 254, 17–22
- [49] Royer, B., Cardoso, N.F., Lima, E.C., Vaghetti, J.C.P., Simon, N.M., Calvate, T., Cataluna Veses, R., 2009, Application of Brazilian pine-fruit shell in natural and carbonized forms as adsorbent to removal of methylene blue from aqueous solution-kinetic and equilibrium study, *Journal of Hazardous Materials*, 164, 1213-1222
- [50] Yang, J., Qiu, K., 2010, Preparation of activated carbons from walnut shells via vacuum chemical activation and their application for methylene blue removal, *Chemical Engineering Journal*, 165, 209-217
- [51] Tan, I., Ahmad, A., Hameed, B., 2008, Adsorption of basic dye using activated carbon prepared from oil palm shell: batch and fixed bed studies, *Desalination*, 25, 13-28

- [52] Ozer, C., Imamoglu, M., Turhan, Y., Boysan, F., 2012, Removal of methylene blue from aqueous solution using phosphoric acid activated carbon prepared from hazelnut husks, *Toxicological and Environmental Chemistry*, 94, 1283-1293
- [53] Gunasekar, V., Ponnusami, V., 2012, Kinetics, equilibrium and thermodynamic studies on adsorption of methylene blue by carbonized leaf plant powder, *Journal of Chemistry*, 13, 1-6
- [54] Malarvizhi, R., Ho, Y.S., 2010, The influence of pH and the structure of the dye molecules on adsorption isotherm modeling using activated carbon, *Desalination*, 264, 97-101
- [55] Nowicki, P., Kazmierczak, J., Pietrzak, R., 2015, Comparison of physicochemical and sorption properties of activated carbons prepared by physical and chemical activation of cherry stones, *Powder Technology*, 269, 312-319
- [56] Theydan, S.K., Ahmed, M.J., 2012, Adsorption of methylene blue onto biomass-based activated carbon by FeCl<sub>3</sub> activation: Equilibrium, kinetics, and thermodynamic studies, *Journal of Analytical and Applied Pyrolysis*, 97, 116-122
- [57] Karagoz, S., Tay, T., Ucar, S., Erdem, M., 2008, Activated carbons from waste biomass by sulfuric acid activation and their use on methylene blue adsorption, *Bioresource Technology*, 2008, 99, 6214-6222

### **3. General conclusions and outlook**

#### **3.1 General conclusions**

The adsorption process is widely used for the environmental remediation and upgrade of the basic wastewater treatment into the municipal wastewater plants. The most used adsorbent material used is the activated carbon and the process results to be cheap, easily to perform and no metabolites are produced from the contaminants. Even if the process is already largely widespread and used, several studies are focused on it to develop it and increase the spectrum of contaminants that can be removed and the situation of application. As reported in the previous sections, the develop of the adsorption process results to be very interesting for the removal of emerging contaminants like plasticizers, personal care and pharmaceutical products, pesticides. Furthermore, the develop of the process results to be very important to guarantee its good performance at lower concentration of typical contaminants treated than nowadays or for the application of it in new situation and setup, like the injection of adsorbent material into the

contaminated groundwater or the coupling of the adsorption with other traditional or advanced process, like biodegradation, advanced oxidation process, photocatalytic degradation etc. For these reason, the investigation of the use of new adsorbent material is very important to develop the adsorption process. This PhD thesis demonstrates the possibility of the use of thermo-plasma expanded graphite as adsorbent material with interesting results and the perspective of the modification of its morphological and physical-chemical properties to use it on new and innovative adsorption setup. Several contaminants were tested to verify the spectrum of potential application of the thermo-plasma expanded graphite for the adsorption process on the field. Because the hydrophobic nature of the thermo-plasma expanded graphite, its ability to remove contaminants was tested on organic compounds. It was demonstrated that compounds like methylene blue, trichloroethylene, toluene, ethylbenzene, xylenes, atrazine, carbamazepine, 17- $\alpha$  ethinylestradiol, bisphenol A, diclofenac, dimethylphthalates, diethylphthalates, dibutylphthalates and di-isobutylphthalates can adsorbed on it. The thermo-plasma expanded graphite was tested in its original commercial form (a very light powder that float on the water) and as modified form prepared during the experimental work. Lab-scale procedures were optimized for the production of a granular form of thermo-plasma expanded graphite by physical entrapment into sodium alginate and for the production of an hydrosoluble form of the thermo-plasma expanded graphite through the sonication of the commercial form. The granular form was used and tested as fixed bed for the filtration of lab-contaminated water and the hydrosoluble form was used and tested as permeable reactive barrier injected at low pressure for the treatment of lab-contaminated groundwater. During the characterization of the adsorption process of all the previous reported contaminants on the thermo-plasma expanded graphite, different parameters were tested to have deep information on it. Kinetics, thermodynamics and isothermal information were obtained, the influence of the pH, the initial concentration of the contaminants, the effect of ionic strength or presence antagonistic molecules, the effect of headspace (for volatile contaminants) and the effect of the contemporaneous presence of contaminants on the adsorption process were tested. For the fixed-bed tests also the effect of the flow rate and bed depth were tested. Furthermore, the regeneration of the adsorbent material were also investigated by thermal recovery and very promising results were obtained. The material preserves its adsorption properties after five cycles of use and regeneration. This PhD thesis demonstrates that thermo-plasma expanded graphite can be used for the typical adsorption setup to remove a large spectrum of contaminants and the lab-scale conducted tests represent the first mandatory optimization step of the process on the field. The most interesting results obtained during this PhD thesis work are the results obtained by modifying the

commercial form of the thermo-plasma expanded graphite. The granular form resulted to be very useful for the adsorption on fixed bed with very high adsorption capacity and the mechanism of production that was optimized allows the coupling of the graphite with other compounds and it can be useful to prepare a material for coupling adsorption to other remediation process (in the outlook section it is better explained). The tests conducted on the hydrosoluble form of the thermo-plasma expanded graphite were very promising and demonstrated the possibility of the use of the material as permeable reactive barrier injectable at low pressure for the treatment of contaminated groundwater.

### **3.2 Outlook**

The thermo-plasma expanded graphite was tested as the commercial form, granular and hydrosoluble form. The promising results suggest to evaluate the performance of the material at lower concentration than the concentration tested during the work to reach the concentration of  $\mu\text{g L}^{-1}$ . Further contaminants can be tested to evaluate the ability of the thermo-plasma expanded graphite and increase the spectrum of compound that can be removed by using that material. The most interesting outlook for the material is the possibility of further modification of its morphology and physical-chemical properties. Further modification can be conducted to improve the characteristic of the thermo-plasma expanded graphite and obtain a material with properties useful for field implementation. One modification could be the magnetization of the material to facilitate the recovery of the adsorbent after its use. It could be very useful for batch application in pump & treat setup or in wastewater treatment plants. Further study can be conducted by entrapping into the granular thermo-plasma expanded graphite molecules of oxide metals with photocatalytic properties to couple the adsorption and the photodegradation. It could be useful to overcome the limitation of the saturation of the adsorbent materials that limits the use of the adsorption process. Other promising modifications can be conducted by entrapping microorganism able to degrade contaminants to couple adsorption and biodegradation with the same benefit described for the coupling of adsorption and photodegradation or by introducing functional groups on the surface of the thermo-plasma expanded graphite. Polar groups can be introduced to enhance the affinity with the water and facilitate the dispersion into the water. It could be useful to increase the diffusion of the contaminants on the surface of the thermo-plasma expanded graphite or to obtain an adsorbent material easily injectable into groundwater. Other specific functional groups could be added to confer to the material a selective adsorption property. The thermo-plasma expanded graphite

could be used for this last purpose by representing an ideal substrate due its optimum mechanical properties.